

**Aspects in the development of Dynamic Noise Perimetry**

**Kholoud Alshaghroud**

**Doctor of Philosophy**

**Cardiff University**

**2014**

## Summary

The purpose of this thesis was to develop further the concept of Dynamic Noise Perimetry (DNP).

The influence of 4 different strengths of Gaussian filter on the DNP stimulus edge, without and with a noise mask, was separately investigated in 15 normal individuals at three eccentricities. The DNP threshold was not affected by the filtering.

The critical check size of the noise mask was investigated in 11 normal individuals at three eccentricities for 8 different checks per cycle. The critical check size at the fovea was 4 checks per cycle and in the periphery between 2 and 4 checks per cycle.

The influence of optical defocus was investigated in 11 normal individuals at three eccentricities. For a defocus of +4.00DS, sensitivity without the noise mask declined by approximately 1dB; with the noise mask sensitivity increased by 1dB.

The original 'Proof of Concept' threshold algorithm, which enabled the estimation of threshold at one location in approximately 3 minutes, underwent numerous modifications. The final iteration permitted threshold estimation at 45 locations in approximately 7 minutes.

Five of the ten individuals with open angle glaucoma who had undergone DNP and standard automated perimetry (SAP) in 2007 were re-examined, using an identical protocol, after a follow-up of four years. The abnormality with DNP at baseline was present at the follow-up in all five individuals and was more severe in 3 individuals. Only 2 individuals exhibited abnormality by SAP.

The influence of the learning effect on the outcome of DNP was evaluated, in one designated eye at each of the five weekly visits, for 10 'young' and 8 'elderly' normal individuals naïve to perimetry. Optimum performance was essentially achieved at the third visit without and with the noise mask.

The outcomes of DNP are adversely influenced by optical defocus and, in the normal eye at least, improve with repeated examinations. Nevertheless, the results from the long-term follow-up of the individuals with open angle glaucoma were sufficiently encouraging to warrant further development of DNP. The next phase of the development should modify the current algorithm to reduce, still further, and without loss of accuracy, the examination duration in normal individuals. The same approach should then be adopted for individuals with manifest glaucomatous field loss.

## **Acknowledgments**

First and foremost, I would like to thank, sincerely, my supervisor, Professor John Wild, for his continuous support, encouragement, guidance and assistance throughout my study.

I thank Dr. Caroline Djiallis for undertaking the ophthalmic examinations of those who participated in the study; Dr. Frank Rakebrant for the mathematical development of the DNP algorithm; Dr. Gavin Powell for the development of the software for DNP; Mr. David Shaw, Senior Medical Statistician, for undertaking the various ANOVAs; and to all those who participated in the study.

I also extend my thanks to my parents and to my brothers and sisters, especially Khalid, Maha and Arwa, for their unconditional love, support, encouragement and patience throughout my study.

Finally, I thank my fellow research students, Aristidis Chandrinou, Saleh Aljarudi and Eleni Malissova for their support. In particular, I am indebted to Eleni, for her, friendship, love, assistance, and encouragement which made my time in Cardiff enjoyable.

I dedicate this thesis to my parents and to the soul of my aunt.

# **Chapter 1: Examination techniques for the investigation of glaucomatous visual field loss**

1.1 Introduction	1
1.1.1 The visual field	1
1.1.2 The differential light threshold	3
1.1.2.1 Kinetic perimetry	3
1.1.2.2 Static perimetry	5
1.2 Physiology associated with the differential light threshold	6
1.2.1 Background luminance	6
1.2.2 Stimulus duration	7
1.2.3 Stimulus size	7
1.2.4 Stimulus grid	8
1.2.5 Units of measurements	9
1.3 Standard automated perimetry	9
1.4 Primary open angle glaucoma	11
1.5 Open angle glaucoma and perimetry	13
1.6 Types of non-standard automated perimetry	16
1.6.1 Flicker Perimetry	16
1.6.1.1 Critical Flicker Fusion Perimetry (CFFP)	16
1.6.1.2 Temporal Modulation Perimetry (TMP)	17
1.6.1.3 Luminance Pedestal Flicker perimetry (LPFP)	18
1.6.2 Short Wavelength Automated Perimetry (SWAP)	18
1.6.3 High-Pass Resolution Perimetry (HPRP)	20
1.6.4 Frequency Doubling Technology (FDT) perimetry	22
1.6.5 Random-dot kinematograms (RDKs)	26
1.6.6 Moorfields Motion Displacement test (MDT)	27
1.6.7 Rarebit Perimetry (RBP)	28
1.6.8 Pulsar Perimetry (PP)	30
1.6.9 Heidelberg edge perimetry (HEP)	32

1.7 The structure-function relationship in open angle glaucoma	33
1.8 Retinal ganglion cell dysfunction	35
<b>Chapter 2: Dynamic Noise Perimetry</b>	
2.1 Background	37
2.1.1 Internal noise	37
2.1.2 External noise	38
2.1.3 The current DNP	42
2.1.3.1 Stimulus parameters	42
2.1.3.2 Examination procedure	44
2.1.4 Output	46
2.1.4.1 Signal Energy ( $E_{th}$ )	46
2.1.4.2 Sampling Efficiency (SE)	47
2.1.4.3 Calculation of equivalent noise ( $N_{eq}$ )	48
2.1.4.4 Further outputs from DNP	48
<b>Chapter 3: Rational</b>	
3.1 Introduction	50
3.1.1 The influence of Gaussian filtering on the outcome of Dynamic Noise Perimetry (Chapter 5)	52
3.1.2 The influence of the strength of the noise mask on the outcome of Dynamic Noise Perimetry (Chapter 6)	53
3.1.3 Further development of the threshold estimation algorithm for Dynamic Noise Perimetry (Chapter 7)	53
3.1.4 The influence of optical defocus on Dynamic Noise Perimetry (Chapter 8)	54
3.1.5 The follow-up of individuals with open angle glaucoma (Chapter 9)	55
3.1.6 The learning effect in Dynamic Noise Perimetry (Chapter Ten)	55
3.2 Logistics	56
3.2.1 Background	56
3.2.2 Methods	56

## **Chapter 4: Calibration of the Dynamic Noise Perimetry high resolution cathode ray tube monitor**

4.1 Introduction	59
4.2 Calibration of the DNP display	60
4.2.1 Introduction	60
4.2.2 Procedure	61
4.2.2.1 Step one: Red, Green and Blue (RGB) colour gun luminance calibration	61
4.2.2.2 Step two: Michelson Contrast validation at the centre of the screen	66
4.2.2.3 Step three: Michelson Contrast validation at each of nine sectors	71
4.3 Transforming the unit of measurement for DNP	77

## **Chapter 5: The influence of the Gaussian filter on Dynamic Noise Perimetry**

5.1 Introduction	79
5.2 Aim	80
5.3 Methods	81
5.3.1 Cohort	81
5.3.2 Examination protocol	81
5.3.3 Analysis	87
5.3.4 Ethical Approval	87
5.4 Results	87
5.5 Discussion	94
5.6 Conclusion	95

## **Chapter 6: The strength of the noise mask on the outcome of Dynamic Noise Perimetry**

6.1 Introduction	96
6.2 Aim	96
6.3 Methods	97
6.3.1 Cohort	97
6.3.2 Examination protocol	99
6.3.3 Analysis	100
6.3.4 Ethical Approval	100
6.4 Results	100
6.5 Discussion	106

## **Chapter 7: Threshold algorithm development for Dynamic Noise Perimetry**

7.1 Background	108
7.2 The ‘Proof of Concept algorithm’	110
7.3 Further development of the ‘Proof of Concept algorithm’	113
7.3.1 First iteration	113
7.3.1.1 Cohort and DNP methodology	119
7.3.1.2 Analysis	121
7.3.1.3 Results	121
7.3.1.4 Discussion	126
7.3.1.5 Conclusion	127
7.3.2 Second iteration	128
7.3.2.1 Preliminary stage	128
7.3.2.1.1 Cohort	128
7.3.2.1.2 Methods	128
7.3.2.1.3 Results	130
7.3.2.2 Polynomial modelling	140
7.3.2.2.1 Derivation of the staircase for the four seed points	141

7.3.2.2.2 Derivation of the staircase for the non-seed points	143
7.3.2.3 Evaluation of the Final Algorithm	144
7.3.2.3.1 Results	145
7.3.2.3.2 Discussion	150
7.3.2.3.3 Conclusion	159
<b>Chapter 8: The influence of foveal optical defocus on Dynamic Noise Perimetry</b>	
8.1 Introduction	162
8.2 Aim	165
8.3 Methods	165
8.3.1 Cohort	165
8.3.2 Examination protocol	165
8.3.3 Analysis	167
8.3.4 Ethical Approval	168
8.4 Results	168
8.4.1 Michelson contrast, expressed as sensitivity (dB)	168
8.4.2 Derivatives from MCN <sub>a</sub> and MCN <sub>p</sub>	176
8.5 Discussion	180
8.6 Conclusion	185
<b>Chapter 9: Long-term follow-up of DNP in open angle glaucoma</b>	
9.1 Introduction	186
9.2 Aim	187
9.3 Methods	187
9.3.1 Cohort	187
9.3.2 Examination protocol	188
9.3.3 Analysis	189
9.3.4 Ethical Approval	189
9.4 Results	189
9.5 Discussion	202

<b>Chapter 10: The Learning Effect in Dynamic Noise Perimetry</b>	
10.1 Introduction	204
10.2 Aim	207
10.3 Methods	207
10.3.1 Cohort	207
10.3.2 Examination protocol	209
10.3.3 Analysis	210
10.3.4 Ethical Approval	211
10.4 Results	213
10.4.1 Mean Sensitivity for the central field	213
10.4.2 Mean Sensitivity at the six central stimulus locations	219
10.4.3 Mean Sensitivity at the six peripheral stimulus locations	225
10.4.4 The ratio of Central to Peripheral Mean Sensitivity	231
10.4.5 Examination Duration	235
10.4.6 The derivatives from $MCN_a$ and $MCN_p$	239
10.5 Discussion	240
<b>Chapter 11: General summary, conclusions and proposals for future work</b>	
11.1 The influence of the Gaussian filter on Dynamic Noise Perimetry	242
11.2 The influence of the strength of the noise mask on the outcome of Dynamic Noise Perimetry	242
11.3 Further development of the ‘Proof of Concept’ DNP Algorithm	243
11.4 The influence of foveal optical defocus on the Dynamic Noise Perimetry	246
11.5 Long-term follow-up of DNP in open angle glaucoma	246
11.6 The Learning Effect in Dynamic Noise Perimetry	247
11.7 Proposals for future work	248
<b>References</b>	251

## Key to the abbreviations used in the text

ASTA	Adaptive Staircase Thresholding Algorithm
CCT	Central corneal thickness
CCD	Charge coupled device
CFFP	Critical Flicker Fusion Perimetry
CRT	Cathode Ray Tube
CSF	Contrast sensitivity function
DNP	Dynamic Noise Perimetry
Eth	Energy threshold
EthN <sub>a</sub>	Energy threshold, in the absence of the noise mask
EthN <sub>p</sub>	Energy threshold, in the presence of the noise mask
FD	Frequency Doubling
FDT	Frequency Doubling Technology perimetry
FDF	Flicker Defined Form perimetry
FWHM	Full Width at Half Maximum
HEP	Heidelberg Edge Perimetry
HPRP	High Pass Resolution Perimetry
IN	Inferior nasally
IOP	Intraocular pressure
IT	Inferior temporally
K	Koniocellular
LPFP	Luminance Pedestal Flicker Perimetry
M	Magnocellular
MC	Michelson contrast
MC N <sub>a</sub>	Michelson contrast in the absence of noise
MC N <sub>p</sub>	Michelson contrast in the presence of noise
MDT	Moorfields Motion Displacement Test
MOBS	Modified binary search
Ne	Noise spectral density
Neq	Equivalent noise
PD	Pattern Deviation
RDKs	Random-dot kinematograms
RGC	Retinal ganglion cell
RNFL	Retinal nerve fibre layer
SD	Standard Deviation
SDI	Signal detection index
SE	Sampling efficiency
SN	Superior nasal
SNR	Signal-to-noise ratio
ST	Superior temporal
SWAP	Short wavelength automated perimetry
TD	Total Deviation
TOP	Tendency-oriented perimetry
TMP	Temporal modulation perimetry
ZEST	Zippy Estimation by Sequential Testing

# Chapter 1

## Examination techniques for the investigation of glaucomatous visual field loss

### 1.1 Introduction

#### 1.1.1 The visual field

The visual field is that part of the environment which is visible to the steadily fixating eye (Anderson and Patella, 1999). The maximum extent of the monocular visual field in a normal individual is approximately 60° superiorly, 70° inferiorly, 60° nasally and 90° temporally (Anderson and Patella, 1999). Clinically, the field within 30° eccentricity from fixation is termed the central field and that beyond 30° eccentricity is termed the peripheral field.

The visual field in the normal individual has been likened to a three-dimensional 'island of vision in a sea of blindness' (Traquair 1927). The height of the island corresponds to the sensitivity of the visual system with the maximum sensitivity (the summit of the hill of vision) occurring, under photopic conditions, at the fovea. The island gradually slopes down (i.e., sensitivity declines) from the summit towards to the shoreline at the sea of blindness. The slope is steepest nasally and flattest temporally. Within the island of vision, at approximately 15° temporally and 1.5° inferiorly to fixation, is the physiological blind spot, which represents the projection of the optic nerve head through the optics of the eye.

The blind spot extends approximately  $5.5^\circ$  horizontally and  $7.5^\circ$  vertically (Reed and Drance, 1972). The analogy of the blind spot, in the concept of the island of vision, is a steep sided well which descends to the bottom of the island of vision.

A normal visual field requires a clear ocular media; a focused image on the retina; and normal image processing along the visual pathway, i.e., from the photoreceptors to the bipolar cells and to the ganglion cells; along the ganglion cell axons, which converge in a characteristic topography and exit the eye as the optic nerve; through the optic chiasm and the optic tract to the lateral geniculate nucleus; and then along the optic radiations, in the temporal and parietal lobes; to the primary visual cortex in the occipital lobe.

Structural damage to the visual pathway appears as functional damage in the form of visual field loss. A reduction in the height of the island of vision (i.e., a sinking into the sea of blindness) represents a generalised depression/ diffuse reduction of sensitivity across the entire visual field. A focal abnormality (also termed a scotoma) describes a localised loss of sensitivity, of varying area and depth, occurring within the boundaries of the visual field. A loss of the peripheral field is termed a constriction and is analogous to an erosion of the shore line of the island of vision. The constriction may be localised to a specific region or may be generalised, as in a concentric constriction. The location of the structural damage and, therefore, the underlying anatomy, governs the characteristics of the visual field defect, i.e., the location, shape, and depth, and this feature is used for the differential diagnosis of abnormality of the visual field.

### **1.1.2 The differential light threshold**

Examination of the visual field, perimetry, involves the estimation of the differential light threshold. The latter is defined as the minimum stimulus luminance ( $\Delta L$ ) necessary to evoke a response against a background of constant known luminance ( $L$ ). It is usually expressed in terms of the differential light sensitivity ( $L/\Delta L$ ).

Standard perimetry uses a white stimulus presented on a white background luminance.

Two different techniques are used to estimate the differential light threshold: kinetic perimetry and static perimetry.

#### **1.1.2.1 Kinetic perimetry**

Kinetic perimetry describes the technique whereby a stimulus of a known size and luminance is moved centripetally, at a constant velocity, along a given meridian towards the visual field. The position at which the stimulus is first 'seen' is designated as the estimated threshold. The stimulus is then moved centripetally along the same meridian towards fixation in order to identify any regions within the visual field which are 'not seen'. The entire procedure is then repeated radially along each meridian. The line joining the positions of the estimated threshold is known as an isopter and is analogous to the contour line of a map. By using various appropriate stimulus sizes and/ or luminances, the contour of the island of vision can be described in terms of a number of isopters. As such, the separation between any two isopters indicates the slope of the hill of vision at any

given location: widely separated isopters indicate a gently sloping contour whilst closely positioned isopters indicate a steep contour.

The ‘gold’ standard for kinetic perimetry was, and to some extent still is, the Goldmann bowl perimeter (Schmidt, 1955). Kinetic perimetry with the Goldmann perimeter is now being replaced by semi-automated kinetic perimetry with the Octopus perimeter (Nowomiejska et al., 2004; Nowomiejska et al., 2005; Vonthein et al., 2007; Nevalainen et al., 2008; Tonagel, Voykov and Schiefer, 2012).

Kinetic perimetry is more efficient for the edge-detection and delineation of advanced visual field loss particularly that exhibiting a steeply sloping border such as advanced arcuate loss, altitudinal loss, concentric constriction, and hemianopsia. In this regard, the technique is less time-consuming and less tiring for both the patient and the perimetrist (Vonthein et al., 2007). It is now becoming the method of choice for examination of the peripheral field given the recognition that the confidence limits associated with the normal values of sensitivity derived by static perimetry using the Goldmann size III stimulus generally exceed the dynamic range of the perimeter. It is also the default method of choice for those unable to undertake static perimetry.

The advent of semi-automated kinetic perimetry has overcome some of the limitations associated with kinetic perimetry undertaken with the Goldmann perimeter. The reaction time of both the patient and the perimetrist can now be quantified and a correction applied to the measured isopters, the stimulus is presented at a constant velocity by means of the computer and the measured field can be compared to age-corrected normal values for the given stimulus combination (Vonthein et al., 2007).

Nevertheless, the moving stimulus tends to be detected more easily in the periphery than the stationary stimulus in static perimetry because of the successive lateral spatial summation (Greve, 1973).

### **1.1.2.2 Static perimetry**

Static perimetry comprises a stationary stimulus presented at various locations in the visual field. The size of the stimulus is fixed and the luminance is varied until an estimation of the threshold is obtained.

Classically, the threshold is usually defined as the stimulus luminance corresponding to a 50%, or sometimes, a 75%, probability of a 'seen' response and is generated from the frequency-of-seeing curve whereby the frequency of a 'seen' response is plotted against, in this instance, the logarithm of the stimulus luminance. The resulting curve is an ogive which is characterized by a linear section in the middle (Weber and Rau, 1992; Chauhan et al., 1993b; Olsson et al., 1993). The slope of the linear portion is indicative of the variability of the threshold estimate: as the variability increases the slope becomes increasingly flat. The frequency-of-seeing techniques could also be applied to kinetic perimetry.

In clinical perimetry, the compilation of a frequency-of-seeing curve at one or more locations would be too time consuming. The threshold estimate is, therefore, achieved by presenting the initial stimulus above (i.e., dimmer) or below (i.e., brighter) than the expected threshold for the given individual. Depending upon the individual's response, the stimulus luminance is increased or decreased in a series of uniform steps until threshold is crossed (i.e., the individual either reports that the stimulus is no longer seen or that it has

just become visible). The threshold can be crossed, again, by reversing the direction of luminance. The accuracy of the threshold estimate can be increased by reducing the step size and/ or increasing the number of reversals and/ or increasing the number of staircases, but at the expense of an increase in the examination duration. The approach by which the stimuli are presented is called an algorithm.

## **1.2 Physiology associated with the differential light threshold**

### **1.2.1 Background luminance**

The adaptation of the eye is determined by the background luminance. Under photopic ( $\geq 10 \text{cdm}^{-2}$ ) conditions, the differential light threshold is an expression of the Weber-Fechner Law i.e.,  $\Delta L/L = c$  where  $c$  is a constant. Under mesopic conditions, the differential light threshold can be described by the Rose-de Vries Law,  $\Delta L/L^{0.5} = c$  and under scotopic conditions (i.e.  $\leq 0.01 \text{cdm}^{-2}$ ) by  $\Delta L = c$  (Greve, 1973).

### **1.2.2 Stimulus duration**

The relationship between the differential light threshold and the stimulus duration,  $t$ , is described by Bloch's Law (Bloch 1885),  $\Delta L * tk = c$ , where  $k$  is the temporal summation coefficient. If the stimulus duration is less than the critical duration, complete temporal summation occurs, i.e.,  $k=1$  and the stimulus appears to become increasingly brighter with increase in stimulus duration. When the examination duration exceeds a critical value, partial temporal summation occurs and  $k$  tends toward zero. When  $k = 0$ , and all other

stimulus parameters remain constant, an increase in stimulus duration has no further effect on the differential light sensitivity.

The critical duration in the normal eye is between 60 and 100msec and depends upon the stimulus eccentricity and the background luminance (Barlow, 1958; Saunders, 1975). Temporal summation increases with decrease in stimulus size (Barlow, 1958; Saunders, 1975) and with decrease in background luminance (Barlow, 1958; Saunders, 1975).

In static perimetry, the stimulus duration is usually between 100 and 200msec depending upon the perimeter. It should not exceed 200msec because the latency of saccadic eye movements is approximately 250msec (Robinson, 1963).

### **1.2.3 Stimulus size**

The relationship between the differential light threshold and the stimulus area,  $a$ , is described by  $\Delta L^* a^k = c$ . The magnitude of  $k$ , the summation coefficient, varies with eccentricity from 0.55 to 0.9 (Wilson, 1970; Anderson and Patella, 1999). When  $k=1$ , complete spatial summation is present and Ricco's Law applies. Partial summation occurs when the stimulus area exceeds a critical area, Ricco's area, and  $k$  is less than unity. Partial summation has been described variously by Pieron's Law ( $k=0.3$ ), Piper's Law ( $k=0.5$ ) and by Goldmann who used a value of  $k=0.8$ . When  $k=0$ , the Weber-Fechner Law applies.

Six Goldmann stimulus sizes were utilised for the Goldmann bowl perimeter. The angular subtends doubled with each increase in stimulus size from the smallest, size 0 ( $0.054^\circ$ ), to

the largest, size V ( $1.724^\circ$ ) and these stimulus sizes are used for semi-automated kinetic perimetry (Vonthein et al., 2007; Nevalainen et al., 2008).

The default stimulus size for standard automated perimetry is Goldmann stimulus size III. With this size, the variability associated with the threshold estimate increases with increase in eccentricity and with decrease in sensitivity to approximately 12 (Heijl, Lindgren and Olsson, 1989b) to 15dB (Gardiner, 2014). The magnitude of the variability, which can exceed the dynamic range of the perimeter, is such as to advocate the use of either Goldmann size V (Wall et al., 2008; Wall et al., 2009; Wall et al., 2010; Vislisel et al., 2011; Wall et al., 2013) or even a size VI (Wall et al., 2013).

#### **1.2.4 Stimulus grid**

The probability of detection of visual field loss increases as the spatial separation of the stimuli decreases; however, this also at the expense of an increase in the examination duration. A stimulus grid with an inter-stimulus separation of  $6^\circ$ , with the stimuli bordering the horizontal and vertical midlines offset by  $3^\circ$ , has become the standard. The probability of detecting a focal defect the size of the blind spot with a  $6^\circ$  square stimulus grid is 95% (Fankhauser and Bebie, 1978). The variability of the threshold estimate with the default Goldmann size III stimulus is such that the  $6^\circ$  square stimulus grid only covers the central field. For late stage disease or for investigation of the visual field out to an eccentricity of approximately  $10^\circ$  a higher resolution grid is used with an inter-stimulus separation of  $2^\circ$ .

### **1.2.5 Units of measurements**

The units of the differential light sensitivity are the candela per square metre ( $\text{cdm}^{-2}$ ) or the apostilb (asb) and both are usually expressed in decibels (dBs). The dB scale is referenced to the maximum luminance of the given perimeter which is specified as 0dB. Consequently, an increase in a dB value corresponds to an increase in sensitivity (Anderson and Patella, 1999).

Since the maximum luminance varies between types of perimeter, identical dB values on two different types of perimeter will not necessarily correspond to the same sensitivity (Schiefer, Patzold and Dannheim, 2005).

### **1.3 Standard automated perimetry**

Standard automated perimetry is the term used to describe static threshold perimetry. The ‘gold’ standard perimeter for standard automated perimetry is the Humphrey Field Analyzer. The initial version of the perimeter was introduced in 1985 (Heijl and Greve, 1985) and the second, and current, version in 1996.

The background luminance of the Humphrey Field Analyzer is  $10\text{cd m}^{-2}$  (31.5asb) which represents a compromise between minimizing the time required for retinal adaptation and maximizing the dynamic range of the perimeter (Heijl and Greve, 1985).

The maximum stimulus luminance ( $\Delta L$ ) is  $3183\text{cdm}^{-2}$  (10,000asb) which gives a dynamic range of approximately 33dB, clinically. The default stimulus size is Goldmann size III.

Four threshold algorithms are available with the Humphrey Field Analyzer: Full Threshold, FASTPAC, SITA Standard and SITA Fast.

The initial algorithm, the Full Threshold utilises a double staircase which crosses threshold in 4dB steps and reverses in 2dB steps (Wild et al., 1999a). The threshold is considered to be the last seen stimulus. The algorithm starts with a stimulus luminance of 25dB at four predetermined seed locations, situated at 9° at each of the four quadrants. The adjacent locations are then tested at 2dB brighter than the expected threshold of the neighbouring stimulus locations derived from the slope of normal hill of vision (Wild et al., 1999a). Ten stimulus locations each include a second determination of threshold which enables an estimation of the within-test variability, i.e., the short-term fluctuation.

The FASTPAC algorithm utilizes a single crossing of threshold with a single 3dB step and the threshold is considered to be the last seen stimulus (O'Brien et al., 1994; Glass, Schaumberger and Lachenmayr, 1995; Roggen et al., 2001). The examination duration of FASTPAC is 35-40% less than the Full Threshold but at the expense of an underestimation in the severity of visual field loss and a 25% increase in the within-test variability (Flanagan et al., 1993; Glass et al., 1995).

The two Swedish Interactive Threshold Algorithms (SITA), SITA Standard and SITA Fast were commercially introduced in 1998. SITA Standard corresponds to Full Threshold and SITA Fast to FASTPAC (Bengtsson et al., 1997; Bengtsson and Heijl, 1998; Bengtsson, Heijl and Olsson, 1998; Nordmann et al., 1998). Both versions of SITA are based upon the ZEST algorithm (See Chapter 7) (Turpin et al., 2003). SITA Standard uses an initial 4dB step, and once the threshold has been crossed, a 2dB step. The staircase at any given

location can be terminated after one crossing of threshold if the standard deviation of the modified probability density function (see Chapter 7) is sufficiently small (Bengtsson et al., 1997). SITA Fast utilizes a single step of 4dB, and the staircase can be terminated at any given location without crossing the threshold (Bengtsson et al., 1997; Bengtsson and Heijl, 1998). Each algorithm is approximately 50% shorter, in normal individuals, relative to its comparative algorithm (Bengtsson and Heijl, 1998; Bengtsson et al., 1998). SITA Fast is 41% shorter than the SITA Standard algorithm (Anderson and Patella, 1999; Wild et al., 1999a; Roggen et al., 2001).

Both versions of SITA repeat the threshold estimation if the initial estimate is more than 12dB from the expected threshold which is wider than the corresponding 4dB disparity with the Full Threshold (Turpin et al., 2003). The test-retest variability at locations exhibiting a sensitivity of  $\geq 25$ dB is better for each SITA version compared to Full Threshold. Below 25dB, SITA Standard exhibits a slightly better, and SITA Fast a slightly poorer, test-retest variability compared to Full Threshold (Artes et al., 2002). Both versions of SITA are more sensitive to the progression of visual field loss (Delgado et al., 2002).

#### **1.4 Primary open angle glaucoma**

Standard automated perimetry is a fundamental tool in the detection and the management of glaucoma.

Glaucoma is a group of conditions in which there is a slowly progressive atrophy of the optic nerve head, characterised by visual field loss and an excavated appearance of the optic nerve head manifested as cupping and a corresponding abnormal neuro-retinal rim. This excavation consists of a loss both of retinal ganglion cell axons in the inner retina, their axons in the optic nerve head and a deformation of connective tissues supporting the optic nerve head (Quigley, 2011; American Academy of Ophthalmology, 2014). Primary open angle glaucoma is a subset of the glaucomas defined by an open and normal appearing anterior chamber angle and raised intraocular pressure, with no other underlying disease. Normal tension glaucoma occurs in the presence of a normal intraocular pressure.

Glaucoma is undiagnosed in nine of ten affected individuals, worldwide, and in 5 of 10 affected individuals in developed countries. By 2020, 79.6 million individuals will be affected by glaucoma, and, of these, 74% will have open angle glaucoma (Quigley and Broman, 2006; Quigley, 2011).

An elevated intraocular pressure is the most important modifiable risk factor for glaucoma. A reduction in intraocular pressure offers, for glaucomatous optic neuropathy, a treatment option that is not available for other neurodegenerative diseases.

The pathophysiology of glaucoma remains largely speculative (Werkmeister et al., 2013) but is likely to involve oxidative stress and mitochondrial dysfunction (Osborne, 2011; Agudo-Barriuso et al., 2013), the immune system (Tezel, 2013), vascular factors (Mozaffarieh and Flammer, 2013) and cortical involvement (Yucel and Gupta, 2008; Nucci et al., 2013).

## 1.5 Open angle glaucoma and perimetry

Morphologically, there are at least four distinct types of retinal ganglion cell in human (Dacey, 1993; Martin et al., 1997). The majority of the ganglion cells are the midget cells which comprise 80% of the total population. These ganglion cells project to the parvocellular layers of the lateral geniculate nucleus and are, therefore, also known as P cells (Rodieck, Binmoeller and Dineen, 1985; Watanabe and Rodieck, 1989; Dacey and Petersen, 1992; Martin et al., 1997). They are sensitive to higher spatial frequencies (detail) and colour. The parasol retinal ganglion cells account for approximately 10% of the total ganglion cell population. They project to the magnocellular layers of the lateral geniculate nucleus and are, therefore, also known as M cells. They are sensitive to high temporal frequencies and fast movement. There are at least two subclasses of M cells: the  $M_x$  cells and the  $M_y$  cells. The  $M_y$  cells are larger than the  $M_x$  cells and comprise approximately 15- 20% of the M cells. The small bistratified retinal ganglion cells account for approximately 10% of the total ganglion cell population. They are smaller than the midget cells and exhibit moderate spatial resolution, moderate conduction velocity, are responsive to moderate contrast stimuli and are implicated in blue-yellow processing. They project to the koniocellular layers of the lateral geniculate nucleus and are also known as K cells (Dacey and Petersen, 1992; Martin et al., 1997). The photosensitive retinal ganglion cells contain melanopsin and respond directly to light (Hankins, Peirson and Foster, 2008). Some of these cells project to the suprachiasmatic nucleus via the retinohypothalamic tract which is responsible for circadian rhythms and others project to the lateral geniculate nucleus and onward to the Edinger-Westphal nucleus and are implicated in the control of the pupillary light reflex.

In the late 1980's and the early 1990's, a number of studies emanated from Quigley's group which reported that between 25% and 50% of the retinal ganglion cells in open angle glaucoma could be damaged before the manifestation of a visual field defect (Quigley et al., 1987; Quigley, Dunkelberger and Green, 1988; Glovinsky, Quigley and Dunkelberger, 1991; Glovinsky, Quigley and Pease, 1993; Kerrigan-Baumrind et al., 2000).

Two hypotheses were advanced to explain the temporal disparity between the loss of retinal ganglion cells and the emergence of visual field loss in early glaucoma.

The first hypothesis suggested that the retinal ganglion cells with larger diameter axons were damaged in early glaucoma. This hypothesis was based upon histological evidence that had shown a greater proportion of the retinal nerve fibres which exceeded the mean diameter were destroyed both in human and monkey open angle glaucoma (Quigley et al., 1987; Quigley et al., 1988; Glovinsky et al., 1991; Glovinsky et al., 1993; Kerrigan-Baumrind et al., 2000). These findings were challenged by Morgan, Uchida and Caprioli (2000) and Morgan (2002) and subsequently by Malik, Swanson and Garway-Heath (2012) and the conclusions are now largely discredited. However, a relatively recent review undertaken on behalf of the American Academy of Ophthalmology (Jampel et al., 2011) still cites this evidence as one of the most important limitations of standard automated perimetry.

The second hypothesis suggested that retinal ganglion cell death in early glaucoma was non-selective. The ganglion cell sub-populations with lower degrees of overlap between adjacent receptive fields would demonstrate functional deficits earlier in the open angle

glaucoma disease process since only a small number of cells must be lost prior to the loss of adequate receptive field coverage. This theory is referred to as the reduced redundancy hypothesis (Johnson, 1994; Johnson 1995).

It was further conjectured that the white stimulus on the white background used in standard automated perimetry had broadband characteristics that activated all the various types of ganglion cells and that, as the large overlap in the ganglion cell network results in considerable redundancy, glaucomatous field loss would be undetected if all types of ganglion cells are stimulated (Soliman et al., 2002).

As a consequence of Quigley's findings (Quigley et al., 1987; Quigley et al., 1988; Glovinsky et al., 1991; Glovinsky et al., 1993; Kerrigan-Baumrind et al., 2000), a number of non-standard types of perimetry were developed through the 1990s and the first decade of this century. These types of perimetry were based either upon specific mediation by the M cells, or upon mediation by a cell type exhibiting minimal redundancy, or both. It was argued that such tests should be better than standard automated perimetry for the detection and follow-up for early glaucoma. Those based upon M cell function (and, therefore, also minimal redundancy) included motion perimetry and flicker perimetry (Tyler, 1981; Silverman, Trick and Hart, 1990; Anderson and O'Brien, 1997; Yoshiyama and Johnson, 1997; Bosworth et al., 1998; Sample et al., 2000; Spry et al., 2005; Matsumoto et al., 2006) whilst those based upon minimal redundancy, only, included short-wavelength automated perimetry (SWAP) (Dacey, 1993; Wild, 2001).

## **1.6 Types of non-standard automated perimetry**

### **1.6.1 Flicker Perimetry**

There are three methods of flicker perimetry: critical fusion frequency perimetry (CFFP), temporal modulation perimetry (TMP) and Luminance Pedestal Flicker perimetry (LPFP). All the three types of perimetry involve the magnocellular pathway and are relatively unaffected by media opacities, defocus, and refractive error compared to luminance based stimuli (i.e. standard automated perimetry and SWAP) (Lachenmayr and Gleissner, 1992).

#### **1.6.1.1 Critical Flicker Fusion Perimetry (CFFP)**

The initial studies of the suitability of CFFP as a stimulus for visual field examination found it to be, at the time, an effective method for detecting glaucomatous damage (Miles, 1950). CFFP modulates the frequency of the flickering stimulus, presented at a fixed contrast usually at or close to 100%, from slow (1-5 Hz) to fast (towards 50 Hz) and measures the maximum frequency at which the flicker can be perceived (Weijland et al., 2004).

The CFFP for normal individuals, using the 1° diameter stimulus presented under photopic conditions, increases with increase in eccentricity from the fovea to the paracentral regions, remains at a high level up to eccentricities of 20° to 30° (Hylkema, 1942), after which it falls below the foveal value (Lachenmayr et al., 1994). It decreases with increase in age (Lachenmayr et al., 1994) and is more resistant to optical defocus than standard automated perimetry (Lachenmayr and Gleissner, 1992).

CFFP detects in normal areas of the visual field by standard automated perimetry are present in glaucoma (Lachenmayr, Gleissner and Rothbacher, 1989) and the technique exhibits a similar diagnostic outcome to Frequency Doubling Technology (FDT) perimetry with the Matrix perimeter (Matsumoto et al., 2006). However, CFFP, although commercially available with the Octopus 300 and 600 series perimeters, has not received further attention.

#### **1.6.1.2 Temporal Modulation Perimetry (TMP)**

Temporal modulation perimetry (TMP) measures the minimum contrast necessary to detect flicker for a fixed temporal frequency (Yoshiyama and Johnson, 1997). TMP measures sensitivity to flicker across a range of frequencies e.g., 2, 8 and 16 Hz sinusoidal flicker (Casson, Johnson and Nelson-Quigg, 1993a; Casson, Johnson and Shapiro, 1993b; Yoshiyama and Johnson, 1997).

Sensitivity for TMP decreases in normal individuals with increase in age and with increase in eccentricity, especially for 16 Hz (Tyler, 1981; Casson et al., 1993a). The sensitivity for TMP at the fovea is independent of age in the normal eye and is similar to CFFP in this regard (Casson et al., 1993a).

The optimal temporal frequency for TMP is considered to be 8Hz since the within- and between-subject variability is lower than that for higher temporal frequencies and the dynamic range is greater because it is near the peak of the normal temporal contrast sensitivity function (Tyler, 1981; Casson et al., 1993a; Casson et al., 1993b; Yoshiyama and Johnson, 1997). However, TMP exhibits abnormality at all temporal frequencies

(Casson et al., 1993b). TMP and CFFP produce similar test-retest reliability in normal individuals but CFFP is slightly better for individuals with open angle glaucoma (Yoshiyama and Johnson, 1997). Both techniques are similar in the identification of abnormality in early glaucoma and in those with OHT who subsequently develop open angle glaucoma (Yoshiyama and Johnson, 1997).

### **1.6.1.3 Luminance Pedestal Flicker perimetry**

Luminance Pedestal Flicker perimetry presents a flickering stimulus on a pedestal of a fixed luminance and determines the temporal frequency necessary to distinguish the stimulus from the pedestal (Anderson and Vingrys, 2000). Currently, this technique is incorporated in the commercially available Medmont M600 perimeter (Medmont, Camberwell, Australia). Nevertheless, the efficacy of LPFP in the detection of open angle glaucoma has not been investigated.

### **1.6.2 Short Wavelength Automated Perimetry (SWAP)**

Short Wavelength Automated Perimetry uses the same projection technique as standard automated perimetry and identical stimulus programs but is modified to use a two-colour increment threshold procedure. SWAP uses a blue narrow band Goldmann stimulus size V which preferentially stimulates the blue or short-wavelength sensitive (SWS) pathway, also known as the S-cone pathway, and a yellow broadband background of 100cdm<sup>-2</sup>. The latter simultaneously suppresses rod activity, whilst leaving the S-cone pathway largely unaffected, and adapts both the green (medium wavelength sensitive, MWS, or M-cone)

pathway and the red, (long wavelength sensitive, LWS, or L-cone) pathway (Wild, 2001; Racette and Sample, 2003; Ferreras et al., 2007). The stimulus duration is 200 msec.

SWS pathway deficits were considered to be more common in individuals with ocular hypertension or with early glaucoma than those obtained with standard automated perimetry (Sample and Weinreb, 1990). In addition, other early studies considered that SWAP could detect glaucomatous visual field loss three to five years earlier than standard automated perimetry (Johnson et al., 1993ab; Sample et al., 1993). Hart et al. in (1990) also recommended that SWAP, rather than standard automated perimetry, should be used for the detection of early open angle glaucoma (Hart et al., 1990).

There are several limitations with SWAP compared to standard automated perimetry. The blue stimulus is affected by absorption as a result of age-related crystalline lens yellowing and is degraded by forward light scattering arising from age-related cataract (Moss, Wild and Whitaker, 1995; Wild et al., 1998; Wild, 2001; San Laureano, 2007) and, as would be expected, the post-operative improvement in the MD following cataract extraction is more pronounced for SWAP (Kim et al., 2001). In addition, SWAP exhibits greater within- and between-examination variability in normal individuals (Kwon et al., 1998; Wild et al., 1998; Hutchings et al., 2001; Blumenthal et al., 2003), in individuals with ocular hypertension and in individuals with open angle glaucoma (Blumenthal et al., 2000a; Hutchings et al., 2001; Blumenthal et al., 2003). It also has a longer examination duration (Wild et al., 1998; Wild, 2001; Soliman et al., 2002; Leeprechanon et al., 2007a; Fogagnolo et al., 2008; Alencar and Medeiros, 2011) and, as a result of processing by the SWS pathway the edge of the stimulus is not sharply bordered and the stimulus is therefore more difficult to detect than that for standard automated perimetry (Alencar and Medeiros, 2011).

A pronounced learning effect is present for SWAP in individuals experienced in standard automated perimetry (Wild et al., 2006) and this will be discussed in detail in Chapter 10. The limited dynamic range of SWAP is insufficiently sensitive to monitor progression in more advanced cases of open angle glaucoma (Alencar and Medeiros, 2011).

Subsequently, several studies found that the sensitivity of SWAP for the early detection of glaucomatous visual field loss was similar to that for standard automated perimetry, regardless of threshold algorithm (Bengtsson and Heijl, 2006; Ng et al., 2009; Tafreshi et al., 2009; Liu et al., 2011b). The sensitivity of the time course for SWAP in detecting those individuals with ocular hypertension who would convert to open angle glaucoma was also found to be similar to standard automated perimetry (van der Schoot et al., 2010). The technique is now seldom used.

### **1.6.3 High-Pass Resolution Perimetry (HPRP)**

High-Pass Resolution Perimetry (HPRP) examines the parvocellular pathway (Frisen, 1987; Frisen, 1993). The stimulus was designed such that both the detection and resolution thresholds were similar and, therefore, proportional to the ganglion cell sampling density (Frisen, 1987). The HPRP stimulus contains high spatial frequencies and is ring-shaped with darker borders ( $15\text{cdm}^{-2}$ ) surrounding a lighter centre ring-shaped ( $25\text{cdm}^{-2}$ ). The average luminance is  $20\text{cdm}^{-2}$ . The detection threshold is estimated using a single-reversal staircase procedure with each stimulus being larger/ smaller than the previous stimulus by a factor of 1.26. The stimulus duration is 165msec.

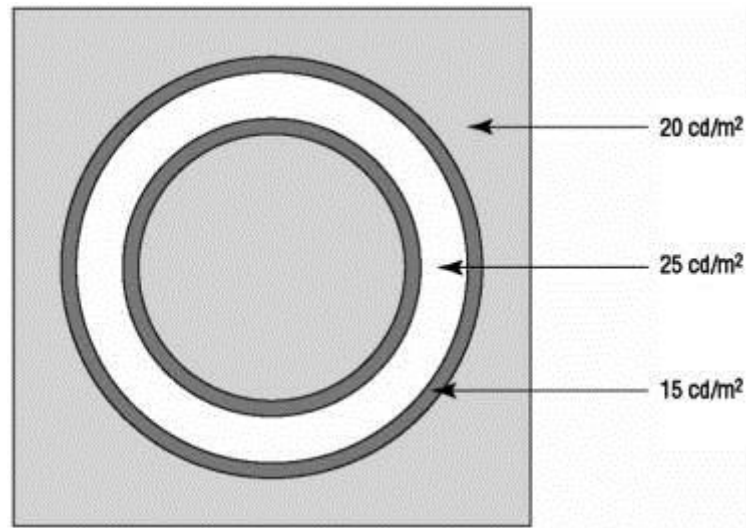


**Figure 1.1 The stimulus for High-Pass Resolution Perimetry.**

The average luminance of the central core ( $25\text{cdm}^{-2}$ ) and of the dark border ( $15\text{cdm}^{-2}$ ) is equal to that of the background ( $20\text{cdm}^{-2}$ ). (Jampel et al., 2011).

HPRP may be diagnostically more sensitive than standard automated perimetry for the early detection of glaucomatous visual field loss (Sample et al., 2006) and it may detect glaucomatous visual field progression earlier than standard automated perimetry (Chauhan et al., 1993a; Martinez, Sample and Weinreb, 1995; Chauhan et al., 1999). However, there have been no recent publications on this topic.

HPRP has also been used in optic neuritis (Wall, 1991).

HPRP is not widely accepted outside of its country of origin, Sweden, (Frisen and Jensen, 2008).

#### **1.6.4 Frequency Doubling Technology (FDT) perimetry**

The concept of Frequency Doubling (FD) was first noted by Kelly (1966) and describes the phenomenon whereby a low spatial frequency sinusoidal grating (<1 cycles per degree) which undergoes high temporal frequency counterphase flicker at 15 Hz, or more, appears to exhibit twice the actual spatial frequency (Kelly, 1981).

The illusion may arise from a spatially non-linear sub-population of retinal ganglion cells, the  $M_y$  cells (Maddess and Henry, 1992; Maddess et al., 1999; Johnson, 2008) which represent approximately 1% of the total number and 10% to 15% (Blakemore and Vital-Durand, 1986) or 15% to 20% (Delgado et al., 2002) of the total number of magnocellular cells. However, there is no evidence of a separate non-linear magnocellular cell system in the primate visual system (White et al., 2002; Quaid, Simpson and Flanagan, 2004) and the principle mechanism for the illusion may be a cortical loss of temporal phase discrimination (White et al., 2002; Zeppieri et al., 2008). However, the ganglion cell type responsible for the processing of the Frequency Doubling illusion, and the extent of the isolation, is unknown. The absence of such knowledge is disconcerting given the popularity of Frequency Doubling Technology (FDT) perimetry in the detection of early glaucoma (Anderson and Johnson, 2002; Ferreras et al., 2007). Interestingly, standard automated perimetry using Goldmann size III is superior to the Frequency Doubling stimulus in preferentially stimulating the magnocellular cells in primate (Swanson et al., 2011).

The initial commercially available version of Frequency Doubling perimetry, the FDT perimeter (Carl Zeiss Meditec, Inc., Dublin, CA), utilized a 0.25 cycles per degree sinusoidal grating embedded within a  $10^\circ$  by  $10^\circ$  square stimulus (Figure 1.1) which

underwent counterphase flicker at 25Hz. The stimulus size at the fovea was a 5° diameter circle. The maximum stimulus eccentricity was 20°. The background luminance was 50cdm<sup>-2</sup> and the stimulus duration 200msec. The threshold, defined as the minimum contrast sensitivity needed to perceive the stimulus, was determined by a modified binary search (MOBS) staircase algorithm.

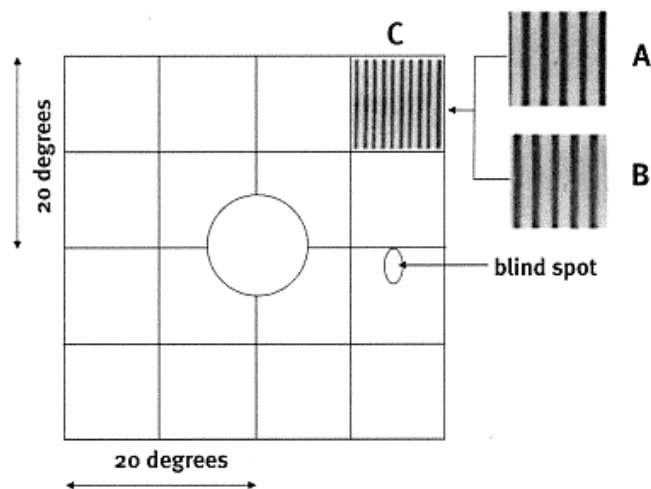


**Figure 1.2** The stimulus for the first generation Frequency Doubling Technology (FDT) perimeter. The 0.5 cycles per degree vertical sine wave grating, counterphased at 25Hz, embedded in a 10° x 10° square stimulus is illustrated at A, B and C. The circular stimulus at the centre has a diameter of 5° (Jampel et al., 2011).

The second commercially available version of FDT, the Humphrey Matrix perimeter, was released in 2005. Three stimulus sizes are used, 10°, 5° and 2° depending upon the program. The 10° square stimulus contains a 0.25 cycles per degree sinusoidal grating which undergoes counterphase flicker at 25Hz and is analogous to that in the original Frequency Doubling Technology perimeter. The 5° and 2° square stimuli contain a 0.5

cycles per degree grating counterphased at 25Hz and 18Hz, respectively. The 5° stimuli are used for the equivalent of Programs 30-2 and 24-2. The threshold is estimated using the Zippy Estimation by Sequential Testing (ZEST) algorithm. ZEST is a Bayesian method and is reliable, fast and accurate in normal and in glaucomatous eyes (Turpin et al., 2003; Anderson et al., 2005). The 2° stimulus is used for the equivalent of Program 10-2 and for the macular threshold program. Flicker sensitivity is estimated with these latter two programs rather than frequency doubling and threshold is determined with the ZEST algorithm. The dynamic range of the Matrix perimeter is compatible to the original FDT perimeter (Anderson et al., 2005).

The clinical implementation of FDT only requires patients to respond to the presence of the stimulus. The task does not depend upon whether the stimulus is perceived as doubled, but simply measures detection thresholds (Anderson and Johnson, 2003a; Ferreras et al., 2007; Johnson, 2008), and this represents the major limitation of FDT.

In the normal eye, sensitivity decreases by approximately 0.7 dB per decade of age across all eccentricities and decreases with increase eccentricity being, typically, 5dB less at the extreme eccentricities (Anderson et al., 2005). Sensitivity in the second eye tested eye is slightly lower than in first eye tested (Anderson et al., 2005) by approximately 5dB (Anderson and McKendrick, 2007) but disappears with translucent patching of the contralateral eye.

As with standard automated perimetry, the Frequency Doubling stimulus is adversely influenced by forward intraocular stray light (Bergin et al., 2011).

FDT is also limited by the learning effect and by the influence of foveal defocus. These issues which are discussed in detail in Chapters 10 and 8, respectively.

Both generations of FDT perimeter, used in suprathreshold and in threshold modes, exhibit acceptable sensitivity and specificity for the detection of glaucomatous field loss compared to standard automated perimetry (Johnson and Samuels, 1997; Quigley, 1998; Alward, 2000; Cello, Nelson-Quigg and Johnson, 2000). The field loss identified by the second generation Matrix perimeter seemingly appears larger and/ or deeper compared to standard automated perimetry (Brusini and Busatto, 1998; Cello et al., 2000; Soliman et al., 2002; Brusini et al., 2006; Ferreras et al., 2007; Leeprechanon et al., 2007b). There is no conclusive evidence to suggest that FDT is able to detect visual field loss prior to standard automated perimetry (Anderson et al., 2005; Burgansky-Eliash et al., 2007; Johnson, 2008). However, an understanding of the depth of glaucomatous field loss as a function of spatial frequency and stimulus size is needed (Harwerth et al., 2010).

The ability of FDT to monitor visual field progression is unknown (Johnson, 2008). Unlike standard automated perimetry, the between-test variability of FDT Matrix perimetry is not influenced by the depth of glaucomatous visual field defect (Artes et al., 2005; Hot, Dul and Swanson, 2008). Such an outcome would favour the use of FDT for the evaluation of progressive field loss particularly in more advanced loss where the variability inherent with standard automated perimetry at a defect depth of approximately 15dB can exceed the dynamic range of the perimeter.

The Matrix provides comparable results to standard automated perimetry in macular disease using Program 10-2 (Anderson, Johnson and Werner, 2011) and in neuroophthalmic disease (Yoon et al., 2012).

The association between structure and function for Frequency Doubling perimetry is comparable with standard automated perimetry particularly in the superior temporal, temporal and inferior-temporal regions (Lamparter et al., 2013).

### **1.6.5 Random-dot kinematograms (RDKs)**

Random-dot kinematograms (RDKs) were considered to be a promising diagnostic tool for the detection of early open angle glaucoma (Bullimore, Wood and Swenson, 1993; Wall and Ketoff, 1995; Bosworth, Sample and Weinreb, 1997). RDKs utilise a stimulus which consists of a series of dots moving at a constant velocity in a given direction against a background of dots moving at a constant velocity in random directions (i.e. visual noise). The numbers of uni-directionally moving dots are increased within the stimulus until the area of these moving dots become visible (i.e. the motion coherence threshold, [MCT]), (Figure 1.3).

Stimuli moving at  $12.5^{\circ}$  per second were found to be more useful for identifying glaucomatous damage compared to stimuli moving at  $4.2^{\circ}$  per second (Trick, Steinman and Amyot, 1995). The stimuli are resistant to the influences of defocus, light scatter and pupil size (Trick et al., 1995; Bosworth et al., 1997).

Later studies found that RDKs identified visual field defects in patients who already showed visual field loss by standard automated perimetry and in a moderate percentage of those with suspected glaucoma and ocular hypertension (Bosworth et al., 1998; Delgado et al., 2002). Nevertheless, the technique has not subsequently been utilised.

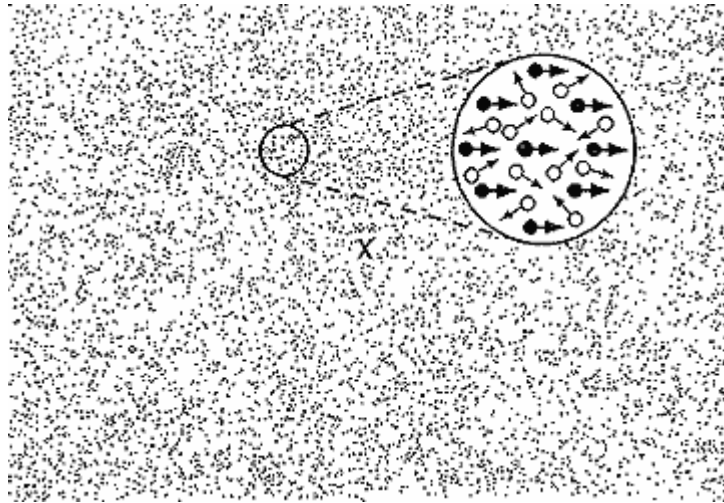


**Figure 1.3 Motion Automated Perimetry.**

The small circle represents the motion stimulus at threshold. The larger circle represents a schematic of the smaller stimulus at threshold: 50% of the dots (illustrated in white) move in random directions and the remaining 50% dots (illustrated in black) all move in a single given direction. The x represents the fixation point (Wall, 2012).

### **1.6.6 Moorfields Motion Displacement test (MDT)**

The Moorfields Motion Displacement test (MMDT; Moorfields Eye Hospital, London, UK) presents a white vertical line stimulus, which is scaled in size to retinal ganglion cell density (Garway-Heath et al., 2000a), on a grey background at a Michelson contrast of 85% at each of 31 stimulus locations arranged according to the Program 24-2 format. Each stimulus presentation comprises three oscillations at 200msec per cycle, i.e., 5Hz (Verdon-Roe et al., 2006; Oleszczuk, Bergin and Sharkawi, 2012). The task is to discriminate the positional change in the line. The threshold is recorded as the minimum detectable displacement. Motion displacement sensitivity is greater than predicted from retinal

ganglion cell spacing and, as such, must be considered as a temporal form of vernier acuity, i.e., a hyperacuity.

The selection of the stimulus locations from the Program 24-2 format is based upon the most recent correlation of the retinal nerve fibre layer at the given stimulus location and the corresponding entry at the optic nerve. The latter model attempts to provide even sampling by disc sector compared to previous iterations (Garway-Heath et al., 2000b).

MMDT is less influenced by intraocular straylight (IOS) compared to standard automated perimetry, FDT perimetry and Flicker Defined Form (FDF) perimetry (Bergin et al., 2011; Oleszczuk et al., 2012).

### **1.6.7 Rarebit Perimetry (RBP)**

Rarebit Perimetry (RBP) purports to detect low to moderate degrees of neural damage within the visual pathway (Frisen, 2002). The name Rarebit Perimetry (RBP) is derived from the use of stimuli which contain a small packet of information (rare bits) to the patient (Chin et al., 2011).

The initial version of Rarebit Perimetry (RBP) consisted of pairs of white high luminance microdots ( $150 \text{ cdm}^{-2}$ ), each half the normal minimum angle of resolution, separated by  $4^\circ$ , and presented for 200msec against a dark background ( $1 \text{ cdm}^{-2}$ ). The test contained 30 stimulus locations within  $30^\circ$  eccentricity: four central stimuli and 26 peripheral stimuli. Each test location comprises a  $5^\circ$  diameter circle, and each circular area is probed five times at random locations within the circle (Frisen, 2002). Each circular area is separated by  $10^\circ$  from centre to centre (Chin et al., 2011; Hackett and Anderson, 2011). The sizes of

the dots increases with increase in eccentricity and were chosen to stimulate a single ganglion cell receptive field, only, at a given eccentricity (Hackett and Anderson, 2011). The observer is required to indicate the number of dots perceived during each presentation. The outcome is the sum of the seen probes divided by the sum of the presented probes and expressed as the Mean or Median Hit Rate (Frisen, 2002).

In normal individuals, the measured sensitivity by RBP declines by 1% per decade of age (Frisen, 2002).

RBP exhibits equivalent sensitivity and specificity to standard automated perimetry in distinguishing between normal and early glaucoma (Martin and Wanger, 2004; Brusini et al., 2005). It is similar/ identical to standard automated perimetry in detecting homonymous hemianopia resulting from occipital lobe infarcts (Gedik, Akman and Akova, 2007) but poorer in detecting visual field loss resulting from idiopathic intracranial hypertension (Celebisoy, Ozturk and Kose, 2010). It is adversely affected by foveal optical defocus (Salvetat et al., 2007) and by cataract (Salvetat et al., 2007; Nilsson et al., 2010).

A learning effect is also present between the first and the second or third examinations (Salvetat et al., 2007).

The current software (version 4.0), divides the examination of the central field into 24 rectangular test areas ranging in size from 6° x 8° centrally to 6° x 14° peripherally (Winther and Frisen, 2010; Chin et al., 2011). The decline in Mean Hit Rate is 4.7% per decade of age in the central field and 6.7% at the fovea (Chin et al., 2011).

### 1.6.8 Pulsar Perimetry (PP)

The Pulsar stimulus comprises an annular stimulus of  $5^\circ$  in diameter and a 100asb ( $31.8\text{cdm}^{-2}$ ) background luminance. The stimulus decreases in contrast from the centre towards the periphery and oscillates at 30Hz below and above the luminance of the background (Figure 1.4). The stimulus duration is 500msec. Threshold is determined by the Tendency Oriented Perimetry (TOP) algorithm. The T30W test examines 66 stimulus locations out to an eccentricity of  $30^\circ$ .

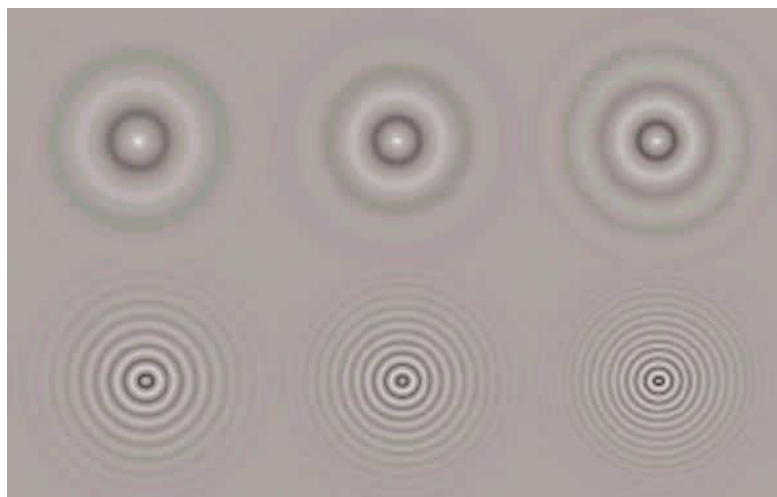


**Figure 1.4** The stimulus for Pulsar Perimetry with different combinations of spatial resolution and contrast (Vidal-Fernandez et al., 2002).

Pulsar perimetry is now incorporated into the Octopus 600 perimeter.

Pulsar perimetry compared to standard automated perimetry, has greater sensitivity in the detection of early visual field loss in patients with OHT (Vidal-Fernandez et al., 2002; Gonzalez-Hernandez et al., 2004; Zeppieri et al., 2010; Gonzalez de la Rosa and Gonzalez-Hernandez, 2013).

The test re-test variability of Pulsar Perimetry is lower compared to both standard automated perimetry and FDT (Salvetat et al., 2013). Nevertheless, it is less affected by age but is significantly influenced by eccentricity and severity of loss (Salvetat et al., 2013).

Pulsar Perimetry is affected by intraocular stray light and defocus as in standard automated perimetry (Gonzalez de la Rosa and Gonzalez-Hernandez, 2013). The main drawback of Pulsar Perimetry is the limited dynamic range which reduces the ability of the technique to determine the full extent of the defect depth.

### **1.6.9 Heidelberg edge perimetry (HEP)**

Flicker defined form perimetry (FDF) utilises an array of randomly positioned black dots against a background of white dots and another array of white dots against a background of black dots. The dots undergo counterphase flicker (i.e., the black dots become white dots and the white dots become black dots). At a temporal frequency of 15Hz, an illusory circular edge contour is perceived against a grey homogenous background (Quaid and Flanagan, 2005a; Goren and Flanagan, 2008) (Figure 1.2). The stimulus patch is  $5^\circ \times 5^\circ$  in diameter and 0.34 cycles per degree and is presented on a background of  $50\text{cdm}^{-2}$  mean luminance. Threshold is determined by the Adaptive Standard Thresholding Algorithm (ASTA) which is based upon an up and down staircase procedure and use likelihood estimates generated from a database of normal values. Seed points in each quadrant are initially measured using a 4-2-2 staircase. The estimated sensitivity is then used as a starting point for the neighbouring locations which are thresholded with a 2-2 staircase (Lamparter et al., 2011). Flicker defined form perimetry is commercially available with the Heidelberg Edge Perimeter (Heidelberg Engineering, Heidelberg, Germany).

The illusion can tolerate decreases in stimulus size (Rogers-Ramachandran and Ramachandran, 1998; Quaid and Flanagan, 2005a).

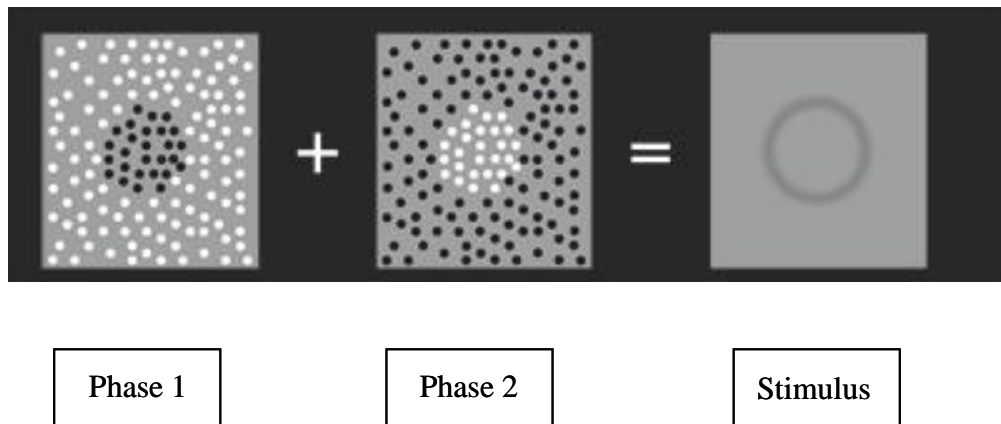


**Figure 1.5** A schematic of the stimulus for Flicker-Defined-Form (FDF) Perimetry.

The perceived low spatial frequency of the illusion is resistant to optical defocus and this increases with increasing eccentricity (Quaid and Flanagan, 2005b). Flicker-Defined-Form perimetry manifests a stronger correlation between structure and function than either FDT or standard automated perimetry (Lamparter et al., 2012). Nevertheless, FDF exhibits a learning effect over three visits (Lamparter et al., 2011).

### **1.7 The structure-function relationship in open angle glaucoma**

It has been realised over the last decade that the temporal disparity in the identification of structural and functional abnormality can be attributed to the difference in the measurement scales of the two outcomes.

The association between the visual field outcome measured in dB and the structural outcome measured in linear units is curvilinear (Garway-Heath et al., 2002). This type of comparison suggests that in early open angle glaucoma, structural loss occurs earlier and/

or appears greater than functional loss, whilst in more advanced disease, it suggests that functional outcomes progress (i.e., worsen) at a greater rate than the structural outcomes. The curvilinear association is a consequence of measuring the visual field outcome in logarithmic units and the structure-function relationship is more linear when the visual field outcome is plotted in linear units (Garway-Heath et al., 2000a).

Consequently, a number of models have been developed for the association between retinal ganglion cell density and the differential light sensitivity (Hood and Kardon, 2007; Drasdo, Mortlock and North, 2008; Gardiner et al., 2008b; Harwerth et al., 2010). The Hood-Kardon model evaluated the curvilinear relationship between the differential light sensitivity in dB and retinal nerve fibre layer thickness in linear units. The models of Drasdo, (2008), Harwerth, (2010) and of Swanson (Swanson, Pan and Lee, 2008; Gardiner et al., 2011; Shafi, Swanson and Dul, 2011) between ganglion cell characteristics and the differential light sensitivity use common scales i.e., both in dBs or both in linear units, and all predict a structure-function slope shallower than unity within the macula and an increase in the slope with increase in retinal eccentricity.

The model of Harwerth is becoming increasingly used in the evaluation of the structure function relationship in open angle glaucoma (Medeiros et al., 2012). The model was developed from histological data in monkey eyes and was validated against human histological data in normal and glaucomatous eyes (Harwerth and Quigley, 2006; Harwerth et al., 2007).

## **1.8 Retinal ganglion cell dysfunction**

There are several theories for retinal ganglion cell death in glaucoma. The main theories are the mechanical theory and the vascular theory.

The mechanical theory involves ganglion cell apoptosis as a result of an elevated intraocular pressure; however, it is not known whether the raised pressure affects the cell body or the axon, or both (Farkas and Grosskreutz, 2001; Kuehn, Fingert and Kwon, 2005; Agarwal et al., 2009). Apoptosis is the programmed cell death pathway designed to remove damaged cells through phagocytosis (Kuehn et al., 2005; Agarwal et al., 2009) and it occurs in the absence of inflammation (Agarwal et al., 2009).

The vascular theory involves a reduced blood supply that may be induced by an elevated intraocular pressure or by reduced ocular blood flow (Flammer, 1994). The disrupted autoregulation leads to ischaemia and inflammation and, in turn, a cascade resulting in pro-apoptotic factors triggering retinal ganglion cell death (Vohra, Tsai and Kolko, 2013).

The loss of retinal ganglion cells is also associated with a loss of neural tissue within the lateral geniculate nucleus and to a lesser extent in the visual cortex (Calkins and Horner, 2012).

It would appear that morphological changes occur in the dendrites of the retinal ganglion cells before the cells become apoptotic (Liu et al., 2011a; Werkmeister et al., 2013; Williams et al., 2013). The dendrites undergo highly dynamic rearrangement during dendritogenesis, both in the addition of dendritic arborization and a loss of existing

dendritic branches (Liu et al., 2011a). Several primate studies have shown that changes in the dendrites, including a thinning, a reduction in the dendritic process diameter at branching points, and alterations to the dendritic tree, precede the loss of neurons in the lateral geniculate nucleus (Weber, Kaufman and Hubbard, 1998; Gupta et al., 2007; Werkmeister et al., 2013). The inner plexiform layer consists of many dendrites and high resolution imaging of this layer has the potential to demonstrate early glaucomatous damage (Liu et al., 2011a).

The residual ganglion cell count predicted from the visual field by the model of Harwerth is frequently greater than that predicted from optical coherence tomography (Harwerth et al., 2007), i.e., the ‘measured structure’ may not be representative of the functioning ganglion cell or axonal number. This finding can be explained by the concept of retinal ganglion cell dysfunction prior to cell death, and is consistent with shrinkage of the axon size and of the dendritic tree (Sun et al., 2008).

Clearly, there is a need for new methods of functional assessment for the early detection of open angle glaucoma. It has been speculated that Dynamic Noise perimetry may provide a psychophysical method for identifying ganglion cell dysfunction.

## **Chapter 2**

### **Dynamic Noise Perimetry**

#### **2.1 Background**

Dynamic Noise Perimetry (DNP) is a new psychophysical test, which has been developed within the Cardiff School of Optometry and Vision Science, Cardiff University, with the aim of detecting ocular disease, particularly open angle glaucoma, at an earlier stage compared to standard automated perimetry.

Dynamic Noise Perimetry is based upon the presence of two types of noise that affect visual performance: internal noise, also known as neural noise, and external noise. The latter relates to the quantal nature of light.

##### **2.1.1 Internal noise**

Internal noise is considered to be the random and spontaneous variation in the inherent neuronal activity which occurs, in the absence of stimulation, in all types of cells from the retina to the cortex (Falkenberg and Bex, 2007). It can be speculated that some forms of ocular disease will result in increased levels of internal noise during the early stages of the disease process. In the case of open angle glaucoma, the retinal ganglion cells undergo shrinkage prior to cell death (Morgan, 2002; Williams et al., 2013) (Section 1.8) and it is hypothesised that this shrinkage will increase the level of internal noise. The magnitude of internal noise can be evaluated, in relative terms, by measuring the difference in the

threshold to a given stimulus in the presence and absence of a given quantity of external noise, usually expressed in terms of the spectral density, and referenced to the given quantity. This difference between the two thresholds is known as the Equivalent noise and the derivation as the equivalent noise input technique (Pelli and Farell, 1999; Pardhan, 2004; McAnany and Alexander, 2009).

### 2.1.2 External noise

External noise can vary both spatially and temporally. There are two types of noise pattern and the type to be used depends upon the stimulus. The first type, when the stimulus comprises a sine wave grating, is an additional sine wave grating that varies from the stimulus in spatial and/ or temporal terms. The second, and more common, type of noise mask is a pixelated pattern that randomly varies, spatially and/ or temporally, in terms of luminance. When the luminance of each pixel, or check, fluctuates both spatially and temporally, the noise mask is known as a spatiotemporal or, more commonly, a dynamic noise mask. A stationary pixelated noise mask is illustrated in Figure 2.1.

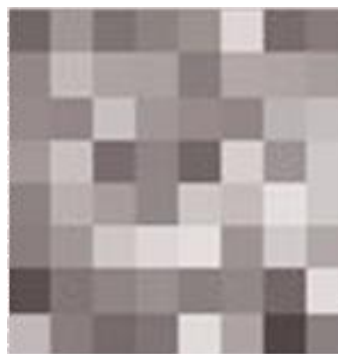


**Figure 2.1** An example of a static two-dimensional noise mask. The pixels vary randomly in luminance across the image and each pixel, or check, is of an equivalent given size.

The parameters of the external noise mask may be quantified in terms of contrast and check size; and, if the mask is dynamic, in terms of check duration. The contrast of an external noise mask is not dependent upon the maximum and minimum luminance values, as is the case with a sine-wave grating. Thus, the contrast is not expressed in terms of Michelson units as such an expression does not account for the distribution of luminance over space. When all of the luminance values within a noise mask are distributed randomly around a mean, it is referred to as a Gaussian noise mask, and it is the spread of the values within the stimulus that provides the best estimate of the contrast (Kukkonen et al., 1993; Hayes and Merigan, 2007; McAnany and Alexander, 2009). The contrast is, therefore, specified in terms of the root mean square (RMS) contrast; the squares of each local contrast over the area of the mask are summed and then averaged, thereby accounting for the relative size of the mask, and are expressed in terms of the square-root of the average (Kukkonen, 1994).

The RMS contrast of the noise mask is limited by the capabilities of the monitor and of the graphics card and when the noise checks are superimposed upon a high contrast grating.

The strength of an external noise mask is referred to as the noise spectral density. The masking power of white pixel noise is best described when the spectral density is calculated by taking into account all dimensions of the noise pixels, i.e., the width, height, and duration, even when there is random luminance in only one of these dimensions.

The spectral density of dynamic noise,  $N_e$ , is defined as:

$$N_e = A * N_{rms}^2 * t_{check} \quad 2.1$$

where  $A$  is the area of each noise check,  $N_{rms}^2$  is the root mean square contrast of the noise mask and  $t_{check}$  is the duration of the noise mask.

An increase in any one of these parameters will increase the noise spectral density, i.e., the strength of the noise mask (Kukkonen et al., 2002).

The ratio of the stimulus energy at threshold to the noise spectral density is constant in the normal eye and is defined as the signal to noise ratio (SNR) (Pelli, 1990). Therefore, when a stimulus is embedded in an external noise mask, the energy at threshold increases in direct proportion to the noise spectral density (Pardhan, 2004; McAnany and Alexander, 2009). A constant SNR is a requirement for estimating equivalent noise and sampling efficiency. When the SNR is constant, the external noise image is considered ‘white’. Although the contrast of the noise mask can be increased, the extent of the increment is limited by the dynamic range of the monitor, especially when assessing the contrast thresholds of individuals with ocular disease. When the critical spatial and temporal parameters of a dynamic noise mask are exceeded, the signal will become increasingly visible, causing the SNR to fall (Rattan, 2010).

The Sampling Efficiency (SE) is a measure of an observer's ability to interpret accurately the available signal information (Legge, Kersten and Burgess, 1987; Pelli and Farell, 1999; Hayes and Merigan, 2007). Sampling efficiency indicates how a 'real-life' observer detects a stimulus compared to the hypothetical 'ideal' observer. In addition to internal noise, detection performance is limited by sub-optimal sampling efficiency (Hayes and Merigan, 2007; McAnany and Alexander, 2009). Sub-optimal sampling efficiency is attributed to differences between stimulus and receptive field properties i.e., incomplete spatial or temporal summation or non-optimal decision strategies (Legge et al., 1987; Hayes and Merigan, 2007). By definition, an 'ideal' observer is able to interpret precisely stimulus information and to achieve optimal sampling efficiency (Abbey and Eckstein, 2006). It follows that both internal noise and sampling efficiency define the limits of visual sensitivity.

The use of external noise paradigms is becoming increasingly topical to determine the limitation (i.e., the Sampling Efficiency (SE) and internal noise) in the ability to either detect a moving or a flickering grating and/ or discriminate the direction of motion of the grating (Falkenberg, Simpson and Dutton, 2014). In several investigations, the use of the Equivalent Noise (EN) model shows that motion sensitivity is limited by both internal noise and reduced sampling efficiency (Legge et al., 1987; Kersten, Hess and Plant, 1988; Pardhan et al., 1996; Pardhan, 2004; Falkenberg and Bex, 2007; Falkenberg et al., 2014).

### **2.1.3 The current DNP**

#### **2.1.3.1 Stimulus parameters**

DNP evaluates the ability to determine the direction of motion of a sine wave grating of a given spatial frequency at any given temporal frequency at any given location in the visual field. The minimum contrast, measured as a Michelson contrast, necessary to detect the direction of drift is determined.

Currently, the stimulus consists of a  $4^\circ \times 4^\circ$  square stimulus containing a 0.5 cycle per degree vertical sine wave grating drifting horizontally, either to the right or to the left, at a temporal frequency of 10Hz (Figure 2.2).



**Figure 2.2** The stimulus for the Dynamic Noise Perimeter: a  $4^\circ$  by  $4^\circ$  square patch containing a 0.5 cycle per degree vertical sine wave grating drifting horizontally, either to the right or to the left, at a temporal frequency of 16 Hz.

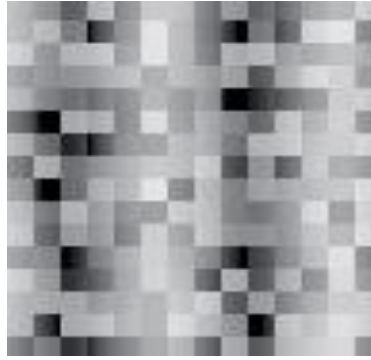


**Figure 2.3** The external noise mask of the Dynamic Noise Perimeter superimposed upon the grating illustrated in Figure 2.2. The grating is visible which indicates that the grating contrast is above threshold. Not to scale.

Each check within the noise mask has a side length of  $0.5^\circ$ . The duration is 30 frames per second which matches the frame rate of the software. The RMS contrast of the noise mask is 0.2 (Figure 2.3).

Given the check side length of  $0.5^\circ$  and the check duration of  $1/30$  seconds, the noise spectral density,  $N_e$ , calculated from Equation 2.1 is  $3.33 \cdot 10^{-4}$ .

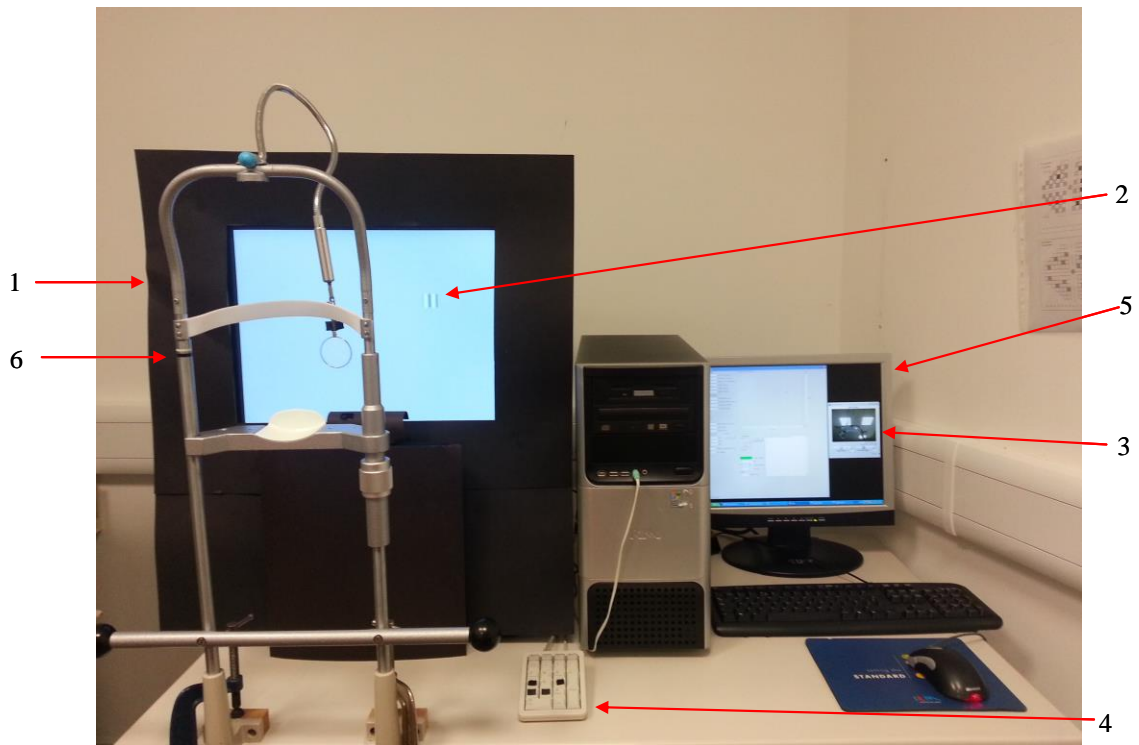


**Figure 2.4** The prototype Dynamic Noise Perimeter. 1, the monitor displaying the stimulus. 2, the stimulus without the noise mask. 3, fixation monitoring. 4, the keyboard for recording a response. 5, the monitor displaying the operating menus. 6, the adjustable chin and forehead rests.

### 2.1.3.2 Examination procedure

The examination is undertaken separately in the presence and in the absence of the noise mask.

The observer fixates a small central spot on the high resolution monitor. The distance between the observer and the monitor is 30cm which is ensured by the use of the adjustable forehead and chin rests. Fixation is monitored by observation of the video image of the observer's eye. If eye movements are made toward an eccentric target, the results for the given trial are discarded.

The threshold contrast for the drifting grating in the absence of the external noise is determined by a two alternative forced-choice procedure. The two stimulus presentations can be separated by any given interval but are currently separated by 500msec. The observer designates the presentation that contained the grating by pressing the appropriate keys on a conventional keyboard. The onset of each stimulus is preceded by an audible signal. A correct response is followed by a different audible signal and an incorrect response by a further different audible signal, both to acknowledge the response and to alert the observer that the next pair of gratings is about to be shown. The onset of a new pair of stimuli commences 200msec after the last response.

The 'Proof of Concept' threshold algorithm is a staircase algorithm comprising 8 reversals. The start level is at least 4dB above the threshold and was selected in order to ensure that the grating is clearly visible at the start of the examination. Subsequent correct answers each reduce the contrast of the 'next' grating by 1dB. The first incorrect response is ignored. A second incorrect response increases the contrast of the 'next' grating by 1dB. This second incorrect response is considered to be the first reversal (a reversal describes a change in the direction of the staircase, i.e., an upward change in direction is associated with an increase in contrast and a downward change in direction with a reduction in contrast). The 'true' start level is taken to be the contrast at the third reversal (the first two reversals are ignored as the responses can result from an unfamiliarity in the requirements of the task).

As described above, throughout the starting phase of the staircase (i.e., upto the third reversal), a single correct answer reduces the level of contrast of the grating by 1dB. This modification was made to enable a sequence to reach, rapidly, the threshold level

(Cornsweet, 1962). The first incorrect response of the subsequent ‘secondary phase’ is ignored and does not change the contrast. A sequence of four correct responses is required to reduce the grating contrast level by 1dB, and one incorrect response to increase the grating contrast level by 1dB (i.e., the second reversal of the ‘secondary phase’). Each subsequent reversal corresponds to a directional change in the staircase (i.e. from a descending to an ascending trend and vice versa). The final threshold is defined as the geometric mean of the last six reversals.

#### **2.1.4 Output**

The output from DNP comprises the minimum Michelson contrast thresholds to identify correctly the grating in the absence of the noise mask ( $MCN_a$ ) and in the presence of noise mask ( $MCN_p$ ). These values enable the calculation of several additional measures, namely, the Signal Energy, the Sampling Efficiency (SE) and the Equivalent Noise ( $N_{eq}$ ).

##### **2.1.4.1 Signal Energy ( $E_{th}$ )**

The  $MCN_a$  and the  $MCN_p$  can each be transformed into signal energy ( $E_{th}$ ), using Equation 2.2. Signal energy is a comprehensive measure of the stimulus at threshold with or without the noise mask, as appropriate, based on size, RMS contrast, spatial frequency, temporal frequency and the duration of presentation.

$$\text{Signal energy, } E_{th} = (C_{rms})^2 * L^2 * T \quad 2.2$$

where  $C_{rms}$  is the RMS contrast of the stimulus at threshold either in the absence or in the presence of the noise mask, as appropriate,  $L$  is the side length of the square stimulus in degrees and  $T$  is the stimulus duration in seconds.

Given that either  $C_{rms} = (MCN_a / \sqrt{2})^2$  or  $C_{rms} = (MCN_p / \sqrt{2})^2$ , as appropriate, and that the side length is  $4^\circ$ , and the stimulus duration is 500msec, Equation 2.2 can be simplified as follows:

$$\begin{aligned}
 \text{The signal energy without the noise mask, } E_{th}N_a &= (MCN_a / \sqrt{2})^2 * 4^2 * 0.5 \\
 &= (MCN_a^2 / 2) * 16 * 0.5 \\
 &= 4 * MCN_a^2 \qquad \qquad \qquad 2.3
 \end{aligned}$$

$$\begin{aligned}
 \text{and the signal energy with the noise mask, } E_{th}N_a &= (MCN_p / \sqrt{2})^2 * 4^2 * 0.5 \\
 &= (MCN_p^2 / 2) * 16 * 0.5 \\
 &= 4 * MCN_p^2
 \end{aligned}$$

#### **2.1.4.2 Sampling Efficiency (SE)**

The SE is derived from the signal energies in the absence of noise,  $E_{th} N_a$ , and in the presence of noise,  $E_{th} N_p$ , and the noise spectral density  $N_e$  ( $3.33 * 10^{-4}$ ):

$$SE = d * N_e / (E_{th} N_e - E_{th} N_0) \quad 2.4$$

where d is 2, based upon the threshold algorithm described above.

#### 2.1.4.3 Calculation of equivalent noise ( $N_{eq}$ )

Similarly, the equivalent noise ( $N_{eq}$ ) can be calculated:

$$N_{eq} = E_{th} N_a * [N_e / (E_{th} N_p - E_{th} N_a)] \quad 2.5$$

#### 2.1.4.4 Further outputs from DNP

To improve the detection capabilities two additional derivatives are used.

Firstly, the ratio of the  $\text{Log}_{10}$  of MC  $N_p$  and the  $\text{Log}_{10}$  of MC  $N_a$ , termed either the  $\text{Log}_{10}$

MC Ratio or the  $\text{Log}_{10}$  Ratio:

$$\text{Log}_{10} \text{ Ratio} = \text{Log}_{10} \text{ MC } N_p / \text{Log}_{10} \text{ MC } N_a \quad 2.6$$

Secondly, the ratio of SE to  $N_{eq}$ , termed the Signal Detection Index (SDI):

$$SDI = SE / N_{eq} \quad 2.7$$

Given that Michelson contrast sensitivity is measured in the absence of a noise mask ( $N_a$ ) and in the presence of a noise mask ( $N_p$ ), two separate signal energy values are derived with DNP.

## **Chapter 3**

### **Rational for, and description of, the research**

#### **3.1 Introduction**

The work described in this thesis continues the development of Dynamic Noise Perimetry (DNP). It has been conjectured/ speculated that one or more of the derivatives of DNP may provide an indication of ganglion cell shrinkage in open angle glaucoma.

The initial work on DNP was undertaken by Dr Rishi Rattan and is described in his Thesis which was awarded the degree of PhD by Cardiff University (Rattan, 2010). The concept of DNP was reviewed in Chapter 2. DNP has been, or is, covered by patents in 14 different countries.

The current thesis describes five aspects of the continued development of DNP.

Prior to commencement of the experimental work, it was necessary to calibrate the high resolution Cathode Ray Tube (CRT) monitor of the DNP. Such a procedure is a relatively complex and time consuming procedure and is described in Chapter 4.

As was described in Chapter 2, the initial DNP stimulus comprised a  $4^\circ \times 4^\circ$  square stimulus containing a sine wave grating with a spatial frequency of 0.5 cycles per degree counterphased at 10Hz and presented on an homogenous grey background of  $50\text{cdm}^{-2}$ . It was uncertain as to whether the change in luminance profile between the stimulus and the background, i.e. the ‘sharp edge’ of the stimulus border, might contribute to the response outcome. The first experimental chapter (Chapter 5) describes an investigation to determine the role of the stimulus border.

It was also necessary to confirm the initial findings concerning the strength of the noise mask as a function of stimulus eccentricity, particularly with reference to the fovea. The investigation of the optimal strength for the noise mask is described in the second experimental chapter (Chapter 6).

The strength of the initial noise mask, 4 checks per grating cycle, was confirmed. Each pixel within the noise mask had a side length of  $0.5^\circ$  at the viewing distance of 30cm. Thus, it could be anticipated that the noise mask might be prone to the effects of optical defocus. The third experimental chapter (Chapter 8) describes the study investigating the effects of defocus on the outcome of DNP.

These three studies were undertaken using the ‘Proof of Concept’ threshold algorithm developed by Dr Rattan. As was described in Chapter 2, the ‘Proof of Concept’ algorithm enabled an estimate of threshold at a single stimulus location in approximately 3 minutes. Clearly, such a time was not clinically viable. Consequently, developmental work on a revised algorithm, which would enable threshold to be determined, without loss of

accuracy, at an increased number of stimulus locations over a shorter examination duration was undertaken in parallel to the three studies. This work is described in Chapter 7

The learning effect for perimetry, whereby the differential light sensitivity improves over the examination with- and between-eyes at the first visit and then between visits up to the second, third or, even the fourth, visit is well documented. The fifth topic for study (Chapter 10) concerned the documentation of the characteristics of the learning effect for DNP and utilised a threshold algorithm which had been developed from the 'Proof of Concept' algorithm.

Finally, the sixth topic of study (described in Chapter 9) comprised the follow-up of the individuals with open angle glaucoma examined by Dr Rattan to determine any progression (i.e. worsening) of sensitivity derived by DNP. By necessity, the follow-up examination utilised the 'Proof of Concept' threshold algorithm.

### **3.1.1 The influence of Gaussian filtering on the outcome of Dynamic Noise Perimetry (Chapter 5)**

The first experimental study determined the influence of 4 different levels of Gaussian filter (0.00, 0.25, 0.50 and 1.00 FWHM) on the outcome of DNP at three stimulus locations ( $0^\circ$ ;  $0^\circ$ ;  $-14^\circ$ ;  $-8^\circ$ ; and  $-22^\circ$ ,  $4^\circ$ ) in the absence and in the presence of the 4 checks per grating cycle noise mask. The cohort comprised 15 normal individuals and each individual was required to attend for four visits each lasting approximately 15 minutes.

### **3.1.2 The influence of the strength of the noise mask on the outcome of Dynamic Noise Perimetry (Chapter 6)**

The second experimental study determined the influence of varying strengths of noise mask (1, 2, 3, 4, 5, 8, 12 and 20 checks/ grating cycle) on the outcome of DNP at three stimulus locations ( $0^\circ$ ,  $0^\circ$ ;  $-14^\circ$ ,  $4^\circ$ ; and  $-22^\circ$ ,  $4^\circ$ ). The cohort comprised 11 normal individuals and each individual was required to attend for two visits each lasting approximately 45 minutes.

### **3.1.3 Further development of the threshold estimation algorithm for Dynamic Noise Perimetry (Chapter 7)**

The development of a modified algorithm evolved from the 'Proof of Concept' algorithm over several iterations.

The first iteration concentrated on reducing the number of reversals from 8 to 4 and altered the criteria for a reversal from either four correct responses to two correct responses or two incorrect responses to one incorrect response. In addition, alterations were made to the step sizes associated with each reversal. This approach enabled the estimation of threshold at 8 locations in approximately 8 minutes and 12 locations in approximately 12 minutes.

The first iteration formed the basis for the second iteration. The latter consisted of two phases. The first phase estimated the threshold at 4 locations, one in each quadrant, using three reversals. The start value at each location was 2dB above the age-corrected normal

value derived from 7 individuals. These locations were termed ‘seed point’ locations. The start value at each location in the second phase was 2dB above the threshold of the respective seed point. The second iteration enabled the estimation of threshold at 45 locations in approximately 7 minutes and, with the noise mask, in approximately 9 minutes.

The development of the modified algorithms involved numerous examinations undertaken on the 7 individuals.

#### **3.1.4 The influence of optical defocus on Dynamic Noise Perimetry (Chapter 8)**

The influence of optical defocus on the outcome of DNP was investigated using four different levels of optical defocus (plano, +1.00DS, +2.00DS and +4.00DS) at each of the three stimulus locations ( $0^\circ, 0^\circ$ ;  $-14^\circ, -8^\circ$ ; and  $-22^\circ, +4^\circ$ ). The interaction between defocus and Gaussian filtering (0.50 FWHM) of the stimulus edges was also investigated. The cohort comprised 11 normal individuals and each individual was required to attend for 4 to 8 visits each lasting approximately 40 minutes. Five additional individuals failed to attend for the required number of visits. The data from these 5 individuals was excluded from the data analysis.

### **3.1.5 The follow-up of individuals with open angle glaucoma (Chapter 9)**

Ten individuals with open angle glaucoma had undergone DNP in 2007 at 5 different stimulus locations ( $0^\circ, 0^\circ$ ;  $10^\circ, 8^\circ$ ;  $-10^\circ, 8^\circ$ ;  $10^\circ, -8^\circ$ ; and  $-10^\circ, -8^\circ$ ) as part of the studies undertaken by Dr Rattan, the results of which are described in his thesis (Rattan, 2010). Five of the 10 individuals agreed to undergo a follow-up examination. Each individual attended for 3 visits and underwent an identical investigative protocol to that of the visits in 2007. Each visit lasted approximately 45 minutes.

### **3.1.6 The learning effect in Dynamic Noise Perimetry (Chapter 10)**

The study used the standard examination protocol for investigating the perimetric learning effect, namely five sessions of DNP each separated by an interval of one week. The threshold estimation algorithm had been developed from the 'Proof of Concept' algorithm and the stimulus program comprised 12 locations. The cohort comprised 10 'young' normal individuals and 8 'elderly' normal individuals. Each session lasted approximately 15 minutes.

## **3.2 Logistics**

### **3.2.1 Background**

The author is an optometrist, registered since 2006, with the Commission for Health Specialties in Saudi Arabia. In October 2007, the author enrolled for a research degree at the Cardiff School of Optometry and Vision Sciences. The period of study was sponsored by the Saudi Arabian Ministry of Higher Education. The research was conducted under the academic supervision of Professor John Wild.

At the end of the first year of research, the author was required to submit a First Year Continuation Report and to undergo a *vive voce* examination of the Report. Following her successful *vive voce* examination, the author continued her research for the degree of PhD from Cardiff University.

### **3.2.2 Methods**

The research was undertaken at the Cardiff School of Optometry and Vision Sciences.

The author initially underwent a training period with Dr. Rattan in the techniques required to calibrate the high resolution CRT monitor. The calibration procedure, described in detail in Chapter 4, was time consuming and took approximately 20 hours per calibration.

The six studies were each approved by the Ethics in Research Committee of the Cardiff School of Optometry and Vision Sciences and followed the tenets of the Declaration of Helsinki.

The normal individuals were recruited from undergraduate and postgraduate students attending, and from the staff of, Cardiff University. The individuals with open angle glaucoma had been recruited from those attending the Cardiff University Eye Clinic. All individuals had received the appropriate written instructions and had signed the respective consent form prior to inclusion in the given study.

The normal individuals were classified as normal on the basis of the ophthalmic examination undertaken by the author, under the supervision of Professor Wild. The ophthalmic examination of the individuals taking part in the study of the learning effect (Chapter 10) and of those with open angle glaucoma (Chapter 9) was undertaken by a research fellow and registered optometrist, Caroline Djalllis, PhD.

The author planned and coordinated the visits of the individuals recruited into the six studies. In total, 49 individuals provided 272 DNP visual fields. The author undertook all

the visual field examinations. The time spent conducting the DNP examinations was approximately 102 hours.

The development of the threshold algorithm was undertaken in collaboration with a mathematician, Frank Rakebrandt, PhD, a software engineer, Gavin Powell, PhD. The author undertook the iterative development of the threshold algorithm and carried out all the DNP examinations.

The Analyses of Variance described in Chapters 5, 6, 8 and 10 were undertaken by David Shaw, MSc, Senior Medical Statistician.

A number of minor difficulties were encountered during the research. The high resolution CRT monitor ceased to work during the first experiment (the influence of the Gaussian filter). The time taken to source a company capable of effecting the repair and for the repair, itself, was three months. Fortunately, a further two high resolution CRT monitors were secured; however, each of these additional monitors required calibration.

Despite the above difficulties, the time spent in further developing DNP was an enjoyable experience both at the scientific, and at the personal, level.

## **Chapter 4**

### **Calibration of the Dynamic Noise Perimetry high resolution**

#### **Cathode Ray Tube monitor**

##### **4.1 Introduction**

Dynamic Noise Perimetry (DNP) utilises a high resolution Cathode Ray Tube (CRT) monitor. High resolution monitors are essential for visual psychophysical research because the output is commonly stable to within approximately 1% and they are suitable for measuring small colour differences (Olds, Cowan and Jolicoeur, 1999).

A CRT monitor must be calibrated to account for the non-linear relationship between the voltage generated by each electron gun and the measured luminance output to the graphics card (Olds et al., 1999). The voltage generated by the CRT is measured in terms of the screen luminance. The relationship between the voltage and the screen luminance is known as a gamma function and this function can be used to calibrate the output of the display (Colombo and Derrington, 2001). The calibration is based upon the relationship between the values in the 'Colour Look Up Table' (CLUT) and the measured output (Brainard, 1989). The CLUT determines the maximum number of colours which can appear on the

screen simultaneously, e.g., 256 colours with a colour depth of 8 bit per pixel. The number of bits per pixel is used to describe the colour of a pixel and the bit depth is used to define the shade of each pixel. A one bit image represents black and white and an 8 bit image is a grey scale that provides 256 levels of grey.

## **4.2 Calibration of the DNP display**

### **4.2.1 Introduction**

The high resolution CRT monitor used in this thesis for DNP was a Mitsubishi Diamond Pro 2045u (Mitsubishi Electric, Kobe, Japan). The maximum resolution was 2048 \* 1536 pixels at a frame rate of 80Hz. The graphics board was a Video Graphics Array (VGA) (Texas Instruments Graphics Architecture (TIGA)) (Dallas, TX) driven by a Research Machines personal computer (Abingdon, Oxfordshire, UK). The graphics board produced an achromatic signal of 256 levels of grey corresponding to 8 bits per pixel. A frame rate of 80Hz was chosen to eliminate any perception of flicker during the presentation of the stimuli. The pixel size was 0.49mm \* 0.49mm, and the average luminance was 50cdm<sup>-2</sup>.

Before any formal study of DNP could be undertaken, it was necessary to undertake visual calibration of the Mitsubishi Diamond Pro 2045u monitor. The calibration was based upon the techniques of Olds et al., (1999), Colombo and Derrington (2001) and Rattan (2010) (Olds et al., 1999; Colombo and Derrington, 2001; Rattan, 2010).

## **4.2.2 Procedure**

### **4.2.2.1 Step one: Red, Green and Blue (RGB) colour gun luminance calibration**

The luminance response of the Mitsubishi Diamond Pro 2045u was separately measured for each of the three individual colour guns, using a Minolta Chroma Meter CS-100 photometer, at 100% contrast and at a screen luminance of 60% of the maximum. These values had been determined previously by Dr Rattan as optimal for achieving a wide range of linearity (Rattan, 2010). The photometer was placed on a tripod perpendicular to the screen at a distance of one metre. The focusing ring in the photometer was then adjusted to one metre. The photometer was set to measure in the 'slow' mode in order to be able to average the transient fluctuations at the level of the drive voltage. The graphics card was instructed, via software developed previously within the School by Dr Jarmo Hallikainen, to generate, separately, the given input luminance at the geometric centre of the screen for each colour gun over a range from 0 to 255 divisions (i.e., steps) of the 60% of the maximum value in successive ascending intervals of 15.

The software presented the output luminance of each individual colour gun as a discreet value. The x and y colour co-ordinates (CIE, 1932) of each colour gun at each output luminance were simultaneously recorded to ensure that the colours remained stable over the range of specified luminance values. All measurements were undertaken, in a dark room, following a 30 minutes warm-up of the monitor. The warm-up period enable stabilisation of the monitor and, therefore, a more accurate calibration.

The procedure was repeated for each of the three guns in sequence on four separate occasions. The time for collection of the output data from the five sets of measurements for each of the three guns was between approximately 4 and 5 hours.

An example of the data for one set of measurements from the most recent calibration of the monitor is illustrated in Table 4.1. The subsequent data displayed in this Chapter are from this most recent calibration.

Index steps	Red			Green			Blue		
	$L_R$	x	y	$L_G$	x	y	$L_B$	x	y
0	0.01	0.307	0.31	0.98	0.304	0.316	0.98	0.31	0.314
15	1.29	0.369	0.324	1.77	0.303	0.402	1.08	0.242	0.228
30	1.71	0.43	0.326	3.02	0.298	0.468	1.5	0.187	0.134
45	2.29	0.481	0.331	4.77	0.295	0.505	1.48	0.187	0.134
60	3.05	0.516	0.335	7.05	0.294	0.53	1.81	0.172	0.114
75	4.01	0.541	0.335	9.96	0.292	0.548	2.24	0.164	0.101
90	5.16	0.561	0.337	13.4	0.291	0.559	2.74	0.159	0.092
105	6.55	0.573	0.337	17.6	0.29	0.566	3.34	0.155	0.087
120	8.16	0.584	0.338	22.4	0.289	0.573	4.05	0.151	0.082
135	10.0	0.591	0.339	28.0	0.288	0.576	4.82	0.150	0.080
150	12.1	0.597	0.34	34.3	0.287	0.58	5.76	0.148	0.077
165	14.5	0.601	0.341	41.2	0.286	0.582	6.71	0.147	0.076
180	17.2	0.604	0.341	48.9	0.286	0.584	7.81	0.147	0.074
195	20.2	0.606	0.341	57.9	0.285	0.585	9.03	0.146	0.073
210	23.2	0.609	0.341	67.2	0.285	0.586	10.3	0.146	0.073
225	26.5	0.611	0.342	76.8	0.284	0.587	11.6	0.145	0.072
240	30.0	0.613	0.342	87.1	0.284	0.587	13.0	0.145	0.071
255	33.7	0.614	0.342	97.6	0.283	0.588	14.5	0.145	0.071

**Table 4.1** The output luminances of the red,  $L_R$ , green,  $L_G$ , and blue,  $L_B$ , colour guns, and the corresponding CIE 1932 co-ordinates, for the given input luminances, specified in index steps, for the first of the five sets of measurements.

The median output luminances of the red,  $L_R$ , green,  $L_G$ , and blue,  $L_B$ , colour guns, and the median of the corresponding CIE 1932 co-ordinates, for the given input luminances specified in index steps, derived from the five sets of measurements are given in Table 4.2.

Index steps	Red $L_m$	Green $L_m$	Blue $L_m$
0	0.94	0.94	0.95
15	1.23	1.73	1.05
30	1.64	2.97	1.23
45	2.22	4.71	1.48
60	2.99	7.01	1.81
75	3.95	9.92	2.24
90	5.09	13.40	2.74
105	6.50	17.60	3.34
120	8.10	22.40	4.04
135	10.00	28.00	4.84
150	12.10	34.30	5.74
165	14.50	41.30	6.75
180	17.20	48.90	7.85
195	20.20	57.70	9.09
210	23.20	66.90	10.40
225	26.50	76.60	11.70
240	30.00	86.70	13.20
255	33.80	97.40	14.60

**Table 4.2** The median output luminances of the red,  $L_R$ , blue,  $L_B$ , and green,  $L_G$ , colour guns and the median of the corresponding CIE 1932 co-ordinates derived from the five sets of measurements.

The characteristics of each colour gun, described by the intercept and the gradient (also known as the gamma value) of the linear function between the  $\log_{10}$  input and the  $\log_{10}$  output luminances, are shown in Figure 4.1.

The gamma value, i.e., the intercept of the linear function and the maximal luminance, of each colour gun was then entered into the stimulus generating software of Dr Hallikainen. The gamma correction was applied to both the generated/requested stimulus and the background in order to equate the requested output from the graphics card and the luminance displayed on the CRT screen.

A 3<sup>rd</sup> order polynomial, constructed from the data set, was used to correct the output of the graphics card over the non-linear range.

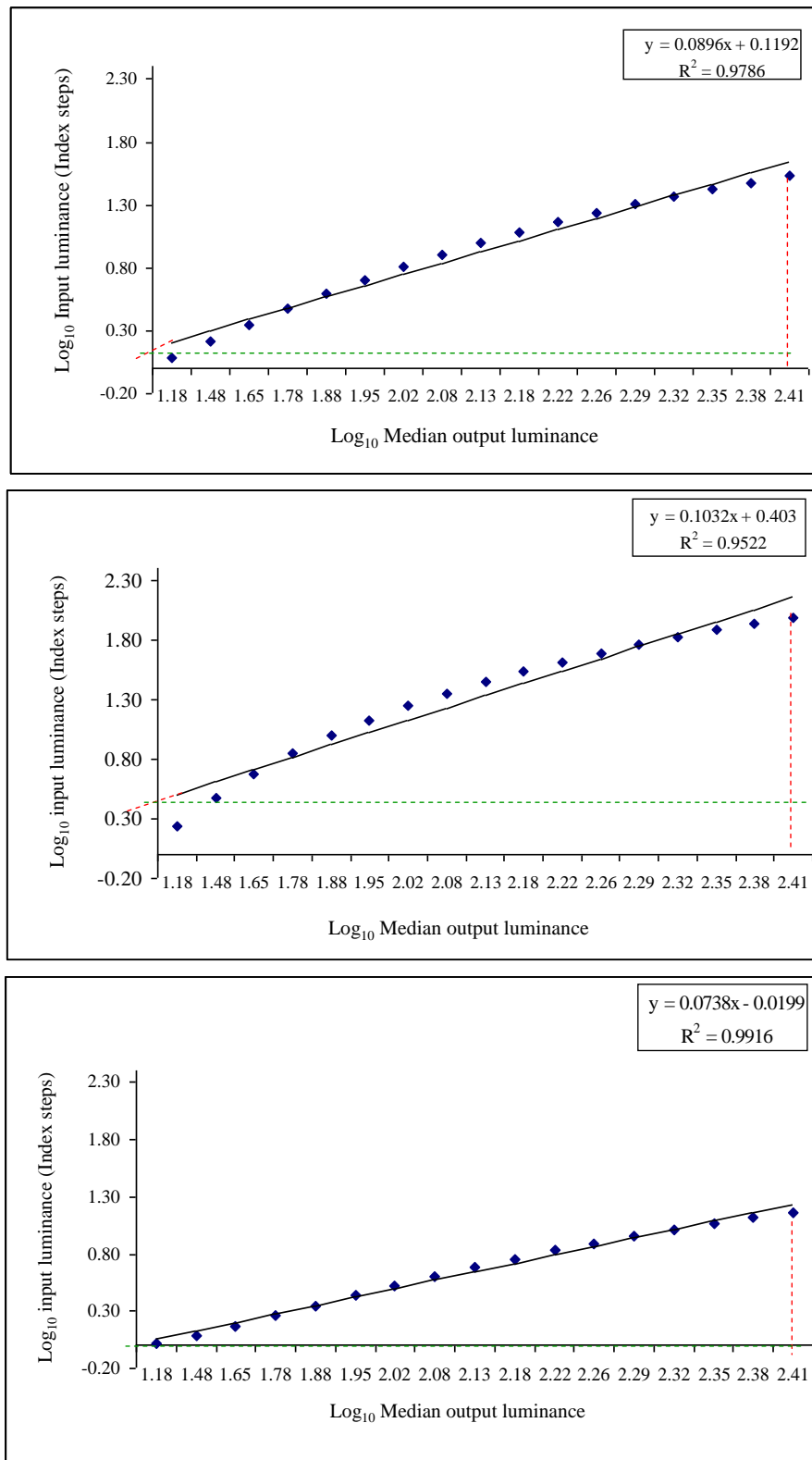


**Figure 4.1** The Log<sub>10</sub> of the input luminance, expressed in index steps, against the Log<sub>10</sub> of the median output luminance for the red (top), green (middle) and blue (bottom) colour guns. The y intercept and the slope of the function, together with the Coefficient of Determination, R<sup>2</sup>, are given in the top right of each panel.

#### **4.2.2.2 Step two: Michelson Contrast validation at the centre of the screen**

To validate the gamma functions for the three guns (i.e., to ensure that the requested input luminance from the graphics card was identical to the output luminance of the CRT screen) a 10cm by 10cm grey stimulus was generated at the geometric centre of the screen against a grey background, via the graphics card and the Hallikainen software, at each of 10 reference Michelson Contrast levels (Figure 4.2) where the Michelson contrast is defined as the difference between the maximum and minimum luminance divided by the sum of the two luminances. The contrast levels ranged from 0.512 to 0.001 in 9 steps with each step being half that of the previous value. The red, green and blue guns were each set at an index value of 127 which corresponded to an average screen luminance of  $50\text{cdm}^{-2}$ .

The luminances necessary to generate each of the given contrast levels, following gamma correction, were measured with the photometer. For any given Michelson contrast, the software presented the square patch at the higher of the two luminances and then at the lower of the two luminances.

Three measurements for each of the two luminance levels were obtained for each of the contrasts between 0.512 and 0.128; seven measurements between 0.064 and 0.016; and nine measurements between 0.008 and 0.001. This approach was used since, with such a procedure, the higher contrast values tend to be the most accurate as the large difference between the maximum and the minimum luminance levels generally offsets any measurement error. The raw data set is illustrated in Table 4.3 and the median for each of the two luminance levels at each of the contrasts in Table 4.4.

The procedure took approximately 2.5 hours.



**Figure 4.2** The 10cm x 10cm square patch used to validate the Michelson Contrast levels following gamma correction. The square patch was initially presented at the higher of the two luminances and then at the lower of the two luminances).

Requested MC	Measured 1		Measured 2		Measured 3		Measured 4		Measured 5		Measured 6		Measured 7		Measured 8		Measured 9	
	L <sub>min</sub>	L <sub>max</sub>																
<b>0.512</b>	22.5	75.5	22.5	75.4	22.5	75.2												
<b>0.256</b>	36.7	63.2	36.7	63.1	36.6	63.0												
<b>0.128</b>	43.4	56.8	43.3	56.8	43.2	56.7												
<b>0.064</b>	46.9	53.6	46.8	53.5	46.7	53.4	46.6	53.3	46.6	53.3	46.6	53.3	46.6	53.2				
<b>0.032</b>	48.5	51.9	48.5	51.9	48.4	51.7	48.2	51.6	48.2	51.6	48.2	51.6	48.2	51.5				
<b>0.016</b>	49.3	51.0	49.3	51.0	49.3	51.0	49.1	50.8	49.1	50.7	49.1	50.7	49.0	50.7				
<b>0.008</b>	49.8	50.6	49.7	50.5	49.6	50.4	49.6	50.4	49.5	50.3	49.4	50.4	49.4	50.3	49.4	50.2	49.4	50.3
<b>0.004</b>	50.0	50.4	49.9	50.3	49.9	50.3	49.7	50.1	49.7	50.2	49.7	50.1	49.7	50.1	49.6	50.0	49.7	50.0
<b>0.002</b>	50.1	50.3	50.0	50.2	50.1	50.1	49.8	50.1	49.8	50.0	49.8	50.0	49.7	49.9	49.7	50.0	49.8	49.9
<b>0.001</b>	50.1	50.2	50.1	50.1	50.1	50.1	49.9	50.0	49.9	50.0	49.8	49.9	49.8	49.9	49.8	49.9	49.7	49.8

**Table 4.3** The measured minimum and the maximum luminance of the square patch array (illustrated in Figure 4.2) generated on the monitor screen, following gamma correction, at each of 10 Michelson contrast (MC) levels. Three measures were obtained for contrasts between 0.512 and 0.128, seven measurements from 0.064 to 0.16 and nine measurements from 0.008 to 0.001.

Requested MC	Median values	
	Measured $L_{min}$	Measured $L_{max}$
<b>0.512</b>	22.5	75.4
<b>0.256</b>	36.7	63.1
<b>0.128</b>	43.3	56.8
<b>0.064</b>	46.6	53.3
<b>0.032</b>	48.2	51.6
<b>0.016</b>	49.1	50.8
<b>0.008</b>	49.5	50.4
<b>0.004</b>	49.7	50.1
<b>0.002</b>	49.8	50.0
<b>0.001</b>	49.9	50.0

**Table 4.4** The median of the measured minimum and of the measured maximum luminances of the square patch array generated on the monitor screen, following gamma correction, at each of the 10 Michelson contrast (MC) levels.

Requested MC	Measured MC	Proportionate difference
<b>0.512</b>	0.540	<b>-5%</b>
<b>0.256</b>	0.265	<b>-4%</b>
<b>0.128</b>	0.135	<b>-5%</b>
<b>0.064</b>	0.067	<b>-5%</b>
<b>0.032</b>	0.034	<b>-6%</b>
<b>0.016</b>	0.017	<b>-6%</b>
<b>0.008</b>	0.009	<b>-13%</b>
<b>0.004</b>	0.004	<b>0%</b>
<b>0.002</b>	0.002	<b>0%</b>
<b>0.001</b>	0.001	<b>0%</b>

**Table 4.5** The Michelson Contrast (MC) requested by the graphics card compared to that obtained from the medians of the measured luminances following gamma correction, tabulated in Table 4.4, and the proportionate difference.

The  $\log_{10}$  of the measured Michelson contrast was then plotted against the  $\log_{10}$  of the requested Michelson contrast (Figure 4.3). A linear fit, with the intercept constrained to pass through the origin at zero was applied to the untransformed data and is shown in Figure 4.3. The fit exhibited a Coefficient of Determination,  $R^2$ , of greater than 0.9999.

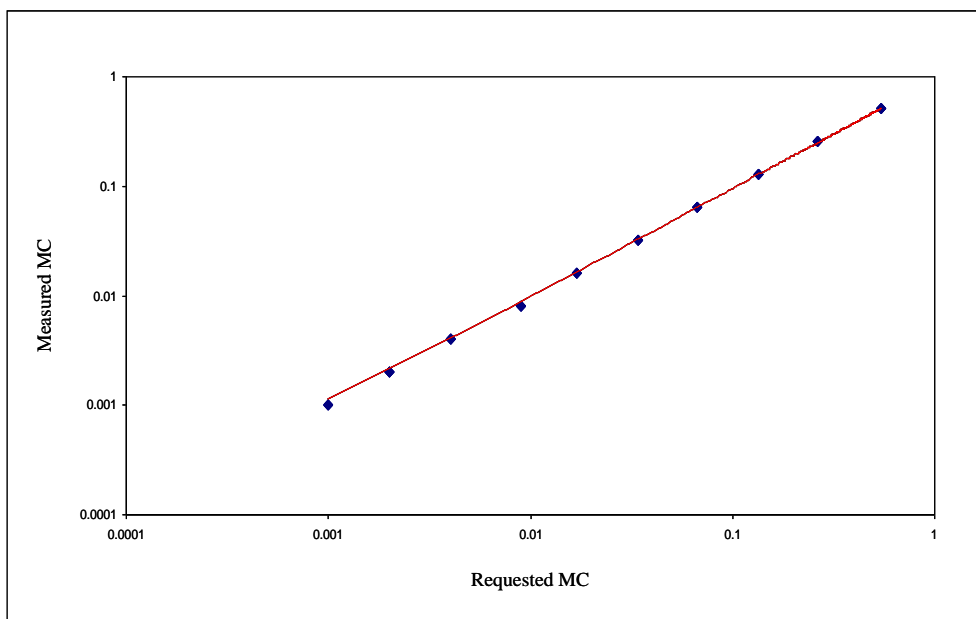


**Figure 4.3** The  $\log_{10}$  of the measured Michelson contrast against the  $\log_{10}$  of the requested Michelson contrast following gamma correction.

Notwithstanding the magnitude of the Coefficient of Determination for the untransformed values, the difference between the requested Michelson contrast and the measured Michelson contrast, following gamma correction, varied as a function of the requested contrast (Table 4.6). The measured contrast over-represented the requested contrast for all values between 0.512 and 0.008 indicating that the combined output from the colour guns was still non-linear. However, the requested MC and the measured MC were essentially equal over the range from 0.004 to 0.001. Fortuitously, the luminance levels responsible for generating this latter range of contrasts were capable of producing the contrast levels for DNP.

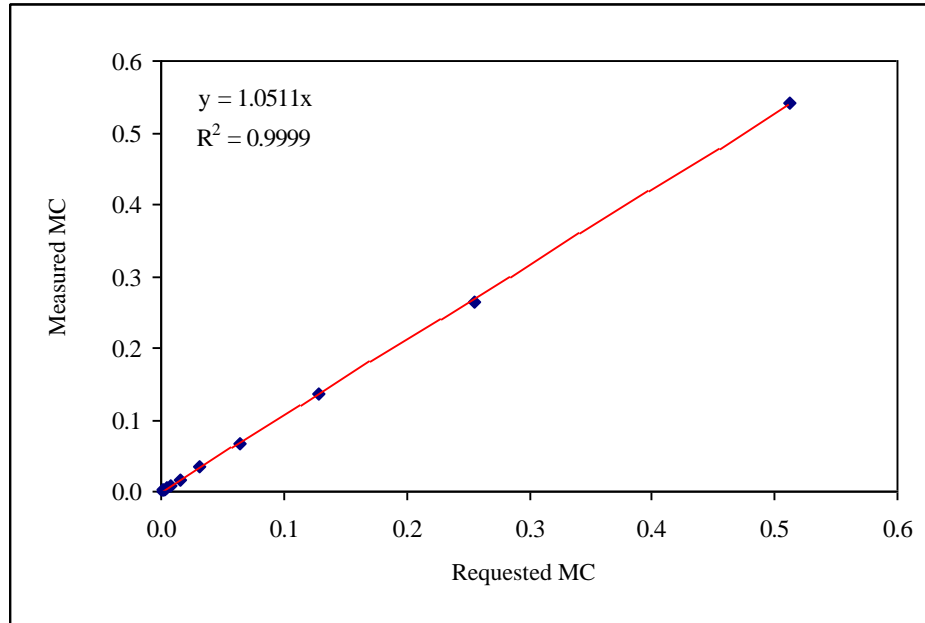


**Figure 4.4** The untransformed measured Michelson contrast against the untransformed requested Michelson contrast following gamma correction. The linear fit is constrained to pass through the origin.

#### 4.2.2.3 Step three: Michelson Contrast validation at each of nine sectors

The calibration process, described above, had been undertaken at the centre of the monitor. It was necessary, therefore, to confirm that the calibration was valid for the remaining sectors of the screen in terms both of the average luminance of  $50\text{cdm}^{-2}$  and of the relationship between the requested and measured Michelson Contrasts.

The screen was divided into a three by three matrix of nine equal sectors (with the centrally located sector excluded since it had already been used for the initial calibration). The calibration process was then undertaken at the centre of each of the remaining 8 sectors.

<b>3</b>	<b>8</b>	<b>7</b>
<b>2</b>	<b>1</b>	<b>6</b>
<b>4</b>	<b>9</b>	<b>5</b>

**Figure 4.5** The nine sectors of the monitor screen. Sector 1 was used for the initial calibration.

The time required to complete the validation was approximately 3 hours.

The difference between the requested MC and the measured MC corresponding to each of the nine sectors are given in Tables 4.6 to 4.14.

<b>Sector 1</b>			
<b>Average luminance 50.0 cdm<sup>-2</sup></b>			
<b>Requested MC</b>	<b>Measured L<sub>min</sub></b>	<b>Measured L<sub>max</sub></b>	<b>Measured MC</b>
<b>0.512</b>	21.8	76.5	<b>0.556</b>
<b>0.256</b>	36.4	63.8	<b>0.273</b>
<b>0.128</b>	43.4	57.4	<b>0.139</b>
<b>0.064</b>	47.0	53.9	<b>0.068</b>
<b>0.032</b>	48.7	52.2	<b>0.035</b>
<b>0.016</b>	49.6	51.3	<b>0.017</b>
<b>0.008</b>	50.1	50.9	<b>0.008</b>
<b>0.004</b>	50.3	50.7	<b>0.004</b>
<b>0.002</b>	50.4	50.6	<b>0.002</b>
<b>0.001</b>	50.4	50.5	<b>0.001</b>

**Table 4.6** The measured MC output corresponding to the graphics card requested MC for Sector 1.

<b>Sector 2</b>			
<b>Average luminance 50.2 cdm<sup>-2</sup></b>			
<b>Requested MC</b>	<b>Measured L<sub>min</sub></b>	<b>Measured L<sub>max</sub></b>	<b>Measured MC</b>
<b>0.512</b>	20.3	73.5	<b>0.567</b>
<b>0.256</b>	34.2	60.8	<b>0.280</b>
<b>0.128</b>	40.9	54.5	<b>0.143</b>
<b>0.064</b>	44.4	51.1	<b>0.070</b>
<b>0.032</b>	46.1	49.5	<b>0.036</b>
<b>0.016</b>	46.9	48.6	<b>0.018</b>
<b>0.008</b>	47.4	48.2	<b>0.008</b>
<b>0.004</b>	47.6	47.9	<b>0.003</b>
<b>0.002</b>	47.7	47.9	<b>0.002</b>
<b>0.001</b>	47.7	47.8	<b>0.001</b>

**Table 4.7** The measured MC output corresponding to the graphics card requested MC for Sector 2.

<b>Sector 3</b>			
<b>Average luminance 49.5 cdm<sup>-2</sup></b>			
<b>Requested MC</b>	<b>Measured L<sub>min</sub></b>	<b>Measured L<sub>max</sub></b>	<b>Measured MC</b>
<b>0.512</b>	21.2	75.9	<b>0.563</b>
<b>0.256</b>	35.7	63.2	<b>0.278</b>
<b>0.128</b>	42.6	56.6	<b>0.141</b>
<b>0.064</b>	46.2	53.3	<b>0.071</b>
<b>0.032</b>	48.0	51.5	<b>0.035</b>
<b>0.016</b>	48.9	50.6	<b>0.017</b>
<b>0.008</b>	49.3	50.2	<b>0.009</b>
<b>0.004</b>	49.5	49.9	<b>0.004</b>
<b>0.002</b>	49.6	49.8	<b>0.002</b>
<b>0.001</b>	49.7	49.8	<b>0.001</b>

**Table 4.8** The measured MC output corresponding to the graphics card requested MC for Sector 3.

<b>Sector 4</b>			
<b>Average luminance 49.7 cdm<sup>-2</sup></b>			
<b>Requested MC</b>	<b>Measured L<sub>min</sub></b>	<b>Measured L<sub>max</sub></b>	<b>Measured MC</b>
<b>0.512</b>	20.2	72.6	<b>0.565</b>
<b>0.256</b>	34.1	60.6	<b>0.280</b>
<b>0.128</b>	40.9	54.4	<b>0.142</b>
<b>0.064</b>	44.3	51.1	<b>0.071</b>
<b>0.032</b>	46.0	49.5	<b>0.037</b>
<b>0.016</b>	46.8	48.5	<b>0.018</b>
<b>0.008</b>	47.3	48.2	<b>0.009</b>
<b>0.004</b>	47.6	47.9	<b>0.003</b>
<b>0.002</b>	47.6	47.8	<b>0.002</b>
<b>0.001</b>	47.7	47.8	<b>0.001</b>

**Table 4.9** The measured MC output corresponding to the graphics card requested MC for Sector 4.

<b>Sector 5</b>			
<b>Average luminance 49.8 cdm<sup>-2</sup></b>			
<b>Requested MC</b>	<b>Measured L<sub>min</sub></b>	<b>Measured L<sub>max</sub></b>	<b>Measured MC</b>
<b>0.512</b>	20.6	75.3	0.570
<b>0.256</b>	35.0	62.5	0.282
<b>0.128</b>	41.8	56.0	0.145
<b>0.064</b>	45.4	52.5	0.073
<b>0.032</b>	47.1	50.6	0.036
<b>0.016</b>	48.1	49.9	0.018
<b>0.008</b>	48.5	49.3	0.008
<b>0.004</b>	48.7	49.1	0.004
<b>0.002</b>	48.8	49.0	0.002
<b>0.001</b>	48.8	48.9	0.001

**Table 4.10** The measured MC output corresponding to the graphics card requested MC for Sector 5.

<b>Sector 6</b>			
<b>Average luminance 50.1 cdm<sup>-2</sup></b>			
<b>Requested MC</b>	<b>Measured L<sub>min</sub></b>	<b>Measured L<sub>max</sub></b>	<b>Measured MC</b>
<b>0.512</b>	20.5	74.4	0.568
<b>0.256</b>	34.7	61.9	0.282
<b>0.128</b>	41.5	55.4	0.143
<b>0.064</b>	45.0	52.0	0.072
<b>0.032</b>	46.8	50.3	0.036
<b>0.016</b>	47.6	49.4	0.019
<b>0.008</b>	48.1	48.9	0.008
<b>0.004</b>	48.3	48.7	0.004
<b>0.002</b>	48.4	48.6	0.002
<b>0.001</b>	48.4	48.5	0.001

**Table 4.11** The measured MC output corresponding to the graphics card requested MC for Sector 6.

<b>Sector 7</b>			
<b>Average luminance 49.6 cdm<sup>-2</sup></b>			
<b>Requested MC</b>	<b>Measured L<sub>min</sub></b>	<b>Measured L<sub>max</sub></b>	<b>Measured MC</b>
<b>0.512</b>	20.1	72.9	0.568
<b>0.256</b>	34.0	60.8	0.283
<b>0.128</b>	40.8	54.5	0.144
<b>0.064</b>	44.3	51.0	0.070
<b>0.032</b>	45.9	49.4	0.037
<b>0.016</b>	46.8	48.5	0.018
<b>0.008</b>	47.3	48.1	0.008
<b>0.004</b>	47.5	47.9	0.004
<b>0.002</b>	47.7	47.9	0.002
<b>0.001</b>	47.7	47.8	0.001

**Table 4.12** The measured MC output corresponding to the graphics card requested MC for Sector 7.

<b>Sector 8</b>			
<b>Average luminance 50.3 cdm<sup>-2</sup></b>			
<b>Requested MC</b>	<b>Measured L<sub>min</sub></b>	<b>Measured L<sub>max</sub></b>	<b>Measured MC</b>
<b>0.512</b>	21.2	77.2	0.569
<b>0.256</b>	35.9	64.3	0.283
<b>0.128</b>	43.0	57.5	0.144
<b>0.064</b>	46.7	54.0	0.072
<b>0.032</b>	48.5	52.2	0.037
<b>0.016</b>	49.4	51.3	0.019
<b>0.008</b>	49.8	50.7	0.009
<b>0.004</b>	50.0	50.5	0.005
<b>0.002</b>	50.2	50.4	0.002
<b>0.001</b>	50.3	50.4	0.001

**Table 4.13** The measured MC output corresponding to the graphics card requested MC for Sector 8.

<b>Sector 9</b>			
<b>Average luminance 49.9 cdm<sup>-2</sup></b>			
<b>Requested MC</b>	<b>Measured L<sub>min</sub></b>	<b>Measured L<sub>max</sub></b>	<b>Measured MC</b>
<b>0.512</b>	20.5	75.2	0.572
<b>0.256</b>	34.7	62.4	0.285
<b>0.128</b>	41.7	55.8	0.145
<b>0.064</b>	45.3	52.3	0.072
<b>0.032</b>	47.0	50.6	0.037
<b>0.016</b>	48.0	49.6	0.016
<b>0.008</b>	48.4	49.2	0.008
<b>0.004</b>	48.6	49.0	0.004
<b>0.002</b>	48.7	48.9	0.002
<b>0.001</b>	48.7	48.8	0.001

**Table 4.14** The measured MC output corresponding to the graphics card requested MC for Sector 9.

However, the author measured each sector and ensured that the relationship between the requested MC and the measured MC at each sector was linear. In this respect the whole measurement were concluded as given in Figure 4.6.

49.5	50.3	49.6
50.2	50.0	50.1
49.7	49.9	49.8

**Figure 4.6** The average luminance in  $\text{cdm}^{-2}$  of each sector, whereas the relationship between the requested MC and Measured MC is linear.

### 4.3 Transforming the unit of measurement for DNP

The Michelson Contrast values for DNP were transformed to a decibel (dB) scale, based upon the capabilities of the CRT monitor and graphics card, in order to make the output more manageable.

Where,

$$\text{dB} = 10 * \text{LOG}_{10}(0.512 / K)$$

and k is the threshold in MC and 0.512 is the maximum contrast.

The dynamic range of the DNP, therefore, was from 0.512 to 0.001MC, equating to thresholds ranging from 0 to 27dB (Table 4.9),

Michelson Contrast (MC)	Decibel level (dB)
0.5120	0
0.4069	1
0.3231	2
0.2560	3
0.2038	4
0.1619	5
0.1280	6
0.1022	7
0.0812	8
0.0640	9
0.0512	10
0.0407	11
0.0320	12
0.0257	13
0.0204	14
0.0160	15
0.0129	16
0.0102	17
0.0080	18
0.0065	19
0.0051	20
0.0040	21
0.0033	22
0.0026	23
0.0020	24
0.0017	25
0.0014	26
0.0010	27

**Table 4.15** The Michelson contrast expressed as sensitivity in decibels (dB) for Dynamic Noise Perimetry.

## Chapter 5

### The influence of the Gaussian filter on Dynamic Noise Perimetry

#### 5.1 Introduction

Edges are a key element in the detection and resolution of an image (Hesse and Georgeson, 2005; Georgeson et al., 2007). The stimulus for DNP, a sine wave grating of 0.5 cycles per degree presented at 16Hz against an homogenous grey background of 50  $\text{cdm}^{-2}$ , contains a sharp edge, i.e., the border between the stimulus and the background. It was necessary, therefore, to determine the influence of the edge on the measured threshold.

The removal, or reduction, of an unwanted component from an image is undertaken by appropriate filtering (Bourne, 2010). Gaussian (low-pass) filtering is used in the visual psychophysical literature to smooth sharp edges (Nurminen, Kilpelainen and Vanni, 2013). A Gaussian filter is characterised in terms of the ‘bell shaped curve’ (Figure 5.1). A one-dimensional Gaussian distribution is described by:

$$f(x) = ae^{-x^2/2\sigma^2}$$

where  $a$  is the height of the distribution,  $x$  is the position of the centre of the distribution and  $\sigma$  is the standard deviation (i.e. the width) of the distribution at the full width at half maximum (FWHM).

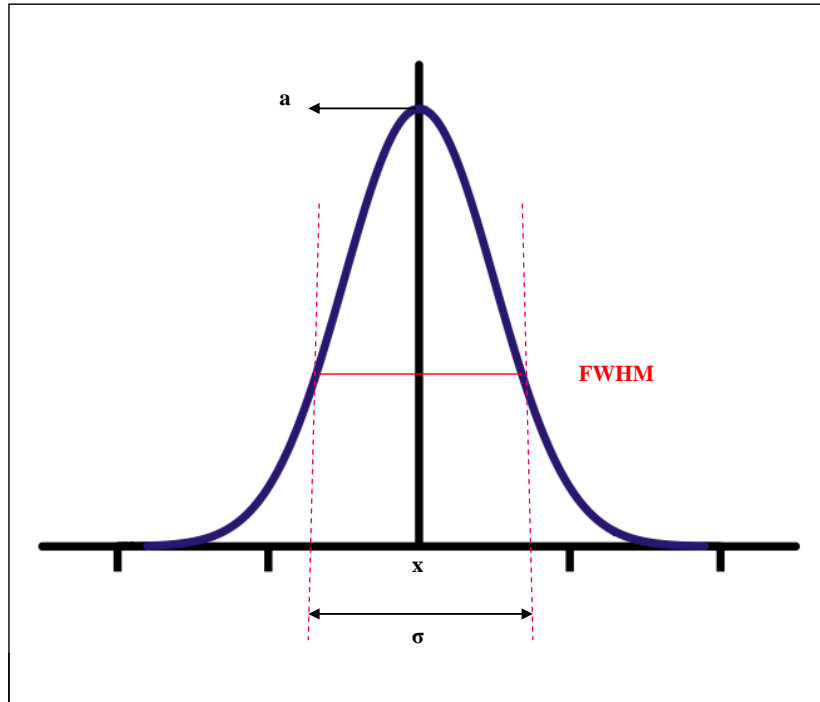


**Figure 5.1** A one-dimensional Gaussian function:  $\sigma$  is the Full Width at Half Maximum height (FWHM),  $a$  is the maximum height and  $x$  is the centre of the distribution.

## 5.2 Aim

The primary aim of the study was to determine, by the use of Gaussian filtering, the influence of the stimulus edge on the threshold in normal individuals. The secondary aim was to determine the threshold as a function of the strength (FWHM) of the Gaussian filter.

## **5.3 Methods**

### **5.3.1 Cohort**

The cohort comprised 15 normal individuals recruited from the student population at the Cardiff School of Optometry and Vision Sciences. The mean age of the individuals was 24.9 years (SD 3.35; range 19 to 30 years).

Each of the individuals underwent a comprehensive ophthalmic examination, to determine eligibility for inclusion in the study. Inclusion criteria comprised no family history of open angle glaucoma; no systemic disease or systemic therapy known to affect the visual field; no ocular surgery or trauma; no current topical ocular medication; a distance refractive error in each eye of not worse than -3.75 dioptres sphere or greater than +1.00DS, together with a cylinder of not larger than 1.50DC; an inter-ocular difference in the distance refractive error of not more than 0.50DS; a distance visual acuity of better than or equal to 6/5 in each eye; a normal anterior eye including normal pupil reflexes; an intraocular pressure, uncorrected for the effect of central corneal thickness, of less than 21mmHg; a normal media; a normal fundal and optic nerve head appearance; and a normal visual field (Program 30-2 and the SITA Standard strategy of the Humphrey Field Analyzer).

### **5.3.2 Examination protocol**

Each individual underwent an initial familiarisation session with DNP, which lasted approximately 15 minutes, and then attended on three separate sessions. The interval between the familiarisation session and the first experimental session ranged from 3 days to one week. The interval between the first and second and between the second and third visits also ranged from 3 days to one week.

At the first visit, each individual underwent DNP in one designated eye for eight separate stimulus combinations, designated at random, of location, filter strength and presence or absence of noise mask (0.2 RMS). The locations comprised  $0^\circ, 0^\circ; -14^\circ, -8^\circ; \text{ and } -22^\circ, 4^\circ$  (in right eye format). The four different strengths of Gaussian filter comprised 0.00, 0.25, 0.50 and 1.00 FWHM. A second array of eight randomly assigned separate stimulus combinations were undertaken at the second visit and the remaining eight at the third visit. The randomisation of the eight stimulus combinations at each of the three visits varied between individuals.

The algorithm used in the study was the ‘Proof of Concept’ algorithm described in Chapter 7, Section 7.2 and illustrated in Figure 7.1.

The Gaussian smoothing (convolution) of the DNP stimulus was undertaken for the two vertical edges of the DNP stimulus, i.e., horizontally in the x direction. The  $4^\circ \times 4^\circ$  square DNP stimulus consisted of 104 pixels x 104 pixels. The number of convoluted pixels varied according to the strength of the Gaussian filter (Figure 5.2.a-c). The number of neighbouring pixels inside the stimulus edge was equal to the number of neighbouring pixels outside the stimulus edge, i.e. around the tangent point.

Each individual wore their distance refractive correction. The non-examined eye was occluded with an opaque patch. Fixation was monitored via the CCD camera which provided an image on the display monitor. Prior to the determination of the first threshold, each individual adapted to the screen luminance ( $50 \text{ cdm}^{-2}$ ) for a minimum of one minute. A one minute enforced rest period was given after every 3 minutes of DNP and immediately after the completion of a given stimulus combination. During the rest period, each individual was required to maintain their adaptation by continuing to view the screen. Each individual received the same instructions throughout each examination at each visit.

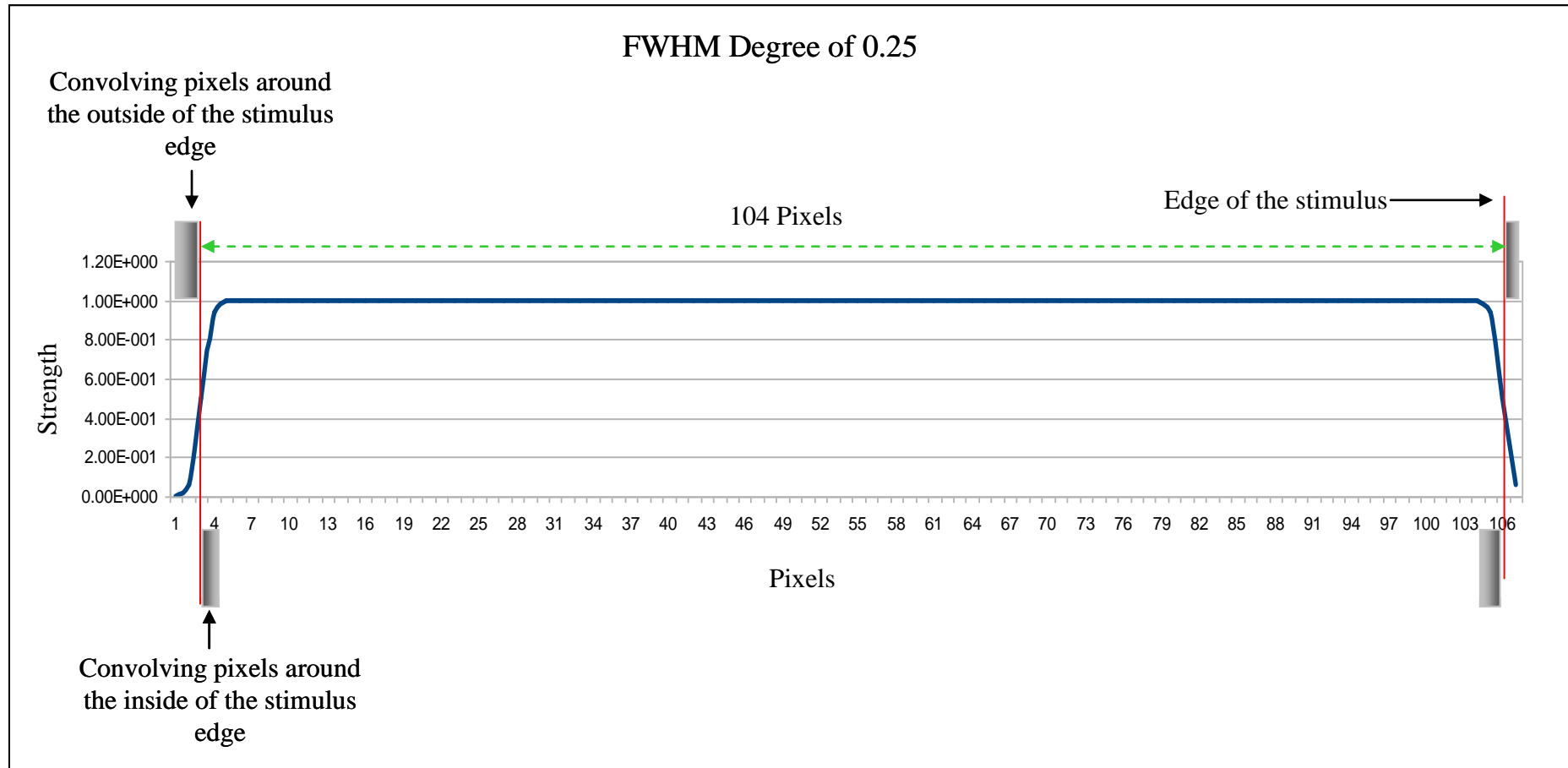


**Figure 5.2.a** A schematic of a Gaussian filter with a 0.25 FWHM. The DNP stimulus size increased horizontally to 108 pixels from the original size of 104 pixels to fit the Gaussian filter of 0.25 FWHM. Two convolving pixels were present either side of each vertical edge, i.e. a total of 4 pixels. The rectangle and the grey scale within the rectangle indicates the presence and strength of the convolution, i.e. a total of 4 pixels. The rectangle and the grey scale within the rectangle indicates the presence and strength of the convolution, i.e. a total of 4 pixels. Note the scale of the x axis is from 0 to 108 pixels.

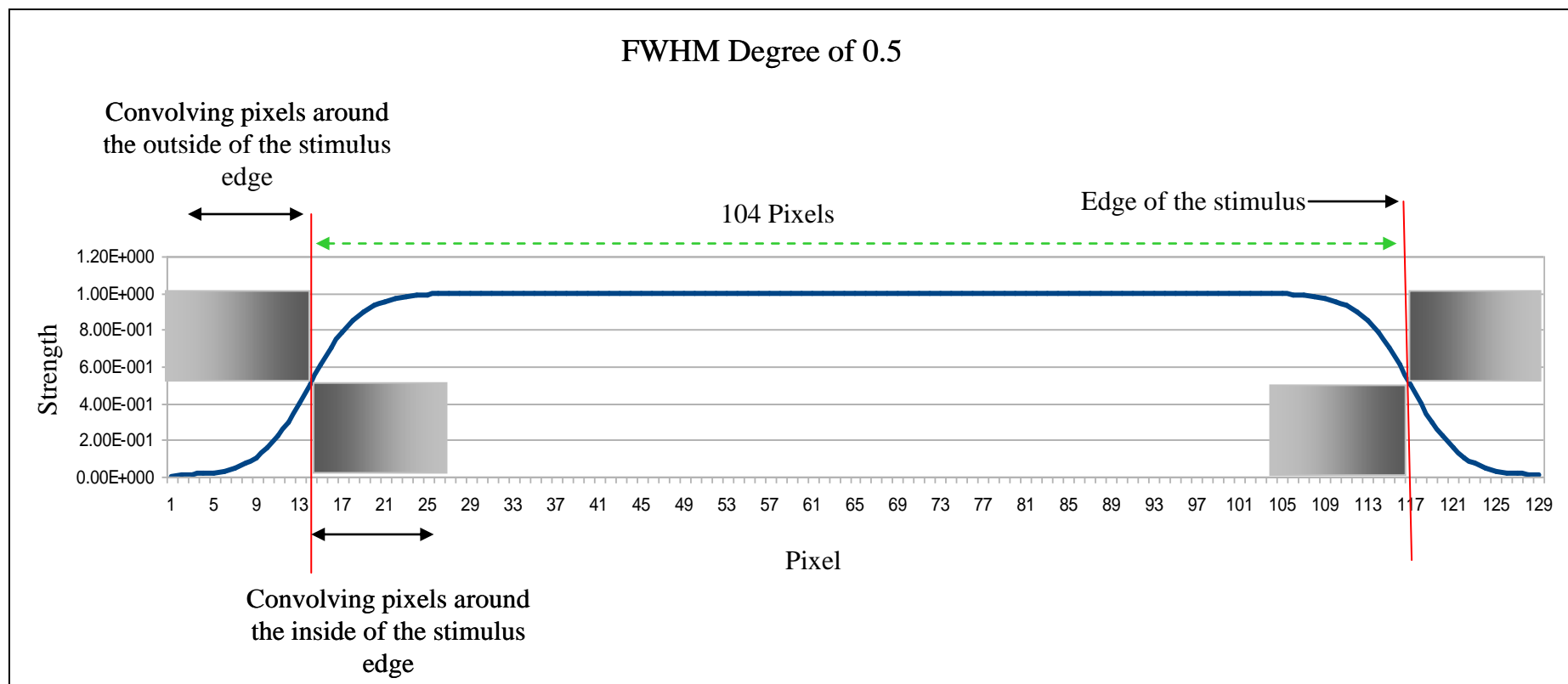


**Figure 5.2.b** A schematic of a Gaussian filter with a 0.50 FWHM. The DNP stimulus size increased horizontally to 130 pixels from the original size of 104 pixels to fit the Gaussian filter of 0.50 FWHM. Thirteen convolving pixels were present either side of each vertical edge, i.e. a total of 26 pixels. The rectangle and the grey scale within the rectangle indicate the presence and strength of the convolution, respectively, where a dark grey indicates the maximum strength of convolution. Note the scale of the x axis is from 0 to 130 pixels.

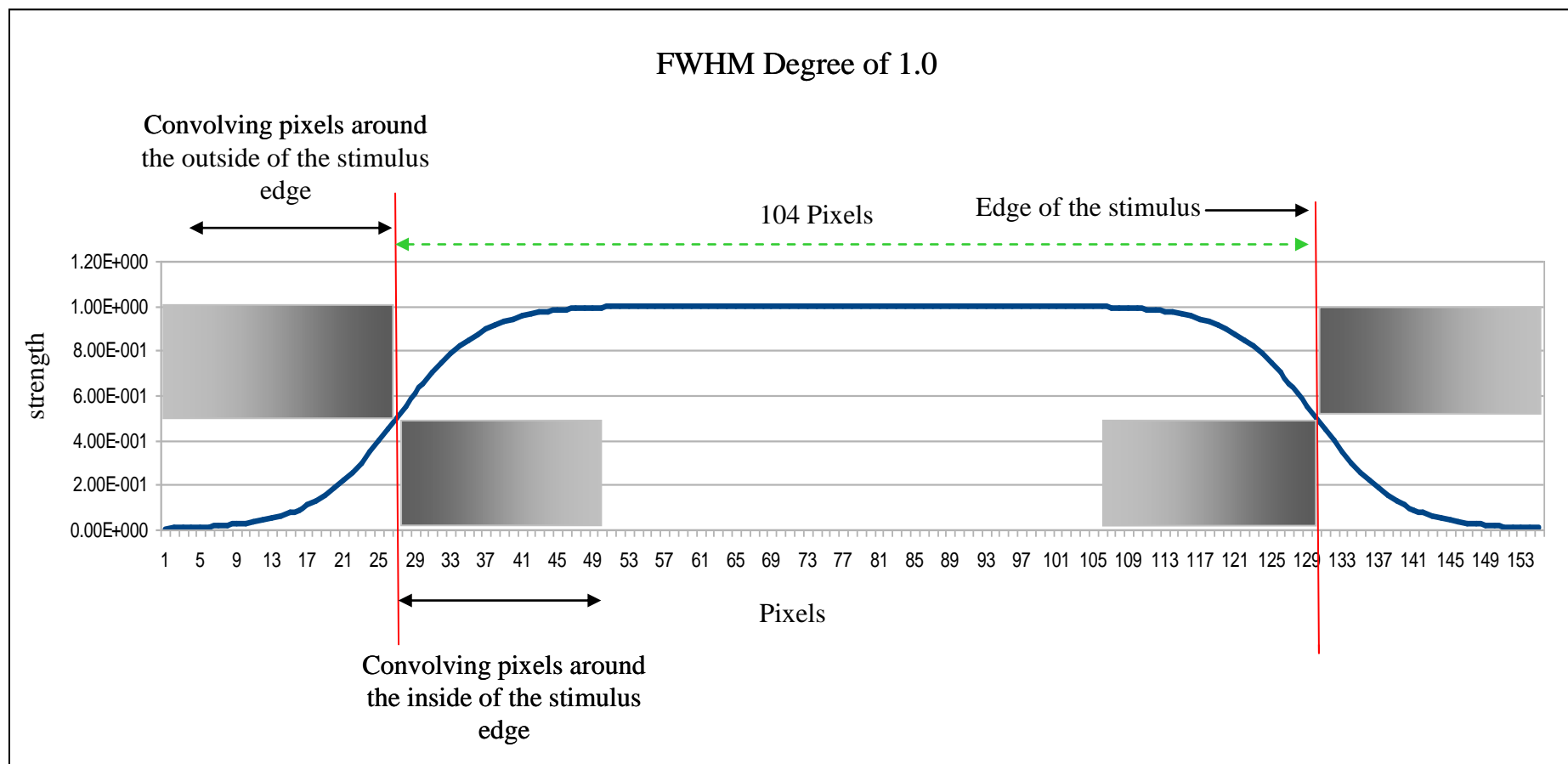


**Figure 5.2.c** A schematic of a Gaussian filter with a 1.00 FWHM. The DNP stimulus size increased horizontally to 156 pixels from the original size of 104 pixels to fit the Gaussian filter of 0.50 FWHM. Twenty-six convolving pixels were present either side of each vertical edge, i.e. a total of 52 pixels. The rectangle and the grey scale within the rectangle indicates the presence and strength of the convolution, respectively, where, a dark grey indicates the maximum strength of convolution. Note the scale of the x axis is from 0 to 156 pixels.

DNP was undertaken with the room lighting 'off'. If a lack of concentration and/ or a misunderstanding of the requirements of the examination were noticed during a given examination, the test was either paused or cancelled and a further explanation was given to the individual. Each test lasted approximately 2.5 to 3.0 minutes and each visit approximately 30 to 35 minutes.

### **5.3.3 Analysis**

Where necessary, the results were converted into right eye format. The results were then analysed using a repeated measures Analysis of Variance (ANOVA) with the presence or absence of the noise mask, the strength of filter and eccentricity as separate within-subject factors.

### **5.3.4 Ethical Approval**

The study was approved by the Ethics in Research Committee of the Cardiff School of Optometry and Vision Sciences which is in accord with the tenets of the Declaration of Helsinki. All individuals had received written instructions and had signed a consent form before undergoing the preliminary familiarisation session.

## **5.4 Results**

The summary statistics (Mean, SD, Median and IQR) of the Michelson contrast, expressed as sensitivity (dB), in the absence and in the presence of the noise mask, for each of the

four levels of the Gaussian filter at each of the 3 stimulus locations are shown in Tables 5.1 to 5.3.

For convenience, the data in Tables 5.1 to 5.3 are re-expressed in Table 5.4 as the Mean sensitivity (dB) for the four Gaussian filters at each stimulus location, in the absence and in the presence of the noise mask and in Table 5.5 as the absolute and proportionate difference, respectively, in the Mean sensitivity in the absence and in the presence of the noise mask.

The corresponding Summary Table for the ANOVA of the absolute values of the Michelson contrast, expressed as sensitivity (dB) in Tables 5.1 to 5.3 is shown in Table 5.6

	Without the noise mask				With the noise mask			
	0.00 FWHM	0.25 FWHM	0.50 FWHM	1.00 FWHM	0.00 FWHM	0.25 FWHM	0.50 FWHM	1.00 FWHM
<b>Individual</b>								
<b>1</b>	18.77	15.63	14.82	13.28	5.22	6.41	3.48	6.09
<b>2</b>	19.20	19.89	19.13	20.06	6.22	6.38	5.26	5.16
<b>3</b>	17.66	19.67	19.67	18.40	8.29	9.46	5.13	7.81
<b>4</b>	15.59	18.20	16.45	14.19	7.73	7.70	6.67	7.90
<b>5</b>	15.38	15.42	17.56	14.44	7.58	6.57	4.07	5.35
<b>6</b>	16.42	15.60	17.45	16.63	6.15	5.56	6.17	5.02
<b>7</b>	14.82	16.63	18.20	14.79	7.28	8.02	7.46	7.41
<b>8</b>	18.83	13.99	17.17	15.63	7.62	6.70	6.81	9.17
<b>9</b>	20.75	20.18	20.21	20.75	5.22	5.35	4.61	4.40
<b>10</b>	16.52	18.20	17.55	18.16	7.13	8.09	6.82	6.98
<b>11</b>	18.17	18.47	18.37	16.01	7.13	6.59	8.90	8.32
<b>12</b>	16.52	18.20	17.55	18.16	7.28	8.02	7.46	7.41
<b>13</b>	15.59	18.20	16.45	14.19	7.73	7.70	6.67	7.90
<b>14</b>	19.20	19.89	19.13	20.06	8.29	9.46	7.49	7.81
<b>15</b>	13.33	14.25	16.10	13.61	6.04	6.65	5.44	6.76
<b>Mean</b>	<b>17.12</b>	<b>17.50</b>	<b>17.72</b>	<b>16.56</b>	<b>6.99</b>	<b>7.24</b>	<b>6.16</b>	<b>6.90</b>
<b>SD</b>	<b>2.02</b>	<b>2.09</b>	<b>1.45</b>	<b>2.54</b>	<b>1.00</b>	<b>1.24</b>	<b>1.47</b>	<b>1.40</b>
<b>Median</b>	<b>16.52</b>	<b>18.20</b>	<b>17.55</b>	<b>16.01</b>	<b>7.28</b>	<b>6.70</b>	<b>6.67</b>	<b>7.41</b>
<b>IQR</b>	<b>15.59, 18.80</b>	<b>15.61, 19.07</b>	<b>16.81, 18.75</b>	<b>14.31, 18.28</b>	<b>6.19, 7.28</b>	<b>6.49, 6.70</b>	<b>5.20, 6.67</b>	<b>5.72, 7.41</b>

**Table 5.1** The summary statistics (Mean, SD, Median and IQR) of the Michelson contrast expressed as sensitivity (dB) at 0°, 0°, in the absence and in the presence of the noise mask, for each of the four levels of the Gaussian filter.

	Without the noise mask				With the noise mask			
	0.00 FWHM	0.25 FWHM	0.50 FWHM	1.00 FWHM	0.00 FWHM	0.25 FWHM	0.50 FWHM	1.00 FWHM
<b>Individual</b>								
<b>1</b>	16.24	8.49	17.05	12.78	11.27	8.57	9.37	9.46
<b>2</b>	16.11	17.64	15.43	15.69	10.09	9.03	8.40	7.80
<b>3</b>	15.05	14.32	16.64	14.90	9.33	10.58	11.25	9.42
<b>4</b>	15.52	16.05	16.45	16.55	8.69	11.50	10.18	10.71
<b>5</b>	16.73	18.53	16.52	14.85	7.99	8.53	6.52	7.33
<b>6</b>	9.80	16.63	17.88	16.39	5.01	6.04	6.37	6.00
<b>7</b>	17.74	16.87	16.56	16.56	5.78	6.50	6.71	6.52
<b>8</b>	18.28	18.35	18.80	19.47	9.03	6.36	7.05	7.60
<b>9</b>	12.08	15.52	15.87	14.59	8.91	9.50	8.77	6.96
<b>10</b>	10.94	14.19	16.52	15.93	6.65	5.90	8.33	9.17
<b>11</b>	15.01	14.40	13.83	15.83	8.26	9.14	8.70	9.46
<b>12</b>	17.74	16.87	16.56	16.56	9.03	6.36	7.05	7.60
<b>13</b>	15.05	14.32	16.64	14.90	9.33	10.58	11.25	9.42
<b>14</b>	14.00	15.52	15.87	14.59	9.85	8.39	8.23	7.52
<b>15</b>	13.99	12.95	13.38	14.51	9.85	8.39	8.23	7.52
<b>Mean</b>	<b>14.95</b>	<b>15.38</b>	<b>16.26</b>	<b>15.61</b>	<b>8.60</b>	<b>8.36</b>	<b>8.43</b>	<b>8.16</b>
<b>SD</b>	<b>2.48</b>	<b>2.51</b>	<b>1.35</b>	<b>1.49</b>	<b>1.67</b>	<b>1.79</b>	<b>1.58</b>	<b>1.34</b>
<b>Median</b>	<b>15.05</b>	<b>15.52</b>	<b>16.52</b>	<b>15.69</b>	<b>9.03</b>	<b>8.53</b>	<b>8.33</b>	<b>7.60</b>
<b>IQR</b>	<b>13.99, 16.49</b>	<b>14.32, 16.87</b>	<b>15.87, 16.64</b>	<b>14.72, 16.47</b>	<b>8.13, 9.59</b>	<b>6.43, 9.32</b>	<b>7.05, 9.07</b>	<b>7.42, 9.42</b>

**Table 5.2** The summary statistics (Mean, SD, Median and IQR) of the Michelson contrast expressed as sensitivity (dB) at  $-14^\circ$ ,  $-8^\circ$ , in the absence and in the presence of the noise mask, for each of the four levels of the Gaussian filter.

	Without the noise mask				With the noise mask			
	0.00 FWHM	0.25 FWHM	0.50 FWHM	1.00 FWHM	0.00 FWHM	0.25 FWHM	0.50 FWHM	1.00 FWHM
<b>Individual</b>								
<b>1</b>	15.55	18.91	16.76	17.14	9.23	7.79	9.42	9.88
<b>2</b>	15.20	16.27	15.55	15.90	8.78	8.53	12.05	8.70
<b>3</b>	15.20	15.60	14.76	14.73	8.66	7.70	9.74	10.33
<b>4</b>	14.73	14.97	14.39	14.75	8.28	8.70	9.39	9.71
<b>5</b>	15.27	15.28	15.32	13.27	5.48	8.25	10.08	9.29
<b>6</b>	16.56	10.10	13.74	14.53	6.13	4.83	7.20	7.74
<b>7</b>	16.65	13.64	16.05	19.40	8.17	6.58	7.45	10.06
<b>8</b>	17.83	19.06	17.32	18.06	5.33	8.34	7.32	8.05
<b>9</b>	13.75	12.95	13.26	12.75	6.07	11.48	9.39	9.17
<b>10</b>	16.87	16.05	16.20	15.76	13.83	9.01	7.29	9.25
<b>11</b>	14.41	13.61	13.48	13.78	9.77	7.33	9.70	9.39
<b>12</b>	16.65	13.64	16.05	19.40	12.15	9.01	7.29	9.25
<b>13</b>	14.73	14.97	14.39	14.75	8.28	8.70	9.39	9.71
<b>14</b>	13.04	11.53	14.19	12.92	8.66	7.70	9.74	10.33
<b>15</b>	13.04	11.53	14.19	12.92	7.93	6.79	8.13	7.49
<b>Mean</b>	<b>15.30</b>	<b>14.54</b>	<b>15.04</b>	<b>15.34</b>	<b>8.45</b>	<b>8.05</b>	<b>8.91</b>	<b>9.22</b>
<b>SD</b>	<b>1.42</b>	<b>2.53</b>	<b>1.24</b>	<b>2.25</b>	<b>2.32</b>	<b>1.46</b>	<b>1.41</b>	<b>0.89</b>
<b>Median</b>	<b>15.20</b>	<b>14.97</b>	<b>14.76</b>	<b>14.75</b>	<b>8.28</b>	<b>8.25</b>	<b>9.39</b>	<b>9.29</b>
<b>IQR</b>	<b>14.57, 16.60</b>	<b>13.28, 15.82</b>	<b>14.19, 16.05</b>	<b>13.53, 16.52</b>	<b>7.03, 9.01</b>	<b>7.51, 8.70</b>	<b>7.39, 9.72</b>	<b>8.94, 9.79</b>

**Table 5.3** The summary statistics (Mean, SD, Median and IQR) of the Michelson contrast expressed as sensitivity (dB) at  $-22^\circ$ ,  $4^\circ$ , in the absence and in the presence of the noise mask, for each of the four levels of the Gaussian filter.

	Without the noise mask			With the noise mask		
	Stimulus location			Stimulus location		
	(0°, 0°)	(-14°, -8°)	(-22°, 4°)	(0°, 0°)	(-14°, -8°)	(-22°, 4°)
<b>Gaussian filter level</b>						
<b>0.00 FWHM</b>	17.12	14.95	15.30	6.99	8.60	8.45
<b>SD</b>	2.02	2.48	1.42	1.00	1.67	2.32
<b>0.25 FWHM</b>	17.50	15.38	14.54	7.24	8.36	8.05
<b>SD</b>	2.09	2.51	2.53	1.24	1.79	1.46
<b>0.50 FWHM</b>	17.72	16.26	15.04	6.16	8.43	8.91
<b>SD</b>	1.45	1.35	1.24	1.47	1.58	1.41
<b>1.00 FWHM</b>	16.56	15.61	15.34	6.90	8.16	9.22
<b>SD</b>	2.54	1.49	2.25	1.40	1.34	0.89

**Table 5.4** The Mean sensitivity (dB) (top) and one SD (bottom) for the four Gaussian filters at each stimulus location, in the absence and in the presence of the noise mask.

	Stimulus location		
	(0°, 0°)	(-14°, -8°)	(-22°, 4°)
<b>Gaussian filter level (FWHM)</b>			
<b>0.00</b>	-10.13 (-59.17)	-6.35 (-42.47)	-6.85 (-44.77)
<b>0.25</b>	-10.26 (-58.63)	-7.02 (-45.64)	-6.49 (-44.64)
<b>0.50</b>	-11.56 (-65.24)	-7.83 (-48.15)	-6.13 (-40.76)
<b>1.00</b>	-9.66 (-58.33)	-7.45 (-47.73)	-6.12 (-39.90)

**Table 5.5** The absolute (dB) and proportionate (%) differences between the group mean sensitivity in the presence of the noise mask and that in the absence of the noise mask at each stimulus location at each of the four levels of Gaussian filter. Note the minus sign indicates the sensitivity was lower in the presence of the noise mask. The proportionate difference is given in parenthesis.

<b>Factor</b>	<b>Numerator Degrees of Freedom</b>	<b>Denominator Degree of Freedom</b>	<b>F value</b>	<b>P value</b>
<b>Eccentricity</b>	2	339	0.24	0.7856
<b>Noise mask</b>	1	339	1576.63	<0.001
<b>Filter strength</b>	3	339	0.27	0.8475
<b>Eccentricity*Noise</b>	2	334	47.31	<0.001
<b>Noise*filter strength</b>	3	334	1.02	0.3849

**Table 5.6** The ANOVA Summary Table for the influences of the presence or absence of the noise mask, the filter strength, and eccentricity on the Michelson contrast expressed as sensitivity (dB).

#### Eccentricity

Overall, sensitivity was not influenced by eccentricity ( $p = 0.786$ ); however, the variation of sensitivity with increase in eccentricity was different between the absence and the presence of the noise mask ( $p < 0.001$ ). Without the noise mask, and in the absence of the Gaussian filter, sensitivity decreased with increase in eccentricity by 1.90dB (Table 5.4). In the presence of the noise mask, and in the absence of the Gaussian filter, sensitivity increased with increase in eccentricity by 1.46dB (Table 5.4).

#### Noise mask

Sensitivity was greater in the absence of the noise mask compared to that derived in the presence of the noise mask ( $p < 0.001$ ).

#### Gaussian filter strength

The varying strengths of filter exerted no influence on the magnitude of the sensitivity ( $p = 0.846$ ) irrespective of the absence or presence of the noise mask ( $p = 0.385$ ).

## 5.5 Discussion

As would be expected, the sensitivity in the absence of the noise mask declined with increase in eccentricity. As would also be expected, the sensitivity in the absence of the noise mask (0.2 RMS) was significantly greater than the sensitivity in the presence of the noise mask. However, in the presence of the noise mask, sensitivity increased with increase in eccentricity.

In the absence of any Gaussian filter, the reduction in sensitivity at the fovea due to the noise mask was approximately 60% whereas that at each of the two peripheral locations was approximately 45%. This finding indicates that the strength of the noise mask may not be optimized for eccentricity. The question of optimization, in terms of the number of checks per grating cycle, will be discussed in further detail in Chapter 6.

Each of the four levels of Gaussian filter exerted little influence on the sensitivity at each of the three eccentricities either in the presence or in the absence of the noise mask (Tables 5.5 to 5.6). This indicates that the stimulus edge of DNP contributed little, if anything, to the perception of the grating. This finding is in accord with that of others, who found that the Gaussian filtering of the stimulus edge did not influence the orientation-identification threshold or the detection threshold for a 0.25 cycles per degree grating presented at 25Hz (Hogg and Anderson, 2009).

## **5.6 Conclusion**

The DNP stimulus edge did not appear to influence the threshold outcome either in the absence of noise or in the presence of noise, i.e., the threshold did not increase for any of the three filters at any of the three eccentricities.

## **Chapter 6**

### **The strength of the noise mask on the outcome of**

### **Dynamic Noise Perimetry**

#### **6.1 Introduction**

The noise mask for the ‘Proof of Concept’ studies undertaken by Dr. Rattan was 4 checks per cycle (Chapter 2). This value had been obtained in a pilot study based upon 4 individuals. Clearly, therefore, it was necessary to validate the selection of 4 checks per cycle on a larger number of individuals.

#### **6.2 Aim**

The aim of the study was twofold. Firstly, to determine the outcome of DNP as a function of the number of checks per cycle of the  $4^\circ \times 4^\circ$  noise mask and, secondly, to ensure that the spatial limits of the optimized noise check size were sufficient to mask the underlying DNP stimulus (0.5 cycles per degree presented at 16Hz).

## **6.3 Methods**

### **6.3.1 Cohort**

The cohort comprised 11 normal individuals recruited from the student population at the Cardiff School of Optometry and Vision Sciences. The mean age of the 11 individuals was 28.1 years (SD 5.01; range 21 to 37 years). Five of the 11 normal individuals had participated in the Gaussian filter experiment described in Chapter 5.

The six new individuals underwent a comprehensive ophthalmic examination to determine their eligibility for inclusion in the study. Inclusion criteria was identical to that described in Chapter 5 and comprised no family history of open angle glaucoma; no systemic disease or systemic therapy known to affect the visual field; no ocular surgery or trauma; no current topical ocular medication; a distance refractive error in each eye of not worse than -3.75 DS or greater than +1.00DS, together with a cylinder of not larger than 1.50DC; an inter-ocular difference in the distance refractive error of not more than 0.50DS; a distance visual acuity of better than or equal to 6/5 in each eye; a minimum pupil size of 4mm; a normal anterior eye including normal pupil reflexes; an intraocular pressure, uncorrected for the effect of central corneal thickness, of less than 21mmHg; a normal media; a normal fundal and optic nerve head appearance; and a normal visual field (Program 30-2 and the SITA Standard strategy of the Humphrey Field Analyzer).

### **6.3.2 Examination protocol**

The five normal individuals who had participated in the previous study of the effect of the Gaussian filter on the outcome of DNP each attended on two separate sessions each

separated by 3 days to one week. Each of the 6 remaining individuals attended for an initial familiarisation session with DNP, which lasted approximately 15 minutes, and then attended on two separate occasions. The interval between the familiarisation session and the first experimental session ranged from 3 days to one week. The interval between the first and second experimental session also ranged from 3 days to one week.

At the first experimental visit, each individual underwent DNP in one designated eye for thirteen separate combinations, designated at random, comprising stimulus location, and the presence or absence of noise mask. The stimulus locations were situated at 0°, 0°; -14°, 4° and -22°, 4° eccentricities, in right eye format. The noise mask contained 1, 2, 3, 4, 5, 8, 12 or 20 checks per cycle.

At the second experimental visit, each individual underwent DNP in the same designated eye for a separate array of fourteen randomly assigned stimulus combinations. The randomisation of the stimulus combinations at each of the two visits varied between individuals.

In total, each individual thus underwent 27 stimulus combinations, i.e., 3 locations \* 8 different noise masks + 3 stimulus locations in the absence of any noise.

The algorithm used in the study was the 'Proof of Concept' algorithm described in Chapter 7, Section 7.2 and illustrated in Figure 7.1.

Each individual wore their distance refractive correction. The fellow eye was occluded with an opaque patch. Fixation was monitored via the CCD camera which provided an

image on the display monitor. Prior to the determination of the first threshold, each individual adapted to the screen luminance ( $50\text{cdm}^{-2}$ ) for at least one minute. A one minute enforced rest period was given after every 3 minutes of DNP and immediately after the completion of a given stimulus combination. During the rest period, each individual was required to maintain their adaptation by continuing to view the screen. Each individual received the same instructions throughout each examination at each visit.

The DNP was undertaken with the room lighting 'off'. If a lack of concentration and/ or a misunderstanding of the requirements of the examination were noticed during a given examination, the test was either paused or cancelled and a further explanation was given to the individual. Each test lasted approximately 2.5 to 3.0 minutes and each visit approximately 45 to 55 minutes including the one minute enforced rest period every 3 minutes and the time following completion of the given stimulus combination.

### **6.3.3 Analysis**

Two separate repeated measures ANOVAs were used with Michelson contrast expressed in dB as the response. The first model included data in the absence of the noise mask and the second model excluded data in the presence of the noise mask. Age was included in both models as a between-subjects factor. Eccentricity and the number of checks per cycle were included as within-subject factors. The interaction of eccentricity and the number of checks per cycle was also included in each model. Each effect was treated as a fixed effect. Subject was included as a random effect.

### **6.3.4 Ethical Approval**

The study was approved by the Ethics in Research Committee of the Cardiff School of Optometry and Vision Sciences which is in accord with the tenets of the Declaration of Helsinki. All individuals had received written instructions and had signed a consent form before undergoing the preliminary familiarisation session.

## **6.4 Results**

The summary statistics (Mean, SD, Median and IQR) of the Michelson contrast, expressed as sensitivity in dB, in the presence and in the absence of the noise mask, for each of the eight different checks per cycle at each of the three stimulus locations are shown in Tables 6.1 to 6.3, and illustrated graphically in Figures 6.1 to 6.3.

The corresponding Summary Tables for the ANOVA are shown in Tables 6.4 and 6.5.

### Eccentricity

Sensitivity in the presence of the noise mask increased with increase in eccentricity ( $p < 0.0001$ ) for both models (Figure 6.4).

### Number of checks per cycle

Sensitivity varied with increase in the number of checks per cycle ( $p < 0.0001$ ) for both models.

### Number of checks per cycle and eccentricity interaction

The change in sensitivity with increase in the number of checks per cycle varied with eccentricity ( $p < 0.0001$ ). At  $0^\circ, 0^\circ$  eccentricity, sensitivity declined with increase in the number of checks per cycle until 4 checks per cycle after which it increased. A similar trend was present at the remaining two eccentricities ( $-14^\circ, 4^\circ$ ; and  $-22^\circ, 4^\circ$ ); in the corresponding minimum was 2 checks per cycle at each eccentricity.

Stimulus location (0°, 0°)									
	With the noise mask								Without the noise mask
	Checks/Cycle								
	1	2	3	4	5	8	12	20	
Individual									
6	9.01	9.87	8.94	8.48	9.11	11.25	13.32	16.10	19.37
9	10.63	7.32	7.49	7.45	9.14	9.50	11.15	15.15	21.75
11	9.71	7.91	7.49	6.71	7.39	8.57	11.67	12.97	18.44
12	10.40	7.33	7.90	5.69	9.33	8.07	12.15	13.90	18.66
15	11.03	6.79	6.41	4.78	7.49	9.02	11.38	12.92	18.53
16	7.79	6.11	6.23	5.45	5.93	9.76	10.71	12.06	18.06
17	9.57	9.71	9.12	8.60	9.14	10.13	11.71	14.75	18.61
18	11.15	8.88	8.49	7.13	8.91	10.96	12.64	14.27	21.62
19	10.88	8.32	7.97	6.99	8.58	9.71	12.02	15.87	17.97
20	10.85	7.68	6.23	7.58	9.35	10.49	13.09	14.53	17.31
21	9.29	9.72	8.06	7.51	8.23	9.36	10.34	14.90	19.52
<b>Mean</b>	<b>10.03</b>	<b>8.15</b>	<b>7.67</b>	<b>6.94</b>	<b>8.42</b>	<b>9.71</b>	<b>11.83</b>	<b>14.31</b>	<b>19.08</b>
<b>SD</b>	<b>1.05</b>	<b>1.27</b>	<b>1.02</b>	<b>1.21</b>	<b>1.08</b>	<b>0.97</b>	<b>0.94</b>	<b>1.26</b>	<b>1.43</b>
<b>Median</b>	<b>10.40</b>	<b>7.91</b>	<b>7.90</b>	<b>7.13</b>	<b>8.91</b>	<b>9.71</b>	<b>11.71</b>	<b>14.53</b>	<b>18.6</b>
<b>IQR</b>	<b>1.43</b>	<b>1.97</b>	<b>1.33</b>	<b>1.35</b>	<b>1.28</b>	<b>1.12</b>	<b>1.13</b>	<b>1.59</b>	<b>1.19</b>

**Table 6.1** The summary statistics (Mean, SD, Median and IQR) of the Michelson contrast expressed as sensitivity (dB) at 0°, 0° eccentricity for each of the 8 different checks per cycle of the given noise mask and without the noise mask.

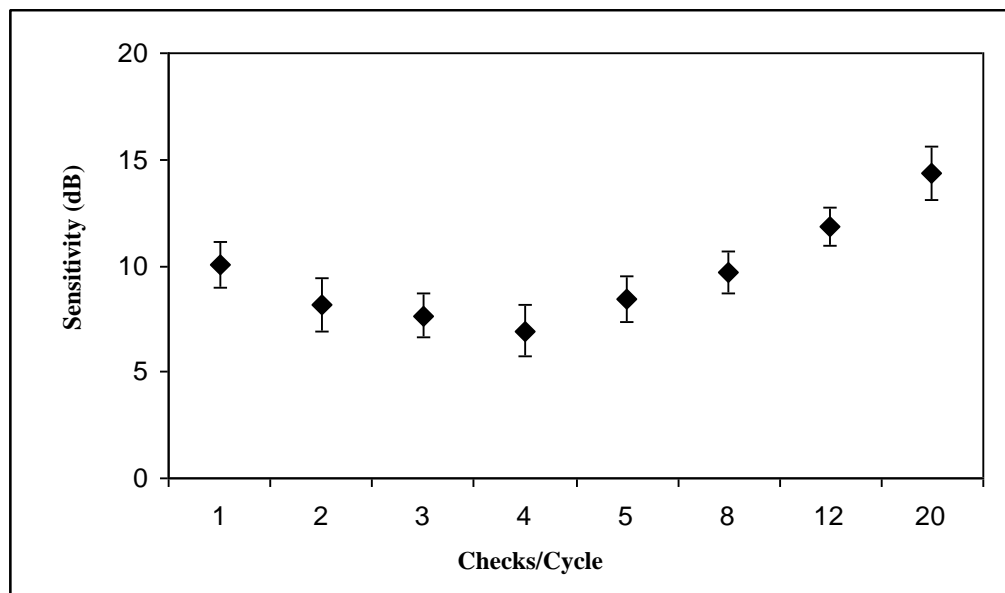


**Figure 6.1** Group mean sensitivity against number of checks per cycle of the given noise mask at 0°, 0° eccentricity for the 11 normal individuals. The error bars indicate one standard deviation of the mean.

Stimulus location (-14°, +4°)									
	With the noise mask								Without the noise mask
	Checks/Cycle								
	1	2	3	4	5	8	12	20	
<b>Individual</b>									
<b>6</b>	11.30	8.39	8.32	8.67	10.34	11.45	14.29	15.96	16.20
<b>9</b>	9.00	8.14	8.27	8.88	10.60	11.06	12.89	13.04	14.24
<b>11</b>	7.84	7.13	8.12	8.60	10.77	12.15	11.82	14.73	16.27
<b>12</b>	8.80	6.35	8.02	9.96	10.14	10.85	13.59	15.93	15.35
<b>15</b>	11.15	6.41	6.90	8.02	7.39	11.43	12.58	15.74	16.15
<b>16</b>	12.58	5.83	6.70	6.75	9.29	9.52	10.96	14.73	16.52
<b>17</b>	11.30	9.80	10.42	9.51	11.49	12.72	16.21	15.73	16.60
<b>18</b>	11.59	9.02	9.79	9.71	11.93	11.85	13.28	16.38	16.73
<b>19</b>	11.46	9.07	9.88	9.58	10.44	12.42	13.43	15.25	16.26
<b>20</b>	9.43	8.68	8.68	7.74	9.85	10.18	11.66	12.05	15.41
<b>21</b>	10.25	9.21	9.51	9.51	11.66	12.70	15.78	16.46	16.61
<b>Mean</b>	<b>10.43</b>	<b>8.00</b>	<b>8.60</b>	<b>8.81</b>	<b>10.36</b>	<b>11.48</b>	<b>13.32</b>	<b>15.09</b>	<b>16.03</b>
<b>SD</b>	<b>1.47</b>	<b>1.35</b>	<b>1.20</b>	<b>0.99</b>	<b>1.26</b>	<b>1.03</b>	<b>1.63</b>	<b>1.40</b>	<b>0.75</b>
<b>Median</b>	<b>11.15</b>	<b>8.39</b>	<b>8.32</b>	<b>8.88</b>	<b>10.44</b>	<b>11.45</b>	<b>13.28</b>	<b>15.73</b>	<b>16.26</b>
<b>IQR</b>	<b>2.17</b>	<b>2.27</b>	<b>1.58</b>	<b>1.24</b>	<b>1.13</b>	<b>1.33</b>	<b>1.74</b>	<b>1.22</b>	<b>0.78</b>

**Table 6.2** The summary statistics (Mean, SD, Median and IQR) of the Michelson contrast expressed as sensitivity (dB) at -14°, 4° eccentricity for each of the 8 different checks per cycle of the given noise mask and without the noise mask.

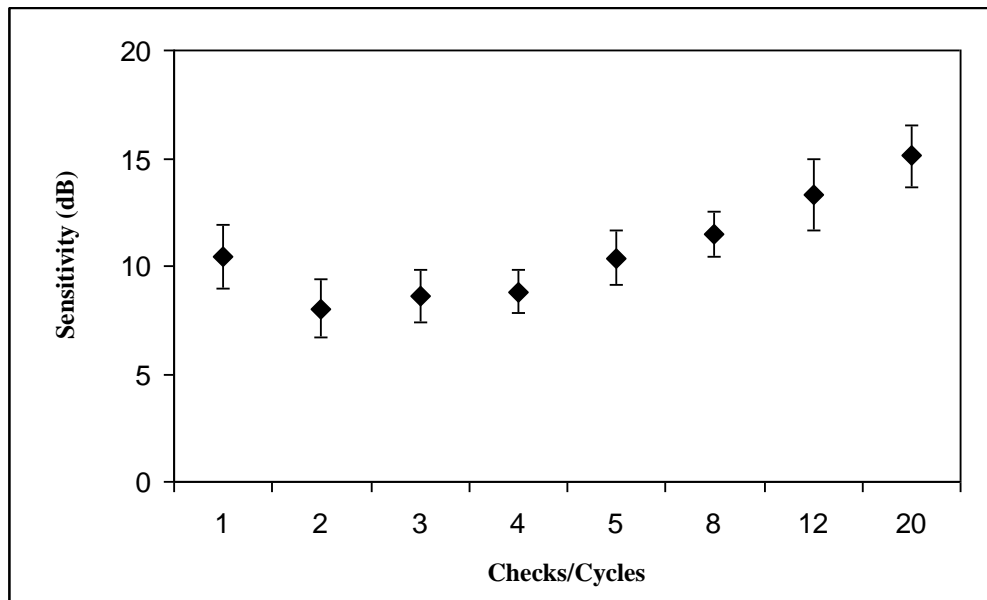


**Figure 6.2** Group mean sensitivity against number of checks per cycle of the given noise mask at -14°, 4° eccentricity for the 11 normal individuals. The error bars indicate one standard deviation of the mean.

Stimulus location (-22°, +4°)									
	With the noise mask								Without the noise mask
	Checks/Cycle								
	1	2	3	4	5	8	12	20	
<b>Individual</b>									
<b>6</b>	10.17	9.01	9.95	9.53	9.95	11.26	11.48	13.08	14.80
<b>9</b>	8.80	8.27	8.02	9.40	10.59	10.60	10.80	12.35	14.73
<b>11</b>	7.79	6.74	7.41	8.39	12.59	11.12	14.31	13.86	15.73
<b>12</b>	6.68	6.23	8.23	8.24	8.91	11.01	13.35	11.59	15.05
<b>15</b>	6.70	5.11	5.38	6.06	8.24	9.74	13.46	12.51	16.21
<b>16</b>	7.77	5.61	5.94	7.66	7.49	10.30	11.96	14.59	14.59
<b>17</b>	10.82	9.80	10.54	10.47	12.89	12.72	13.04	15.98	15.73
<b>18</b>	10.63	9.74	10.89	8.60	12.72	12.72	13.04	14.51	14.96
<b>19</b>	9.51	8.36	8.10	8.75	8.91	11.55	12.76	15.77	16.00
<b>20</b>	9.95	9.37	8.18	9.80	10.35	12.54	13.88	12.25	15.45
<b>21</b>	8.16	6.39	7.86	7.37	9.62	11.68	13.74	14.93	14.48
<b>Mean</b>	<b>8.82</b>	<b>7.69</b>	<b>8.23</b>	<b>8.57</b>	<b>10.21</b>	<b>11.39</b>	<b>12.89</b>	<b>13.77</b>	<b>15.25</b>
<b>SD</b>	<b>1.50</b>	<b>1.72</b>	<b>1.72</b>	<b>1.24</b>	<b>1.85</b>	<b>0.99</b>	<b>1.07</b>	<b>1.50</b>	<b>0.60</b>
<b>Median</b>	<b>8.80</b>	<b>8.27</b>	<b>8.10</b>	<b>8.60</b>	<b>9.95</b>	<b>11.26</b>	<b>13.04</b>	<b>13.86</b>	<b>15.05</b>
<b>IQR</b>	<b>2.28</b>	<b>2.88</b>	<b>1.45</b>	<b>1.52</b>	<b>2.68</b>	<b>1.31</b>	<b>1.24</b>	<b>2.33</b>	<b>0.97</b>

**Table 6.3** The summary statistics (Mean, SD, Median and IQR) of the Michelson contrast expressed as sensitivity (dB) at -22°, +4° eccentricity for each of the 8 different checks per cycle of the given noise mask and without the noise mask.

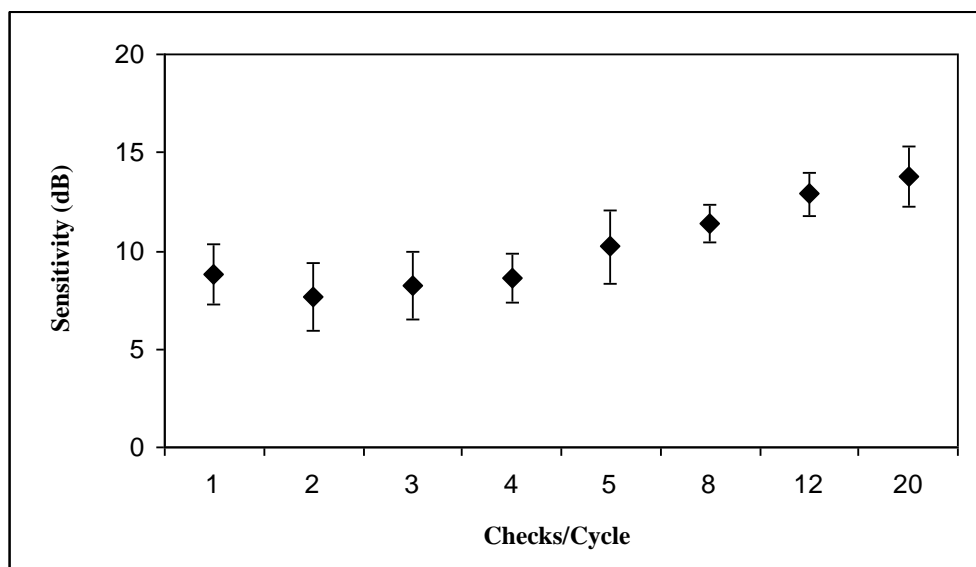


**Figure 6.3** Group mean sensitivity against number of checks per cycle of the given noise mask at -22°, 4° eccentricity for the 11 normal individuals. The error bars indicate one standard deviation of the mean.

Factor	Numerator Degrees of Freedom	Denominator Degrees of Freedom	F value	P value
<b>Eccentricity</b>	2	260	12.29	<0.0001
<b>Checks per cycle</b>	8	260	296.22	<0.0001
<b>Checks/cycle*eccentricity</b>	16	260	10.40	<0.0001
<b>Age</b>	1	9	0.16	0.7005

**Table 6.4** The ANOVA Summary Table for the Michelson contrast expressed as sensitivity (dB). The data in the absence of the noise mask is included.

Factor	Numerator Degrees of Freedom	Denominator Degrees of Freedom	F value	P value
<b>Eccentricity</b>	2	230	26.89	<0.0001
<b>Checks per cycle</b>	7	230	172.90	<0.0001
<b>Checks/cycle*eccentricity</b>	14	230	3.99	<0.0001
<b>Age</b>	1	9	0.23	0.6425

**Table 6.5** The ANOVA Summary Table for the Michelson contrast expressed as sensitivity (dB). The data in the absence of the noise mask is excluded.

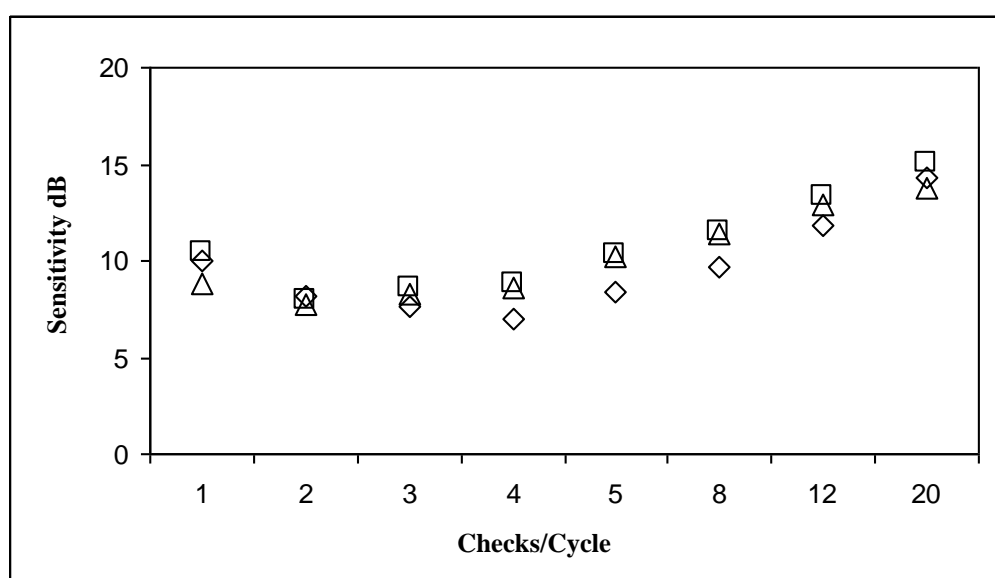


**Figure 6.4** Group mean sensitivity against number of checks per cycle of the given noise mask by eccentricity for the 11 normal individuals. The error bars have been omitted for clarity. The diamonds, squares and triangles represent eccentricities of 0°, 0°, -14°, 4° and -22°, 4°, respectively.

## Age

Sensitivity, overall, was not influenced by age ( $p = 0.642$ ) in either model even though the age range of the individuals varied from 21 to 37 years.

## **6.5 Discussion**

The optimum (in terms of the minimum Mean, SD, Median and IQR) noise mask at the fovea was 3 and 4 checks per grating cycle. The optimum noise mask at the two more peripheral stimulus locations was less clear; however, 4 checks per grating cycle resulted in the proportionally smallest SD for each of the two peripheral locations. These findings were in accord with that of Kukkonen et. al. (1995) who found that the critical check size is influenced by the temporal and spatial parameters of the underlying stimulus. For low to medium spatial frequency gratings, i.e. 1 to 4 cycles per degree, the critical check size was 4.2 checks per cycle and for 64 cycles per degree, the critical check size was 2.6 checks per cycle (Kukkonen, Rovamo and Nasanen, 1995). Given that the stimulus size subtended  $4^\circ \times 4^\circ$  and contained 2 grating cycles, it was convenient to utilize the 4 checks per cycle noise mask for each stimulus location.

In terms of Michelson contrast, the 4 checks per grating cycle resulted in the required 3 fold reduction in the Michelson contrast; however, the Michelson contrast in the presence of the noise mask, expressed as sensitivity in dB, increased within increase in eccentricity. Such a sensitivity gradient is unique in clinical perimetry. Nevertheless, given that the identification of an abnormal response, at any given stimulus location, is dependent upon the statistical comparison of the measured sensitivity with that of the age-corrected

sensitivity, the shape/ and or slope of the sensitivity gradient is immaterial. The use of a noise mask containing 2 checks per grating cycle at the peripheral locations would result in an approximately flat sensitivity gradient, which is more familiar in clinical perimetry, i.e., the Esterman Test, but at the expense of a reduction in dynamic range in the more peripheral regions.

## Chapter 7

### Threshold algorithm development for Dynamic Noise Perimetry

#### 7.1 Background

The classical non-adaptive method for determining threshold is the Method of Limits, whereby the stimulus luminance varies in small steps either in an ascending or a descending direction with the start and reversing values corresponding to the upper and lower limits of a predefined range. A large amount of information is wasted with this technique because the start value is presented far from the threshold and an excessive time is taken to obtain the threshold (Treutwein, 1995; Phipps et al., 2001).

The adaptive method is the current approach, whereby the stimulus luminance varies dependent upon the individual's previous responses. The procedure is termed the staircase, or bracketing, method (Wetherill and Levitt, 1965). The staircase presents a series of 'up' and 'down' steps around the threshold and the steps vary in size. This method also avoids the problems of the classical method by presenting the stimulus at, or near, the expected threshold (Treutwein, 1995). The examination duration for the determination of threshold is shorter than the non-adaptive method (Phipps et al., 2001).

The binary search staircase is an efficient means of searching an ordered array, which, in a manner similar to the bracketing strategy, utilizes information gained with each stimulus presentation to determine the next step of the search (Tyrrell and Owens, 1988). The

modified binary search (MOBS) staircase was developed to offer improvements in both accuracy and efficiency for threshold determination (Tyrrell and Owens, 1988).

A further type of threshold algorithm is the maximum likelihood estimation. This algorithm is more computationally complex than the staircase method. Examples include the Parameter Estimation by Sequential Testing (PEST) (Taylor and Douglas Creelman, 1967; Treutwein, 1995); the Zippy Estimation by Sequential Testing (ZEST) (Turpin et al., 2003; McKendrick, 2005; Anderson and Johnson, 2006); and the Quick Estimation by Sequential Testing (QUEST) (Watson and Pelli, 1983). The maximum likelihood estimation is different to the staircase method in that the start value, at any given location, is based upon a prior distribution of expected values at that location and is termed a probability density function (pdf) (Tyrrell and Owens, 1988). The probability density function reduces the examination duration by placing the start value close to the most likely endpoint thereby ensuring the minimum number of responses to obtain the threshold (Phipps et al., 2001).

The best PEST algorithm starts with a binary staircase and then, after the first reversal, adopts the QUEST logic.

The ZEST algorithm presents the initial stimulus luminance at a level equal to the mean of the initial pdf and uses the response to generate a new pdf by multiplying the old pdf by a likelihood function that is similar to the frequency-of-seeing curve (Turpin et al., 2003). After determination of the new pdf, the new mean is calculated and the stimulus intensity equal to that mean is presented. The process is repeated until a termination criterion is met

(i.e., the SD of the pdf is  $<0.50\text{dB}$ ). The output threshold is the mean of the final pdf (Turpin et al., 2003).

The QUEST algorithm uses the mode of the new pdf, instead of the mean as in ZEST. Both the mode in QUEST and/ or the mean in ZEST of the final pdf is considered the best estimate of the individual threshold.

## **7.2 The ‘Proof of Concept algorithm’**

The algorithm developed by Dr. Rattan for his pilot studies of DNP was termed the ‘Proof of Concept algorithm’ (Rattan, 2010).

The ‘Proof of Concept algorithm’ was a combination of two maximum likelihood methods of determining threshold, PEST and ZEST (Anderson and Johnson, 2006) and utilised the up-and-down transformed response rule (Wetherill and Levitt, 1965). The length of the threshold sequence was dependent upon the number of correct responses required to reduce the contrast of the grating by a step size of 1dB.

A schematic of the ‘Proof of Concept algorithm’ is illustrated in Figure 7.1 and was used both in the absence and in the presence of the noise mask. Based on pilot studies, Dr Rattan had selected the starting level for the contrast of the grating to be at least 4dB above threshold, both in the absence and in the presence of the noise mask, respectively, in order to ensure that the grating was clearly visible. This approach allowed individuals to familiarise themselves with both tasks before the staircase commenced. Throughout the

initial, or starting, phase of the staircase, a single correct answer reduced the level of contrast of the grating by 1dB. This approach was adopted to enable the sequence to reach rapidly the threshold region (Cornsweet, 1962). The first incorrect response did not change the contrast (i.e., the response was ignored). However, a second incorrect response at the same level of contrast increased the contrast of the grating by 1dB and, with the second incorrect response, the direction of contrast of the grating changed from a descending trend (reducing the level of contrast) to an ascending trend (increasing the level of contrast) and was considered as the first ‘reversal’ of the staircase. Then, from the ‘secondary phase’ of the staircase onwards, a sequence of four correct responses was required to reduce the grating contrast level by 1dB, and one incorrect response to increase the grating contrast level by 1dB. Four correct responses corresponded to a probability of 0.84 of seeing the threshold (Rovamo et al., 1993a; Rovamo, Luntinen and Nasanen, 1993b; Kukkonen et al., 1995; Rovamo and Kukkonen, 1996; Kukkonen et al., 2002). Each subsequent reversal corresponded to a directional change in the staircase (i.e. from a descending to an ascending trend or vice versa).

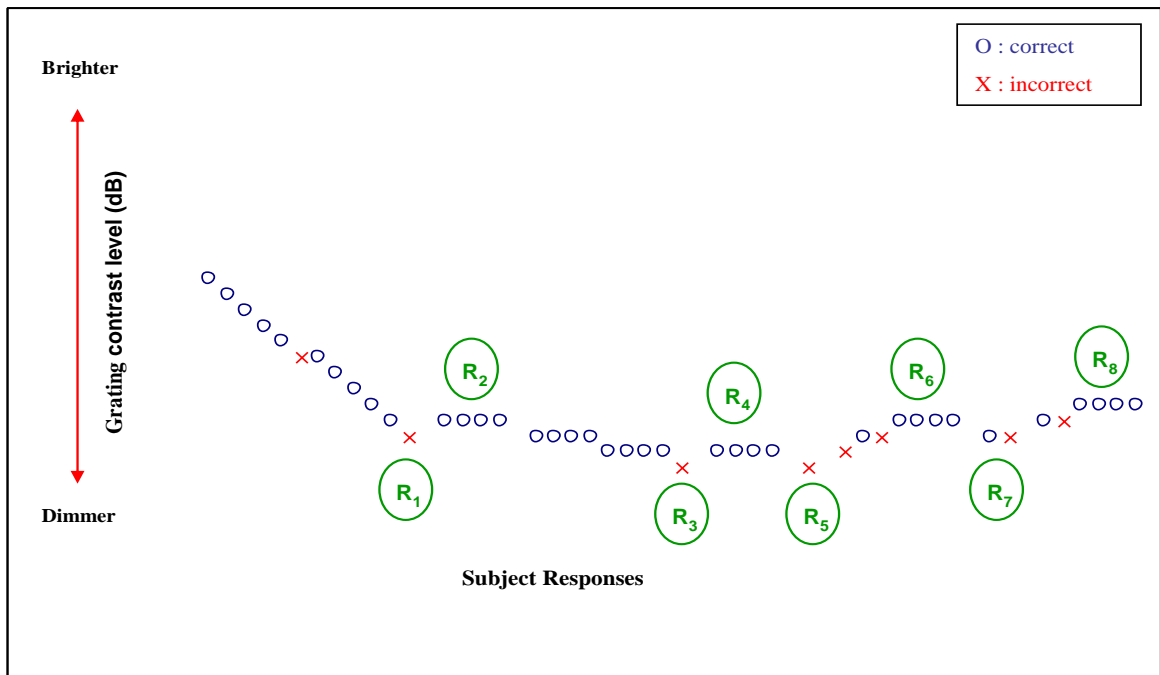


**Figure 7.1** A schematic of the ‘Proof of Concept algorithm’ where 8 reversals determines the length of the staircase, and the geometric mean of the last 6 reversals is used to calculate the final threshold. R<sub>1</sub> through to R<sub>8</sub> represents the corresponding reversal.

The accuracy of the final threshold estimation increases as the number of reversals increases (Wetherill and Levitt, 1965). However, the time taken to reach threshold increases with increase in the number of reversals. Other comparable studies in the visual psychophysical literature have indicated that six to eight reversals are acceptable for determining the threshold (Kukkonen et al., 1995). Dr Rattan adopted eight reversals, and the final threshold value was considered to be the geometric mean of the last six reversals.

The duration of the thresholding procedure at a single stimulus location was between approximately 2 and 2.5 minutes (i.e. a total of four to five minutes to obtain the threshold at one stimulus location in the absence and then in the presence of the noise mask).

The aim of the work described in this chapter was to make DNP suitable for clinical purposes by reducing the examination duration and by increasing the number of stimulus locations whilst maintaining the accuracy and efficiency of the threshold estimation.

### **7.3 Further development of the ‘Proof of concept algorithm’**

The further development of the algorithm for DNP was undertaken in stages with particular regard to the variability associated with, and the time taken for, determining the threshold. The initial modifications were based upon changes to the ‘Proof of Concept algorithm.’ The development was undertaken with an iterative approach.

#### **7.3.1 First iteration**

The first iteration was divided into two phases with each phase sharing the same algorithm but using a different number of stimulus locations. Eight stimulus locations were selected for the first phase and twelve locations for the second phase. The stimulus locations were selected on the basis of the structural and functional topographic mapping of the retinal nerve fibre layer (Garway-Heath et al., 2000b).

The eight stimulus locations for the first phase were selected, in right eye format, as  $0^\circ, 0^\circ$ ;  $-10^\circ, +8^\circ$ ;  $-10^\circ, -8^\circ$ ;  $-26^\circ, +4^\circ$ ;  $+6^\circ, +4^\circ$ ;  $+10^\circ, -12^\circ$ ;  $+10^\circ, +12^\circ$ ; and  $-6^\circ, +16^\circ$ . The additional four stimulus locations for the second phase were selected, in right eye format, as  $-26^\circ, -4^\circ$ ;  $-18^\circ, +12^\circ$ ;  $-18^\circ, -12^\circ$ ; and  $-6^\circ, -16^\circ$  (Figure 7.2).

The essential modification to the staircase sequence with each phase comprised a variable step size and a shorter sequence of stimulus presentations.

The starting level of contrast was selected to be 4dB above the age-corrected value based upon Dr Rattan's database of 23 normal individuals ranging in age from 15 to 84 years (mean age 53.0 years, SD 20.7). Four reversals were required to determine the final threshold at each location.

During the first reversal of the staircase, a single correct answer reduced the contrast of the grating by 4dB. This modification was made in order to ensure that the threshold level was approached rapidly. After the first correct answer, each subsequent correct answer reduced the contrast of the grating by 1dB. The first incorrect answer did not change the contrast level (i.e., the response was ignored); however, a second successive incorrect response resulted in a 4dB increase in contrast.

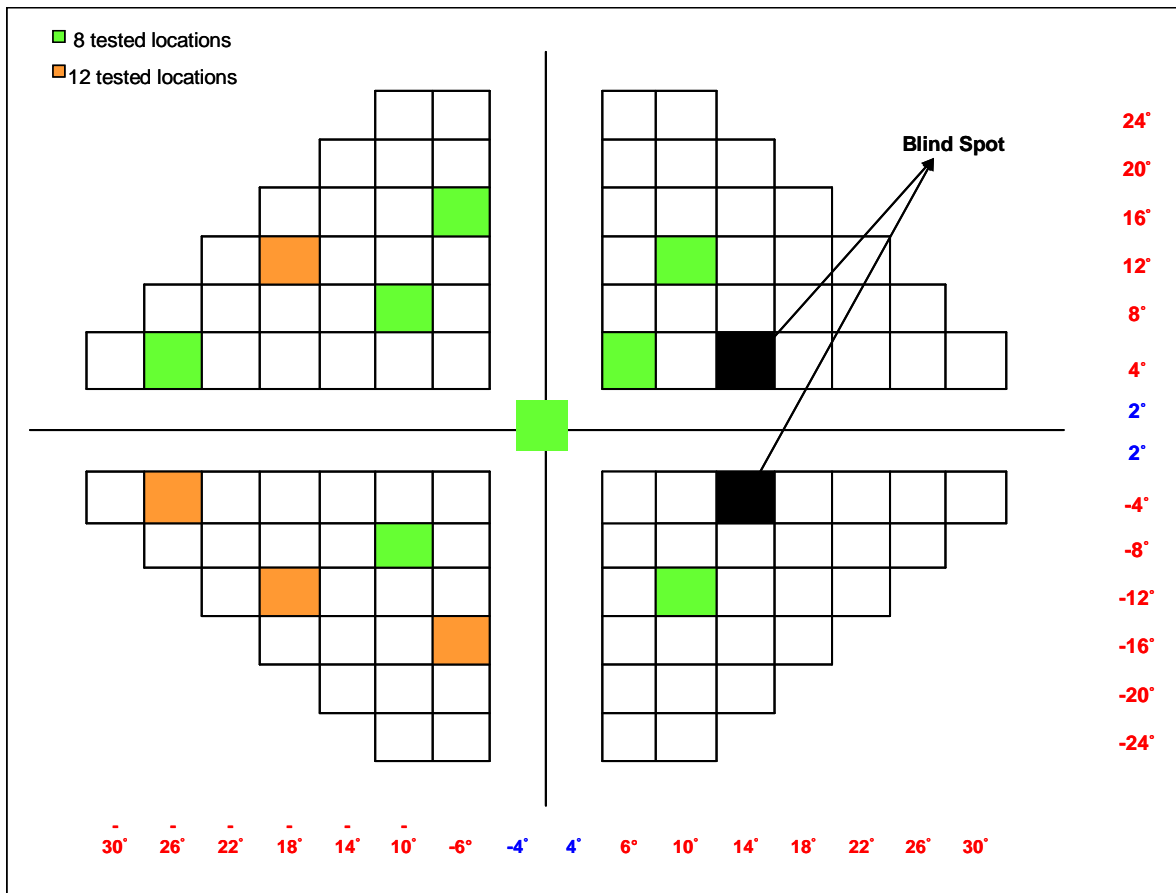


**Figure 7.2** The stimulus grid for DNP in right eye format. The eight stimulus locations used in the first phase are highlighted in green and the additional four stimulus locations used in the second phase are highlighted in orange. The black squares indicate the blind spot.

For the second and the third reversals of the staircase, a sequence of two correct responses was required for a reduction in the contrast of the grating by 1dB and one incorrect response to raise the contrast by 1dB. For the fourth reversal, where the staircase of the algorithm terminated, a sequence of either three successive correct responses or one incorrect response, only, was required to reach the endpoint of the algorithm.

The threshold value was defined as the average of the last reversal (i.e. the average of the value of the incorrect response and of the correct response).

A schematic of the staircase procedure that determined a threshold which was located at 1.5dB above the age-corrected value is illustrated in Figure 7.3. Similarly, the procedure for determining the threshold which was 1.5dB below the age-corrected value is illustrated in Figure 7.4.

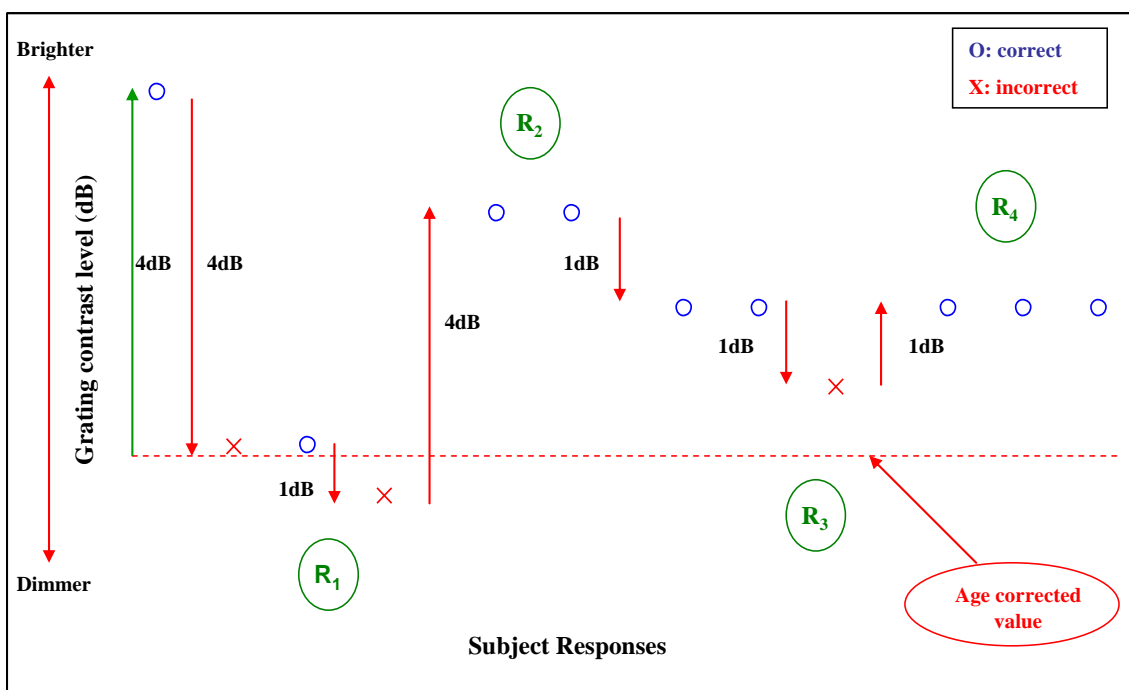


**Figure 7.3** A schematic of the staircase algorithm where 4 reversals determine the length of the staircase, and the final reversal is used to calculate threshold. The final threshold is 1.5dB above the age-corrected value. R<sub>1</sub> through to R<sub>4</sub> represents the corresponding reversal.

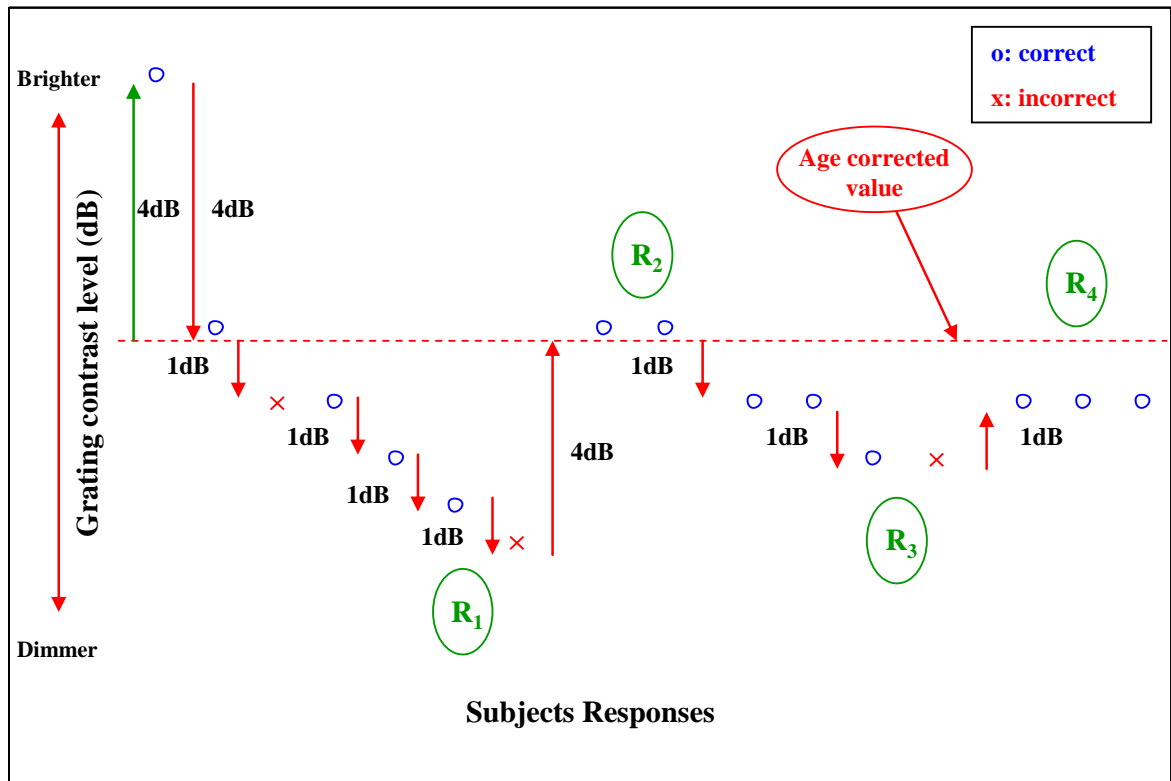


**Figure 7.4** A schematic of the staircase algorithm where 4 reversals determine the length of the staircase, and the final reversal is used to calculate threshold. The final threshold is 1.50dB below the age-corrected value. R<sub>1</sub> through to R<sub>4</sub> represents the corresponding reversal.

During the first reversal, an incorrect response after the first correct response resulted in a 4dB increase in the contrast of the grating. A subsequent successive (i.e., second) single incorrect response raised the contrast by 1dB. A further successive (i.e., third) single incorrect response terminated the threshold sequence. A schematic of the staircase procedure is illustrated in Figure 7.5.

Similarly, during the first reversal, if the first response at the start value was incorrect, the contrast level of the grating was increased by 1dB. A further (i.e., second) successive incorrect response, increased the contrast by 1dB and a third successive incorrect response terminated the determination at the given location. A schematic of the staircase procedure with three single successive incorrect responses during the first reversal is illustrated in Figure 7.6.

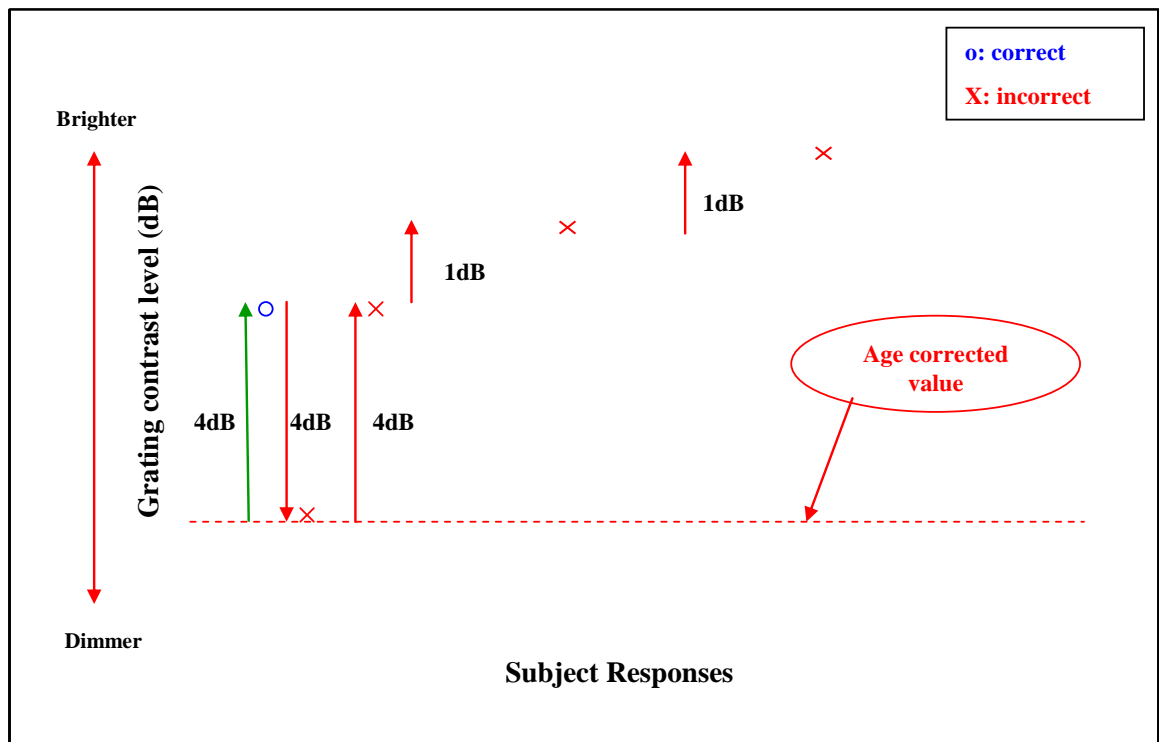


**Figure 7.5** A schematic where, during the first reversal, four consecutive incorrect responses after the first correct response at the start value terminates the threshold sequence.

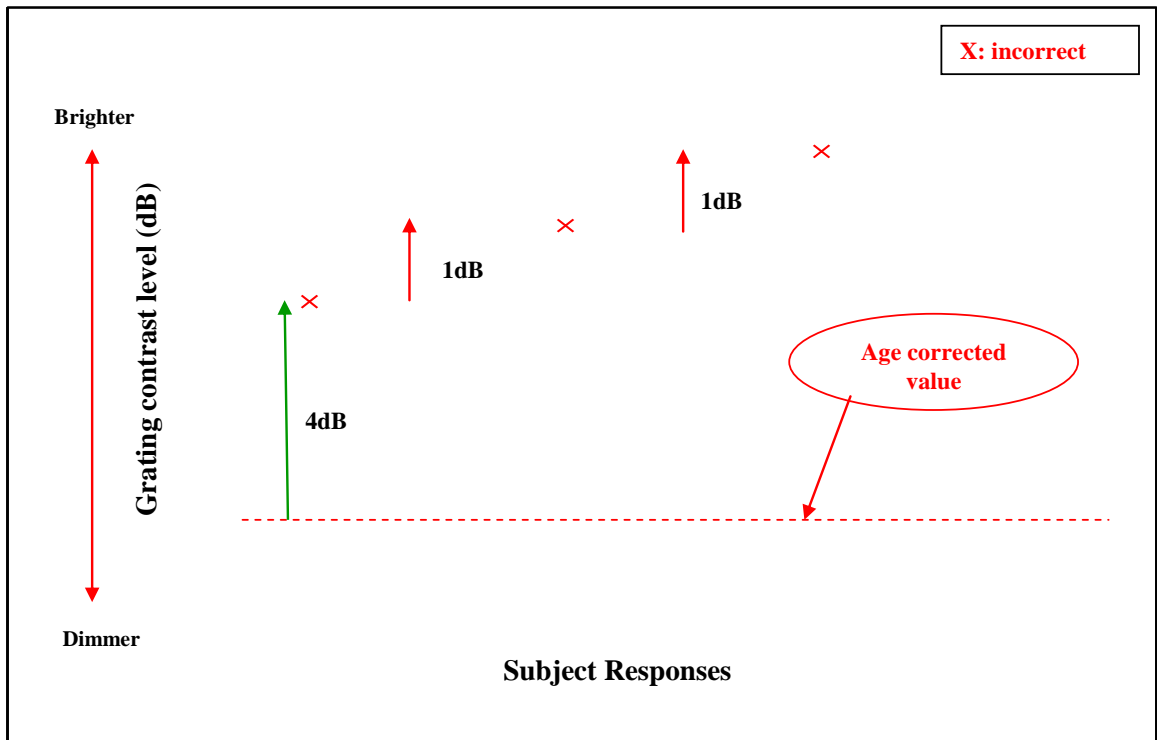


**Figure 7.6** A schematic where, during the first reversal, three consecutive incorrect responses including that at the start value terminates the threshold sequence.

### 7.3.1.1 Cohort and DNP methodology

The final version of the first iteration was formally evaluated over two phases.

The first phase was undertaken by four normal individuals and the second phase by the same four normal individuals and a further two normal individuals.

The purpose of the first phase was to determine the variability of the threshold response and the duration of the examination. The purpose of the second phase was twofold: firstly, to collect an additional data set from a further two individuals and, secondly, to determine

the time necessary to obtain the threshold at an additional 4 stimulus locations, i.e., 12 in total, for each of the six individuals.

All six individuals were recruited from the students and the staff of the Cardiff School of Optometry and Vision Sciences, were highly experienced in visual psychophysical experiments and were familiar with the DNP thresholding logic. Prior to the study, each individual had undergone an ophthalmic examination to ensure conformity with the inclusion criteria for entry into the study. The inclusion criteria were as those described in Chapters 5, 6, 8.

The ages of the four individuals who took part in both phases were 29, 33, 39 and 57 years, respectively. The ages of the two additional normal individuals who took part in the second phase were 26 and 45 years.

The four individuals underwent DNP, in one randomly designated eye, in the absence of, and then in the presence of, the noise mask for each of the two phases. The first phase was undertaken before the second phase. For the first phase, the thresholds for each of the 8 stimulus locations were obtained on three separate visits, with each visit separated by one week. For the second phase, the thresholds for each of the 12 stimulus locations were obtained at a fourth visit.

The two additional individuals underwent DNP, in one randomly designated eye, in the absence of, and then in the presence of, the noise mask for the second phase. The thresholds for each of the 12 stimulus locations were obtained on three separate visits with each visit separated by one week.

All six individuals wore their distance refractive correction in trial lens form, corrected where necessary for the 30 cm viewing distance of the monitor. Rest periods of one minute were given approximately every three minutes, and of approximately 5 minutes between tests, to minimise the fatigue effect.

### **7.3.1.2 Analysis**

The analysis of variability of the threshold response at each stimulus location over the three visits, both in the absence and in the presence of the noise mask, was undertaken in terms of the Coefficient of Variation (defined as the SD divided by the Mean). The examination duration was considered in terms of that at the fourth visit for the 4 individuals and in terms of the last of the three visits for the additional two individuals.

### **7.3.1.3 Results**

The mean and SD of the Michelson contrast, in the absence of the noise mask, expressed as sensitivity (dB), across the three visits by stimulus location for each of the six individuals is given in Table 7.1 and in the presence of the noise mask in Table 7.2. The mean and SD of the examination duration, in the absence and in the presence of the noise mask, for the corresponding three visits is also given in Tables 7.1 and 7.2, respectively.

Locations	26 years sensitivity (dB)	29 years sensitivity (dB)	33 years sensitivity (dB)	36 years sensitivity (dB)	39 years sensitivity (dB)	57 years sensitivity (dB)
0°, 0°	16.66 (0.60)	17.64 (0.45)	18.40 (1.13)	18.17 (0.09)	17.14 (1.11)	16.56 (1.10)
+6°, +4°	15.09 (0.24)	15.90 (0.83)	17.87 (1.08)	17.44 (0.58)	16.97 (1.30)	14.91 (0.85)
-10°, +8°	14.90 (1.58)	16.08 (1.39)	15.39 (0.58)	16.82 (0.63)	14.93 (0.35)	14.22 (0.37)
-10°, -8°	14.55 (1.59)	15.86 (0.69)	16.38 (0.28)	16.83 (0.45)	14.58 (0.56)	14.78 (0.60)
+10°, +12°	15.75 (0.51)	16.85 (1.06)	16.25 (1.05)	16.19 (1.29)	16.22 (1.16)	14.17 (0.63)
+10°, -12°	17.14 (1.54)	18.00 (0.27)	16.20 (0.24)	15.45 (1.08)	14.53 (1.32)	16.08 (1.11)
-6°, +16°	15.40 (0.82)	16.17 (0.82)	16.11 (0.55)	15.05 (1.01)	13.51 (0.43)	15.18 (0.92)
-26°, +4°	13.43 (0.66)	16.09 (1.23)	14.66 (0.56)	15.18 (0.59)	13.38 (0.67)	11.84 (0.88)
<b>Duration (sec)</b>	<b>274.3 (25.5)</b>	<b>302.2 (32.0)</b>	<b>300.1 (25.0)</b>	<b>312.0 (27.4)</b>	<b>323.2 (31.2)</b>	<b>335.3 (31.2)</b>

**Table 7.1** The Mean (SD) of the Michelson contrast, in the absence of the noise mask, expressed as sensitivity (dB) across the three visits for each of the eight stimulus locations for each of the six individuals. The Mean and SD of the examination duration across the three visits for each individual are also shown.

Locations	26 years sensitivity (dB)	29 years sensitivity (dB)	33 years sensitivity (dB)	36 years sensitivity (dB)	39 years sensitivity (dB)	57 years sensitivity (dB)
0°, 0°	8.07 (1.00)	8.40 (1.09)	9.13 (1.48)	7.76 (1.91)	9.02 (0.56)	8.78 (0.71)
+6°, +4°	8.79 (1.04)	8.22 (0.50)	9.58 (0.40)	9.79 (1.04)	8.72 (0.53)	7.27 (0.86)
-10°, +8°	7.54 (1.09)	9.43 (0.30)	10.38 (0.38)	9.07 (0.17)	8.10 (0.91)	7.91 (0.98)
-10°, -8°	9.67 (1.13)	9.85 (1.09)	9.93 (0.48)	9.59 (0.64)	8.90 (0.84)	8.97 (0.80)
+10°, +12°	9.14 (1.01)	9.05 (1.54)	8.95 (0.62)	8.53 (1.50)	8.77 (0.91)	8.27 (1.16)
+10°, -12°	9.74 (1.25)	8.92 (1.07)	9.39 (1.33)	11.79 (1.72)	9.37 (0.86)	8.70 (0.59)
-6°, +16°	9.85 (0.17)	9.03 (0.84)	9.62 (0.80)	9.57 (0.18)	9.19 (0.32)	8.85 (1.86)
-26°, +4°	9.80 (1.09)	7.64 (0.82)	9.72 (0.82)	10.67 (0.00)	7.58 (0.49)	8.56 (0.30)
<b>Duration (sec)</b>	<b>315.3 (10.3)</b>	<b>306.0 (15.1)</b>	<b>316.2 (18.1)</b>	<b>330.0 (20.0)</b>	<b>346.3 (23.5)</b>	<b>377.5 (49.0)</b>

**Table 7.2** The Mean (SD) of the Michelson contrast, in the presence of the noise mask, expressed as sensitivity (dB) across the three visits for each of the eight stimulus locations for each of the six individuals. The Mean and SD of the examination duration across the three visits for each individual are also shown.

The Coefficient of Variation, for the data sets illustrated in Tables 7.3 and 7.4 are shown in Tables 7.4 and 7.5, respectively.

Locations	26 years sensitivity (dB)	29 years sensitivity (dB)	33 years sensitivity (dB)	36 years sensitivity (dB)	39 years sensitivity (dB)	57 years sensitivity (dB)
0°, 0°	3.6	2.6	6.1	0.5	6.5	6.6
+6°, +4°	1.6	5.2	6.0	3.3	7.7	5.7
-10°, +8°	10.6	8.6	3.8	3.8	2.3	2.6
-10°, -8°	11.0	4.4	1.7	2.7	3.8	4.1
+10°, +12°	3.3	6.3	6.5	8.0	7.2	4.4
+10°, -12°	9.0	1.5	1.5	7.0	9.1	6.9
-6°, +16°	5.3	5.1	3.4	6.7	3.2	6.1
-26°, +4°	4.9	7.6	3.8	3.9	5.0	7.4

**Table 7.3** The Coefficient of Variation (%) of the Michelson contrast, in the absence of the noise mask, expressed as sensitivity (dB), for the three visits for each of the eight stimulus locations for each of the six individuals.

Locations	26 years sensitivity (dB)	29 years sensitivity (dB)	33 years sensitivity (dB)	36 years sensitivity (dB)	39 years sensitivity (dB)	57 years sensitivity (dB)
0°, 0°	12.4	13.0	16.2	24.6	6.2	8.1
+6°, +4°	11.9	6.1	4.2	10.6	6.1	11.8
-10°, +8°	14.5	3.2	3.7	1.9	11.2	12.4
-10°, -8°	11.7	11.1	4.8	6.6	9.4	8.9
+10°, +12°	11.0	17.0	6.9	17.6	10.4	14.0
+10°, -12°	12.9	12.0	14.2	14.6	9.2	6.8
-6°, +16°	1.8	9.3	8.3	4.4	3.5	21.0
-26°, +4°	11.1	10.7	8.4	0.0	6.5	3.5

**Table 7.4** The Coefficient of Variation (%) of the Michelson contrast, in the presence of the noise mask, expressed as sensitivity (dB), for the three visits for each of the eight stimulus locations for each of the six individuals.

Locations	26 years sensitivity (dB)	29 years sensitivity (dB)	33 years sensitivity (dB)	36 years sensitivity (dB)	39 years sensitivity (dB)	57 years sensitivity (dB)
0°, 0°	3.4	5.1	2.6	47.6	1.0	1.2
+6°, +4°	7.6	1.8	2.4	3.2	1.1	3.5
-10°, +8°	1.4	1.2	2.8	0.5	2.5	2.2
-10°, -8°	1.1	0.4	1.1	2.5	1.5	3.2
+10°, +12°	1.2	2.5	0.7	2.2	0.8	2.1
+10°, -12°	1.4	2.7	1.0	2.1	4.8	4.8
-6°, +16°	0.3	1.4	2.2	0.3	1.3	0.5
-26°, +4°	2.3	8.0	9.6	0.0	1.0	1.0

**Table 7.4** The ratio of the Coefficient of Variation in the presence of the noise mask to that in the absence of the noise mask.

The Michelson contrast, in the absence of the noise mask, expressed as sensitivity (dB) for the 12 stimulus locations for each of the six individuals is given in Table 7.5 and in the presence of the noise mask in Table 7.6. The corresponding examination durations, are also given in Tables 7.5 and 7.6, respectively.

Locations	26 years sensitivity (dB)	29 years sensitivity (dB)	33 years sensitivity (dB)	36 years sensitivity (dB)	39 years sensitivity (dB)	57 years sensitivity (dB)
0°, 0°	17.09	18.22	17.48	18.06	17.82	17.78
+6°, +4°	15.55	15.74	18.10	16.77	15.75	15.81
-10°, +8°	16.25	19.29	16.62	17.26	16.13	15.24
-10°, -8°	18.42	17.12	14.45	15.23	16.13	15.16
+10°, +12°	12.71	15.66	15.81	16.85	14.40	12.31
+10°, -12°	13.16	15.13	16.09	14.63	14.12	14.80
-6°, +16°	15.27	16.35	17.05	17.23	17.13	15.81
-6°, -16°	13.74	17.36	15.59	15.80	14.84	14.80
-18°, +12°	15.38	15.23	14.04	14.98	13.12	13.42
-18°, -12°	11.51	12.63	16.09	13.88	14.14	15.43
-26°, +4°	13.12	14.65	15.09	14.91	15.66	17.33
-26°, -4°	12.42	16.22	10.60	13.80	14.66	14.21
<b>Duration (sec)</b>	<b>721.2</b>	<b>720.0</b>	<b>720.3</b>	<b>670.2</b>	<b>760.0</b>	<b>840.3</b>

**Table 7.5** The Michelson contrast, in the absence of the noise mask, expressed as sensitivity (dB) for each of the 12 stimulus locations for each of the six individuals. The examination duration is also shown.

Locations	26 years sensitivity (dB)	29 years sensitivity (dB)	33 years sensitivity (dB)	36 years sensitivity (dB)	39 years sensitivity (dB)	57 years sensitivity (dB)
0°, 0°	8.04	9.67	7.68	6.65	8.96	8.47
+6°, +4°	8.75	8.42	9.20	9.20	8.18	8.28
-10°, +8°	6.64	9.70	9.97	8.97	8.30	7.80
-10°, -8°	9.74	8.69	9.42	9.22	8.77	7.88
+10°, +12°	9.23	9.73	8.36	7.66	8.88	9.34
+10°, -12°	8.34	7.69	10.40	12.78	8.28	8.34
-6°, +16°	9.75	8.71	9.67	9.67	8.66	9.30
-6°, -16°	8.33	9.72	10.45	10.45	8.66	9.85
-18°, +12°	9.28	8.70	9.81	9.81	8.27	8.05
-18°, -12°	8.75	8.05	10.67	10.67	7.66	6.33
-26°, +4°	9.75	7.89	10.57	10.67	7.66	9.34
-26°, -4°	8.40	7.90	10.43	10.68	7.21	9.42
<b>Duration (sec)</b>	<b>823.3</b>	<b>750.0</b>	<b>773.1</b>	<b>690.3</b>	<b>720.5</b>	<b>1020.1</b>

**Table 7.6** The Michelson contrast, in the presence of the noise mask, expressed as sensitivity (dB) for each of the 12 stimulus locations for each of the six individuals. The examination duration is also shown.

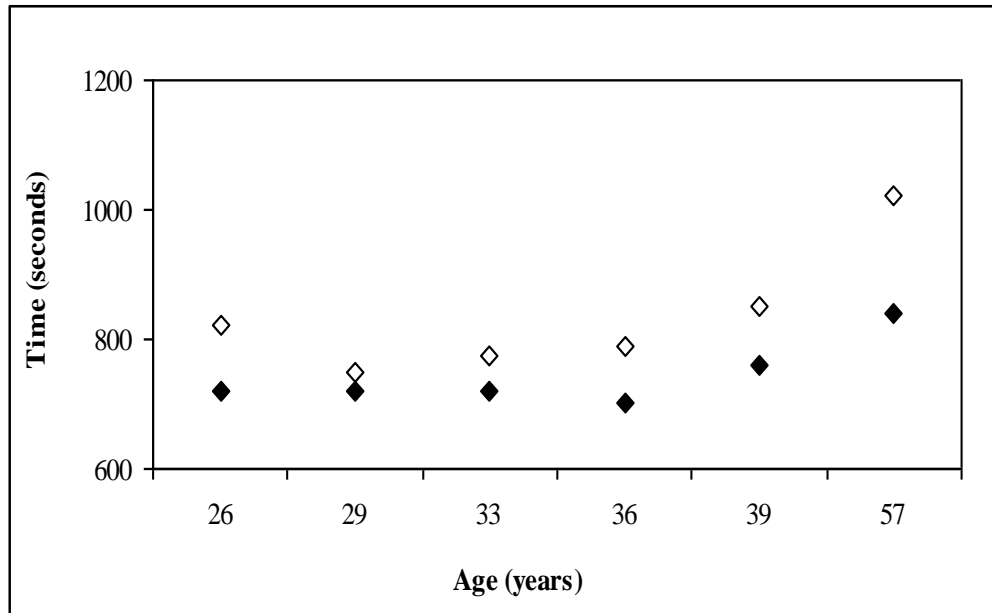


**Figure 7.7** The examination duration (sec) for the 12 stimulus locations in the absence (filled symbols) and in the presence (open symbols) of the noise mask for the six individuals.

#### **7.3.1.4 Discussion**

The use of the Coefficient of Variation is dependent upon heteroscedasticity of the given dataset, i.e., the magnitude of the SD increases with the magnitude of the mean. Classically, the variability associated with the differential light sensitivity, expressed in dB, increases as the sensitivity declines upto approximately 12-15dB after which it declines (Heijl, Lindgren and Olsson, 1989; Russell et al., 2012; Gardiner, 2014). Nevertheless, the Coefficient of Variation, has been used in relation to High Pass Resolution perimetry (Wall, Lefante and Conway, 1991), short-wavelength automated perimetry and standard automated perimetry (Wild et al., 1998; Acton, Gibson and Cubbidge, 2012) and short-wavelength automated perimetry, alone (Cubbidge, Hosking and Embleton, 2002).

The 'acceptable' magnitude for a Coefficient of Variation is empirical. The results for variability of the first iteration of the algorithm can be placed in the context of the Coefficient of Variation for an objective measurement such as the measurement of the peripapillary retinal nerve fibre layer thickness. By Time-domain optical coherence tomography, the Coefficient of Variation, for 5 circular scans at each of 8 sessions, was approximately 7% in 10 normal individuals and 12% in 10 individuals with open angle glaucoma (Blumenthal et al., 2000b). For, Spectral-domain optical coherence tomography, the CVs ranged from 1.45% for the global retinal nerve fibre layer thickness to 2.59% for the temporal quadrant thickness in 45 normal individuals and from 1.74% to 3.22%, respectively, in 33 individuals with open angle glaucoma. However, the Coefficient of Variation for the multifocal visual evoked potential would appear to be larger: in 5 normal individuals over 5 visits, it was less than 20% at most stimulus locations (i.e., range 6.8% - 25.9%; mean 15.2% SD 4.5%).

For standard automated perimetry, using Program 30-2 of the Humphrey Field Analyzer, the Coefficient of Variation, based upon 51 normal individuals, increased with increase in eccentricity from approximately 5-7% at an eccentricity of 3°, paracentrally, to between approximately 16-25% at an eccentricity of approximately 28° superiorly. The corresponding Coefficients of Variation for short-wavelength automated perimetry were approximately 2.7 times larger (Wild et al., 1998). Similarly, the Coefficients of Variation for standard automated perimetry, using program 10-2 of the Humphrey Field Analyzer, were approximately 5% in normal individuals compared to 6%, and 44% in individuals with stage 0-1 and with stage 4 age-related macular degeneration (Acton et al., 2012). The corresponding values for short-wavelength automated perimetry were approximately 16%, 21% and 105%).

No obvious relationship was present between the Coefficient of Variation and either eccentricity or age, both in the absence and in the presence of the noise mask. The median (IQR) Coefficient of Variation amongst the 6 individuals in the absence of the noise mask was 5.1% (3.4 to 6.6) and in the presence of the noise mask 9.9% (6.2 to 12.4), i.e. an approximate doubling (Table 7.4).

### **7.3.1.5 Conclusion**

Clearly, the Coefficient of Variations both in the absence and in the presence of the noise mask compared favourably to those encountered in standard automated perimetry. It was, therefore, decided that the algorithm developed as the first iteration could be used in the development of the second iteration algorithm.

## **7.3.2 Second iteration**

### **7.3.2.1 Preliminary stage**

The Second iteration algorithm was based upon the development, and use, of expected 'start' values at each of 45 locations, within an eccentricity of 30°, for the Michelson contrast, expressed in dB, both in the absence and in the presence of the noise mask.

The expected 'start' values at all locations were modelled in terms of a second order polynomial describing the given sensitivity in terms of the given stimulus location. Such an approach is common in the algorithms used for SAP (Wild et al., 1993). The modelling commenced with the acquisition of the threshold estimate at each of the locations using the final version of the first iteration algorithm.

#### **7.3.2.1.1 Cohort**

Seven normal individuals were recruited across a representative age range (29 – 70 years). Five of the seven normal individuals had participated in the first iteration algorithm. The two additional individuals, also recruited from amongst the students and staff of the Cardiff School of Optometry and Vision Sciences, were familiar with the requirements of DNP and underwent a practice session before taking part in the development work.

#### **7.3.2.1.2 Methods**

The 45 stimulus locations are illustrated in Figure 7.8.

Each individual attended for five visits. At each visit, threshold was obtained using the first iteration algorithm at each of 9 pseudo-randomly chosen stimulus locations (one from a designated ‘set’ of five) in the absence and in the presence of the noise mask. The designated set of locations for a given individual were different in the absence and in the presence of the noise mask. The order of the absence or the presence of the noise mask was randomised within an individual at each visit. Each visit was separated by an interval of 3 days. A one minute rest period was given every three minutes of DNP and a five minute rest period between each test.

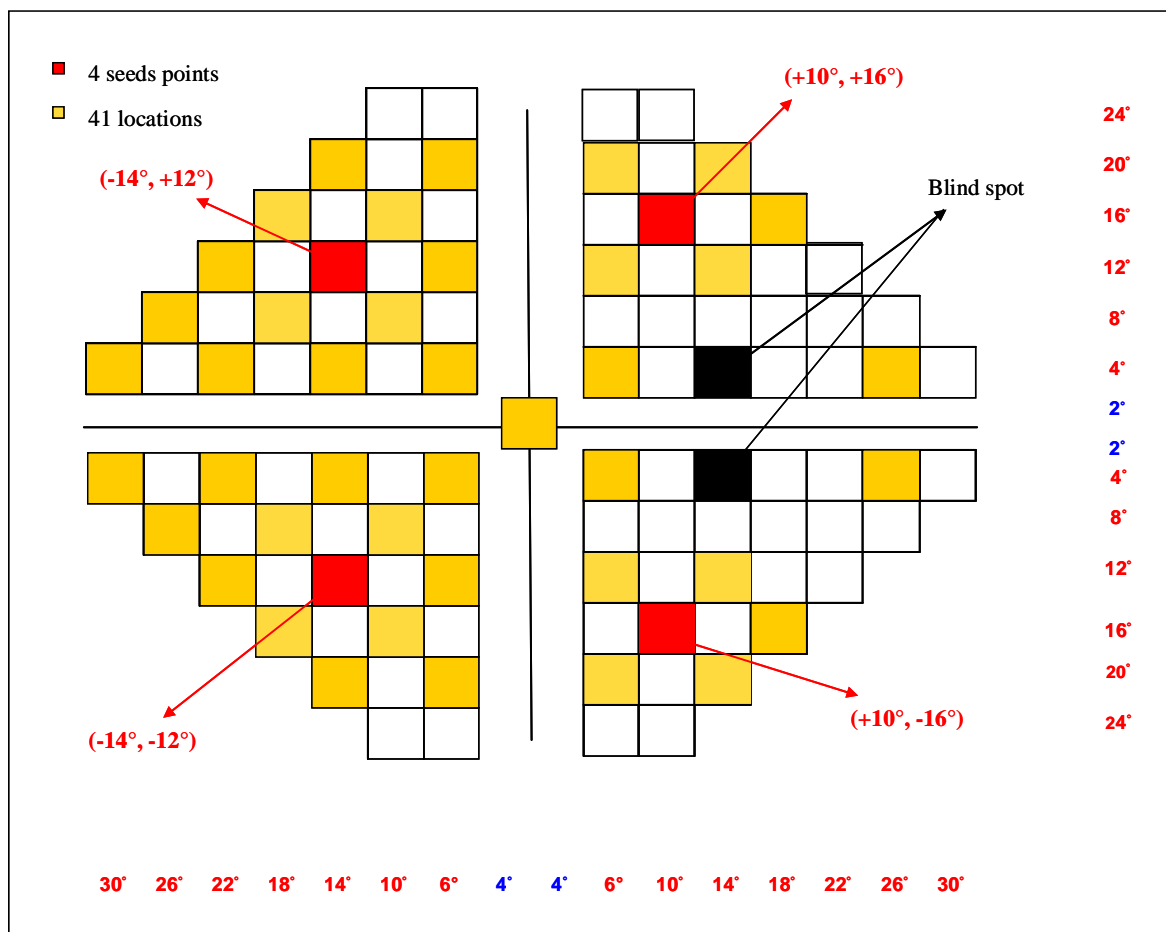


**Figure 7.8** The stimulus grid for the second iteration of the algorithm for DNP, in right eye format. The four seed points are illustrated in red and the remaining 41 locations are illustrated in orange. The black squares indicate the blind spot.

The threshold at each of the nine stimulus locations lasted approximately 5 to 6 minutes in the absence and, again, in the presence of the noise mask, i.e., 10 to 12 minutes in total.

### 7.3.2.1.3 Results

The threshold estimate, expressed as sensitivity in dB, for each of the seven individuals at each stimulus location in each of the designated sets of nine stimulus locations in the absence and in the presence of the noise mask is shown in Tables 7.7 to 7.11 and in Tables 7.12 to 7.16, respectively.

Locations	29 years sensitivity (dB)	33 years sensitivity (dB)	39 years sensitivity (dB)	45 years Sensitivity (dB)	57 years Sensitivity (dB)	65 years Sensitivity (dB)	70 years Sensitivity (dB)
-14°, +20°	15.48	16.08	15.71	15.46	13.33	14.28	12.32
-6°, +12°	17.70	16.09	17.02	16.09	14.81	13.71	13.67
-10°, +8°	16.70	15.13	16.26	16.96	15.68	14.71	10.95
+6°, +4°	18.70	17.38	17.41	15.95	16.82	17.27	12.73
-14°, -4°	18.23	17.11	17.13	16.52	16.82	13.48	14.59
-18°, -8°	15.13	16.09	14.01	18.64	13.81	13.71	13.29
+6°, -12°	16.45	16.09	15.02	13.95	15.81	14.71	14.71
-10°, -16°	16.34	15.62	16.02	15.66	14.81	15.82	14.97
+18°, -16°	18.17	18.67	17.50	16.48	14.77	15.34	13.89
<b>Duration (sec)</b>	<b>348.0</b>	<b>366.1</b>	<b>376.0</b>	<b>393.4</b>	<b>426.2</b>	<b>457.0</b>	<b>480.1</b>

**Table 7.7** The Michelson contrast, expressed as sensitivity in dB, for each of the seven individuals at each stimulus location in the first designated set of nine stimulus locations, and the corresponding examination duration, in the absence of the noise mask.

Locations	29 years sensitivity (dB)	33 years sensitivity (dB)	39 years sensitivity (dB)	45 years Sensitivity (dB)	57 years Sensitivity (dB)	65 years Sensitivity (dB)	70 years Sensitivity (dB)
-6°, +20°	16.37	15.23	16.18	14.81	13.42	12.71	11.79
+10°, +16°	14.94	14.94	14.61	13.48	12.80	12.44	11.68
+6°, +12°	17.17	15.95	15.02	14.06	13.77	13.93	11.61
-30°, +4°	15.13	13.61	14.28	14.71	12.52	11.26	10.20
+26°, +4°	16.12	13.04	16.49	13.95	14.15	12.93	10.04
-6°, -4°	20.19	18.23	17.75	15.94	14.81	15.64	13.88
-10°, -8°	18.70	17.05	16.87	15.33	14.31	17.85	12.70
+14°, -12°	17.09	16.09	15.13	15.48	15.82	16.80	11.32
-14°, -20°	17.41	17.08	16.02	15.95	15.91	14.24	11.65
<b>Duration (sec)</b>	<b>316.2</b>	<b>336.0</b>	<b>369.0</b>	<b>393.4</b>	<b>404.1</b>	<b>430.3</b>	<b>426.0</b>

**Table 7.8** The Michelson contrast, expressed as sensitivity in dB, for each of the seven individuals at each stimulus location in the second designated set of nine stimulus locations, and the corresponding examination duration, in the absence of the noise mask.

Locations	29 years sensitivity (dB)	33 years sensitivity (dB)	39 years sensitivity (dB)	45 years Sensitivity (dB)	57 years Sensitivity (dB)	65 years Sensitivity (dB)	70 years Sensitivity (dB)
+6°, +20°	14.81	15.08	14.02	13.36	13.81	14.19	13.79
+18°, +16°	15.13	15.62	13.53	15.00	13.81	11.26	12.89
-14°, +12°	15.66	15.05	15.02	15.19	14.81	14.71	11.32
-22°, +4°	15.14	15.76	15.02	15.95	12.80	13.71	12.32
0°, 0°	20.28	19.17	18.06	17.15	16.60	16.68	15.00
+6°, -4°	16.23	17.50	17.01	16.93	16.09	16.68	11.88
-22°, -12°	15.51	15.00	13.01	13.48	13.87	12.10	12.65
-18°, -16°	15.33	15.95	14.35	13.42	13.81	13.71	12.32
-6°, -20°	15.13	15.08	13.63	12.26	13.81	14.81	13.67
<b>Duration (sec)</b>	<b>312.0</b>	<b>347.4</b>	<b>353.0</b>	<b>378.1</b>	<b>380.0</b>	<b>432.4</b>	<b>431.1</b>

**Table 7.9** The Michelson contrast, expressed as sensitivity in dB, for each of the seven individuals at each stimulus location in the third designated set of nine stimulus locations, and the corresponding examination duration, in the absence of the noise mask.

Locations	29 years sensitivity (dB)	33 years sensitivity (dB)	39 years sensitivity (dB)	45 years Sensitivity (dB)	57 years Sensitivity (dB)	65 years Sensitivity (dB)	70 years Sensitivity (dB)
+14°, +20°	15.13	13.24	14.02	13.49	13.38	11.66	11.08
-10°, +16°	17.80	17.04	16.02	15.95	12.63	13.71	13.85
-22°, +12°	14.10	15.08	13.89	13.96	13.30	11.75	12.65
-26°, +8°	16.12	14.08	13.63	15.54	12.31	11.71	11.96
-14°, +4°	17.55	17.85	16.02	16.02	13.17	14.72	13.42
-30°, -4°	15.63	13.33	13.94	15.02	11.31	12.00	11.65
+26°, -4°	15.14	14.17	14.74	14.26	13.81	13.76	12.66
-14°, -12°	17.95	15.19	13.89	13.27	14.13	13.81	14.15
+6°, -20°	16.68	15.08	14.37	13.61	14.84	15.16	13.67
<b>Duration (sec)</b>	<b>308.3</b>	<b>310.2</b>	<b>332.1</b>	<b>354.1</b>	<b>342.4</b>	<b>408.0</b>	<b>412.4</b>

**Table 7.10** The Michelson contrast, expressed as sensitivity in dB, for each of the seven individuals at each stimulus location in the fourth designated set of nine stimulus locations, and the corresponding examination duration, in the absence of the noise mask.

Locations	29 years sensitivity (dB)	33 years sensitivity (dB)	39 years sensitivity (dB)	45 years Sensitivity (dB)	57 years Sensitivity (dB)	65 years Sensitivity (dB)	70 years Sensitivity (dB)
-18°, +16°	15.13	14.08	15.02	15.66	13.36	11.66	11.08
+14°, +12°	15.76	14.81	13.53	14.94	14.81	13.71	13.85
-18°, +8°	16.23	15.63	15.36	16.84	14.61	11.75	12.65
-6°, +4°	17.41	16.52	16.02	17.12	16.50	16.71	15.96
-22°, -4°	15.11	16.09	14.02	15.95	14.81	16.72	13.42
-26°, -8°	15.79	14.13	14.02	14.47	12.80	12.00	11.65
-6°, -12°	17.12	16.08	15.02	15.95	14.92	13.76	14.66
+10°, -16°	18.56	16.08	16.02	15.95	15.66	13.81	14.15
+14°, -20°	14.52	16.09	14.15	13.95	15.22	15.16	13.67
<b>Duration (sec)</b>	<b>335.1</b>	<b>351.4</b>	<b>354.1</b>	<b>361.0</b>	<b>397.0</b>	<b>410.3</b>	<b>457.2</b>

**Table 7.11** The Michelson contrast, expressed as sensitivity in dB, for each of the seven individuals at each stimulus location in the fifth designated set of nine stimulus locations, and the corresponding examination duration, in the absence of the noise mask.

Locations	29 years sensitivity (dB)	33 years sensitivity (dB)	39 years sensitivity (dB)	45 years Sensitivity (dB)	57 years Sensitivity (dB)	65 years Sensitivity (dB)	70 years Sensitivity (dB)
-14°, +20°	9.73	9.20	9.21	8.51	9.70	9.38	7.25
-6°, +12°	10.40	9.67	9.30	8.47	9.38	7.27	8.57
-10°, +8°	9.72	8.77	8.59	7.51	8.57	7.81	8.07
+6°, +4°	10.78	10.39	9.54	7.27	8.37	6.80	6.21
-14°, -4°	9.21	8.28	9.12	9.52	9.38	8.76	7.32
-18°, -8°	9.82	8.62	8.78	8.79	8.33	6.27	9.57
+6°, -12°	9.72	9.67	7.54	8.70	8.13	7.27	9.23
-10°, -16°	8.24	9.67	9.59	9.52	8.37	9.39	9.74
+18°, -16°	8.33	7.66	8.13	8.52	8.91	7.51	8.21
<b>Duration (sec)</b>	<b>368.3</b>	<b>389.1</b>	<b>427.5</b>	<b>457.3</b>	<b>471.3</b>	<b>488.0</b>	<b>493.1</b>

**Table 7.12** The Michelson contrast, expressed as sensitivity in dB, for each of the seven individuals at each stimulus location in the first designated set of nine stimulus locations, and the corresponding examination duration, in the presence of the noise mask.

Locations	29 years sensitivity (dB)	33 years sensitivity (dB)	39 years sensitivity (dB)	45 years Sensitivity (dB)	57 years Sensitivity (dB)	65 years Sensitivity (dB)	70 years Sensitivity (dB)
-6°, +20°	8.24	9.78	8.59	9.30	9.91	6.55	6.75
+10°, +16°	7.67	9.68	9.47	7.08	7.37	8.18	6.21
+6°, +12°	9.78	7.66	9.60	7.47	9.81	9.16	8.51
-30°, +4°	7.24	8.68	9.67	6.52	7.37	9.56	7.17
+26°, +4°	7.71	9.68	9.60	6.51	7.74	7.56	7.52
-6°, -4°	8.71	9.08	6.58	8.06	7.99	7.06	8.75
-10°, -8°	6.84	8.67	7.53	7.16	8.37	8.24	7.33
+14°, -12°	8.72	8.99	9.60	10.48	8.39	7.27	6.21
-14°, -20°	9.25	10.78	10.56	9.63	7.37	8.39	7.95
<b>Duration (sec)</b>	<b>365.0</b>	<b>372.2</b>	<b>431.0</b>	<b>448.2</b>	<b>463.3</b>	<b>478.0</b>	<b>484.1</b>

**Table 7.13** The Michelson contrast, expressed as sensitivity in dB, for each of the seven individuals at each stimulus location in the second designated set of nine stimulus locations, and the corresponding examination duration, in the presence of the noise mask.

Locations	29 years sensitivity (dB)	33 years sensitivity (dB)	39 years sensitivity (dB)	45 years Sensitivity (dB)	57 years Sensitivity (dB)	65 years Sensitivity (dB)	70 years Sensitivity (dB)
+6°, +20°	9.72	9.67	10.70	9.30	9.65	8.39	7.07
+18°, +16°	10.23	10.67	8.96	8.52	9.96	7.81	6.30
-14°, +12°	8.72	9.96	8.59	8.46	7.37	7.54	7.18
-22°, +4°	9.81	8.57	8.22	9.74	7.39	7.96	7.75
0°, 0°	9.95	8.95	9.84	7.00	7.51	6.91	6.29
+6°, -4°	8.86	8.67	9.63	7.04	6.37	7.03	6.50
+22°, -12°	7.70	8.74	9.60	8.01	8.90	7.29	7.67
-18°, -16°	7.07	8.73	7.93	8.52	7.68	8.28	7.19
-6°, -20°	8.27	9.63	8.59	8.30	9.66	9.06	7.26
<b>Duration (sec)</b>	<b>360.1</b>	<b>383.4</b>	<b>457.2</b>	<b>462.0</b>	<b>485.4</b>	<b>479.2</b>	<b>501.4</b>

**Table 7.14** The Michelson contrast, expressed as sensitivity in dB, for each of the seven individuals at each stimulus location in the third designated set of nine stimulus locations, and the corresponding examination duration, in the presence of the noise mask.

Locations	29 years sensitivity (dB)	33 years sensitivity (dB)	39 years sensitivity (dB)	45 years Sensitivity (dB)	57 years Sensitivity (dB)	65 years Sensitivity (dB)	70 years Sensitivity (dB)
+14°, +20°	9.92	10.59	9.15	8.56	7.40	8.28	6.83
-10°, +16°	7.71	8.17	7.55	8.52	9.57	8.24	8.21
-22°, +12°	8.29	8.67	8.59	8.01	8.91	7.48	7.32
-26°, +8°	8.29	7.67	8.59	8.52	7.08	6.29	6.45
-14°, +4°	7.71	9.42	7.58	7.62	8.08	6.27	7.38
-30°, -4°	7.57	7.65	8.12	8.00	6.92	5.81	7.23
+26°, -4°	8.85	7.92	7.55	8.59	8.37	7.27	6.46
-14°, -12°	7.71	8.08	9.70	7.51	7.37	8.84	7.23
+6°, -20°	7.67	8.67	7.12	8.01	8.38	8.56	6.10
<b>Duration (sec)</b>	<b>336.1</b>	<b>351.5</b>	<b>401.0</b>	<b>439.1</b>	<b>467.0</b>	<b>465.3</b>	<b>473.0</b>

**Table 7.15** The Michelson contrast, expressed as sensitivity in dB, for each of the seven individuals at each stimulus location in the fourth designated set of nine stimulus locations, and the corresponding examination duration, in the presence of the noise mask.

Locations	29 years sensitivity (dB)	33 years sensitivity (dB)	39 years sensitivity (dB)	45 years Sensitivity (dB)	57 years Sensitivity (dB)	65 years Sensitivity (dB)	70 years Sensitivity (dB)
-18°, 16°	8.24	9.67	9.19	7.09	8.35	8.28	7.21
+14°, +12°	9.29	8.55	7.37	7.46	7.24	8.24	8.10
-18°, +8°	7.13	7.39	6.90	6.81	7.51	6.27	8.01
-6°, +4°	9.71	8.67	8.75	7.04	8.33	8.24	7.33
-22°, -4°	7.78	8.61	8.59	9.74	8.37	7.96	7.21
-26°, -8°	6.70	7.20	8.59	8.49	7.83	9.29	8.35
-6°, -12°	8.72	8.81	8.54	8.18	7.05	9.16	8.98
+10°, -16°	8.44	7.12	7.88	8.52	7.38	8.24	6.32
+14°, -20°	9.73	8.68	9.33	8.72	7.91	8.28	7.22
<b>Duration (sec)</b>	<b>309.4</b>	<b>364.0</b>	<b>401.2</b>	<b>436.0</b>	<b>454.1</b>	<b>451.0</b>	<b>468.0</b>

**Table 7.16** The Michelson contrast, expressed as sensitivity in dB, for each of the seven individuals at each stimulus location in the fifth designated set of nine stimulus locations, and the corresponding examination duration, in the presence of the noise mask.

Following collection of the dataset for the 45 stimulus locations, one location in each quadrant was designated as a ‘seed point’. The four seed points were situated, in right eye format, at +10°, +16°; +10°, -16°; -14°, +12°; and -14°, -12°. Each selected location was required to be surrounded by four other locations in the same quadrant with each being designated as ‘neighbour locations’. The regression of Michelson contrast, expressed as sensitivity in dB, against age for each of four seed points in the absence and in the presence of the noise mask is given in Figures 7.9 to 7.12 and in Figures 7.13 to 7.16, respectively.

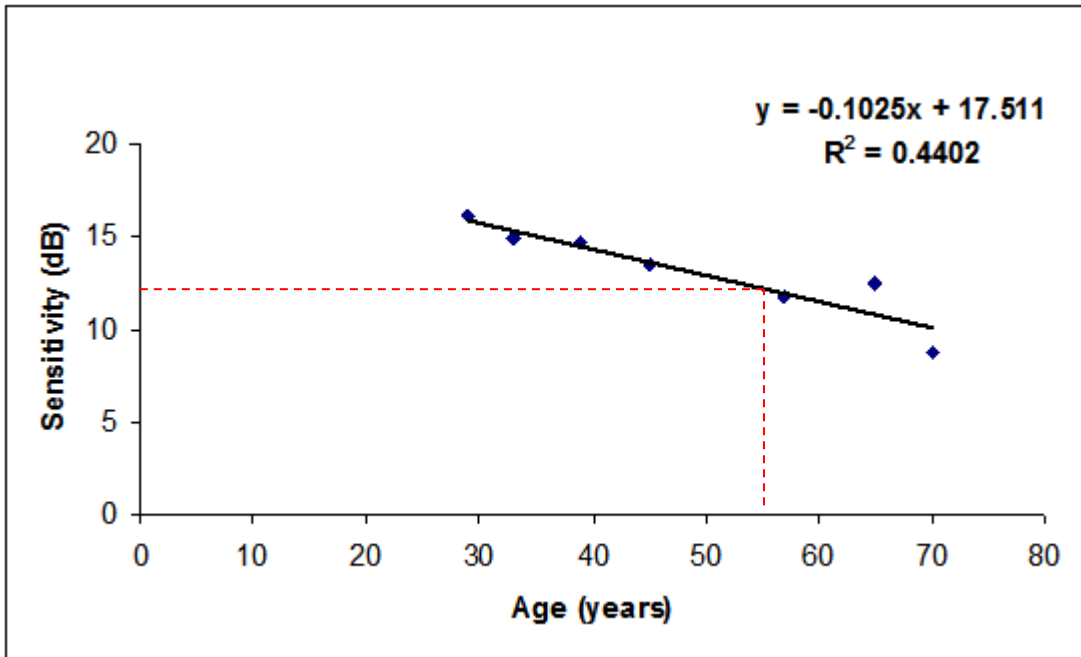


**Figure 7.9** The relationship between Michelson contrast, expressed as sensitivity in dB, against age and in the absence of the noise mask, for the seed point at  $+10^\circ, +16^\circ$ . The dashed red line indicates, as an example, the ‘start’ value of 12dB for an individual aged 55 years.

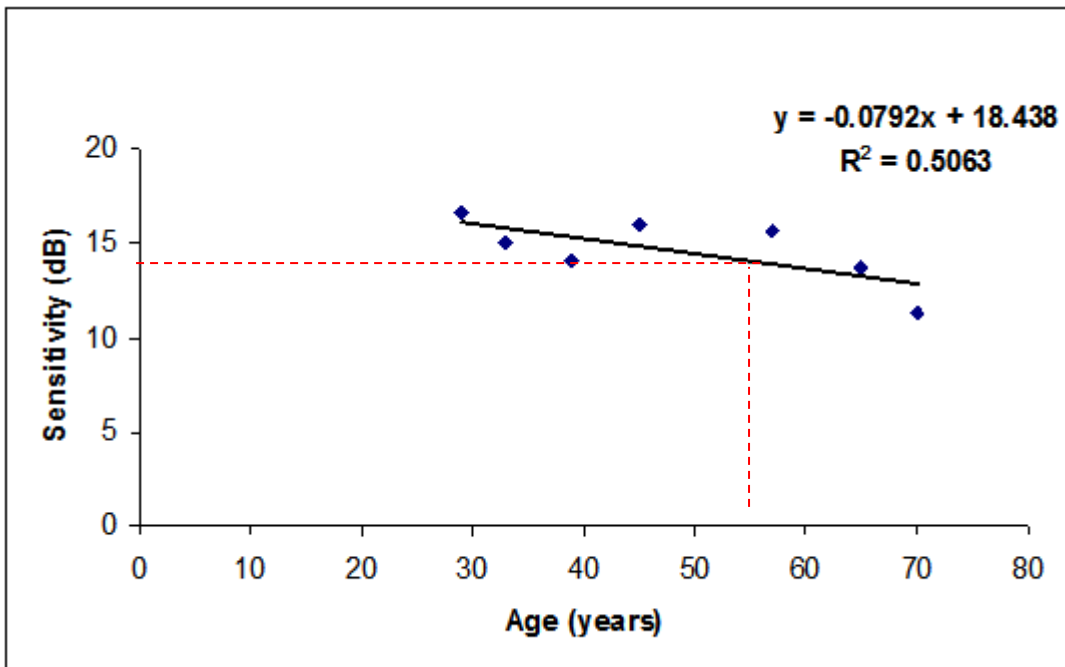


**Figure 7.10** The relationship between Michelson contrast, expressed as sensitivity in dB, against age and in the absence of the noise mask, for the seed point at  $+10^\circ, -16^\circ$ . The dashed red line indicates, as an example, the ‘start’ value of 14dB for an individual aged 55 years.

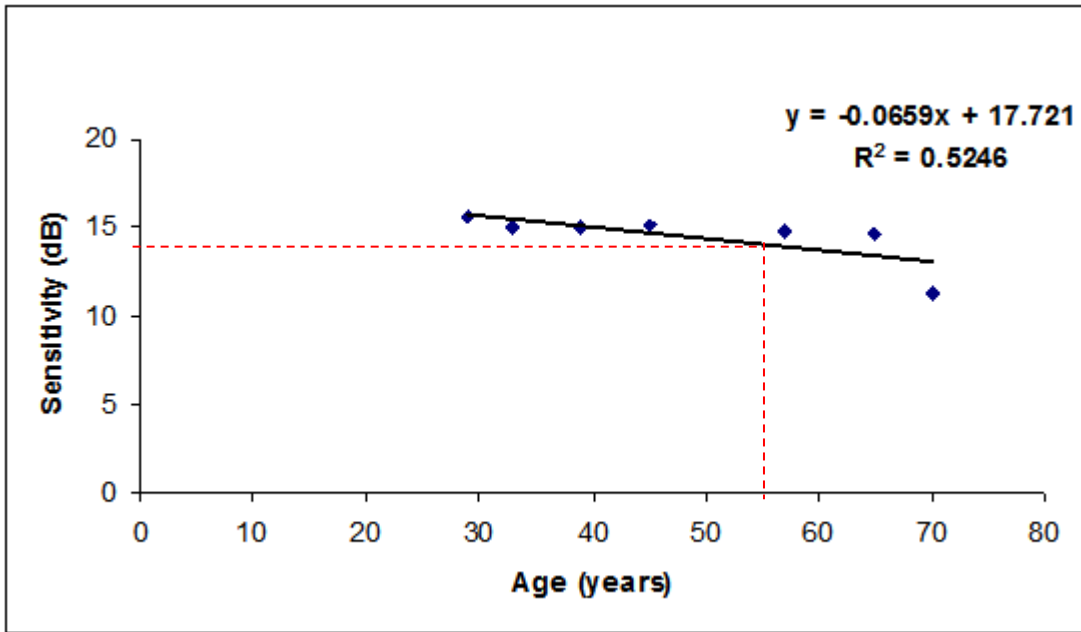


**Figure 7.11** The relationship between Michelson contrast, expressed as sensitivity in dB, against age and in the absence of the noise mask, for the seed point at  $-14^\circ, +12^\circ$ . The dashed red line indicates, as an example, the ‘start’ value of 14dB for an individual aged 55 years.

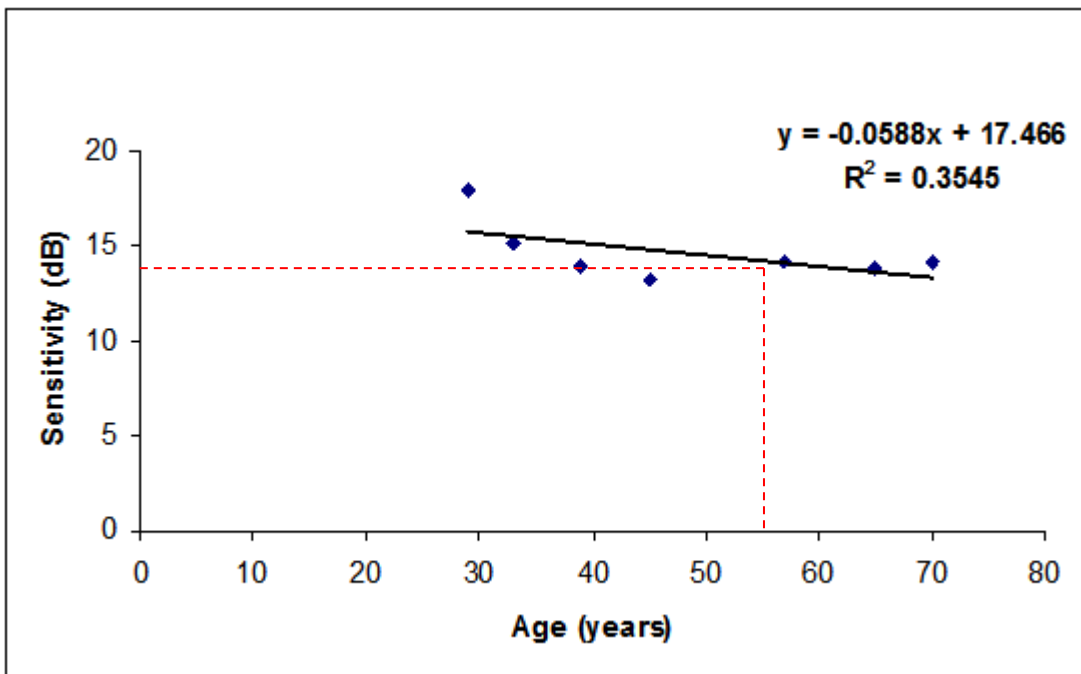


**Figure 7.12** The relationship between Michelson contrast, expressed as sensitivity in dB, against age and in the absence of the noise mask, for the seed point at  $-14^\circ, -12^\circ$ . The dashed red line indicates, as an example, the ‘start’ value of 14dB for an individual aged 55 years.

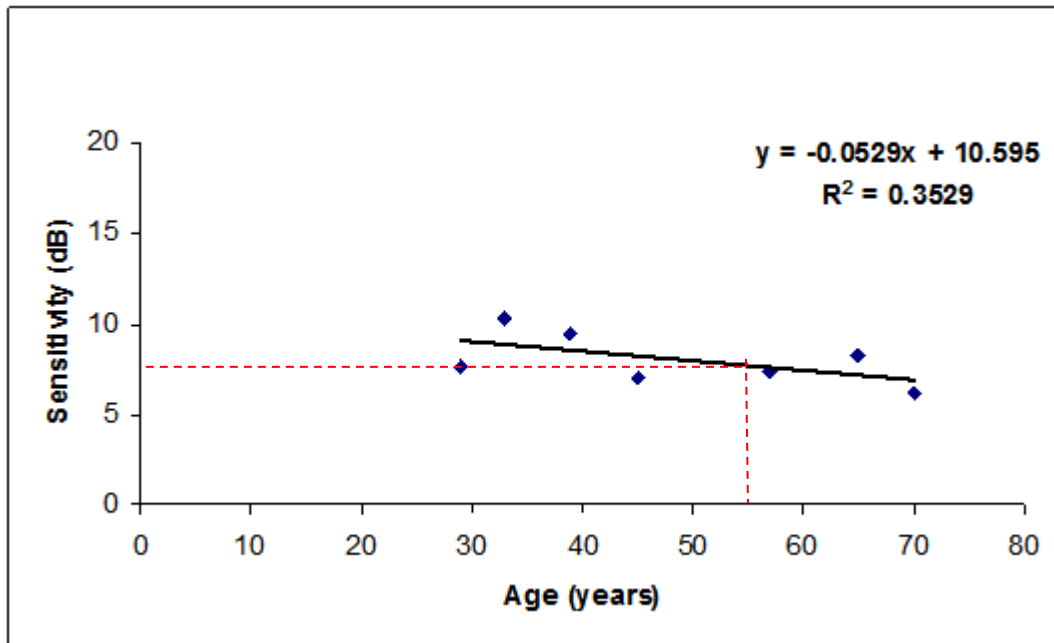


**Figure 7.13** The relationship between Michelson contrast, expressed as sensitivity in dB, against age and in the presence of the noise mask, for the seed point at  $+10^\circ, +16^\circ$ . The dashed red line indicates, as an example, the ‘start’ value of 7.5dB for an individual aged 55 years.

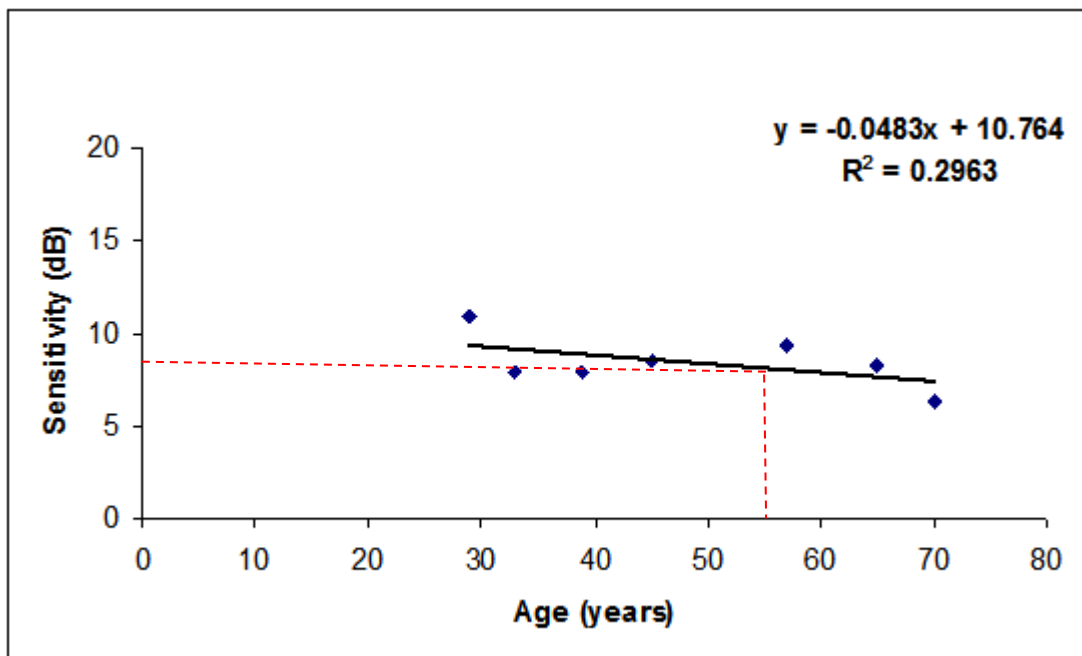


**Figure 7.14** The relationship between Michelson contrast, expressed as sensitivity in dB, against age and in the presence of the noise mask, for the seed point at  $+10^\circ, -16^\circ$ . The dashed red line indicates, as an example, the ‘start’ value of 8dB for an individual aged 55 years.

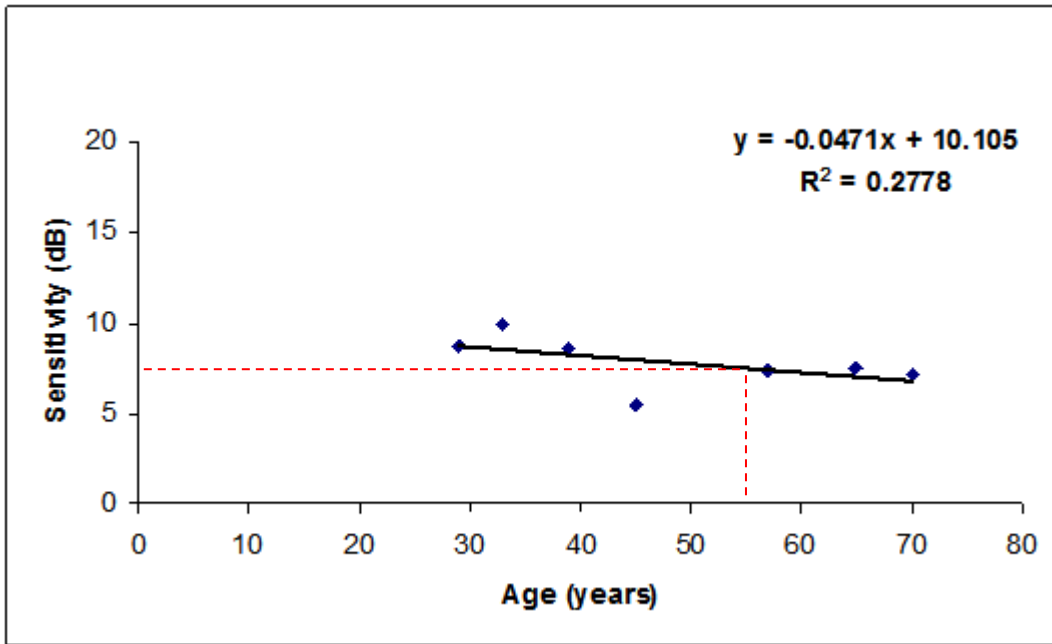


**Figure 7.15** The relationship between Michelson contrast, expressed as sensitivity in dB, against age and in the presence of the noise mask, for the seed point at  $-14^\circ, +12^\circ$ . The dashed red line indicates, as an example, the ‘start’ value of 7.5dB for an individual aged 55 years.

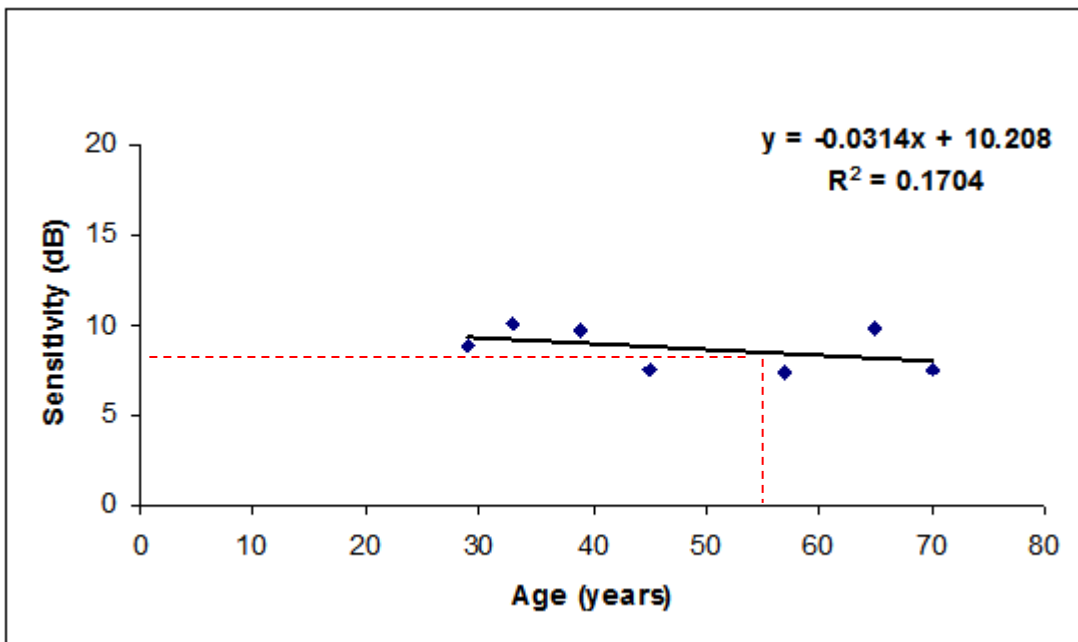


**Figure 7.16** The relationship between Michelson contrast, expressed as sensitivity in dB, against age and in the presence of the noise mask, for the seed point at  $-14^\circ, -12^\circ$ . The dashed red line indicates, as an example, the ‘start’ value of 8dB for an individual aged 55 years.

### 7.3.2.2 Polynomial modelling

In order to determine the expected threshold for each seed location, the mean of the Michelson contrasts for the 7 individuals, across the four locations, in the absence and in the presence of the noise mask, respectively, were then separately modelled, using polyfitn within Matlab software version 6.5.1 (The Math Works Inc, Natick, MA, USA) in terms of a second order polynomial:

$$z(x, y) = x^2*VAL(1) + x*y*VAL(2) + x*VAL(3) + y^2*VAL(4) + y*VAL(5) + c$$

where:

$z$  is the Michelson contrast at the given stimulus location  $(x, y)$  and  $VAL(1)$  to  $VAL(5)$ , inclusive, are the respective coefficients of the polynomial and  $c$  is a constant representing the offset.

The offset value,  $c$ , was then used to calculate, separately, the expected Michelson contrast at each of the four seed points in the absence and in the presence of the noise mask.

The threshold, in the absence and in the presence of the noise mask, was then to be calculated at each of these seed points using a staircase based upon the respective expected Michelson contrasts. Following the acquisition of the threshold at the given seed point, in the absence or in the presence of the noise mask, the given threshold was substituted into the original polynomial to calculate a new value of  $c$  for the given quadrant. From a knowledge of the quadrant-specific  $c$  value, the expected Michelson contrast was then calculated for each stimulus location within the given quadrant.

Due to the importance of the given seed points in determining the expected values at the remaining locations, it was necessary to implement a detailed staircase in order to obtain an accurate estimate of threshold compatible with a realistic test time. The staircase for the determination of threshold at the remaining locations would then be less detailed.

#### **7.3.2.2.1 Derivation of the staircase for the four seed points**

The start level for each of the four seed points was based upon the final version of the first iteration algorithm and was 2dB above the expected value derived from the polynomial. Throughout the starting phase, i.e., the first reversal of the staircase, two consecutive correct responses were required to reduce the contrast level of the grating by 2dB. A further two consecutive correct responses were required to decrease the level of contrast of the grating by 1dB. In the case of an incorrect response following the first crossing of threshold, one incorrect response was required to increase the level of contrast of the grating by 2dB. A subsequent incorrect response increased the level of contrast of the grating by an additional 1dB. A further incorrect response terminated the staircase at the given location. During the second and third reversals, two consecutive correct responses were required to decrease the contrast level of the grating by 1dB, and one incorrect response to increase the contrast level of the grating by 1dB. For any one seed point, a schematic of the staircase with two consecutive correct responses at the first reversal is shown in Figure 7.17 and with three consecutive incorrect responses at the first reversal is shown in Figure 7.18.

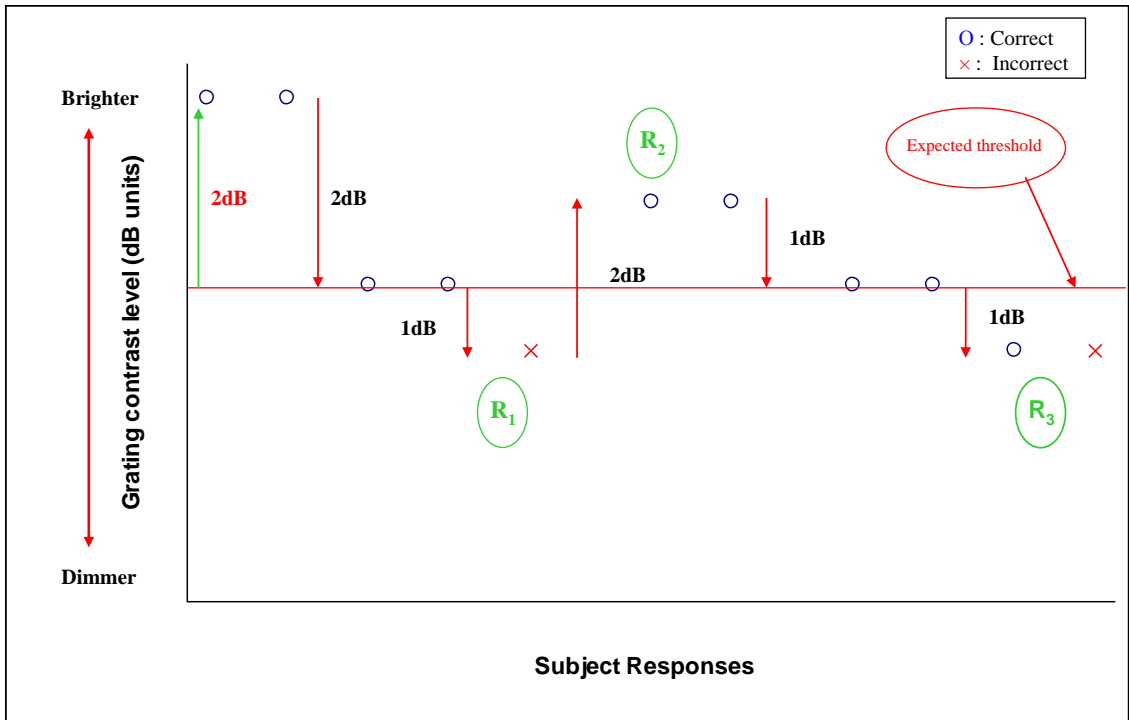


**Figure 7.17** A schematic of the staircase, for any one seed point, where 3 reversals determine the length of the staircase, and the final reversal is used to calculate the threshold (i.e., the average of the first incorrect and the last correct responses).

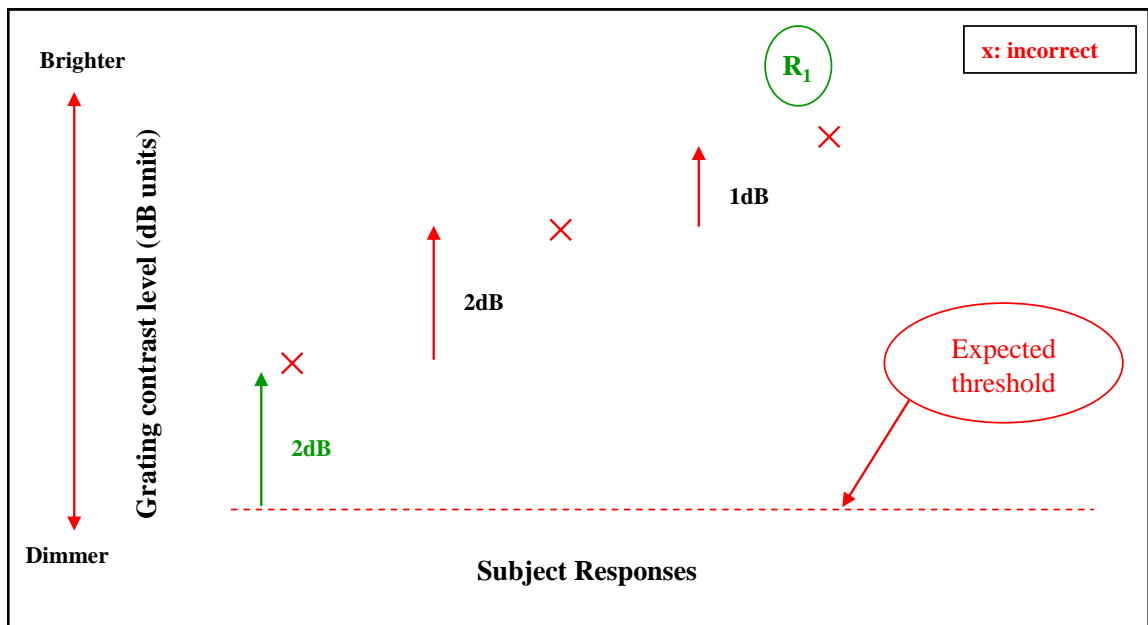


**Figure 7.18** A schematic of the staircase for any one seed point, illustrated in Figure 7.17, where three consecutive incorrect responses terminate the staircase.

### 7.3.2.2.2 Derivation of the staircase for the non-seed points

The start value at each of the remaining 41 locations (i.e., the non-seed points) was 2dB above the corresponding predicted threshold derived from the given polynomial. The first two consecutive correct responses decreased the level of contrast of the grating by 2dB. One incorrect response increased the contrast level of the grating by 2dB. A second consecutive incorrect response increased the level of contrast of the grating by 1dB, and a further incorrect response terminated the staircase (Figure 7.19).

Following the first 2dB decrease in the contrast of the grating, a 1dB decrease in contrast occurred after two consecutive correct responses, until an incorrect response was recorded (Figure 7.20).

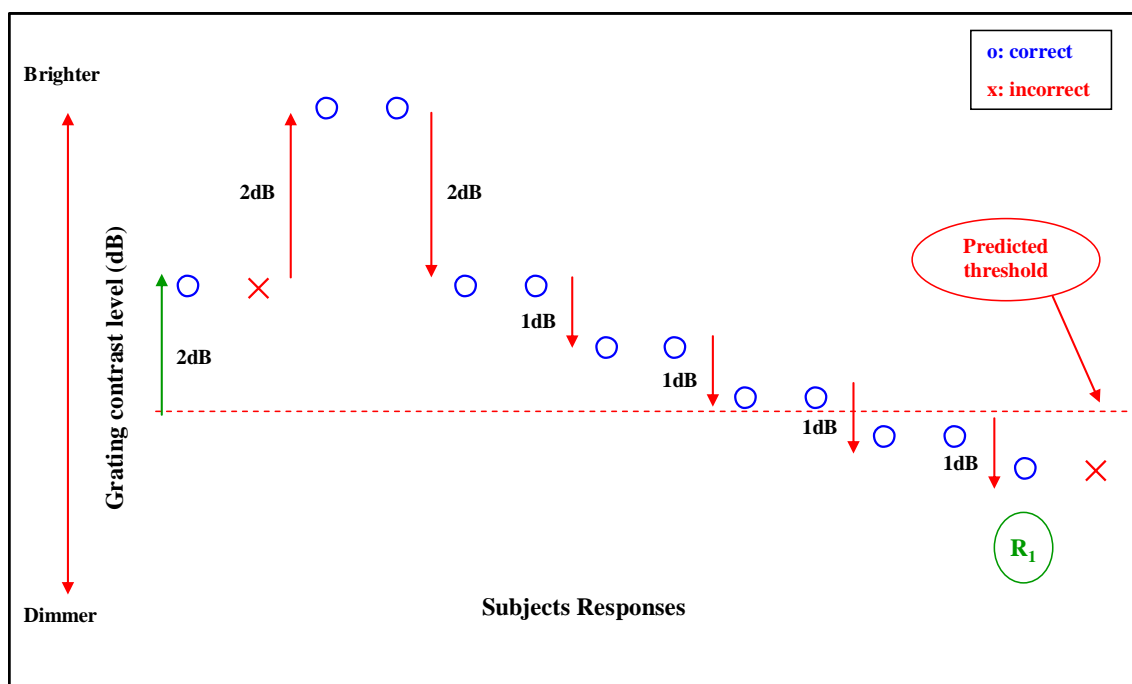


**Figure 7.19** A schematic of the staircase algorithm for any one of the 41 non-seed points, where one reversal determines the length of the staircase.

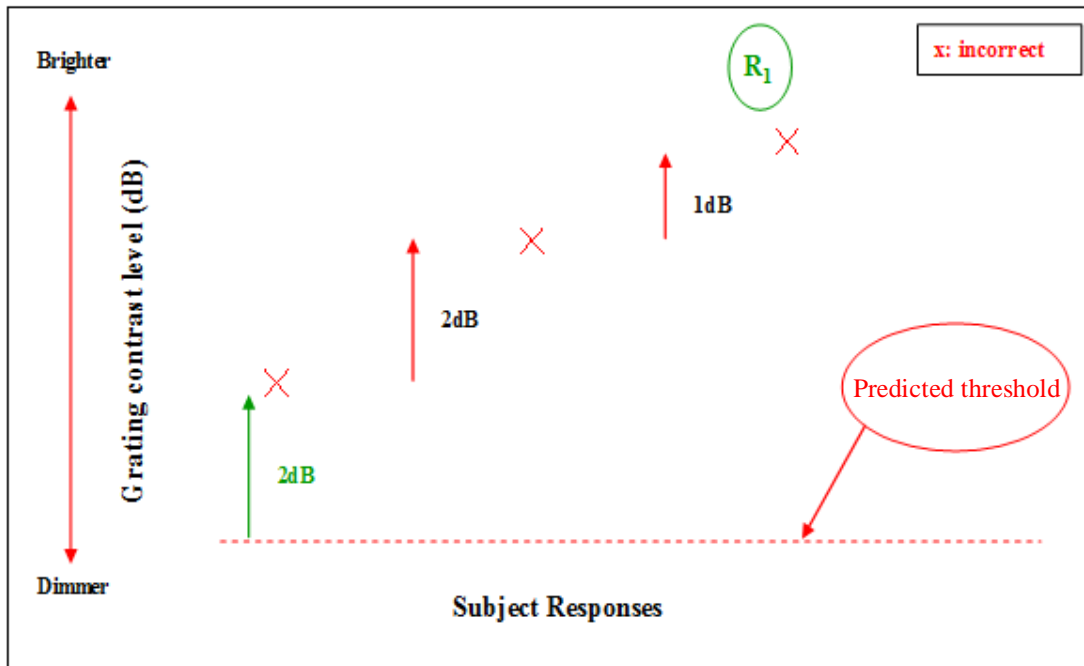


**Figure 7.20** A schematic of the staircase algorithm for any one of the 41 non-seed points, where three incorrect responses terminate the staircase.

### 7.3.2.3 Evaluation of the Final Algorithm

The algorithm incorporating the two staircase modalities was evaluated, in the absence and in the presence of the noise mask, on the same seven individuals at two single examinations.

In order to assess the utility of the start values determined by the second order polynomial function in the final algorithm (i.e., that incorporating the two staircase modalities), the Michelson contrast, expressed as sensitivity in dB, derived with the Final Algorithm was compared to that derived with the first iteration algorithm at each stimulus location for each individual using the technique of Bland and Altman (1986) whereby the difference between the two outcomes is referenced to the mean of the two outcomes.

### 7.3.2.3.1 Results

The threshold estimate for each of the seven individuals at each of the 45 stimulus locations, in the absence and in the presence of the noise mask, for the Final Algorithm are shown in Tables 7.17 and 7.18, respectively. The corresponding examination durations are also given in the two Tables.

Number of location	Locations	29 years sensitivity (dB)	33 years sensitivity (dB)	39 years sensitivity (dB)	45 years sensitivity (dB)	57 years sensitivity (dB)	65 years sensitivity (dB)	70 years sensitivity (dB)
1	-14°, 20°	16.58	15.04	16.83	14.26	14.95	12.24	10.20
2	-6°, 12°	19.07	14.48	16.44	16.58	13.90	13.56	12.52
3	-10°, 8°	18.81	14.44	15.96	17.09	14.87	13.07	13.03
4	6°, 4°	19.11	18.28	18.42	17.06	16.14	15.04	13.00
5	-14°, -4°	19.10	18.63	17.63	17.57	16.51	15.55	13.51
6	-18°, -8°	16.87	17.87	16.86	16.22	14.24	13.21	12.16
7	6°, -12°	18.15	16.36	15.46	13.73	16.20	14.71	12.67
8	-10°, -16°	16.50	15.52	15.93	15.53	14.94	13.51	11.47
9	18°, -16°	18.05	18.16	17.66	15.99	15.52	13.97	11.93
10	-6°, 20°	15.85	17.21	16.15	14.82	14.54	12.80	10.76
11	10°, 16°	15.70	14.83	14.60	13.63	12.77	11.61	10.57
12	6°, 12°	17.94	16.18	16.30	14.52	14.08	12.50	10.46
13	-30°, 4°	14.64	14.07	14.93	13.47	13.92	12.45	10.41
14	26°, 4°	16.38	15.21	15.29	14.55	13.99	12.53	10.49
15	-6°, -4°	19.46	18.20	17.22	16.46	15.96	15.44	13.40
16	-10°, -8°	18.32	18.86	17.72	16.69	16.16	14.67	12.63
17	14°, -12°	18.85	16.88	15.86	15.71	15.81	14.69	12.65
18	-14°, -20°	16.01	14.86	15.32	15.47	15.77	13.45	11.41
19	6°, 20°	14.73	15.14	14.44	13.51	12.04	12.49	11.45
20	18°, 16°	15.28	15.57	13.42	13.12	13.47	11.10	10.06
21	-14°, 12°	17.31	14.84	15.01	16.10	15.13	14.08	12.04
22	-22°, 4°	16.57	15.47	15.25	13.23	13.37	12.21	12.17
23	0°, 0°	19.92	18.24	18.29	17.90	16.12	15.88	14.84
24	6°, -4°	18.80	17.19	17.00	17.77	16.99	15.75	13.71
25	-22°, -12°	15.51	16.86	13.64	14.93	14.74	12.91	11.87

26	-18°, -16°	16.39	14.43	14.14	15.28	14.35	13.26	11.22
27	-6°, -20°	16.85	16.95	14.52	14.93	14.80	13.91	12.87
Number of location	Locations	29 years sensitivity (dB)	33 years sensitivity (dB)	39 years sensitivity (dB)	45 years sensitivity (dB)	57 years sensitivity (dB)	65 years sensitivity (dB)	70 years sensitivity (dB)
28	14°, 20°	14.59	14.98	14.56	12.65	13.74	11.63	10.59
29	-10°, 16°	16.79	18.72	15.71	15.60	13.50	13.58	11.54
30	-22°, 12°	15.55	14.16	13.25	14.94	13.58	12.92	10.88
31	-26°, 8°	16.51	16.08	13.70	14.85	14.93	11.83	10.79
32	-14°, 4°	17.99	17.71	16.24	17.32	14.06	13.30	13.26
33	-30°, -4°	14.98	15.75	14.06	13.72	12.64	11.70	10.66
34	26°, -4°	15.94	14.88	14.24	17.06	15.73	15.04	13.00
35	-14°, -12°	16.39	15.84	14.59	15.96	15.77	13.94	11.90
36	6°, -20°	15.75	15.43	15.13	15.95	15.29	13.94	12.89
37	-18°, 16°	14.73	15.16	15.12	14.74	14.04	12.72	10.68
38	14°, 12°	17.01	14.37	15.78	14.53	15.24	12.51	10.47
39	-18°, 8°	16.77	15.30	15.31	16.31	15.17	14.29	12.25
40	-6°, 4°	18.06	16.66	16.53	17.72	14.55	15.71	13.66
41	-22°, -4°	15.52	15.04	14.68	16.32	14.80	14.30	12.26
42	-26°, -8°	15.37	15.10	13.44	14.40	13.90	12.39	10.34
43	-6°, -12°	19.03	17.72	16.48	15.64	16.07	13.62	11.58
44	10°, -16°	17.97	16.20	15.52	15.33	13.12	14.32	12.27
45	14°, -20°	15.62	15.64	14.93	14.80	15.47	13.78	11.74
<b>Duration (sec)</b>		<b>420.0</b>	<b>435.2</b>	<b>480.1</b>	<b>510.0</b>	<b>513.1</b>	<b>540.3</b>	<b>600.4</b>

**Table 7.17** The Michelson contrast, expressed as sensitivity in dB, for each of the seven individuals at each of the 45 stimulus locations, in the absence of the noise mask, and the corresponding examination duration, for the Final Algorithm (i.e., that incorporating the two staircase modalities).

Number of location	Locations	29 years sensitivity (dB)	33 years sensitivity (dB)	39 years sensitivity (dB)	45 years sensitivity (dB)	57 years sensitivity (dB)	65 years sensitivity (dB)	70 years sensitivity (dB)
1	-14°, 20°	9.52	9.36	8.95	7.71	8.79	8.35	7.35
2	-6°, 12°	7.55	9.17	8.84	9.42	9.49	7.19	8.29
3	-10°, 8°	7.96	8.23	7.63	7.61	9.68	7.56	7.87
4	6°, 4°	9.12	10.66	9.76	8.98	9.05	7.92	8.69
5	-14°, -4°	8.59	9.34	9.09	9.70	8.77	8.65	7.99
6	-18°, -8°	9.57	8.44	7.18	8.79	8.85	8.73	6.58
7	6°, -12°	9.42	9.21	8.19	9.59	7.18	8.54	8.18
8	-10°, -16°	7.81	9.69	8.87	9.01	9.08	9.95	8.73
9	18°, -16°	8.53	7.98	8.26	8.80	8.88	8.75	8.46
10	-6°, 20°	8.15	8.92	8.52	9.31	8.41	6.30	7.87
11	10°, 16°	8.81	9.44	9.82	9.71	8.53	6.97	7.12
12	6°, 12°	9.14	8.37	8.86	7.57	8.66	9.51	7.51
13	-30°, 4°	7.99	7.73	8.18	7.03	7.10	7.97	7.76
14	26°, 4°	7.57	7.87	8.50	7.30	7.35	7.23	6.45
15	-6°, -4°	8.28	8.90	9.20	8.96	9.50	8.40	8.72
16	-10°, -8°	8.69	8.92	8.25	8.00	9.14	8.53	8.31
17	14°, -12°	9.62	9.20	9.85	8.95	8.52	7.89	7.37
18	-14°, -20°	8.71	9.22	9.71	8.98	7.55	8.39	8.78
19	6°, 20°	8.78	9.01	9.54	8.27	9.36	9.22	8.09
20	18°, 16°	9.40	10.02	9.41	9.27	8.34	8.20	7.88
21	-14°, 12°	9.25	8.93	8.89	9.46	7.47	7.41	6.47
22	-22°, 4°	8.51	9.24	7.21	9.62	9.69	7.56	7.72
23	0°, 0°	9.11	9.69	9.63	9.00	9.08	8.95	7.32
24	6°, -4°	9.01	8.78	9.55	8.18	9.38	7.29	6.25
25	-22°, -12°	6.39	8.75	9.53	8.76	8.24	8.12	8.64
26	-18°, -16°	7.44	8.41	8.68	8.27	8.83	7.72	7.41
27	-6°, -20°	7.61	9.99	8.82	8.89	8.87	8.21	7.76
28	14°, 20°	8.79	10.56	8.56	8.35	9.96	8.84	7.58
29	-10°, 16°	8.29	9.35	8.17	7.66	8.89	7.78	7.19
30	-22°, 12°	8.45	8.38	8.93	8.58	8.22	8.08	7.58
31	-26°, 8°	7.46	7.89	8.20	8.07	7.19	7.52	6.53
32	-14°, 4°	7.28	8.77	7.11	7.95	9.16	8.02	7.83
33	-30°, -4°	7.60	7.19	6.99	8.30	7.51	6.70	6.46
34	26°, -4°	8.67	7.61	8.38	9.15	8.39	7.37	7.81
35	-14°, -12°	8.46	9.67	9.02	7.59	8.89	8.05	7.90
36	6°, -20°	7.21	9.87	8.95	8.60	8.23	8.09	6.93
37	-18°, 16°	8.77	9.41	6.38	8.36	8.68	8.53	7.22
38	14°, 12°	9.10	8.69	8.20	7.64	9.93	8.77	8.91
39	-18°, 8°	7.85	7.45	7.02	7.78	8.72	8.57	7.61
40	-6°, 4°	8.98	9.13	9.87	8.25	9.86	7.70	8.47
41	-22°, -4°	7.76	7.34	8.40	8.23	6.83	7.20	6.73

42	-26°, -8°	7.85	7.96	6.83	8.01	7.83	8.17	7.69
Number of location	Locations	29 years sensitivity (dB)	33 years sensitivity (dB)	39 years sensitivity (dB)	45 years sensitivity (dB)	57 years sensitivity (dB)	65 years sensitivity (dB)	70 years sensitivity (dB)
43	-6°, -12°	8.97	8.69	7.31	8.33	8.08	7.96	7.73
44	10°, -16°	8.30	8.51	7.97	7.97	8.18	7.68	6.27
45	14°, -20°	9.42	9.65	8.98	9.06	8.89	8.26	8.85
<b>Duration (sec)</b>		<b>510.3</b>	<b>540.0</b>	<b>552.1</b>	<b>562.5</b>	<b>578.1</b>	<b>600.1</b>	<b>660.0</b>

**Table 7.18** The Michelson contrast, expressed as sensitivity in dB, for each of the seven individuals at each of the 45 stimulus locations, in the presence of the noise mask, and the corresponding examination duration, for the Final Algorithm (i.e., that incorporating the two staircase modalities).

The examination duration for the seven individuals, in the absence and in the presence of the noise mask, is also illustrated graphically in Figure 7.21. The examination duration increased linearly with increase in age both in the absence and in the presence of the noise mask. As expected, the duration was longer in the presence of the noise mask; however, the difference between the two examinations durations reduced with increase in age.

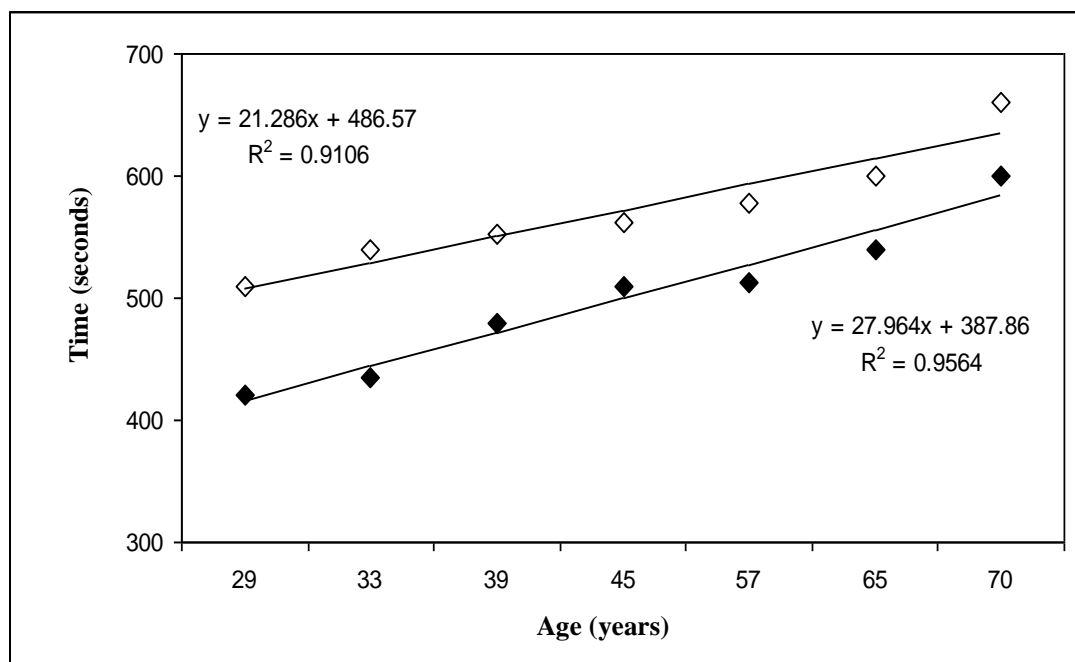


**Figure 7.21** The examination duration (seconds) for each individual, in the absence (filled symbols) and in the presence (open symbols) of the noise mask, for the Final Algorithm.

The mean (SD) of the differences in Michelson contrast, expressed as sensitivity in dB, across the 45 stimulus locations between the Final and the First Iteration algorithms in the absence and in the presence of the noise mask for each of the 7 individuals is given in Table 7.19

The difference in the Michelson contrast, expressed as sensitivity in dB, between the Final and First Iteration algorithms against that of the mean for the two algorithms in the absence of the noise mask (top) and in the presence of the noise mask (bottom) for each of the seven individuals is given in Figures 7.22 to Figures 7.28.

		Without the noise mask	With the noise mask
Individual	Age	Mean (SD) of the difference	Mean (SD) of the difference
1	29	0.45 (1.01)	-0.23 (0.86)
2	33	0.36 (1.14)	-0.01 (0.75)
3	39	0.31 (0.76)	-0.18 (0.96)
4	45	0.22 (1.24)	0.31 (0.85)
5	57	0.39 (1.00)	0.38 (1.12)
6	65	-0.54 (1.20)	0.20 (0.96)
7	70	-0.97 (1.26)	-5.18 (1.29)

**Table 7.19** The mean (SD) of the differences in Michelson contrast, expressed as sensitivity in dB, across the 45 stimulus locations between the Final and the First Iteration algorithms in the absence (left) and in the presence (right) of the noise mask for each of the 7 individuals.

In the absence of the noise mask, the Final Algorithm slightly overestimated the Michelson contrast, expressed as sensitivity in dB, compared to the First Iteration algorithm for the

first five individuals ranked by increasing age. The algorithm then overestimated the sensitivity for the oldest two individuals.

In the presence of the noise mask, the Final Algorithm underestimated the Michelson contrast, expressed as sensitivity in dB, compared to the First Iteration algorithm for the first three individuals ranked by increasing age and then overestimated the sensitivity for the next three ranked individuals.

Clearly, the results for individual number 7, aged 70 years, in the presence of the noise mask must be considered as outlying values.

#### **7.3.2.3.2 Discussion**

The polynomial function used, in the Final Algorithm, for the description of the start value at each eccentricity facilitated the threshold evaluation of a substantial increase in the number of stimulus locations without an apparent loss of accuracy.

The lower SD of the difference between means in the presence of the noise mask would be expected given the lower dynamic range in the presence of the noise mask compared to that in the absence of the mask.

The reason for the outlying values for the oldest individual is unclear but may reflect the weakness of the polynomial function in individuals of approximately 70 years and beyond. In standard automated perimetry, the decline in sensitivity with increase in age is usually considered to be linear. However, there is considerable evidence that the function becomes non-linear beyond approximately 70 years of age (Johnson and Marshall, 1995). The

incorporation of a term for age into the model would seem to be an obvious next step in the development of the algorithm.

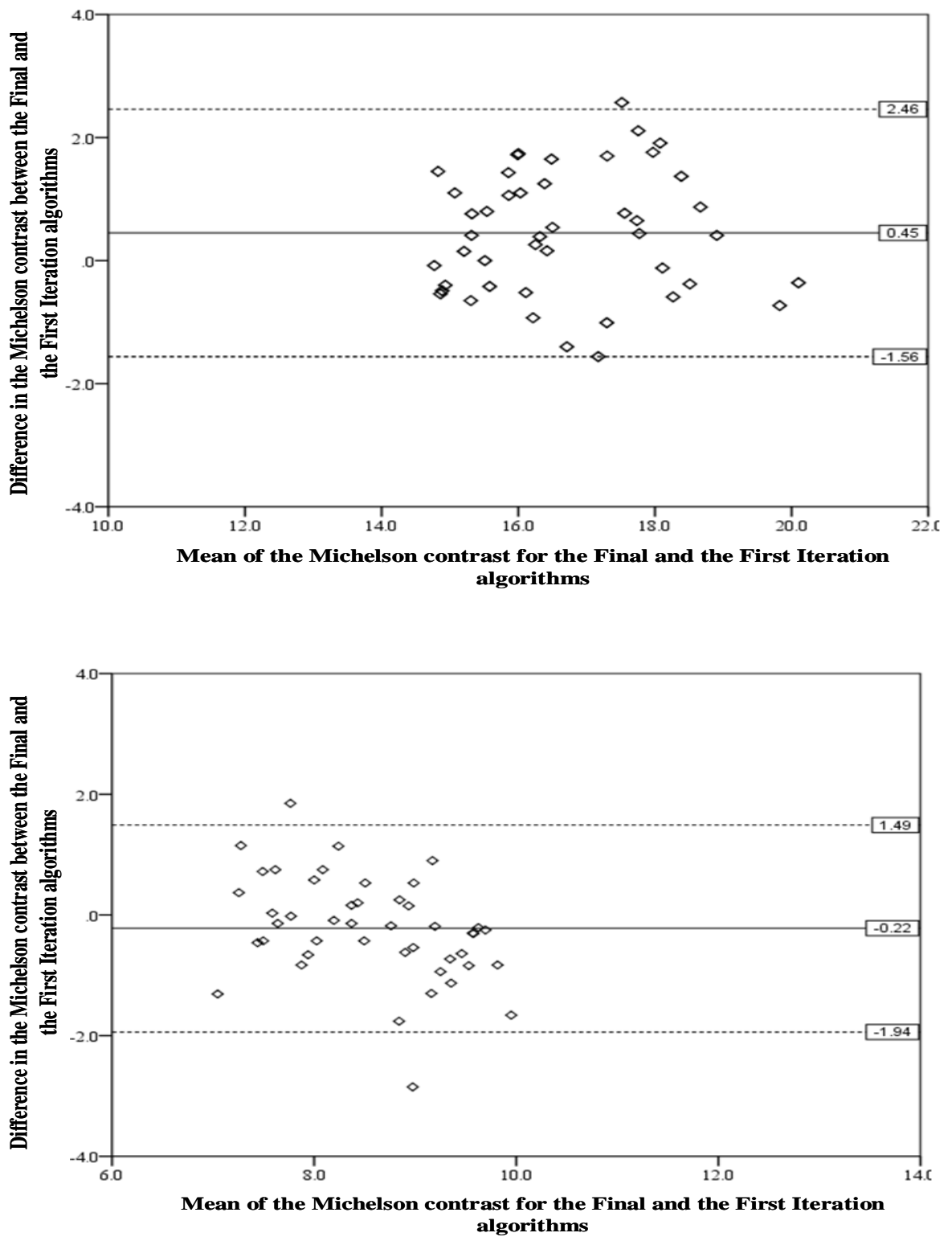


**Figure 7.22** The difference in the Michelson contrast, expressed as sensitivity in dB, between the Final and First Iteration algorithms against that of the mean for the two algorithms in the absence of the noise mask (top) and in the presence of the noise mask

(bottom) for the individual aged 29 years. The solid and dotted lines represent the mean and 2SDs of the differences, respectively. Note the difference in the scaling for the abscissa.

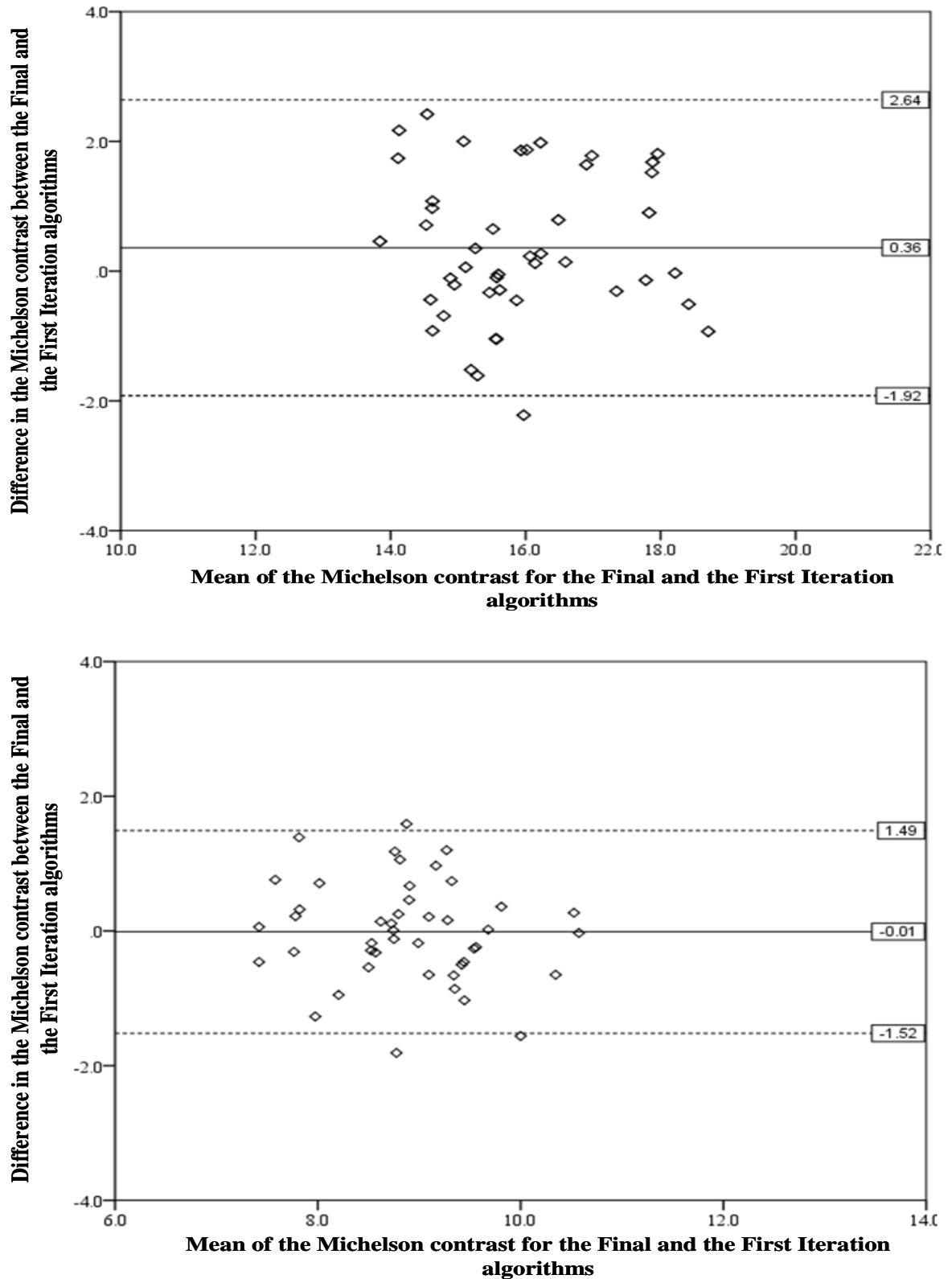


**Figure 7.23** The difference in the Michelson contrast, expressed as sensitivity in dB, between the Final and First Iteration algorithms against that of the mean for the two algorithms in the absence of the noise mask (top) and in the presence of the noise mask (bottom) for the individual aged 33 years. The solid and dotted lines represent the mean

and 2SDs of the differences, respectively. Note the difference in the scaling for the abscissa.

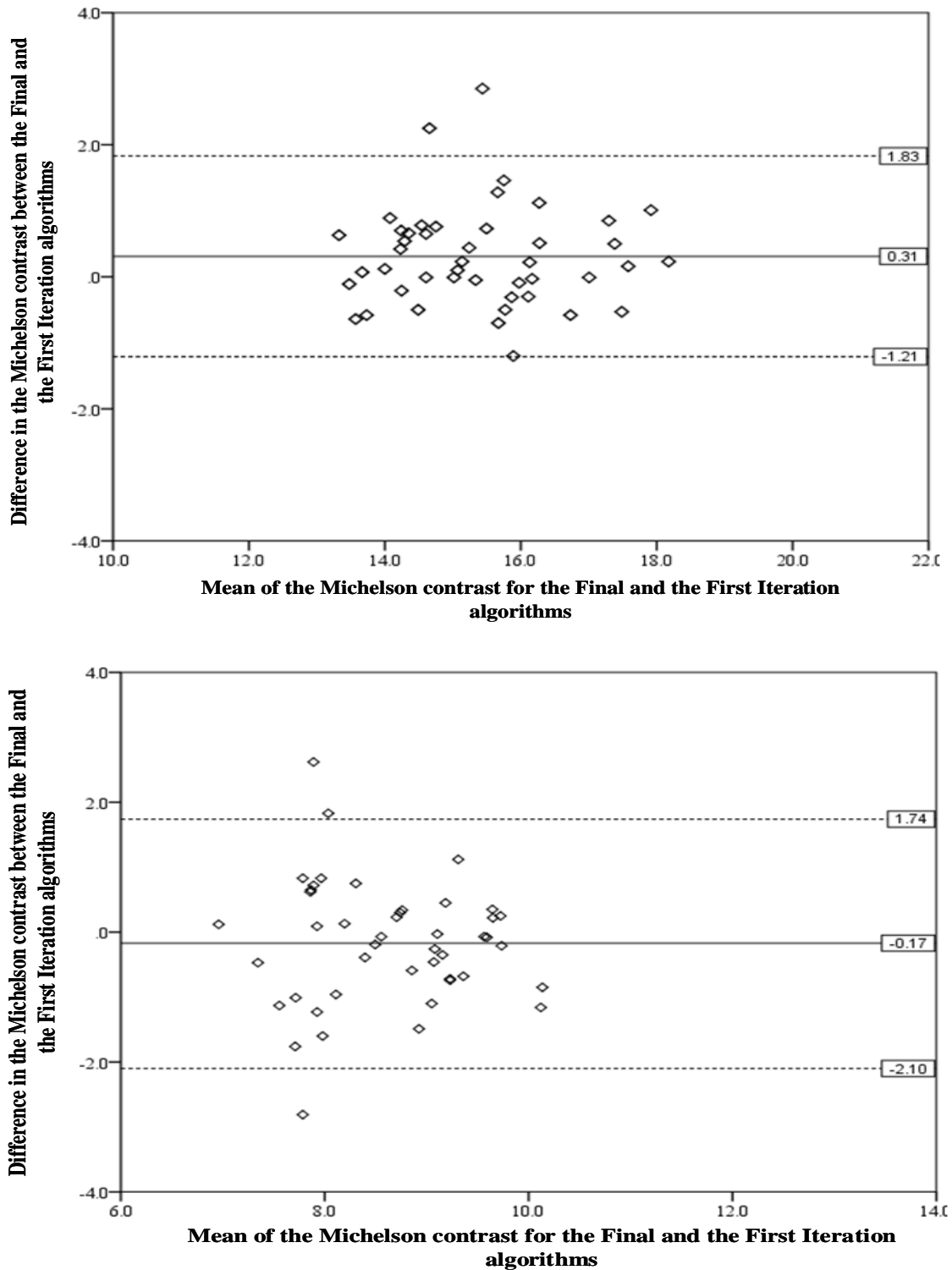


**Figure 7.24** The difference in the Michelson contrast, expressed as sensitivity in dB, between the Final and First Iteration algorithms against that of the mean for the two algorithms in the absence of the noise mask (top) and in the presence of the noise mask (bottom) for the individual aged 39 years. The solid and dotted lines represent the mean

and 2SDs of the differences, respectively. Note the difference in the scaling for the abscissa.

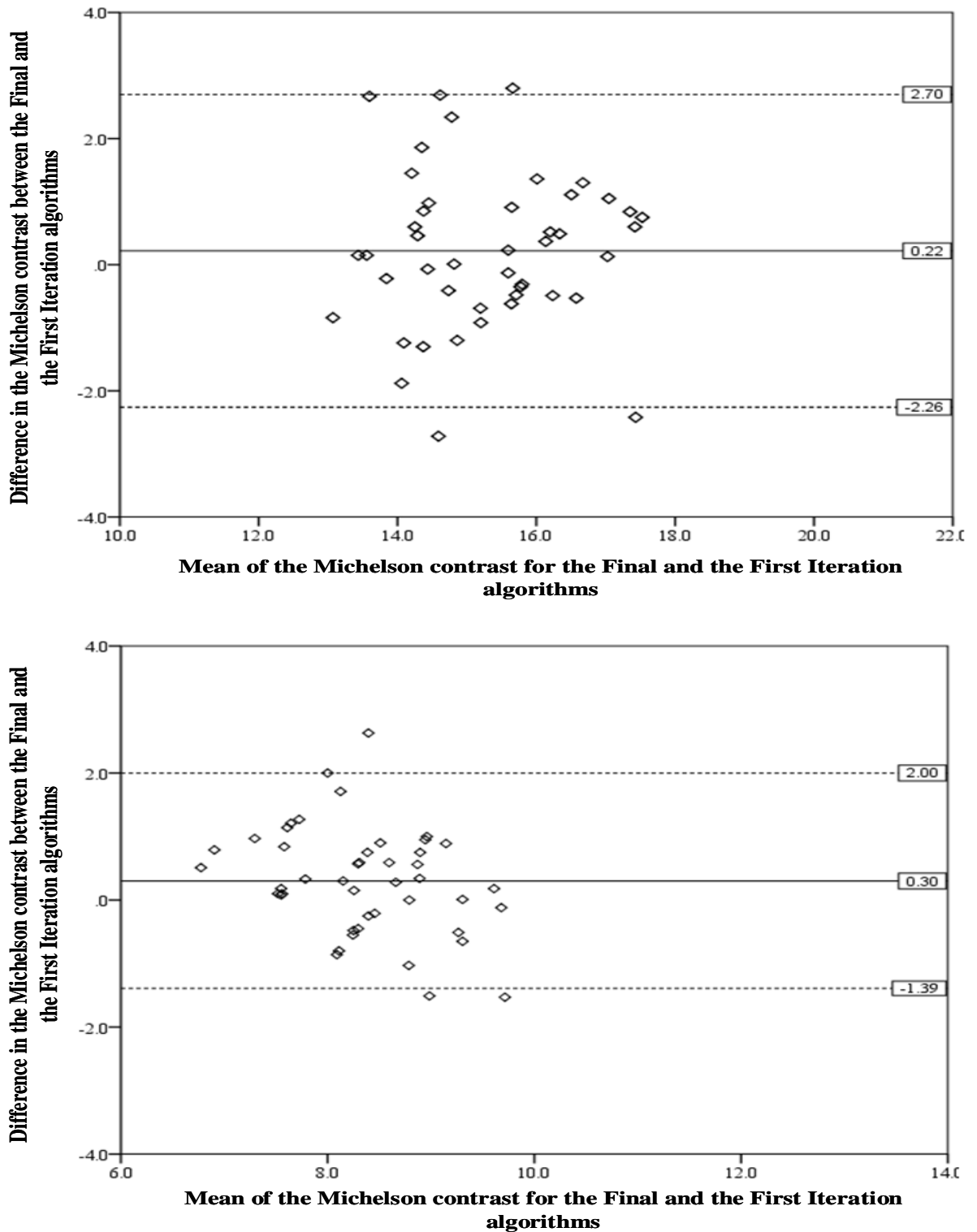


**Figure 7.25** The difference in the Michelson contrast, expressed as sensitivity in dB, between the Final and First Iteration algorithms against that of the mean for the two algorithms in the absence of the noise mask (top) and in the presence of the noise mask (bottom) for the individual aged 45 years. The solid and dotted lines represent the mean

and 2SDs of the differences, respectively. Note the difference in the scaling for the abscissa.

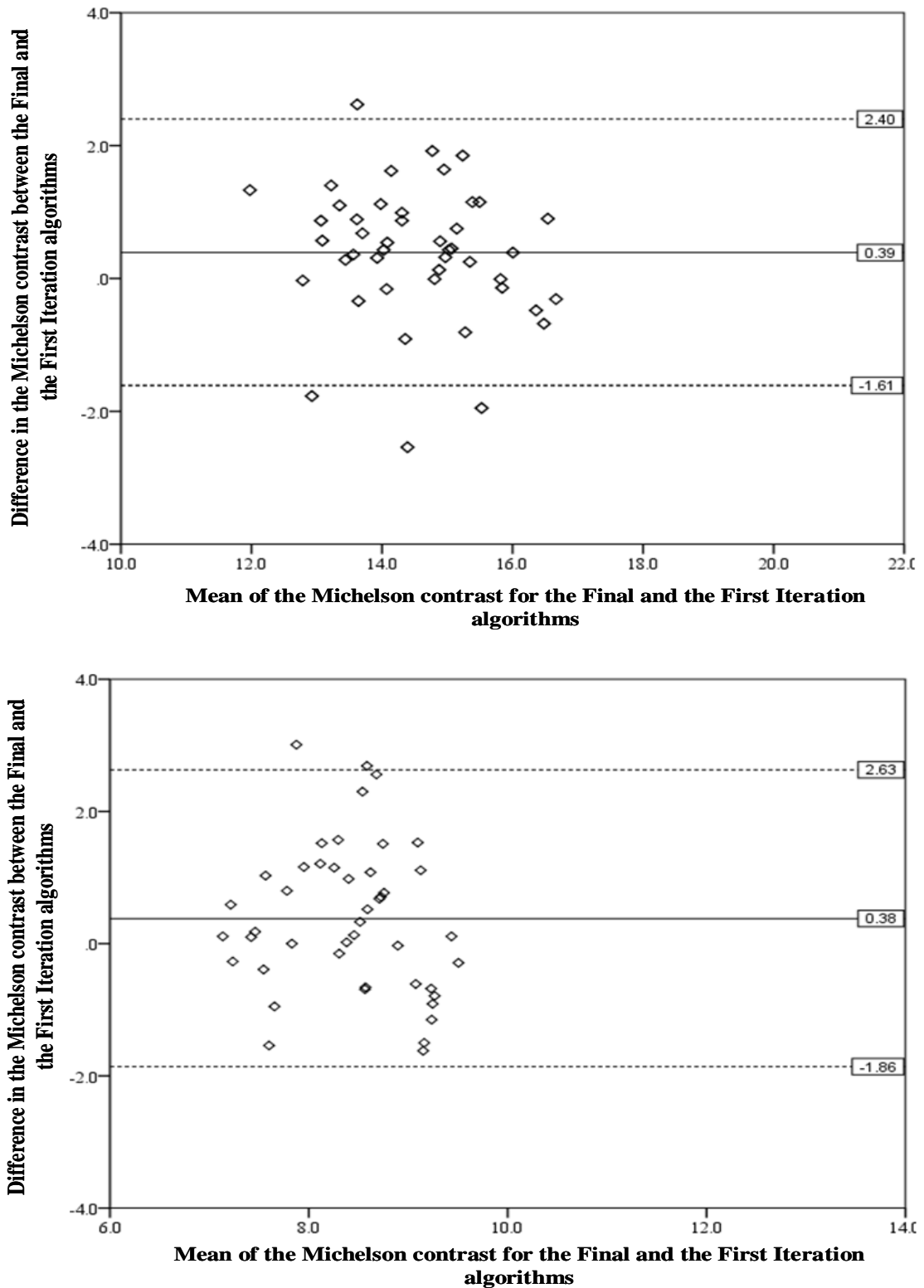


**Figure 7.26** The difference in the Michelson contrast, expressed as sensitivity in dB, between the Final and First Iteration algorithms against that of the mean for the two algorithms in the absence of the noise mask (top) and in the presence of the noise mask (bottom) for the individual aged 57 years. The solid and dotted lines represent the mean

and 2SDs of the differences, respectively. Note the difference in the scaling for the abscissa.

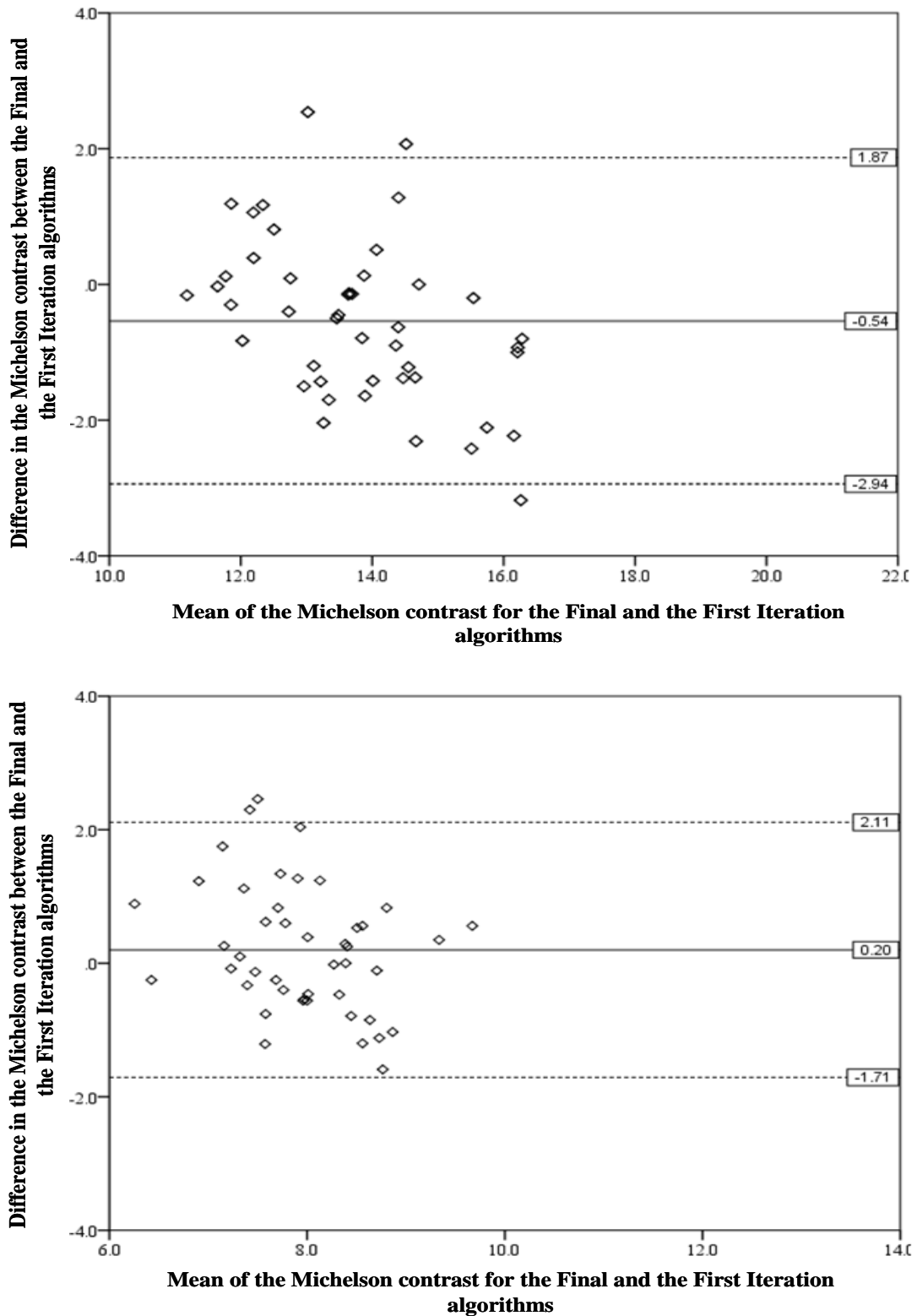


**Figure 7.27** The difference in the Michelson contrast, expressed as sensitivity in dB, between the Final and First Iteration algorithms against that of the mean for the two algorithms in the absence of the noise mask (top) and in the presence of the noise mask (bottom) for the individual aged 65 years. The solid and dotted lines represent the mean

and 2SDs of the differences, respectively. Note the difference in the scaling for the abscissa.

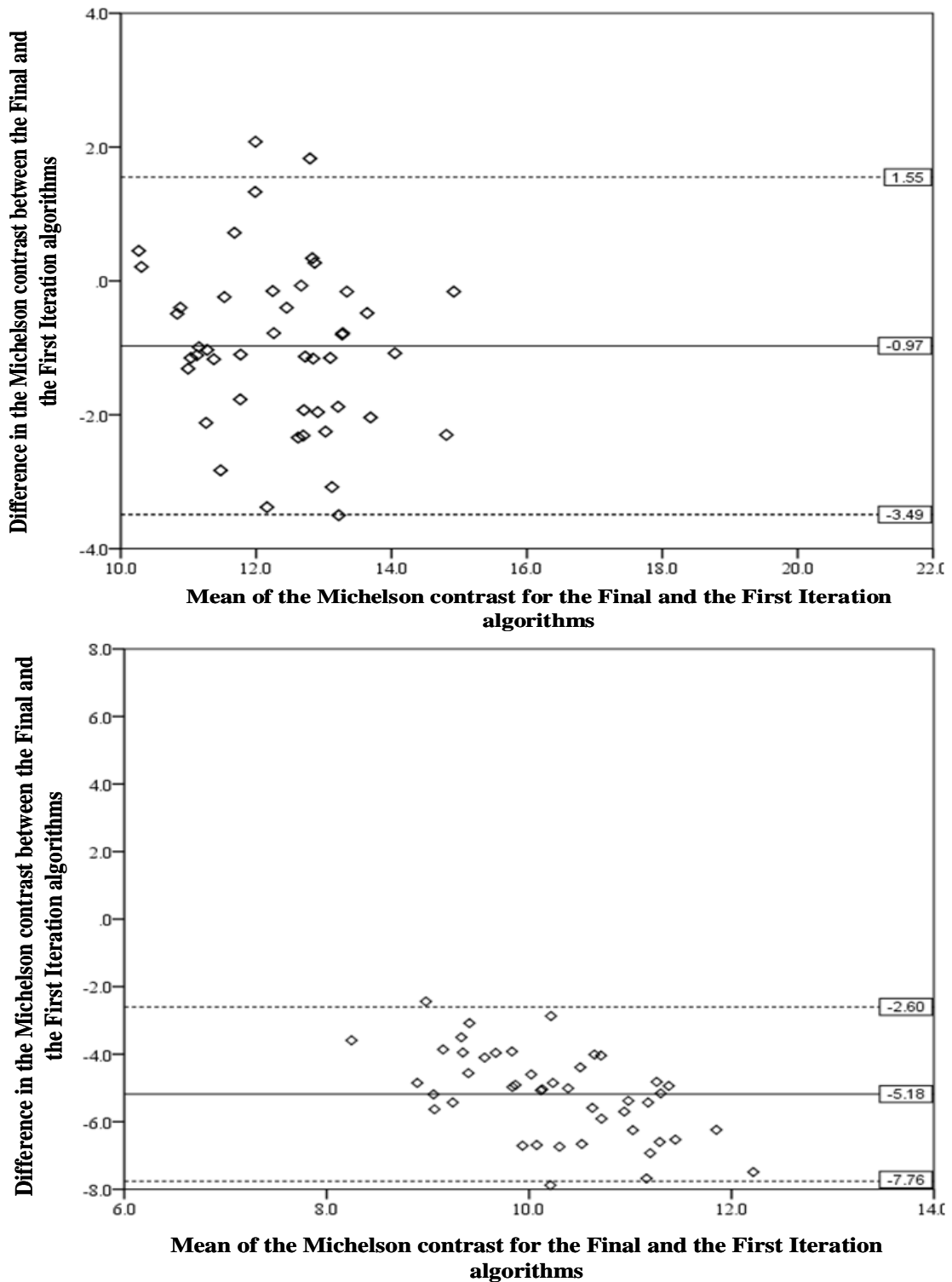


**Figure 7.28** The difference in the Michelson contrast, expressed as sensitivity in dB, between the Final and First Iteration algorithms against that of the mean for the two algorithms in the absence of the noise mask (top) and in the presence of the noise mask (bottom) for the individual aged 70 years. The solid and dotted lines represent the mean

and 2SDs of the differences, respectively. Note the difference in the scaling for the abscissa.

The majority of the time saving with the Final Algorithm arose from the use of eccentricity corrected start values. Four individuals, those aged 29, 33, 39 and 57 years old, provided data for all the stages in the development of the Final Algorithm. The mean examination duration, in the absence of the noise mask, of these four individuals was 315.2 seconds (17.0 SD) for the 8 stimulus location algorithm, 760.2 seconds (56.6 SD) for the 12 location algorithm and 462.1 seconds (42.5 SD) for the 45 location final algorithm (Figure 7.29). The corresponding values in the presence of the noise mask were 336.5 seconds (32.2 SD), 815.9 seconds (137.8 SD) and 545.1 seconds (28.1 SD). For the 29 year old, the examination duration necessary to obtain the threshold at a single stimulus location in the absence of the noise mask was 120 seconds for the Proof of Concept algorithm, 302 and 720 seconds for the 8 and 12 stimulus location algorithms, respectively, and 420 seconds for the 45 locations of the Final Algorithm.

The examination duration for the final algorithm, in the absence and in the presence of the noise mask, was longer compared to that of the most immediately comparable algorithm for standard automated perimetry, namely SITA Standard of the Humphrey Field Analyzer, which in normal individuals for the 56 stimulus locations of Program 24-2 is, on average, 368 seconds (Bengtsson et al., 1998) and in individuals with open angle glaucoma approximately 483 seconds (Nordmann et al., 1998; Wild et al., 1999b). The time for DNP was more immediately comparable to the less accurate FASTPAC algorithm which for Program 24-2 in normal individuals is approximately 240 seconds (Bengtsson et al., 1998) and in individuals with open angle glaucoma approximately 574 seconds (Flanagan et al., 1993; Wild et al., 1999b). Indeed, the examination duration of the Final Algorithm was

considered to be sufficiently short to be used in pilot studies of individuals with ocular disease to test the concept of DNP rather than in a full-scale study.

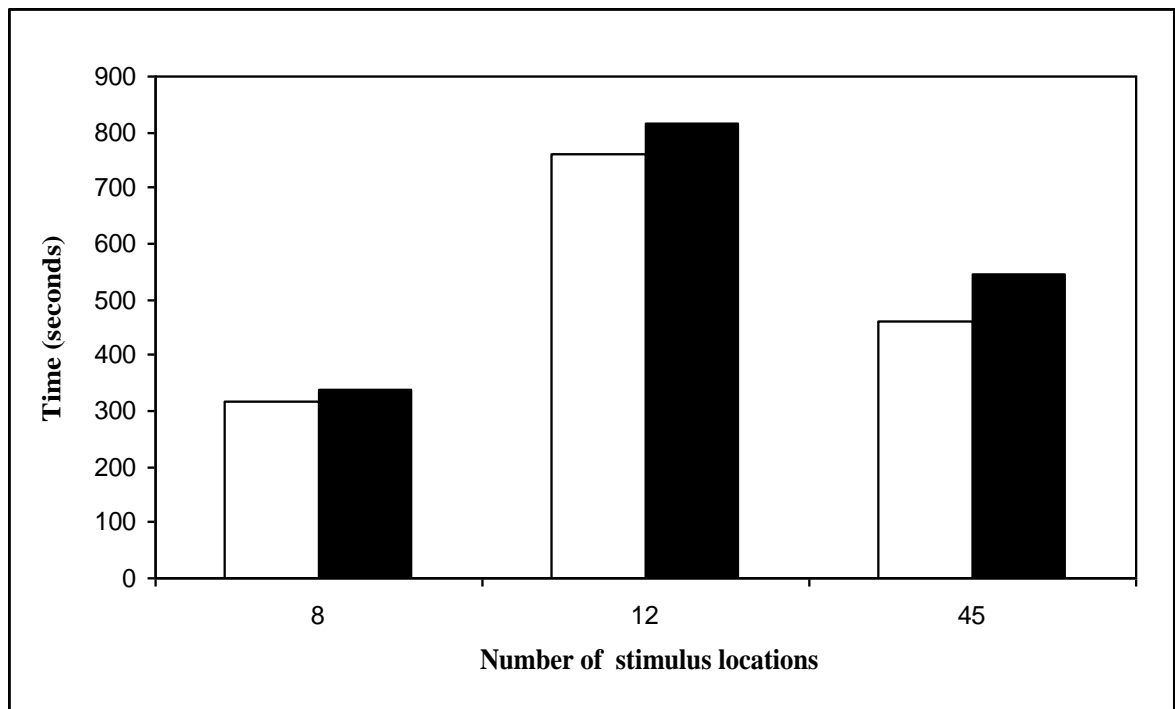


**Figure 7.29** The mean examination duration (SD) of four individuals, aged 29, 33, 39 and 57 years, for the 8 and 12 stimulus location algorithms and for the Final (45 location) Algorithm in the absence of the noise mask (open bars), and in the presence of the noise mask (solid bars).

### 7.3.2.3.3 Conclusion

The continued development of the algorithm should concentrate on a number of aspects. The data set of normal individuals needs to be increased beyond that of the seven individuals. Such an increase should consider the nature of the decline in sensitivity with increase in age, particularly beyond the age of approximately 70 years. With the increase in a representative data set, the start values generated by the polynomial modelling at each location should become more representative of the ‘true’ value and should reduce the number of confirmatory steps (and therefore the examination duration) within the

subsequent algorithm. The polynomial for each location should also incorporate a term for age.

Furthermore, since the start value at any given 'seed' points is relatively close to the expected threshold, the initial stimulus may not be seen by some individuals. It is preferable for the start value to be sufficiently visible to an individual of any age in order for the threshold to be approached precisely. An initial presentation with the contrast level at 4dB greater than the expected threshold would generate a 'seen' response in most normal individuals. A correct response to this stimulus would be followed by two successive presentations with the contrast at 1dB less than the expected threshold. The first incorrect response to these presentations would result in a reversal (i.e., the first reversal). The subsequent presentation would be at an increased contrast level of 2dB and would require two consecutive correct responses to complete the staircase. Two consecutive incorrect responses would also terminate the staircase. The final threshold would be the average of the last seen and the last not seen stimuli. The use of the initial 4dB step would reduce the potential for an initial period where a stimulus is not apparent and would therefore reduce the opportunity for guessing. The removal of the third reversal could lead to some loss in accuracy; however, the majority of algorithms in perimetry incorporate a maximum of two reversals (Flanagan et al., 1993; Glass et al., 1995; Bengtsson et al., 1997; Nordmann et al., 1998; Sekhar et al., 2000; Schiefer et al., 2009).

A further reduction in the examination duration would result from the modification of the start value at any given location based upon the final threshold at any given surrounding location. Such an approach is used in the modern perimetric algorithms (Bengtsson et al., 1997; Bengtsson and Heijl, 1998; Bengtsson et al., 1998; Nordmann et al., 1998; Wild et

al., 1999b; Sekhar et al., 2000; Artes et al., 2002; Turpin et al., 2003; Aoki, Takahashi and Kitahara, 2007; Bourne et al., 2007; Ng et al., 2009; Schiefer et al., 2009).

A small reduction in the examination duration could occur from the introduction of a time window in which the observer either would be required to make the response (including guessing) between one of a pair of consecutively presented stimuli. An initial response occurring outside the time window would be discounted and would increase the contrast level of the next presentation by 2dB. Consecutive responses outside the time window would terminate the staircase at the given location. The magnitude of the time window might be expected to vary between the absence and the presence of the noise mask, with increase in eccentricity, with increase in reaction time and with increase in age. It could be speculated that the time window might be reduced with increasing familiarity of DNP (i.e., as the learning effect declines).

## Chapter 8

### The influence of foveal optical defocus on Dynamic Noise Perimetry

#### 8.1 Introduction

A number of studies have investigated the effects of optical defocus at the fovea on the outcome of SAP determined using Goldmann stimulus size III within 30° eccentricity (Weinreb and Perlman, 1986; Atchison, 1987; Goldstick and Weinreb, 1987; Herse, 1992). The differential light sensitivity within this region declines by approximately 1.4dB per dioptre of foveal defocus irrespective of eccentricity (Heuer et al., 1987). The influence of optical defocus at the fovea increases with reduction in Goldmann stimulus size for those Goldmann stimulus smaller than size III, out to 30° to 40° eccentricity (Atchison, 1987). Ametropia and presbyopia should, therefore, be corrected prior to perimetry (Anderson, McDowell and Ennis, 2001). Lower spatial frequencies are less affected by foveal defocus than are the higher spatial frequencies (Green and Campbell, 1965) and this explains why the larger Goldmann stimuli are more robust to the effects of foveal defocus (Green and Campbell, 1965; Anderson and Patella, 1999; Anderson et al., 2001).

Foveal defocus up to +4.00 dioptres at 30° eccentricity, having corrected for the peripheral refractive error, exerts little influence for a stimulus size approximately equivalent to a Goldmann size VI. However, the decline in sensitivity with increase in foveal defocus increases with reduction in stimulus size (Anderson et al., 2001).

The effect of foveal defocus is less marked at 30° eccentricity compared to that at the fovea (Anderson et al., 2001). The differences in the sensitivity between the fovea and the periphery can be explained by the corresponding differences in the ganglion cell receptive field size (Anderson et al., 2001). At the fovea, the receptive fields are small; therefore, a small stimulus stimulates the given receptive field. Increases in stimulus size result in stimulation of adjoining receptive fields and merely produce small increases in sensitivity. In the periphery, the receptive fields are larger and successive increases in stimulus size result in an increase in sensitivity until the receptive field is completely covered by the stimulus (Anderson et al., 2001).

The influence of foveal defocus has been studied for other types of perimetry including Critical Flicker Fusion (CFF) perimetry, Frequency Doubling Technology (FDT) perimetry, Motion Automated Perimetry (MAP), Rarebit Perimetry (RBP) and Heidelberg Edge Perimetry (HEP).

For CFF, a 1° diameter stimulus is resistant to foveal defocus of up to +3.00DS out to 25° eccentricity; however, CFF declines with increase in foveal defocus up to +9.00DS which was the maximum employed (Lachenmayr and Gleissner, 1992). Conversely, CFF with Goldmann stimulus size III is resistant to foveal defocus up to +10.00 dioptres within 15° eccentricity (Matsumoto et al., 1997).

FDT perimetry is less influenced by foveal defocus because the stimulus consists of a low spatial frequency (0.25 cycle per degree and 0.5 cycle per degree). Sensitivity declines by up to 0.5dB per dioptre of foveal defocus up to +6.00 dioptres (Artes et al., 2003; Dul, 2013). This resistance to foveal defocus is clinically useful in the context of the

examination of patients with high levels of defocus (Anderson and Johnson, 2003b). It is difficult to compare directly the results from SAP and FDT because they each use different contrast metrics, Michelson versus Weber contrasts, respectively (Anderson and Johnson, 2003b).

Motion contrast thresholds (MCT) are not affected by foveal defocus of up to +3.25 dioptres for a range of stimulus displacements and velocities (Barton et al., 1996). However, between +3.25 and +8.00 dioptres of foveal defocus, MCTs are slightly elevated (Trick et al., 1995).

Rarebit Perimetry is affected by foveal defocus of at least upto +6.00 dioptres. The Mean Hit Rate (MHR) decreases and the standard deviation of the MHR (MHR-SD) increases with increase in defocus (Salvetat et al., 2007).

Heidelberg Edge Perimetry (HEP) is increasingly resistant to foveal defocus with increase in eccentricity. The stimulus is resistant to foveal defocus of up to +4.00 dioptres within 3° eccentricity, of up to +6.00 dioptres at 9° eccentricity, and of up to +10.00 dioptres at 15° and 21° eccentricities, respectively (Quaid and Flanagan, 2005b).

The stimulus for Dynamic Noise Perimetry is a low spatial frequency grating (0.5 cycles per degree) presented at 16Hz. The noise mask is currently 4 checks per cycle (See Chapter 2). As such, it would be expected that the grating would be relatively resistant to optical defocus. However, the mask contains high frequency components and it is not known to what extent, if any, the mask will be degraded by optical defocus.

## **8.2 Aim**

The primary aim of the study was to determine, in normal individuals, the influence of foveal optical defocus on the outcome of DNP with and without the noise mask. The secondary aim was to determine any influence of foveal defocus on the DNP stimuli with and without the presence of Gaussian filter of FWHM 0.5.

## **8.3 Methods**

### **8.3.1 Cohort**

The cohort comprised 11 normal individuals, recruited from the student population at the Cardiff School of Optometry and Vision Sciences, who had previously taken part in either the Gaussian Filter study (Chapter 5) or the noise mask study (Chapter 6). Five of the 11 individuals had undertaken both of the studies, 4 had undertaken the filter study, only, and 2 had undertaken the noise mask study, only. The inclusion criteria for the spherical component of the refractive error ranged from +0.50DS to -1.00DS and of the cylindrical component from -0.25 to -0.50DC. The spherical equivalent refractive error ranged from +0.50 to -1.00. All individuals a distance visual acuity of 6/5 or better in each eye and a minimum pupil size of 4mm.

### **8.3.2 Examination protocol**

Seven of the 11 individuals (Group 1) underwent DNP in one designated eye for 48 separate stimulus combinations of location (3), level of defocus (4), presence or absence of

the noise mask (4 checks per cycle; 0.2 RMS) and presence or absence of the Gaussian filter (0.50 FWHM). One randomly assigned set of 12 stimulus combinations was undertaken at each of four visits. The randomisation of the twelve stimulus combinations at each of the four visits, varied between individuals.

The stimulus locations comprised  $0^\circ, 0^\circ; -14^\circ, -8^\circ$  and  $-22^\circ, 4^\circ$  (in right eye format). The four different levels of foveal defocus comprised Plano, +1.00, +2.00 and +4.00DS.

The interval between the first and the second visits ranged between 3 days to one week. The interval between the second and third and between the third and fourth visits, also ranged between 3 days to one week. The remaining 4 individuals (Group 2) underwent an identical protocol to those of the 7 individuals with the exception that the 0.50 FWHM filter was always present. This reduced protocol necessitated two sets of 12 randomly assigned stimulus combinations; with each set undertaken at one of two visits. The interval between the first visit and the second visit ranged from 3 days to one week.

The algorithm used in the study was the ‘Proof of Concept Algorithm’ described in Chapter 7, Section 7.2 and illustrated in Figure 7.1.

Each individual wore their distance refractive correction together with an additional +3.00DS for the 30cm viewing distance of the screen. The fellow eye was occluded with an opaque patch. Fixation was monitored via the CCD camera which provided an image on the display monitor. The DNP was undertaken with the room lighting ‘off’. Prior to the determination of the first threshold, each individual adapted to the screen luminance ( $50\text{cdm}^{-2}$ ) for at least one minute.

A one minute enforced rest period was given after every 3 minutes of DNP and immediately after the completion of a given stimulus combination. During the rest period, each individual was required to maintain their adaptation by continuing to view the screen. Each individual received the same instructions throughout each examination at each visit. If a lack of concentration and/ or a misunderstanding of the requirements of the examination became apparent during a given examination, the test was either paused or cancelled, as appropriate, and a further explanation given to the individual.

Each test lasted approximately 2.5 to 3.0 minutes and each visit lasted approximately 45 to 55 minutes including rest periods.

### **8.3.3 Analysis**

The results were converted into right eye format, where appropriate.

The results for the Michelson contrast, expressed as sensitivity in dB, were analysed using a separate repeated measures ANOVA with sensitivity as the response. Age was included as a between-subjects factor and eccentricity, the absence or the presence of the noise mask, and the absence or the presence of the Gaussian filter, as separate within-subject factors. All 2-way interactions of eccentricity noise mask, and Gaussian filter were included in the model. Each effect was treated as a fixed effect. Subject was included as a random effect.

The derivatives from  $MCN_a$  and  $MCN_p$  were tabulated in terms of descriptive statistics.

### **8.3.4 Ethical Approval**

The study was approved by the Ethics in Research Committee of the Cardiff School of Optometry and Vision Sciences which is in accord with the tenets of the Declaration of Helsinki. All individuals had received written instructions and had signed a consent form prior to the onset of the study.

## **8.4 Results**

The mean age of the 7 individuals in Group One was 26.7 years (SD 3.2; range 21 to 31 years) and of those in Group Two was 25.1 years (SD 3.45; range 21 to 31 years).

### **8.4.1 Michelson contrast, expressed as sensitivity (dB)**

The summary statistics (Mean, SD, Median and IQR) for the seven individuals at each of the three stimulus locations for each of the four levels of defocus, in the absence and in the presence of the noise mask, and without the filter are shown in Table 8.1. The corresponding values for the 11 individuals with the filter are shown in Table 8.2. The results are illustrated graphically in Figures 8.1 and 8.2.

The summary table for the ANOVA is given in Table 8.5.

### Eccentricity

Sensitivity changed with increase in eccentricity ( $p < 0.0001$ ); however, the polarity of the change differed between that for the presence and that for the absence of the noise mask ( $p < 0.0001$ ).

In the absence of the noise mask (and no Gaussian filter), sensitivity declined from a mean of 19.6dB (SD 0.9) at the fovea to a mean of 14.9dB (SD 1.1) at the most peripheral location (i.e. a reduction of 4.6dB or 31%) representing a deterioration of 0.207dB per degree of eccentricity.

Similarly, in the absence of the noise mask, but with the Gaussian filter in situ, sensitivity declined from a mean of 19.1dB (SD 0.9) at the fovea to a mean of 14.7dB (SD 0.8) at the most peripheral location (i.e. a reduction of 4.4dB or 23%) representing a deterioration of 0.196dB per degree of eccentricity.

In the presence of the noise mask but without the Gaussian filter, the sensitivity increased from a mean of 7.8dB (SD 0.9) at the fovea to a mean of 9.6dB (SD 1.5) at the most peripheral location (i.e. an increase of 1.8dB or 23%) representing an increase of 0.08dB per degree of eccentricity.

Similarly, in the presence of the noise mask, but with the Gaussian filter in situ, the sensitivity increased from a mean of 8.1dB (0.6) at the fovea to a mean of 9.3 (SD 1.1) at the most peripheral location (i.e. an increase of 1.2dB or 15%) representing an increase of 0.05dB per degree of eccentricity.

<b>N=7: Without the noise mask, No filter</b>												
<b>Eccentricity</b>	<b>(0°, 0°)</b>				<b>(-14°, -8°)</b>				<b>(-22°, +4°)</b>			
<b>Defocus (DS)</b>	<b>0.00</b>	<b>+1.00</b>	<b>+2.00</b>	<b>+4.00</b>	<b>0.00</b>	<b>+1.00</b>	<b>+2.00</b>	<b>+4.00</b>	<b>0.00</b>	<b>+1.00</b>	<b>+2.00</b>	<b>+4.00</b>
<b>Individual</b>												
<b>2</b>	20.09	19.21	19.72	19.18	16.06	15.06	13.05	12.80	14.09	12.91	12.05	11.32
<b>7</b>	19.85	17.95	18.41	16.10	15.52	14.70	16.24	13.12	15.24	15.52	13.70	13.12
<b>9</b>	20.84	21.54	18.56	18.02	14.16	13.31	12.31	14.65	13.33	13.72	12.71	13.16
<b>12</b>	18.99	18.41	18.06	18.33	16.24	15.55	16.05	14.33	15.02	14.73	14.16	13.72
<b>15</b>	18.21	19.53	15.46	17.17	14.51	12.48	13.94	13.39	14.93	13.71	13.90	13.01
<b>17</b>	18.80	19.07	19.25	16.41	15.19	16.26	15.39	15.90	14.93	15.05	15.23	14.39
<b>21</b>	20.09	19.53	18.99	18.83	14.26	15.87	14.75	13.31	16.92	16.27	15.00	14.26
<b>Mean</b>	<b>19.55</b>	<b>19.32</b>	<b>18.35</b>	<b>17.72</b>	<b>15.13</b>	<b>14.75</b>	<b>14.53</b>	<b>13.93</b>	<b>14.92</b>	<b>14.56</b>	<b>13.82</b>	<b>13.28</b>
<b>SD</b>	<b>0.92</b>	<b>1.14</b>	<b>1.39</b>	<b>1.19</b>	<b>0.85</b>	<b>1.39</b>	<b>1.50</b>	<b>1.09</b>	<b>1.11</b>	<b>1.17</b>	<b>1.15</b>	<b>1.03</b>
<b>Median</b>	<b>19.85</b>	<b>19.21</b>	<b>18.56</b>	<b>18.02</b>	<b>15.19</b>	<b>15.06</b>	<b>14.75</b>	<b>13.39</b>	<b>14.93</b>	<b>14.73</b>	<b>13.90</b>	<b>13.16</b>
<b>IQR</b>	<b>18.90, 20.09</b>	<b>18.74, 19.53</b>	<b>18.23, 19.12</b>	<b>16.79, 18.58</b>	<b>14.39, 15.79</b>	<b>14.01, 15.71</b>	<b>13.49, 15.72</b>	<b>13.22, 14.49</b>	<b>14.51, 15.13</b>	<b>13.71, 15.28</b>	<b>13.21, 14.58</b>	<b>13.07, 13.99</b>
<b>N=7: With the noise mask, No filter</b>												
<b>Eccentricity</b>	<b>(0°, 0°)</b>				<b>(-14°, -8°)</b>				<b>(-22°, +4°)</b>			
<b>Defocus (DS)</b>	<b>0.00</b>	<b>+1.00</b>	<b>+2.00</b>	<b>+4.00</b>	<b>0.00</b>	<b>+1.00</b>	<b>+2.00</b>	<b>+4.00</b>	<b>0.00</b>	<b>+1.00</b>	<b>+2.00</b>	<b>+4.00</b>
<b>Individual</b>												
<b>2</b>	6.82	8.94	7.90	9.02	8.63	9.53	8.99	9.00	8.93	9.03	9.07	10.99
<b>7</b>	8.00	8.51	7.48	9.04	8.35	8.25	9.02	10.01	9.44	9.28	9.40	10.06
<b>9</b>	8.07	8.08	8.49	8.70	11.61	10.24	10.82	10.36	11.81	8.96	10.18	10.53
<b>12</b>	9.11	8.84	7.53	7.20	6.65	8.02	9.97	10.50	7.99	9.37	10.95	11.00
<b>15</b>	6.56	6.48	7.04	7.12	8.76	9.81	8.88	9.20	8.57	8.73	9.75	11.00
<b>17</b>	8.00	8.94	9.42	10.50	9.60	10.80	10.50	11.74	11.50	11.38	11.71	10.63
<b>21</b>	8.33	8.65	9.85	9.21	8.08	8.78	9.25	10.55	9.20	9.55	11.00	11.40
<b>Mean</b>	<b>7.84</b>	<b>8.35</b>	<b>8.25</b>	<b>8.68</b>	<b>8.81</b>	<b>9.35</b>	<b>9.63</b>	<b>10.19</b>	<b>9.63</b>	<b>9.47</b>	<b>10.30</b>	<b>10.80</b>
<b>SD</b>	<b>0.88</b>	<b>0.88</b>	<b>1.06</b>	<b>1.19</b>	<b>1.52</b>	<b>1.04</b>	<b>0.79</b>	<b>0.92</b>	<b>1.46</b>	<b>0.88</b>	<b>0.96</b>	<b>0.43</b>
<b>Median</b>	<b>8.00</b>	<b>8.65</b>	<b>7.90</b>	<b>9.02</b>	<b>8.63</b>	<b>9.53</b>	<b>9.25</b>	<b>10.36</b>	<b>9.20</b>	<b>9.28</b>	<b>10.18</b>	<b>10.99</b>
<b>IQR</b>	<b>7.41, 8.20</b>	<b>8.29, 8.89</b>	<b>7.51, 8.96</b>	<b>7.95, 9.13</b>	<b>8.21, 9.18</b>	<b>8.51, 10.02</b>	<b>9.01, 10.23</b>	<b>9.60, 10.52</b>	<b>8.75, 10.47</b>	<b>8.99, 9.46</b>	<b>9.58, 10.97</b>	<b>10.58, 11.00</b>

**Table 8.1** The summary statistics (Mean, SD, Median and IQR) of the sensitivity (dB) for the 7 individuals at each of the three stimulus locations for each of the four levels of foveal defocus, without the noise mask and without the filter (top) and with the noise mask and without the filter (bottom).

<b>N=11: Without the noise mask, Filter</b>												
<b>Eccentricity</b>	<b>(0°, 0°)</b>				<b>(-14°, -8°)</b>				<b>(-22°, +4°)</b>			
<b>Defocus (DS)</b>	<b>0.00</b>	<b>+1.00</b>	<b>+2.00</b>	<b>+4.00</b>	<b>0.00</b>	<b>+1.00</b>	<b>+2.00</b>	<b>+4.00</b>	<b>0.00</b>	<b>+1.00</b>	<b>+2.00</b>	<b>+4.00</b>
<b>Individual</b>												
<b>1</b>	19.74	18.06	16.17	18.53	15.05	14.23	14.65	15.52	14.94	14.69	13.34	13.26
<b>2</b>	20.18	20.34	20.21	18.53	15.72	15.73	15.16	14.82	13.44	12.19	13.33	13.40
<b>3</b>	18.46	18.40	17.90	19.06	15.15	14.87	14.67	15.82	15.36	14.13	15.33	13.76
<b>4</b>	18.99	18.41	18.06	18.33	17.60	16.24	16.05	15.55	15.02	14.73	14.16	13.72
<b>5</b>	18.61	19.33	20.55	14.86	14.33	13.29	13.72	11.91	15.63	15.47	13.35	12.22
<b>7</b>	18.56	18.80	19.69	18.98	16.07	14.25	15.43	14.09	15.34	13.88	14.88	13.45
<b>9</b>	20.75	18.17	18.50	19.12	15.00	13.28	11.85	13.84	13.31	14.11	12.12	14.64
<b>12</b>	19.16	18.02	18.05	17.95	16.11	15.02	16.00	15.90	15.54	14.30	15.18	14.59
<b>15</b>	18.10	19.36	16.80	18.06	15.89	13.06	13.96	13.88	14.74	14.12	14.75	13.26
<b>17</b>	18.07	20.21	19.40	18.88	15.39	15.96	14.92	13.65	14.16	15.90	14.59	15.52
<b>21</b>	19.21	18.52	16.73	16.73	15.73	14.20	15.26	12.93	13.96	13.02	12.84	12.00
<b>Mean</b>	<b>19.07</b>	<b>18.87</b>	<b>18.37</b>	<b>18.09</b>	<b>15.64</b>	<b>14.56</b>	<b>14.70</b>	<b>14.36</b>	<b>14.68</b>	<b>14.23</b>	<b>13.99</b>	<b>13.62</b>
<b>SD</b>	<b>0.86</b>	<b>0.83</b>	<b>1.46</b>	<b>1.27</b>	<b>0.84</b>	<b>1.11</b>	<b>1.19</b>	<b>1.29</b>	<b>0.83</b>	<b>1.03</b>	<b>1.05</b>	<b>1.03</b>
<b>Median</b>	<b>18.99</b>	<b>18.52</b>	<b>18.06</b>	<b>18.53</b>	<b>15.72</b>	<b>14.25</b>	<b>14.92</b>	<b>14.09</b>	<b>14.94</b>	<b>14.13</b>	<b>14.16</b>	<b>13.45</b>
<b>IQR</b>	<b>18.51, 19.48</b>	<b>18.29, 19.35</b>	<b>17.35, 19.55</b>	<b>18.00, 18.93</b>	<b>15.10, 15.81</b>	<b>13.75, 15.98</b>	<b>14.31, 15.34</b>	<b>13.74, 15.54</b>	<b>14.06, 15.35</b>	<b>14.00, 14.71</b>	<b>13.33, 14.82</b>	<b>13.26, 14.18</b>
<b>N=11: With the noise mask, Filter</b>												
<b>Eccentricity</b>	<b>(0°, 0°)</b>				<b>(-14°, -8°)</b>				<b>(-22°, +4°)</b>			
<b>Defocus (DS)</b>	<b>0.00</b>	<b>+1.00</b>	<b>+2.00</b>	<b>+4.00</b>	<b>0.00</b>	<b>+1.00</b>	<b>+2.00</b>	<b>+4.00</b>	<b>0.00</b>	<b>+1.00</b>	<b>+2.00</b>	<b>+4.00</b>
<b>Individual</b>												
<b>1</b>	7.90	8.52	7.49	9.05	8.01	8.26	9.72	10.00	8.99	9.30	10.04	10.43
<b>2</b>	7.29	9.66	8.70	9.50	8.36	9.50	8.68	10.61	8.08	8.70	9.07	10.12
<b>3</b>	8.88	9.14	9.37	8.81	8.78	8.10	9.05	11.24	9.17	8.57	9.66	10.24
<b>4</b>	8.47	8.84	9.04	9.60	8.02	7.47	8.11	9.54	7.95	8.33	9.20	9.92
<b>5</b>	7.93	8.21	11.50	8.96	8.50	8.58	9.02	10.95	9.17	8.14	9.99	11.05
<b>7</b>	8.70	8.03	9.58	9.37	8.70	9.25	9.03	11.06	11.41	11.40	10.97	10.09
<b>9</b>	7.49	7.91	9.34	10.89	9.10	11.03	10.03	10.58	10.58	10.22	10.96	11.05
<b>12</b>	9.02	8.80	7.00	6.88	7.31	8.33	10.95	10.01	8.11	8.94	10.93	10.92
<b>15</b>	7.96	8.12	8.56	8.95	8.26	8.99	9.05	11.17	8.92	9.30	9.55	10.07
<b>17</b>	7.99	8.73	10.50	10.71	9.71	10.18	10.96	11.61	10.42	11.03	11.15	10.32
<b>21</b>	7.87	8.70	9.05	9.94	8.00	8.38	8.98	10.19	9.85	10.67	10.99	8.79
<b>Mean</b>	<b>8.14</b>	<b>8.61</b>	<b>9.10</b>	<b>9.33</b>	<b>8.43</b>	<b>8.91</b>	<b>9.42</b>	<b>10.63</b>	<b>9.33</b>	<b>9.51</b>	<b>10.23</b>	<b>10.27</b>
<b>SD</b>	<b>0.56</b>	<b>0.52</b>	<b>1.25</b>	<b>1.07</b>	<b>0.64</b>	<b>1.02</b>	<b>0.91</b>	<b>0.64</b>	<b>1.12</b>	<b>1.14</b>	<b>0.79</b>	<b>0.64</b>
<b>Median</b>	<b>7.96</b>	<b>8.70</b>	<b>9.05</b>	<b>9.37</b>	<b>8.36</b>	<b>8.58</b>	<b>9.05</b>	<b>10.61</b>	<b>9.17</b>	<b>9.30</b>	<b>10.04</b>	<b>10.32</b>
<b>IQR</b>	<b>7.89, 8.59</b>	<b>8.16, 8.82</b>	<b>8.63, 9.47</b>	<b>8.95, 9.77</b>	<b>8.01, 8.74</b>	<b>8.30, 9.37</b>	<b>9.00, 9.87</b>	<b>10.10, 11.11</b>	<b>8.51, 10.13</b>	<b>8.64, 10.44</b>	<b>9.60, 10.96</b>	<b>10.08, 10.68</b>

**Table 8.2** The summary statistics (Mean, SD, Median and IQR) of the sensitivity (dB) for the 11 individuals at each of the three stimulus locations for each of the four levels of foveal defocus, without the noise mask and with the filter (top) and with the noise mask and with the filter (bottom).

<b>Factor</b>	<b>Numerator Degrees of Freedom</b>	<b>Denominator Degrees of Freedom</b>	<b>F value</b>	<b>P value</b>
<b>Eccentricity</b>	2	397	118.66	<0.0001
<b>Noise</b>	1	397	4728.62	<0.0001
<b>Filter</b>	1	405	0.02	0.875
<b>Defocus</b>	3	397	0.07	0.975
<b>Eccentricity*noise</b>	2	397	374.44	<0.0001
<b>Eccentricity*filter</b>	2	397	0.87	0.419
<b>Eccentricity*defocus</b>	6	397	1.06	0.388
<b>Noise*filter</b>	1	397	0.02	0.894
<b>Noise*defocus</b>	3	397	36.54	<0.0001
<b>Filter*defocus</b>	3	397	1.31	0.272
<b>Age</b>	1	9.64	0.58	0.463

**Table 8.3** The ANOVA Summary Table for the influence of eccentricity, the presence or absence of the noise mask, the presence or absence of the Gaussian filter (0.50 FWHM), the level of foveal defocus, and the age of the subjects, on the sensitivity derived by DNP.

#### Noise Mask

Overall, as would be expected, sensitivity was lower in the presence of the noise mask ( $p < 0.0001$ ).

#### Gaussian Filter

Overall, sensitivity was not influenced by a Gaussian Filter of 0.5FWHM ( $p = 0.875$ ).

#### Foveal defocus

Overall, sensitivity was not influenced by foveal defocus ( $p = 0.975$ ). However, the effect of the defocus (Figure 8.1) differed between that for the presence and that for the absence of the noise mask ( $p < 0.0001$ ).

In the absence of the noise mask (and no Gaussian filter), the sensitivity at the fovea declined from a mean of 19.6dB (SD 0.9) with zero foveal defocus to a mean of 17.7dB (SD 1.2) with a foveal defocus of 4.00DS (i.e. a reduction of 1.8dB or approximately 0.5dB per dioptre of foveal defocus) and at the most peripheral location from a mean of 14.9dB (SD 1.1) to a mean of 13.3dB (SD 1.0) (i.e. a reduction of 1.6dB or approximately 0.4dB per dioptre of foveal defocus).

Similarly, in the absence of the noise mask, but with the Gaussian filter in situ, the sensitivity at the fovea declined from a mean of 19.1dB (SD 0.9) with zero foveal defocus to a mean of 18.1dB (SD 1.3) with a foveal defocus of 4.00DS (i.e. a reduction of 1.00dB or 0.25dB per dioptre of foveal defocus) and at the most peripheral location from a mean of 14.7dB (SD 0.8) to a mean of 13.6dB (SD 1.0) (i.e. a reduction of 1.1dB or approximately 0.25dB per dioptre of foveal defocus).

In the presence of the noise mask (and no Gaussian filter), the sensitivity at the fovea increased from a mean of 7.8dB (SD 0.9) with zero foveal defocus to a mean of 8.7dB (SD 1.2) with a foveal defocus of 4.00Ds (i.e. an increase of 0.9dB or approximately 0.20dB per dioptre of foveal defocus) and an increase at the most peripheral location from a mean of 9.6dB (SD 1.5) to a mean of 10.8dB (SD 0.4) (i.e. an increase of 1.2dB or approximately 0.30dB per dioptre of foveal defocus).

Similarly, in the presence of the noise mask but with the Gaussian filter in situ, the sensitivity at the fovea increased from a mean of 8.1dB (SD 0.6) with zero foveal defocus to a mean of 9.3dB (SD 1.1) with a foveal defocus of 4.00DS (i.e. an increase of 1.2dB or 0.30dB per dioptre of foveal defocus) and at the most peripheral location increased from a

mean of 9.3dB (SD 1.1) to a mean of 10.3dB (SD 0.6) (i.e. an increase of 0.9dB or approximately 0.25dB per dioptre of foveal defocus).

### Age

As would be expected from the restricted age range (21 to 31 years) of the individuals, sensitivity, overall, was not influenced by age ( $p=0.463$ ).

The outcome of foveal defocus on the derivatives from  $MCN_a$  and  $MCN_p$ , are given in Tables 8.3 to 8.5 inclusive.

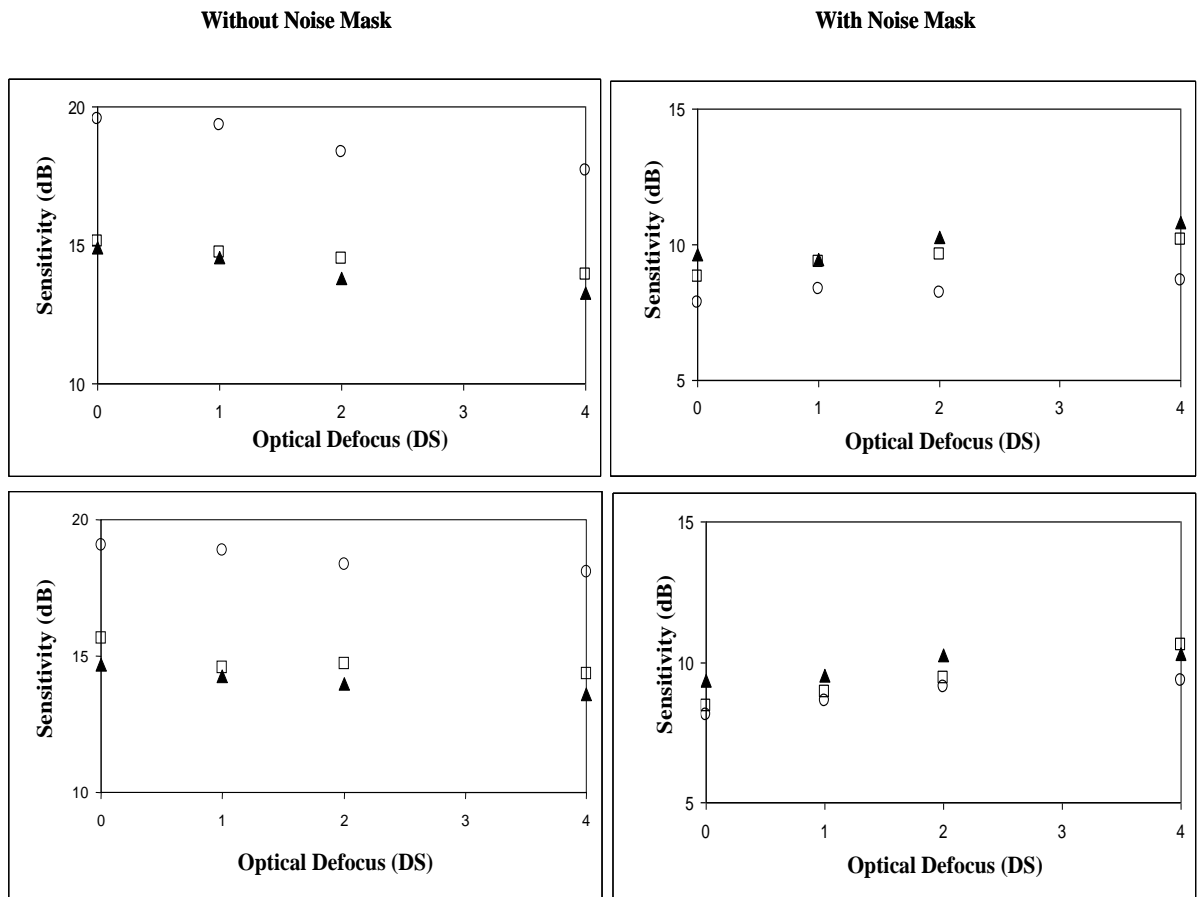


**Figure 8.1** The mean sensitivity at each of the three stimulus locations for the 7 individuals (top) without the Gaussian filter in the absence of the noise mask (top left) and in the presence of the noise mask (top right) at each level of foveal optical defocus and for the 11 individuals (bottom) with the Gaussian filter (0.50FWHM) in the absence of the noise mask (bottom left) and in the presence of the noise mask (bottom right). The open circles indicate the foveal stimulus location ( $0^\circ, 0^\circ$ ). The open square indicates the mid-peripheral stimulus location ( $-14^\circ, -8^\circ$ ) and the filled triangle indicates the peripheral stimulus location ( $-22^\circ, +4^\circ$ ). Note the difference in scaling of the vertical axis between the left and right hand sections of the figure. The error bars have been omitted for clarity.

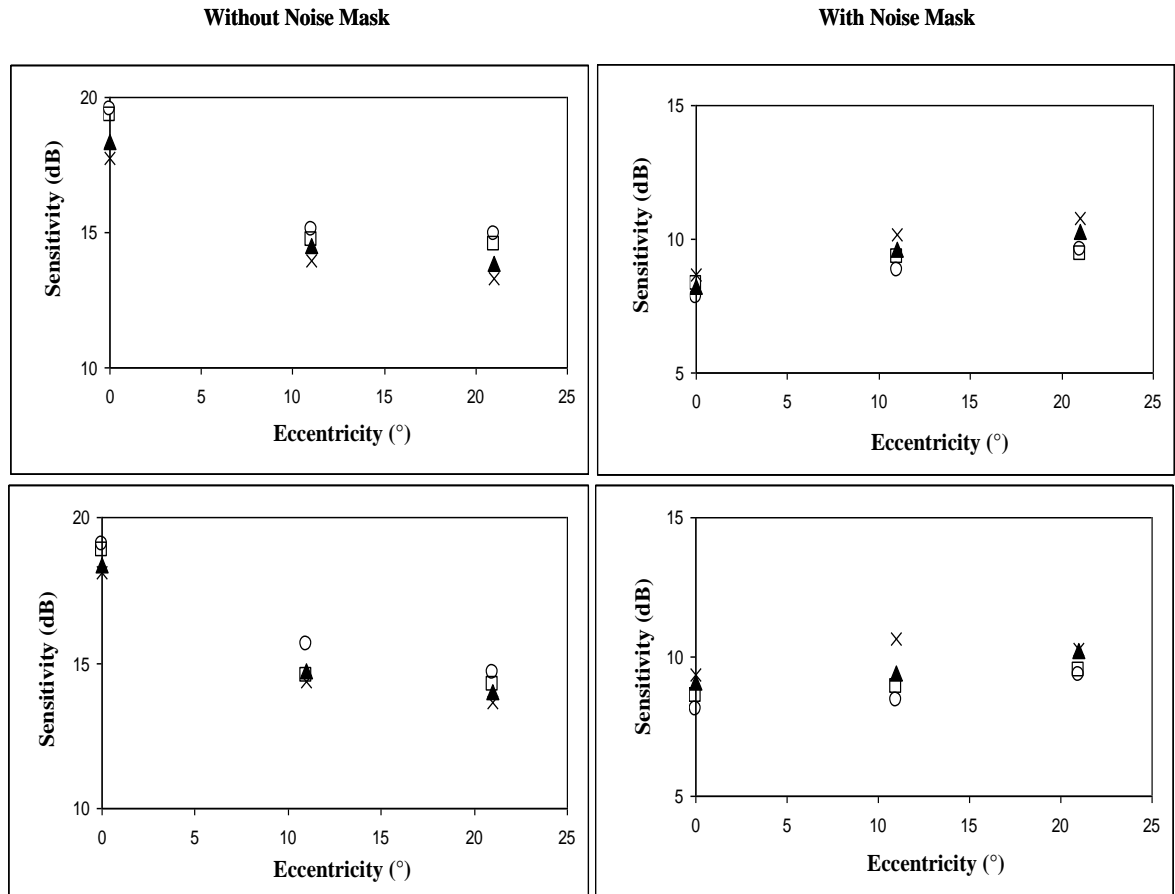


**Figure 8.2** The mean sensitivity for the 7 individuals (top) without the Gaussian filter in the absence of the noise mask (top left) and in the presence of the noise mask (top right), at each stimulus eccentricity and for the 11 individuals (bottom) with the Gaussian filter (0.50FWHM) in the absence of the noise mask (bottom left) and in the presence of the noise mask (bottom right). The open circle indicates zero foveal optical defocus. The open squares, filled triangles and the crosses indicate +1.00, +2.00 and +4.00 dioptres of foveal optical defocus, respectively. Note the difference in scaling of the vertical axis between the left and right hand sections of the figure. The error bars have been omitted for clarity.

#### 8.4.2 Derivatives from $MCN_a$ and $MCN_p$

The summary statistics (Mean, SD, Median and IQR) for the seven individuals for each of the derivatives from  $MCN_a$  and  $MCN_p$  at each of the three stimulus locations for each of the four levels of foveal defocus without the Gaussian filter are shown in Table 8.4 and for the 11 individuals with the Gaussian filter in Table 8.5.

<b>0°, 0°</b>							
<b>Foveal defocus (DS)</b>		<b>MCN<sub>a</sub></b>	<b>MCN<sub>p</sub></b>	<b>N<sub>eq</sub></b>	<b>SE</b>	<b>LOG Ratio</b>	<b>SDI</b>
<b>Plano</b>	<b>Mean</b>	0.006	0.086	0.000002	0.025	0.479	16718.25
	<b>SD</b>	0.001	0.018	0.000001	0.010	0.041	6784.17
<b>+1.00</b>	<b>Mean</b>	0.006	0.076	0.000003	0.032	0.508	15969.24
	<b>SD</b>	0.001	0.018	0.000001	0.010	0.053	10490.31
<b>+2.00</b>	<b>Mean</b>	0.008	0.079	0.000004	0.032	0.525	10201.88
	<b>SD</b>	0.003	0.018	0.000002	0.017	0.039	4578.04
<b>+4.00</b>	<b>mean</b>	0.009	0.072	0.000008	0.041	0.564	7529.42
	<b>SD</b>	0.002	0.020	0.000008	0.023	0.075	3766.19
<b>15°, -9°</b>							
<b>Foveal defocus (DS)</b>		<b>MCN<sub>a</sub></b>	<b>MCN<sub>p</sub></b>	<b>N<sub>eq</sub></b>	<b>SE</b>	<b>LOG Ratio</b>	<b>SDI</b>
<b>Plano</b>	<b>Mean</b>	0.016	0.071	0.000036	0.057	0.653	2165.67
	<b>SD</b>	0.003	0.023	0.000051	0.061	0.107	840.48
<b>+1.00</b>	<b>Mean</b>	0.018	0.061	0.000049	0.061	0.699	1974.46
	<b>SD</b>	0.006	0.014	0.000051	0.031	0.092	1021.78
<b>+2.00</b>	<b>Mean</b>	0.019	0.056	0.000077	0.075	0.725	1848.28
	<b>SD</b>	0.007	0.010	0.000117	0.052	0.088	1108.05
<b>+4.00</b>	<b>Mean</b>	0.021	0.050	0.000077	0.092	0.778	1313.99
	<b>SD</b>	0.005	0.010	0.000029	0.040	0.030	774.55
<b>-21°, 3°</b>							
<b>Foveal defocus (DS)</b>		<b>MCN<sub>a</sub></b>	<b>MCN<sub>p</sub></b>	<b>N<sub>eq</sub></b>	<b>SE</b>	<b>LOG<sub>10</sub> Ratio</b>	<b>SDI</b>
<b>Plano</b>	<b>Mean</b>	0.0169	0.058	0.000074	0.093	0.708	2071.35
	<b>SD</b>	0.0041	0.018	0.000115	0.098	0.111	1206.14
<b>+1.00</b>	<b>Mean</b>	0.0185	0.059	0.000041	0.062	0.710	1760.01
	<b>SD</b>	0.0049	0.010	0.000022	0.038	0.051	941.54
<b>+2.00</b>	<b>Mean</b>	0.0219	0.049	0.000088	0.100	0.790	1241.09
	<b>SD</b>	0.0060	0.011	0.000035	0.044	0.034	601.63
<b>+4.00</b>	<b>Mean</b>	0.0247	0.043	0.000403	0.213	0.850	940.67
	<b>SD</b>	0.0064	0.004	0.000718	0.221	0.063	375.85

**Table 8.4** The summary statistics (Mean and SD) of the Michelson contrast, without the Gaussian filter (0.50FWHM), in the absence (MCN<sub>a</sub>) and in the presence (MCN<sub>p</sub>) of the noise mask and of the four derivatives: Equivalent noise (N<sub>eq</sub>); Sampling efficiency (SE); LOG<sub>10</sub> of the ratio MCN<sub>p</sub> : MCN<sub>a</sub> and Signal Detection Index (SDI) for the 7 normal individuals at each stimulus eccentricity at each level of foveal optical defocus.

<b>0°, 0°</b>							
<b>Foveal defocus (DS)</b>		<b>MCN<sub>a</sub></b>	<b>MCN<sub>p</sub></b>	<b>N<sub>eq</sub></b>	<b>SE</b>	<b>LOG<sub>10</sub> Ratio</b>	<b>SDI</b>
<b>Plano</b>	<b>Mean</b>	0.006	0.079	0.000002	0.0280	0.50	13438.52
	<b>SD</b>	0.001	0.010	0.000001	0.0074	0.04	5939.20
<b>+1.00</b>	<b>Mean</b>	0.007	0.071	0.000003	0.0347	0.53	12192.70
	<b>SD</b>	0.001	0.008	0.000001	0.0089	0.03	5189.00
<b>+2.00</b>	<b>Mean</b>	0.008	0.065	0.000005	0.0498	0.56	10982.56
	<b>SD</b>	0.003	0.019	0.000002	0.0314	0.04	7169.87
<b>+4.00</b>	<b>Mean</b>	0.008	0.061	0.000008	0.0528	0.58	8895.33
	<b>SD</b>	0.003	0.017	0.000006	0.0238	0.06	3448.09
<b>-15°, -9°</b>							
<b>Foveal defocus (DS)</b>		<b>MCN<sub>a</sub></b>	<b>MCN<sub>p</sub></b>	<b>N<sub>eq</sub></b>	<b>SE</b>	<b>LOG<sub>10</sub> Ratio</b>	<b>SDI</b>
<b>Plano</b>	<b>Mean</b>	0.0142	0.0742	0.000015	0.0337	0.61	2764.60
	<b>SD</b>	0.0026	0.0108	0.000008	0.0112	0.05	1304.85
<b>+1.00</b>	<b>Mean</b>	0.0185	0.0673	0.000041	0.0510	0.68	1750.61
	<b>SD</b>	0.0046	0.0146	0.000049	0.0386	0.08	895.19
<b>+2.00</b>	<b>Mean</b>	0.0180	0.0597	0.000051	0.0624	0.70	1857.02
	<b>SD</b>	0.0058	0.0117	0.000068	0.0338	0.08	800.01
<b>+4.00</b>	<b>Mean</b>	0.0196	0.0447	0.000133	0.1279	0.79	1640.54
	<b>SD</b>	0.0061	0.0067	0.000166	0.0675	0.08	862.36
<b>-21°, 3°</b>							
<b>Foveal defocus (DS)</b>		<b>MCN<sub>a</sub></b>	<b>MCN<sub>p</sub></b>	<b>N<sub>eq</sub></b>	<b>SE</b>	<b>LOG<sub>10</sub> Ratio</b>	<b>SDI</b>
<b>Plano</b>	<b>Mean</b>	0.0177	0.0615	0.000043	0.0621	0.70	1748.35
	<b>SD</b>	0.0035	0.0150	0.000037	0.0398	0.08	601.77
<b>+1.00</b>	<b>Mean</b>	0.0198	0.0591	0.000061	0.0718	0.73	1474.85
	<b>SD</b>	0.0049	0.0145	0.000054	0.0491	0.08	672.03
<b>+2.00</b>	<b>Mean</b>	0.0210	0.0493	0.000114	0.1051	0.78	1323.44
	<b>SD</b>	0.0052	0.0091	0.000132	0.0597	0.07	586.14
<b>+4.00</b>	<b>Mean</b>	0.0228	0.0486	0.000120	0.1043	0.80	1120.76
	<b>SD</b>	0.0053	0.0076	0.000118	0.0525	0.05	560.82

**Table 8.5** The summary statistics (Mean and SD) of the Michelson contrast, with the Gaussian filter (0.50FWHM), in the absence (MCN<sub>a</sub>) and in the presence (MCN<sub>p</sub>) of the noise mask and of the four derivatives: Equivalent noise (N<sub>eq</sub>); Sampling efficiency (SE); LOG<sub>10</sub> of the ratio MCN<sub>p</sub> : MCN<sub>a</sub> and Signal Detection Index (SDI) for the 11 normal individuals at each stimulus eccentricity at each level of foveal optical defocus.

Stimulus location		MCN <sub>a</sub>	MCN <sub>p</sub>	N <sub>eq</sub>	SE	LOG <sub>10</sub> Ratio	SDI
0°, 0°	Median	33.75	-18.35	323.11	51.13	20.05	-44.10
	IQR	25.14; 82.41	-30.55; - 12,79	139.63; 618.97	32.60; 122.63	12.70; 29.45	-69.72; - 36.10
-15°, -9°	Median	29.48	-31.75	523.86	171.43	24.66	-40.35
	IQR	6.87; 64.31	-41.17; - 8.89	116.17; 624.48	35.94; 249.61	11.80; 30.76	-62.62; - 5.05
-21°, 3°	Median	55.58	-37.80	871.53	267.21	35.79	-58.68
	IQR	24.01; 73.70	-41.35; 4.53	157.32; 1108.10	13.89; 407.99	7.85; 37.04	-66.45; - 33.51
Stimulus location		MCN <sub>a</sub>	MCN <sub>p</sub>	N <sub>eq</sub>	SE	LOG <sub>10</sub> Ratio	SDI
0°, 0°	Median	32.10	-22.8	144.79	70.06	16.90	-42.70
	IQR	- 4.20;46.0	-38.9; - 17.4	37.08; 622.61	47.68; 175.25	6.54; 31.75	-53.06; 9.90
-15°, -9°	Median	49.30	-40.37	444.56	264.93	27.16	-55.14
	IQR	13.96; 59.55	-43.22; - 36.12	303.85; 1029.11	189.29; 275.23	23.06; 37.74	-60.71; - 21.52
-21°, 3°	Median	40.57	-23.29	300.10	105.72	19.25	-49.39
	IQR	12.64; 50.78	-35.73; - 3.95	52.27; 430.30	-1.83; 193.44	2.50; 25.49	-55.94; - 18.52

**Table 8.6** The summary statistics (Median and IQR) of the proportionate difference (%) between the +4.00DS and zero levels of foveal optical defocus, in the absence of the Gaussian filter, for the Michelson contrast in the absence (MCN<sub>a</sub>) and in the presence (MCN<sub>p</sub>) of the noise mask and of the four derivatives: Equivalent noise (N<sub>eq</sub>); Sampling efficiency (SE); LOG<sub>10</sub> of the ratio MCN<sub>p</sub> : MCN<sub>a</sub>; and Signal Detection Index (SDI) for the 7 normal individuals (top) and 11 normal individuals (bottom) at each of the three given locations, without and with the Gaussian filter (0.50FWHM), respectively. All values exhibit a deterioration with increase in defocus.

## 8.5 Discussion

The Gaussian filtering of the stimulus edge did not influence sensitivity.

The presence of the noise mask, as would be expected, attenuated the sensitivity compared to that in the absence of the noise mask ( $p < 0.0001$ ).

With increase in eccentricity, sensitivity decreased in the absence of the noise mask at a rate of approximately -0.2dB per degree of eccentricity but increased in the presence of the noise mask at a rate of approximately 0.07dB per degree of eccentricity ( $p < 0.0001$ ). The sensitivity profile in the presence of the noise mask was approximately 1.5dB higher at the most peripheral location compared to that at fixation.

The decline in sensitivity, in the absence of the noise mask, with increase in eccentricity is compatible with other types of clinical perimetry (Raninen and Rovamo, 1986; Wall et al., 1991; Johnson, Cioffi and Van Buskirk, 1999; Blumenthal et al., 2003; Anderson et al., 2005; Salvetat et al., 2013).

The increase in sensitivity with increase in eccentricity, in the presence of the 4 checks per cycle noise mask is similar to that obtained in Chapter 6. The difference between the foveal sensitivity in the presence of noise mask, and in the absence of defocus, in the current study was 1.2dB compared to 1.6dB at the same locations described in Chapter 6. It must also be appreciated that the noise mask can never be of such strength as to render the sensitivity gradient parallel to that in the absence of the noise mask (Chapter 6).

With increase in defocus, regardless of the presence or absence of the Gaussian filter, sensitivity in the absence of the noise mask declined at each of the three stimulus locations by approximately 0.25 to 0.5dB per dioptre of defocus ( $p < 0.0001$ ). The reduction of approximately 0.25 to 0.5dB per dioptre of defocus can be compared to that of 0.63dB units per dioptre for a near identical pupil size (range 3.5 to 6mm) and stimulus condition, namely a  $5^\circ$  square stimulus containing a 0.5 cycles per degree grating superimposed on a background with an average luminance of  $50\text{cdm}^{-2}$  and specified in terms of Michelson contrast (Anderson and Johnson, 2003a). A similar gradient of up to 0.5dB per dioptre of foveal defocus was also found for the larger  $10^\circ \times 10^\circ$  stimuli of the initial commercially available FDT perimeter which presents, at 25Hz, a 0.5 cycle per degree grating for the central stimulus and a 0.25 cycle per degree grating for the peripheral stimuli (Artes et al., 2003). For a  $0.5^\circ$  spatial SD Gabor stimulus containing a 0.5 cycle per degree grating presented at 5Hz, the gradient was approximately 0.5dB per dioptre of defocus between  $2^\circ$  and  $7^\circ$  (Horner et al., 2013). Defocus by 6.00 dioptres resulted in a reduction of sensitivity for spatial frequencies of 0.14 to 0.5 cycles per degree and spatial SDs, scaled appropriately for eccentricity, from  $0.5^\circ$  to  $1.8^\circ$ , by 0.27dB between  $0^\circ$  and  $10^\circ$  eccentricity, by 0.20dB between  $10^\circ$  and  $20^\circ$  and by 0.13dB between  $20^\circ$  and  $27^\circ$  (Horner et al 2013). Equally, the gradient for a  $0.4^\circ$  circular white stimulus on a white background was 0.43dB per dioptre of defocus at the fovea (Anderson et al., 2001). The results can also be placed in the context of the reduction for the size III stimulus of standard automated perimetry of 1.84dB per dioptre for an 8mm pupil and of -1.10dB per dioptre for a 3mm pupil out to  $4.2^\circ$  eccentricity (Herse, 1992); and, for pharmacologically dilated pupils, over the central field of 0.24dB per dioptre (Weinreb and Perlman, 1986) and 0.37dB per dioptre (Heuer et al., 1987). However, caution must be exercised in this latter regard since the concept of DNP is based upon Michelson contrast whilst that of standard automated

perimetry is based upon Weberian contrast. Frequency Doubling Perimetry is also based upon Michelson contrast.

When a stimulus is defocused by optical blur, the diameter of the stimulus increases but the overall luminance remains the same; a blur circle is formed at the retina and the point luminance decreases. If the blur circle is limited within a single ganglion cell receptive field, the threshold will not be significantly altered; but as defocus increases and the blur circle spreads out onto multiple ganglion cell receptive fields, the energy on one ganglion cell receptive field decreases; thereby increasing the threshold (Anderson et al., 2001).

With the noise mask, sensitivity increased by approximately 0.2 to 0.4dB per dioptre of defocus.

The low frequency stimulus (0.5 cycle per degree sine wave grating) of DNP was, as would be expected, relatively immune to the optical defocus (Green and Campbell, 1965; Atchison, Woods and Bradley, 1998; Strang, Atchison and Woods, 1999). The noise mask contains higher frequency components which should be more affected by the foveal defocus. The sharp border between each pixel is degraded with increasing defocus resulting in a reduction in the effect (strength) of the noise mask. The increase in sensitivity at all three locations within increase in defocus indicates that the effective strength of the noise mask is reduced by 1dB in the presence of a +4.00DS foveal defocus. The subjective visual impression with the +4.00DS foveal defocus was that the noise mask checks had merged with the grating giving the appearance of a 'cloud' superimposed upon the grating.

The retinal image is also magnified by the given defocus lens. The vergence of the light entering the eye,  $L_c$ , can be expressed as:

$$L_c = L / 1 - [(d/n) L]$$

where  $L$  = the power of the defocus lens,  $d$  = the back vertex distance, and  $n$  = refractive index of air. For a defocus lens of +4.00 and a back vertex distance of 12mm,  $L_c = 4.20$ .

The magnification due to the defocus lens,  $M$ , can be expressed as:

$$M = L_c/L_d$$

where  $L_d$  is the vergence of the light from the stimulus =  $(1/ax)*n + F$

and where, for example, for the Emsley Standard Reduced Eye,  $ax$  is the axial length of 22.22mm, and  $n$  is the refractive index of 1.333 and  $F$  is the power of the eye of +60.00 dioptres. With these values,  $L_d = +60.06$  dioptres.

Thus,  $M = 4.20/60.06 = 7.0\%$ .

However, no attempt was made to correct the stimulus for the effect of magnification.

Quite marked between-individual variations exist in the magnitude of the peripheral refractive error at any given location (Taberner et al., 2011). It is possible that the given

lens used to induce the foveal defocus could have either partially corrected or exacerbated the given peripheral refractive error at any given location for any given individual. However, there was no systematic change in the magnitudes of the SDs at any given eccentricity with increase in foveal defocus. Interestingly, peripheral contrast sensitivity is more robust to defocus, even following correction of peripheral refractive error (Anderson et al., 2001).

The study was undertaken on young individuals with natural pupils. Clearly, it will be important to ascertain the impact not only of the foveal defocus on the lower sensitivity profile for older individuals for DNP, both in the absence and in the presence of the noise mask, but also of the interaction between the smaller pupil size, occurring due to older age, and the magnitude of foveal defocus on the DNP sensitivity profile.

The vulnerability of the noise mask to foveal defocus suggests that it would also be vulnerable to the effect of forward intra-ocular light scatter arising from age-related cataract. Forward intra-ocular light scatter causes a loss of stimulus contrast due to the veiling glare even for low spatial frequencies and it can also be hypothesised that the 0.5 cycles per degree DNP stimulus would also be attenuated. Indeed, the overall reduction in sensitivity arising from the straylight affects all types of perimetry but to varying levels (Bergin et al., 2011; Oleszczuk et al., 2012).

It can be conjectured that any reduction in sensitivity derived by the grating arising from foveal defocus would have a more pronounced effect on focal visual field loss arising from glaucomatous damage in that the defocus may lead to an underestimation of the borders of the defect. Such an outcome occurs with the reduced image quality arising from forward

intra-ocular light scatter in age-related cataract. Following improved image quality as a result of cataract extraction and intra-ocular lens implantation, the MD index improves, as would be expected, but the PSD index worsens (Siddiqui, Azuara-Blanco and Neville, 2005; Rao et al., 2013).

A detailed inferential analysis of the four derivatives of Michelson contrast in the absence and in the presence of the noise mask was not undertaken since it was felt necessary to fully understand the impact of foveal defocus on the Michelson contrasts in the absence and in the presence of the noise mask.

## **8.6 Conclusion**

The DNP stimulus is relatively robust to optical defocus up to +4.00DS in the fovea and in the periphery: In the absence of the noise mask, a +4.00DS foveal defocus results in an approximate 1dB attenuation in sensitivity. In the presence of the noise mask, a +4.00DS foveal defocus results in an approximate 1dB increase in sensitivity, i.e., a reduction in the effective strength of the noise mask by 1dB. The utilization of appropriate refractive correction is recommended for the DNP especially in the presence of the noise mask.

## **Chapter 9**

### **Long-term follow-up of DNP in open angle glaucoma**

#### **9.1 Introduction**

In 2007, Dr. Rattan had undertaken an exploratory cross-sectional study of the utility of DNP in 10 individuals with either open angle glaucoma or considered as a glaucoma suspect. Michelson contrasts, with and without the noise mask, had been determined at the same four locations for all ten individuals. The results, including the four derivatives from the Michelson contrasts with and without the noise mask, for each individual at each location, had been compared to the corresponding 90<sup>th</sup> percentile obtained from 16 normal individuals. The results had also been compared to standard automated perimetry and to optical coherence tomography. DNP identified abnormality which was present with standard automated perimetry but also seemed to identify additional abnormality. In order to validate the additional abnormality, a longer-term follow-up was envisaged, to allow for disease progression, whereby the outcome could be compared to the initial findings and to that from the concurrent standard automated perimetry.

## **9.2 Aim**

The aim of the study was to compare, in the 10 individuals, firstly, the results of DNP and standard automated perimetry at follow-up and, secondly, to compare the results with those obtained at the initial visit.

## **9.3 Methods**

### **9.3.1 Cohort**

Nine of the 10 individuals responded to the invitation to participate in the follow-up study. Six of the nine responded in the affirmative; however, one individual repeatedly failed to attend for her appointments. The remaining five individuals (4 males, 1 female) all had open angle glaucoma. The mean age was 73.4 years (SD 11.3) with a range from 59 to 85 years. The baseline examination had been undertaken approximately three and a half years earlier (mean 3.6 years, SD 0.1).

As would be expected, all individuals exhibited an optic nerve head characteristic of open angle glaucoma (including one or more of an increase in cup size, increase in cup to disc ratio, disc asymmetry, changes in the lamina cribrosa, loss of neuroretinal rim, disc pallor, evidence of peripapillary atrophy, vessel changes or disc margin haemorrhage). All individuals with open angle glaucoma were under the care of Mr. James Morgan,

Consultant Ophthalmologist, and were being treated with ocular hypotensive medication. All individuals manifested well-controlled intraocular pressures

### **9.3.2 Examination protocol**

The five individuals attended for 4 visits each separated by one week. At the first visit, the individuals underwent an ophthalmic examination by an optometrist, Dr. Caroline Djalllis, to confirm the inclusion criteria, namely, a visual acuity of 6/9 or better in each eye; a distance refractive error less than or equal to 5 DS mean sphere and less than 2.5 D cylinder; lenticular changes not greater than NCIII, NOIII, CI, or PI by the Lens Opacity Classification System III (Chylack et al., 1993); no systemic medication known to affect the visual field; and no history or family history of diabetes mellitus. Threshold perimetry was then undertaken using Program 24-2 and the SITA Standard algorithm of the Humphrey Field Analyzer 750 (Carl Zeiss Meditec, Dublin, CA).

At the second visit, the contrast thresholds were obtained in the designated eye, in the absence of noise (MC N<sub>a</sub>) and in the presence of the noise mask (MC N<sub>p</sub>) at five stimulus locations: 0°, 0°; 10°, 8°; -10°, 8°; 10°, -8°; and -10°, -8° using the Proof of Concept algorithm. The order of the stimulus locations was randomised as was the order of the absence or presence of the noise mask. Individuals wore the distance refraction corrected for the 30cm viewing distance of the screen. The protocol was identical to that adopted by Dr Rattan at the baseline visits. The procedure was repeated at a third and a fourth visit.

### **9.3.3 Analysis**

The results obtained at the final (fourth) visit were analysed. Results were converted into right eye format where necessary.

The values of Michelson contrast in the absence (MC  $N_a$ ) and in the presence (MC  $N_p$ ) of the noise mask, the Equivalent ( $N_{eq}$ ), the Sampling Efficiency (SE), the Log<sub>10</sub> MC Ratio (Log<sub>10</sub> Ratio) and the Signal Detection Index (SDI) were compared to the corresponding 90<sup>th</sup> percentile derived from the results of 16 of the 20 normal individuals (mean age 65.1 (SD 10.2); median 64.5 and IQR 14.3). The remaining 4 normal individuals, used by Dr Rattan, were omitted from the revised data set due to young age.

### **9.3.4 Ethical Approval**

The study was approved by the South East Wales Research and Ethics committee and was in accord with the tenets of the Declaration of Helsinki. All individuals had received written instructions and had signed a consent form prior to the onset of the study.

## **9.4 Results**

The Overview printout of the Humphrey Field Analyzer displaying the results of the baseline and follow-up visual field examinations, together with the corresponding results of DNP, for each of the five individuals are given in Figures 9.1 to 9.5.

The results for each DNP outcome measure, at each stimulus location, for each individual are also given as a composite table in Table 9.1. The latter table also contains the corresponding values obtained at the Baseline examination in 2007.

The 90<sup>th</sup> percentile of the distribution amongst the 16 normal individuals for each of the DNP outcome measures are given in Table 9.2.

### **Case #1**

Case #1 had exhibited an early inferior arcuate defect, and an apparent early nasal step, in the left eye by standard automated perimetry at Baseline as evidenced in the Pattern Deviation probability map. The outcome measures for DNP had all been normal.

At follow-up, the inferior loss by standard automated perimetry appeared to have increased both in depth and in area. The outcome for DNP at the superior temporal stimulus location exhibited abnormality for both Michelson contrasts and for all four derivatives. The outcome at the superior nasal quadrant location was abnormal for the Michelson contrast in the absence of noise and for three of the four derivatives. The corresponding stimulus locations for standard automated perimetry exhibited sensitivity within the normal range. The sensitivity was also within the normal range for standard automated perimetry at the two inferior stimulus locations corresponding to those of DNP. However, the Sampling Efficiency for DNP at the inferior nasal location was beyond the 90<sup>th</sup> percentile.

## **Case #2**

Case #2 had exhibited a possible early inferior arcuate defect, together with a possible early nasal step, in the right eye by standard automated perimetry at the baseline visit as evidenced in the Pattern Deviation probability map. The Michelson contrasts and each of the four derivatives were normal at the superior temporal quadrant location. The Michelson contrast in the absence of noise and the Signal Detection Index were abnormal at the superior nasal location. Interestingly, the Michelson contrast in the presence of the noise mask and the Sampling Efficiency were both abnormal at the inferior nasal location.

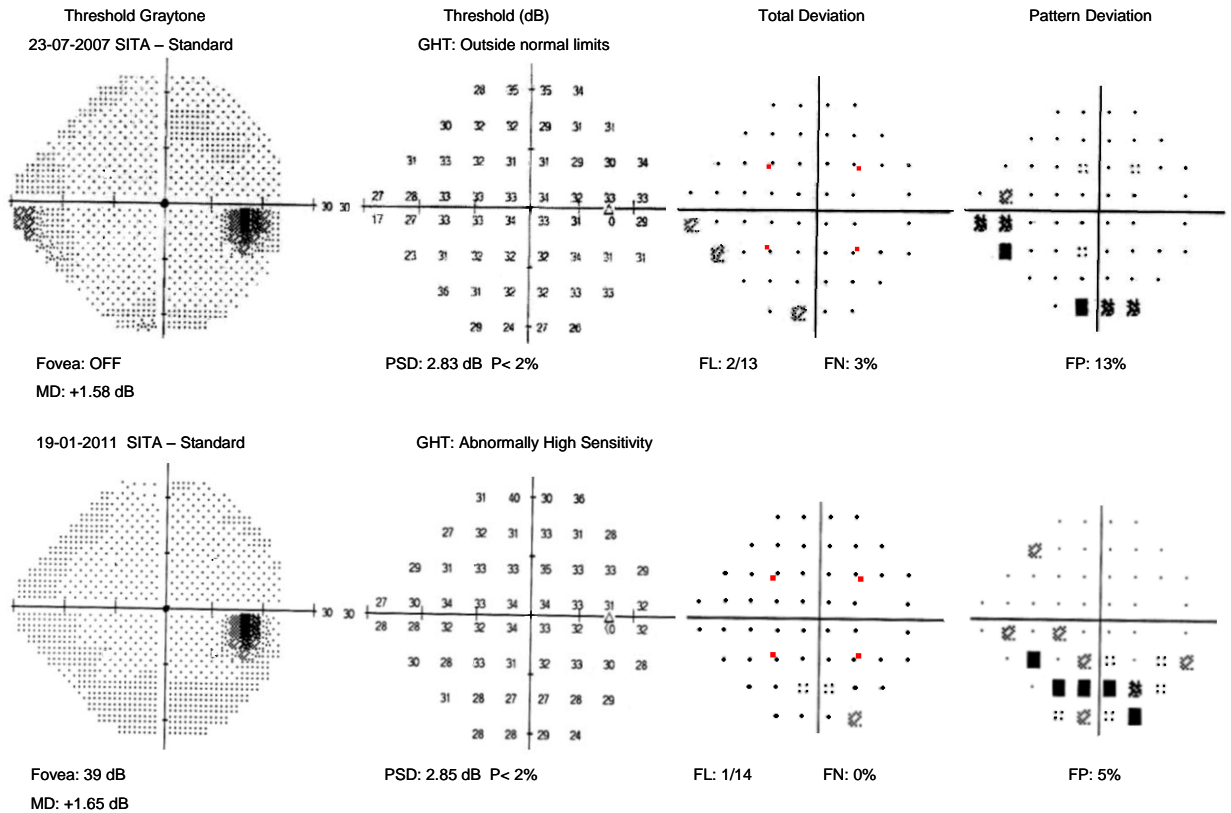
At follow-up, a diffuse loss was present by standard automated perimetry, as evidenced by the Total Deviation probability map. The appearance of the Pattern Deviation probability map suggested a possible reduction in the extent of the inferior focal loss by standard automated perimetry although the suspicion of an early inferior arcuate defect was still present. The outcome of DNP at the follow-up was most likely attributable to the diffuse loss. Abnormalities were present at all four stimulus locations examined. The Michelson contrast in the presence of the noise mask and the Sampling Efficiency were abnormal at all four locations. The Michelson contrast in the absence of the noise mask and the Signal Detection Index were abnormal at each of the same three stimulus locations.

## CASE #1 Right Eye

Eye: Right  
DOB: 04-02-1935

Name:  
ID:

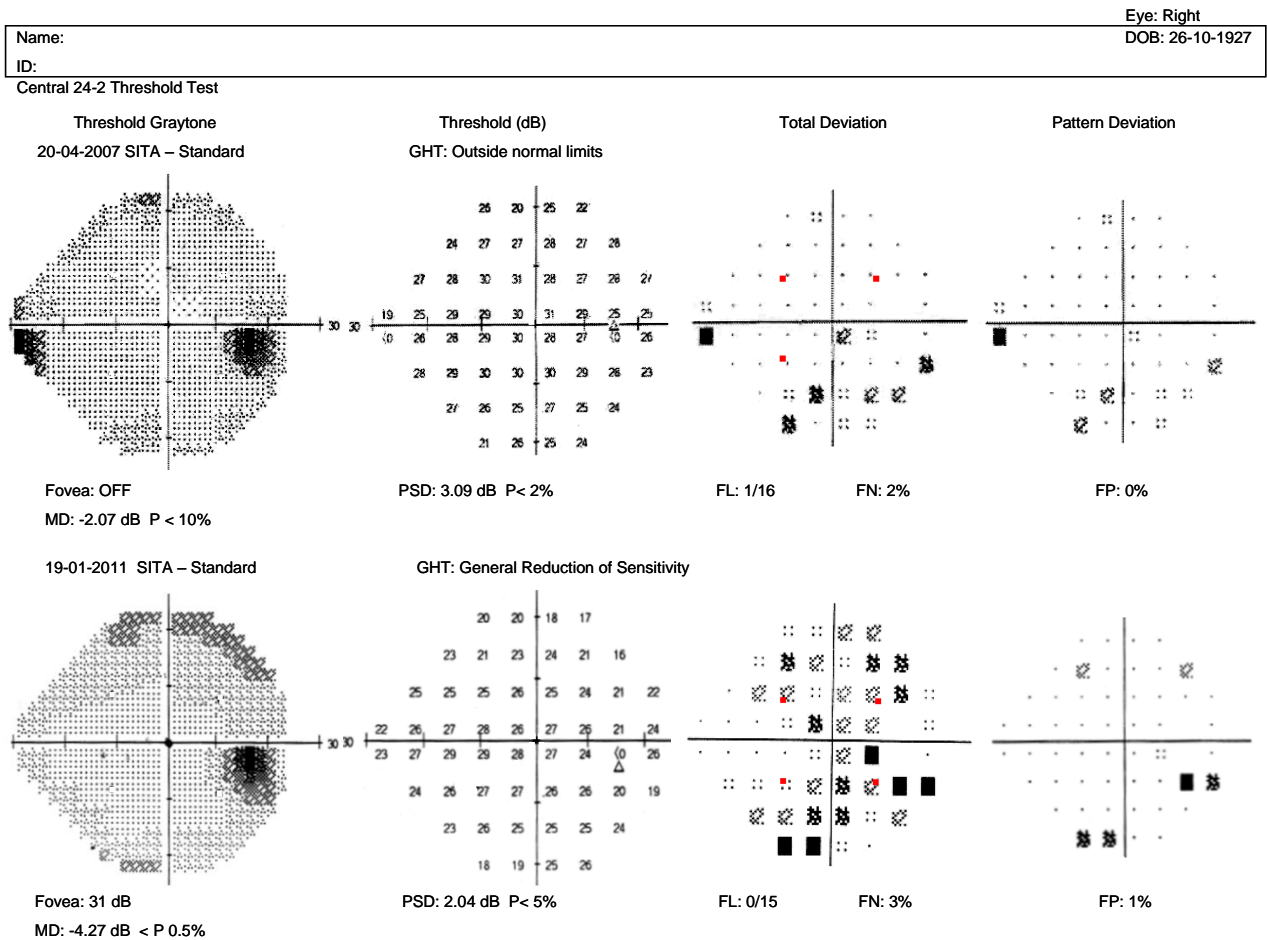
Central 24-2 Threshold Test



Case	Year	Location	Quad rant	Pattern Deviation probability	MC Na	MC Np	Neq	SE	Log10 Ratio	SDI
<b>1: Right eye</b>										
	2007	10°, 8°	ST	< 5%	0.017	0.110	8.52E-06	0.014	0.545	1655
	2011	10°, 8°	ST	N	0.115	0.224	1.18E-04	0.004	0.690	38
	2007	-10°, 8°	SN	N	0.017	0.124	6.08E-06	0.011	0.509	1818
	2011	-10°, 8°	SN	N	0.021	0.098	1.61E-05	0.018	0.601	1123
	2007	-10°, -8°	IN	N	0.014	0.103	6.73E-06	0.016	0.537	2383
	2011	-10°, -8°	IN	N	0.015	0.163	2.88E-06	0.006	0.432	2191
	2007	10°, -8°	IT	N	0.012	0.093	5.50E-06	0.020	0.536	3567
	2011	10°, -8°	IT	N	0.017	0.118	7.14E-06	0.012	0.525	1709

**Figure 9.1** The Overview printout of the Baseline and Follow-up standard automated perimetry examinations for the field of the right eye of individual #1. Note the apparent progression of the inferior visual field.

## CASE #2 Right Eye



Case	Year	Location	Quad rant	Pattern Deviation probability	MC Na	MC Np	Neq	SE	Log10 Ratio	SDI	
<b>2: Right eye</b>											
	2007	10°, 8°	ST	N	0.022	0.115	1.25E-05	0.013	0.566	1042	
	2011	10°, 8°	ST	N	0.021	0.275	.94E-06	0.002	0.334	1137	
	2007	-10°, 8°	SN	N	0.024	0.160	7.43E-06	0.007	0.489	891	
	2011	-10°, 8°	SN	N	0.062	0.287	1.64E-05	0.002	0.449	129	
	2007	-10°, -8°	IN	N	0.016	0.294	1.01E-06	0.002	0.297	1917	
	2011	-10°, -8°	IN	N	0.031	0.210	7.27E-06	0.004	0.448	531	
	2007	10°, -8°	IT	Not Done							
	2011	10°, -8°	IT	N	0.030	0.213	6.98E-06	0.004	0.443	537	

**Figure 9.2** The Overview printout of the Baseline and Follow-up standard automated perimetry examinations for the field of the right eye of individual #2. Note the apparent emergence of an age-related cataract as evidenced by the worsening of the Total Deviation map.

### Case #3

Case #3 had exhibited an apparent early inferior paracentral defect in the left eye by standard automated perimetry at the Baseline visit as evidenced in the Pattern Deviation probability map. The outcome measures for DNP had all been normal at the superior nasal quadrant location. However, the Equivalent Noise and the Log<sub>10</sub> Ratio were abnormal at each of the same three stimulus locations, inferiorly. In addition, the Michelson contrast in the absence of noise and the Signal Detection Index were both abnormal at two of these three locations although only one of these locations exhibited abnormality for both. Clearly, there was a good correspondence between standard automated perimetry and DNP.

At Follow-up, the inferior loss appeared to have increased both in depth and in area standard automated perimetry. The outcome for DNP at the superior nasal quadrant exhibited abnormality for the Equivalent Noise and the Log<sub>10</sub> Ratio. The three inferior locations each exhibited abnormality for the Michelson contrast in the absence of the noise mask and for the Equivalent Noise and for the Signal Detection Index. The Sampling Efficiency and the Log<sub>10</sub> Ratio was abnormal at each of two of the inferior locations; although only one location exhibited abnormality for both derivatives.

The repeatability of the DNP outcomes, in terms of probability level, was excellent. In addition, the Michelson contrast in the absence of the noise mask and that in the presence of the noise mask, the Sampling Efficiency and the Signal Detection Index became

abnormal at the Follow-up at one, one, two, and three of the inferior locations, respectively.

In conclusion, the outcome of DNP was at least comparable to, if not better than, that of standard automated perimetry in the detection and progression of early visual field loss.

#### **Case #4**

Case #4 had exhibited a deep and extensive inferior arcuate defect in the left eye by standard automated perimetry at the baseline visit as evidenced in the Pattern Deviation probability map. The outcome measures for DNP had all been normal at the two superior quadrant locations. The Michelson contrast in the absence, and in the presence, of the noise mask and the Sampling Efficiency were all abnormal at the inferior temporal location which, itself, lay within the focal loss identified by standard automated perimetry.

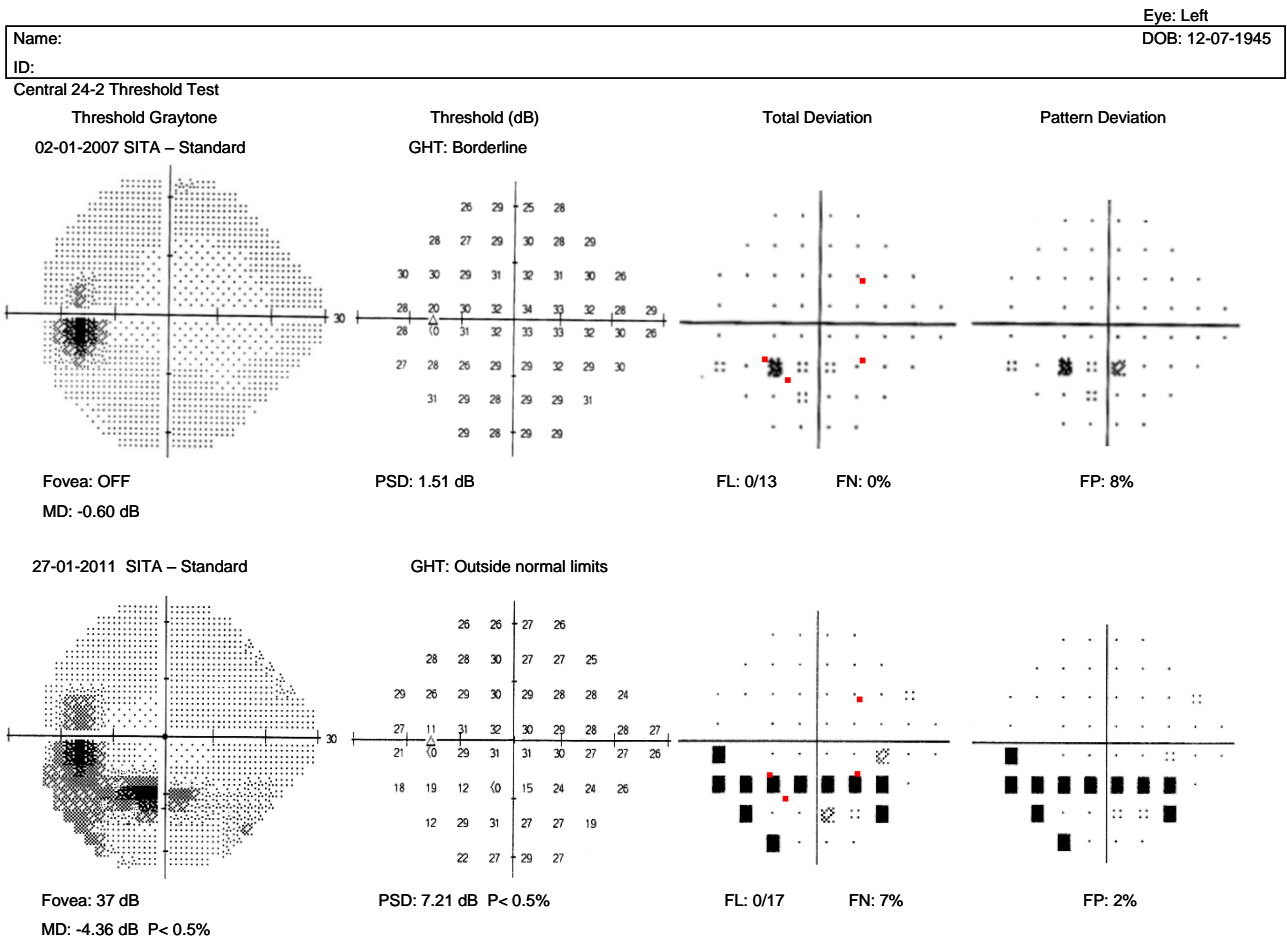
At Follow-up, the inferior arcuate defect was seemingly wider than that at the Baseline. The Michelson contrasts and all four derivatives were abnormal at the inferior location with the Equivalent Noise, the Log<sub>10</sub> Ratio and the Signal Detection Index each having progressed from normal to abnormal. The superior temporal location also exhibited apparent progressive loss as manifested by abnormality in the Michelson contrast in the absence of the noise mask, the Equivalent Noise, and the Signal Detection Index.

## Case #5

Case #5 had exhibited an essentially normal field for the right eye by standard automated perimetry at the Baseline visit as evidenced in the Pattern Deviation probability map. However, there was a slight suspicion of a superior nasal step. The outcome measures for DNP had all been normal at the two superior quadrant locations and at the inferior temporal location. However, the inferior nasal location had exhibited abnormality for the Michelson contrast in the absence of noise, the Sampling Efficiency and the Signal Detection Index.

At Follow-up, the superior nasal step appeared to have widened and deepened. Apparent abnormalities were present for DNP at the superior nasal location in the Equivalent Noise, the Log<sub>10</sub> Ratio and the Signal Detection Index. Interestingly, the abnormalities at the inferior nasal location in the Michelson contrast in the absence of noise, the Sampling Efficiency and the Signal Detection Index were still present at follow-up together with progression to abnormality of the Michelson contrast obtained in the presence of the noise mask. The two temporal locations each exhibited apparent progression from normality to abnormality for the Michelson contrast in the absence of the noise mask and for the Signal Detection Index.

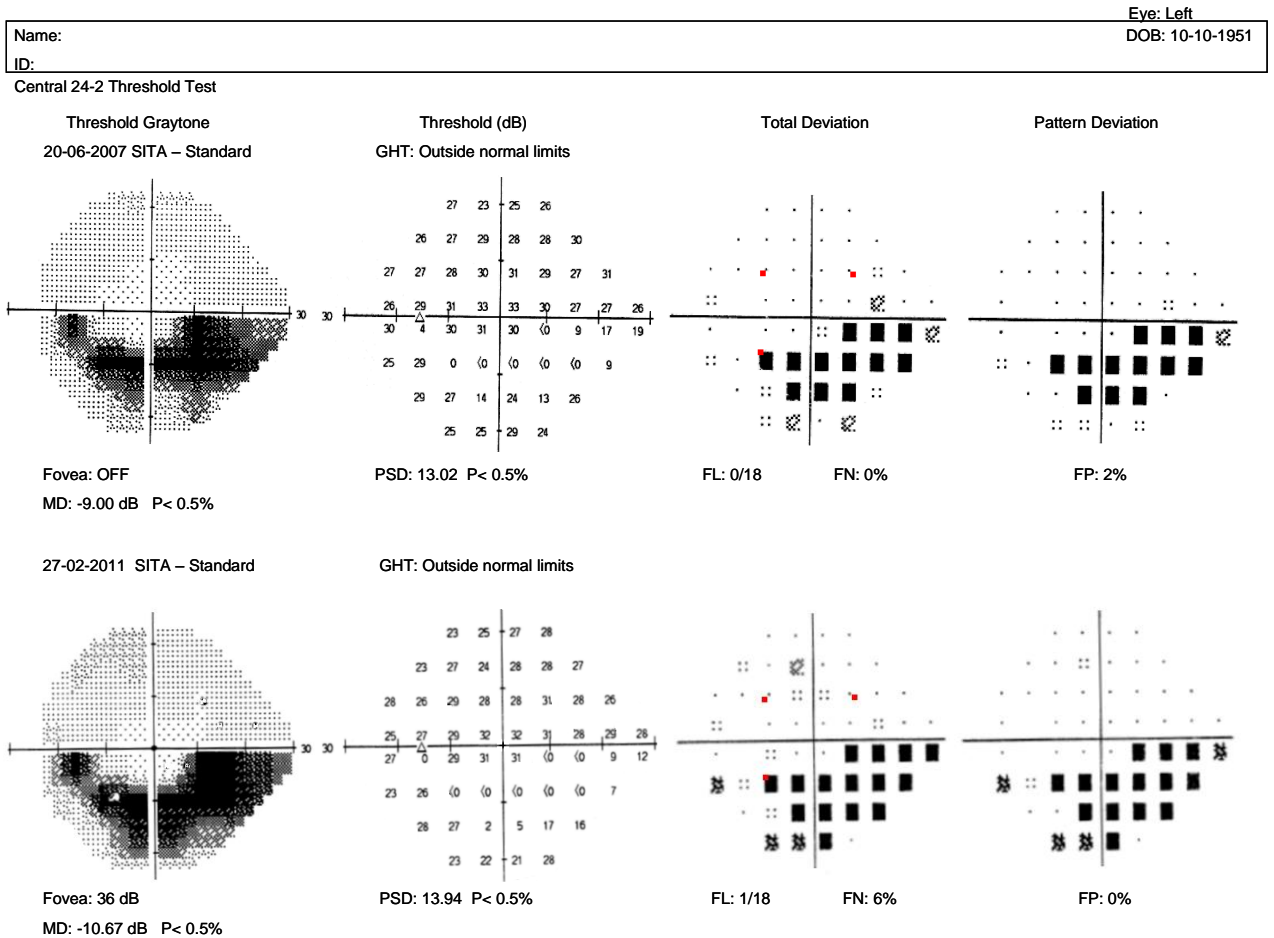
**CASE #3 Left Eye**



Case	Year	Location	Quad rant	Pattern Deviation probability	MC N <sub>a</sub>	MC N <sub>p</sub>	N <sub>eq</sub>	SE	Log <sub>10</sub> Ratio	SDI
<b>Left eye</b>										
3	2007	10°, 8°	SN	N	0.014	0.107	6.19E-06	0.015	0.527	2383
	2011	10°, 8°	SN	N	0.023	0.055	7.26E-05	0.066	0.771	914
	2007	10°, -8°	IN	N	0.028	0.122	1.87E-05	0.012	0.589	633
	2011	10°, -8°	IN	< 5%	0.053	0.272	1.30E-05	0.002	0.443	180
	2007	-10°, -8°	IT	< 1%	0.019	0.083	1.85E-05	0.025	0.628	1368
	2011	-10°, -8°	IT	< 0.5%	0.042	0.082	1.23E-04	0.034	0.792	279
	2007	-6°, -12°	IT	N	0.030	0.091	4.18E-05	0.023	0.686	539
	2011	-6°, -12°	IT	N	0.072	0.085	8.40E-04	0.082	0.937	97

**Figure 9.3** The Overview printout of the Baseline and Follow-up standard automated perimetry examinations for the field of the left eye of individual #3. Note the apparent progression of the inferior visual field by both standard automated perimetry and DNP.

## CASE #4 Left Eye



Case	Year	Location	Quad rant	Pattern Deviation probability	MC N <sub>a</sub>	MC N <sub>p</sub>	N <sub>eq</sub>	SE	Log <sub>10</sub> Ratio	SDI
<b>Left eye</b>										
4	2007	-10°, 8°	ST	N	0.015	0.134	4.19E-06	0.009	0.478	2247
	2011	-10°, 8°	ST	N	0.028	0.127	1.74E-05	0.011	0.579	627
	2007	10°, 8°	SN	N	0.014	0.183	2.04E-06	0.005	0.400	2469
	2011	10°, 8°	SN	N	0.019	0.084	1.81E-05	0.025	0.625	1360
	2007	-10°, -8°	IN	< 0.5	0.016	0.174	2.99E-06	0.006	0.426	1858
	2011	-10°, -8°	IN	< 0.5	0.079	0.202	5.95E-05	0.005	0.629	81

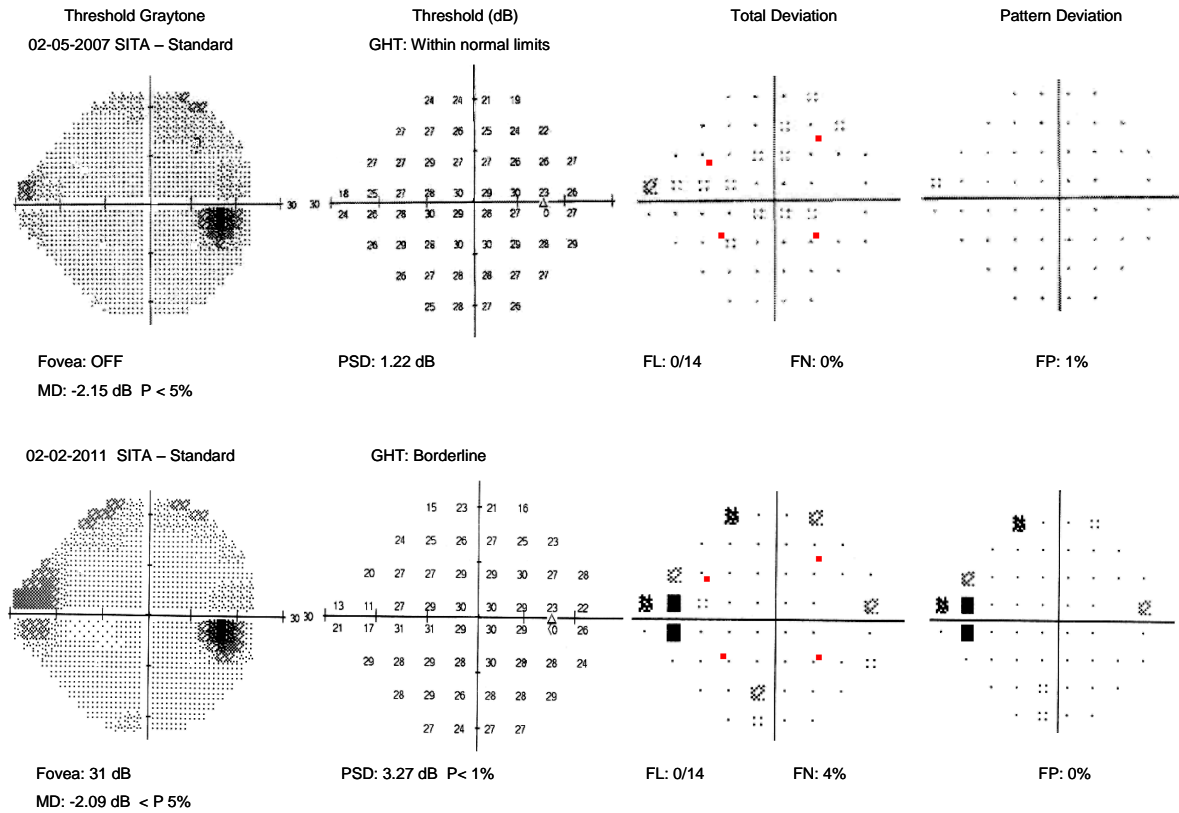
**Figure 9.4** The Overview printout of the Baseline and Follow-up standard automated perimetry examinations for the field of the left eye of individual #4. Note the possible widening of the inferior visual field loss at Follow-up by standard automated perimetry.

## CASE #5 Right Eye

Eye: Right  
DOB: 18-02-1929

Name:  
ID:

Central 24-2 Threshold Test



Case	Year	Location	Quad rant	Pattern Deviation probability	MC N <sub>a</sub>	MC N <sub>p</sub>	N <sub>eq</sub>	SE	Log <sub>10</sub> Ratio	SDI
<b>Right eye</b>										
5	2007	10°, 12°	ST	N	0.021	0.133	8.83E-06	0.010	0.524	1088
	2011	10°, 12°	ST	N	0.031	0.188	9.60E-06	0.005	0.483	505
	2007	-14°, 8°	SN	N	0.018	0.188	3.24E-06	0.005	0.419	1475
	2011	-14°, 8°	SN	N	0.029	0.125	1.87E-05	0.011	0.586	605
	2007	-10°, -8°	IN	N	0.018	0.162	4.14E-06	0.006	0.453	1555
	2011	-10°, -8°	IN	N	0.023	0.168	6.60E-06	0.006	0.475	906
	2007	10°, -8°	IT	N	0.016	0.139	4.33E-06	0.009	0.475	2007
	2011	10°, -8°	IT	N	0.029	0.154	1.19E-05	0.007	0.526	615

**Figure 9.5** The Overview printout of the Baseline and Follow-up standard automated perimetry examinations for the field of the right eye of individual #5. Note the apparent progression of the superior nasal step.

Case	Year	Location	Quad rant	Pattern Deviation probability	MC N <sub>a</sub>	MC N <sub>p</sub>	N <sub>eq</sub>	SE	Log <sub>10</sub> Ratio	SDI	
<b>1: Right eye</b>											
	2007	10°, 8°	ST	< 5%	0.017	0.110	8.52E-06	0.014	0.545	1655	
	2011	10°, 8°	ST	N	0.115	0.224	1.18E-04	0.004	0.690	38	
	2007	-10°, 8°	SN	N	0.017	0.124	6.08E-06	0.011	0.509	1818	
	2011	-10°, 8°	SN	N	0.021	0.098	1.61E-05	0.018	0.601	1123	
	2007	-10°, -8°	IN	N	0.014	0.103	6.73E-06	0.016	0.537	2383	
	2011	-10°, -8°	IN	N	0.015	0.163	2.88E-06	0.006	0.432	2191	
	2007	10°, -8°	IT	N	0.012	0.093	5.50E-06	0.020	0.536	3567	
	2011	10°, -8°	IT	N	0.017	0.118	7.14E-06	0.012	0.525	1709	
<b>2: Right eye</b>											
	2007	10°, 8°	ST	N	0.022	0.115	1.25E-05	0.013	0.566	1042	
	2011	10°, 8°	ST	N	0.021	0.275	.94E-06	0.002	0.334	1137	
	2007	-10°, 8°	SN	N	0.024	0.160	7.43E-06	0.007	0.489	891	
	2011	-10°, 8°	SN	N	0.062	0.287	1.64E-05	0.002	0.449	129	
	2007	-10°, -8°	IN	N	0.016	0.294	1.01E-06	0.002	0.297	1917	
	2011	-10°, -8°	IN	N	0.031	0.210	7.27E-06	0.004	0.448	531	
	2007	10°, -8°	IT	Not Done							
	2011	10°, -8°	IT	N	0.030	0.213	6.98E-06	0.004	0.443	537	
<b>Left eye</b>											
3	2007	10°, 8°	SN	N	0.014	0.107	6.19E-06	0.015	0.527	2383	
	2011	10°, 8°	SN	N	0.023	0.055	7.26E-05	0.066	0.771	914	
	2007	10°, -8°	IN	N	0.028	0.122	1.87E-05	0.012	0.589	633	
	2011	10°, -8°	IN	< 5%	0.053	0.272	1.30E-05	0.002	0.443	180	
	2007	-10°, -8°	IT	< 1%	0.019	0.083	1.85E-05	0.025	0.628	1368	
	2011	-10°, -8°	IT	< 0.5%	0.042	0.082	1.23E-04	0.034	0.792	279	
	2007	-6°, -12°	IT	N	0.030	0.091	4.18E-05	0.023	0.686	539	
	2011	-6°, -12°	IT	N	0.072	0.085	8.40E-04	0.082	0.937	97	
<b>Left eye</b>											
4	2007	-10°, 8°	ST	N	0.015	0.134	4.19E-06	0.009	0.478	2247	
	2011	-10°, 8°	ST	N	0.028	0.127	1.74E-05	0.011	0.579	627	
	2007	10°, 8°	SN	N	0.014	0.183	2.04E-06	0.005	0.400	2469	
	2011	10°, 8°	SN	N	0.019	0.084	1.81E-05	0.025	0.625	1360	
	2007	-10°, -8°	IN	< 0.5	0.016	0.174	2.99E-06	0.006	0.426	1858	
	2011	-10°, -8°	IN	< 0.5	0.079	0.202	5.95E-05	0.005	0.629	81	

Right eye										
5	2007	10°, 12°	ST	N	0.021	0.133	8.83E-06	0.010	0.524	1088
	2011	10°, 12°	ST	N	0.031	0.188	9.60E-06	0.005	0.483	505
	2007	-14°, 8°	SN	N	0.018	0.188	3.24E-06	0.005	0.419	1475
	2011	-14°, 8°	SN	N	0.029	0.125	1.87E-05	0.011	0.586	605
	2007	-10°, -8°	IN	N	0.018	0.162	4.14E-06	0.006	0.453	1555
	2011	-10°, -8°	IN	N	0.023	0.168	6.60E-06	0.006	0.475	906
	2007	10°, -8°	IT	N	0.016	0.139	4.33E-06	0.009	0.475	2007
	2011	10°, -8°	IT	N	0.029	0.154	1.19E-05	0.007	0.526	615

**Table 9.1** The summary table of the results over the follow-up period for the various outcome measures of DNP for each of the five individuals with open angle glaucoma at the given stimulus locations. The green and red highlighting indicates a value lying inside or outside, respectively, the 90<sup>th</sup> percentile of the values for the 16 normal individuals. The corresponding pattern deviation probability value at the given location is highlighted in yellow, brown or salmon.

Location	MC N <sub>a</sub>	MC N <sub>p</sub>	N <sub>eq</sub>	SE	Log <sub>10</sub> Ratio	SDI
10°, 8°	<0.0260	<0.2021	<1.80E-05	>0.0042	<0.6044	>739.13
10°, -8°	<0.0195	<0.1684	<1.47E-05	>0.0059	<0.5985	>1317.08
-10°, -8°	<0.0170	<0.1670	<1.28E-05	>0.0060	<0.5769	>1740.12
-10°, 8°	<0.0218	<0.1825	<1.56E-05	>0.0050	<0.6011	>1055.78
-6°, -12°	<0.0717	<0.0913	<8.40E-04	>0.0816	<0.9366	>538.761
10°, 12°	<0.0314	<0.1619	<9.60E-06	>0.0102	<0.5863	>505.123
-14°, 8°	<0.0287	<0.2038	<1.87E-05	>0.0102	<0.0588	>605.378

**Table 9.2** The summary table of the 90<sup>th</sup> percentile of the values for the 16 normal individuals at the given stimulus location for each of the various outcome measures of DNP.

## **9.5 Discussion**

The outcome for DNP at the follow-up of the five individuals with open angle glaucoma yielded promising results compared to those obtained by standard automated perimetry.

One of the striking features of DNP was that an abnormality in a given outcome measure at a given stimulus location remained abnormal at Follow-up, i.e., the apparent abnormality was repeatable after an interval of approximately three and half years. In addition, some locations which were normal at Baseline exhibited abnormality in one or more of the outcome measures at follow-up. However, the opposite was not the case i.e., apparent abnormalities at Baseline did not revert to normal at Follow-up. In a number of cases, abnormality identified by DNP at Baseline was subsequently confirmed as abnormal by standard automated perimetry at Follow-up.

There was no particular pattern in the abnormality of the given outcome measure of DNP between the five individuals.

The results, however, must be placed in the context of the fact only two DNP and standard automated perimetry examinations were undertaken during the three and a half years of follow-up. It is conceivable, therefore, that one or more of the examinations of a given individual could have exhibited a marked degree of variability, thus, undermining the conclusions about any given level of sensitivity at any given location.

The results of this limited pilot study was sufficient to warrant a larger scale study of the role of DNP in 'early' open angle glaucoma with particular reference not only to standard automated perimetry but also to retinal nerve fibre layer thickness and ganglion cell layer thickness. It was discussed in Chapter 7 whether such a study should be undertaken with the final 45 location algorithm or with a further, yet to be designed, iteration of this algorithm. The question remains unresolved.

## Chapter 10

### The Learning Effect in Dynamic Noise Perimetry

#### 10.1 Introduction

The learning effect has been known in standard automated perimetry for many years (Wood et al., 1987; Werner, Adelson and Krupin, 1988; Heijl et al., 1989b; Wild et al., 1989; Kulze, Stewart and Sutherland, 1990; Werner et al., 1990; Searle et al., 1991; Wild et al., 1991; Heijl and Bengtsson, 1996; Nordmann et al., 1998; Castro, Kawase and Melo, 2008). It occurs as the patient becomes increasingly familiar with the requirements of the perimetric task and manifests as an improvement in sensitivity and a decrease in measurement variability over time. It is present in normal individuals (Heijl et al., 1989b; Castro et al., 2008), in ocular hypertension (Wild et al., 1989; Wild et al., 1991) and in open angle glaucoma (Wild et al., 1991; Heijl and Bengtsson, 1996).

The learning effect has been shown to be present for the first eye examined at the initial visit (Searle et al., 1991), to be transferred between eyes at the first visit (Searle et al., 1991) and to be present between visits, both within- (Searle et al., 1991) and between-eyes (Heijl et al., 1989b; Searle et al., 1991; Heijl and Bengtsson, 1996). It is present generally up to at least the end of the second or third visit (Wood et al., 1987; Heijl et al., 1989b; Searle et al., 1991; Heijl and Bengtsson, 1996; Matsuo et al., 2002; Castro et al., 2008).

The improvement in sensitivity increases with increase in eccentricity from fixation (Miles, 1950; Wood et al., 1987; Heijl, 1989; Heijl et al., 1989b; Heijl et al., 1989c; Wild et al., 1989; Werner et al., 1990; Searle et al., 1991; Heijl and Bengtsson, 1996; Castro et al., 2008) and is greatest in areas of relative loss (Heijl et al., 1989b; Wild et al., 1989).

The learning effect presents a major clinical problem in the management of open angle glaucoma in that the appearance of the recorded visual field at the initial examinations is often more severe than the 'true' field loss.

The characteristics of the learning effect for SWAP are similar to that for standard automated perimetry (Wild and Moss, 1996; Wild, 2001; Bayer and Erb, 2002; Racette and Sample, 2003; Chiselita et al., 2006; Rossetti et al., 2006; Wild et al., 2006). The learning effect for SWAP is present in normal individuals, in patients with ocular hypertension and in patients with open angle glaucoma (Rossetti et al., 2006; Wild et al., 2006). It is present for patients experienced in standard automated perimetry and can result in an overestimation of the area and depth of field loss, particularly over the initial three examinations (Chiselita et al., 2006; Rossetti et al., 2006; Wild et al., 2006). Individuals either with open angle glaucoma or considered to be glaucoma suspects who underwent annual perimetry for eight years exhibited an increase in Mean Sensitivity between years 1 and 2 which remained approximately stable for several years before declining from year 6 onwards. However, Mean Sensitivity for SWAP increased until year 6 before declining (Gardiner, Demirel and Johnson, 2008a). The SITA SWAP algorithm is less influenced by

the learning effect compared to the Full Threshold algorithm for SWAP (Rossetti et al., 2006; Fogagnolo et al., 2010).

A learning effect for FDT perimetry is also present in normal individuals (Iester et al., 2000; Horani et al., 2002; Joson, Kamantigue and Chen, 2002; Heeg, Ponsioen and Jansonius, 2003; Contestabile et al., 2007; Fogagnolo et al., 2008), in ocular hypertension (Centofanti et al., 2008) and in open angle glaucoma (Joson et al., 2002; Matsuo et al., 2002; Heeg et al., 2003). It generally occurs between the first and second visits in normal individuals (Fujimoto et al., 2002; Horani et al., 2002; Matsuo et al., 2002; Contestabile et al., 2007; Horn et al., 2007) and in individuals with ocular hypertension and in individuals with open angle glaucoma (Fujimoto et al., 2002; Matsuo et al., 2002; Horn et al., 2007). Moreover, the learning effect for FDT perimetry using the Humphrey Matrix perimeter for those with no perimetric experience lasts until the third visit in normal individuals (Pierre-Filho Pde et al., 2010), and in individuals with open angle glaucoma (De Tarso Pierre-Filho et al., 2010).

In summary, individuals experienced in standard automated perimetry show a residual learning effect for FDT perimetry and for SWAP (Wild et al., 1989; Heijl and Bengtsson, 1996; Kwon et al., 1998; Chauhan and Johnson, 1999; Fujimoto et al., 2002; Salvetat et al., 2007).

The learning effect for CFF perimetry occurs between the first and second visits in normal individuals (Bernardi, Costa and Shiroma, 2007).

Flicker Defined Form perimetry exhibits a learning effect over the first three visits for Mean Sensitivity, Mean Deviation, and Pattern Deviation and a reduction in the variability associated with the estimation of the threshold (Lamparter et al., 2011).

It can be hypothesised that a learning effect is likely to be associated with DNP both in the absence and in the presence of the noise mask. Clearly it is important to determine the characteristics of such an effect.

## **10.2 Aim**

The aim of the study, therefore, was to determine the extent of any increase in sensitivity derived by Dynamic Noise Perimetry (DNP) with repeated examinations in normal individuals, both in the absence and in the presence of the noise mask.

## **10.3 Methods**

### **10.3.1 Cohort**

The cohort comprised 18 normal individuals divided into two age groups: 10 ‘young’ individuals with a mean age of 25.9 years (SD 3.7; range from 20 to 31 years) and 8 ‘old’ individuals with a mean age of 66.6 years (SD 7.2; range 58 to 75years). The younger individuals were recruited from the undergraduate and postgraduate student community of

Cardiff University whilst the older individuals were recruited from the Eye Clinic of the Cardiff School of Optometry and Vision Sciences.

At the enrolment visit, each individual underwent a comprehensive ophthalmic examination by an optometrist, Dr. Caroline Djalllis, to confirm the inclusion criteria.

Inclusion criteria for all individuals comprised a negative family history of open angle glaucoma; no chronic systemic disease, no systemic medication known to affect the visual field; no current topical ocular medication; no ocular surgery or trauma; a distance refractive error of  $\leq \pm 5$  dioptres sphere and  $\leq \pm 3$  dioptres cylinder; a distance visual acuity of better than or equal to 6/5 in each eye for the young individuals and better than or equal to 6/9 for the elderly individuals; a normal anterior eye, including a pupil diameter of greater than 3mm and normal pupil reflexes; an intraocular pressure, uncorrected for the effect of central corneal thickness of  $\leq 21$ mmHg; a normal crystalline lens appearance for the young group and, in the elderly group, of better than nuclear colour 2.0, nuclear opalescence, 2.0, cortical 1.0, or posterior subcapsular 1.0 according to the Lens Opacity Classification System (LOCS III) (Chylack et al., 1993); a normal fundal and optic nerve head appearance; and a normal visual field (Program 24-2 and the SITA Standard strategy of the Humphrey Field Analyzer).

Each then underwent a familiarisation session to ensure an understanding of the procedures for DNP.

### **10.3.2 Examination protocol**

Each individual then attended for a further five visits and underwent DNP in one randomly designated eye at each visit using an identical protocol.

The study used the First Iteration algorithm approach, second phase, described in Chapter 7. The stimulus program, shown in Figure (7.2), comprised twelve stimulus locations at eccentricities of: 0, 0; -10, +8; -10, -8; -26, +4; +6, +4; +10, -12; +10, +12; -6, +16; -26, -4; -18, +12; -18, -12; and -6, -16. The noise mask contained 4 checks per cycle at each stimulus eccentricity. The order of the sequence of the noise mask first was randomized within each individual between each visit.

Each individual wore the appropriate refractive correction for the viewing distance of 30cm. The fellow eye was occluded with an opaque patch. Fixation was monitored via the CCD camera which provided an image on the display monitor.

An enforced rest period of 1 minute was given every three minutes and a rest period of 5 minutes between the two examination sessions (i.e. either in the absence of the noise mask or in the presence of the noise mask session). If a lack of concentration or a misunderstanding of the requirements of the examination occurred, the test was paused and a further explanation was given to the individual.

At the first visit of the five DNP visits, each individual was provided with verbal and written information concerning the study procedure and then underwent a practice session for 5 minutes in order to ensure compliance with the DNP concept.

Each of the five visits was separated by a one week interval and the time of day at which DNP was initially undertaken was maintained for each individual over each of the remaining four visits.

Each individual received the same instructions at each visit.

### **10.3.3 Analysis**

The results were converted to right eye format where necessary.

The primary analysis comprised three separate repeated measures ANOVA.

For the first model, the mean Michelson contrast, expressed as sensitivity in dB, for all 12 stimulus locations was taken as the response and, in the second model, the ratio of the central sensitivity to the peripheral sensitivity. Age was included in all three models as a between-subjects factor. The absence or presence of the noise mask and visits were included in the models as separate within-subject factors. Two-way interactions of all three factors were also included in each of the three models. Each effect was treated as a fixed effect. Subject was included as a random effect.

Two further models were included, for the six central locations and for the six peripheral locations, respectively, merely for comparative purposes.

The secondary analysis comprised a representation of the data in terms of the proportionate change from Baseline. This latter analysis was undertaken in order to obtain an appreciation of the data from a clinical perspective and to permit a comparison of the perimetric learning effect with other studies.

The derivatives from  $MCN_a$  and  $MCN_p$  were tabulated in terms of descriptive statistics for the proportionate change from Visit 1 to Visit 5.

#### **10.3.4 Ethical Approval**

The study was approved by the Ethics in Research Committee of the Cardiff School of Optometry and Vision Sciences which is in accord with the tenets of the Declaration of Helsinki. All individuals had received written instructions and had signed a consent form prior to the onset of the study.

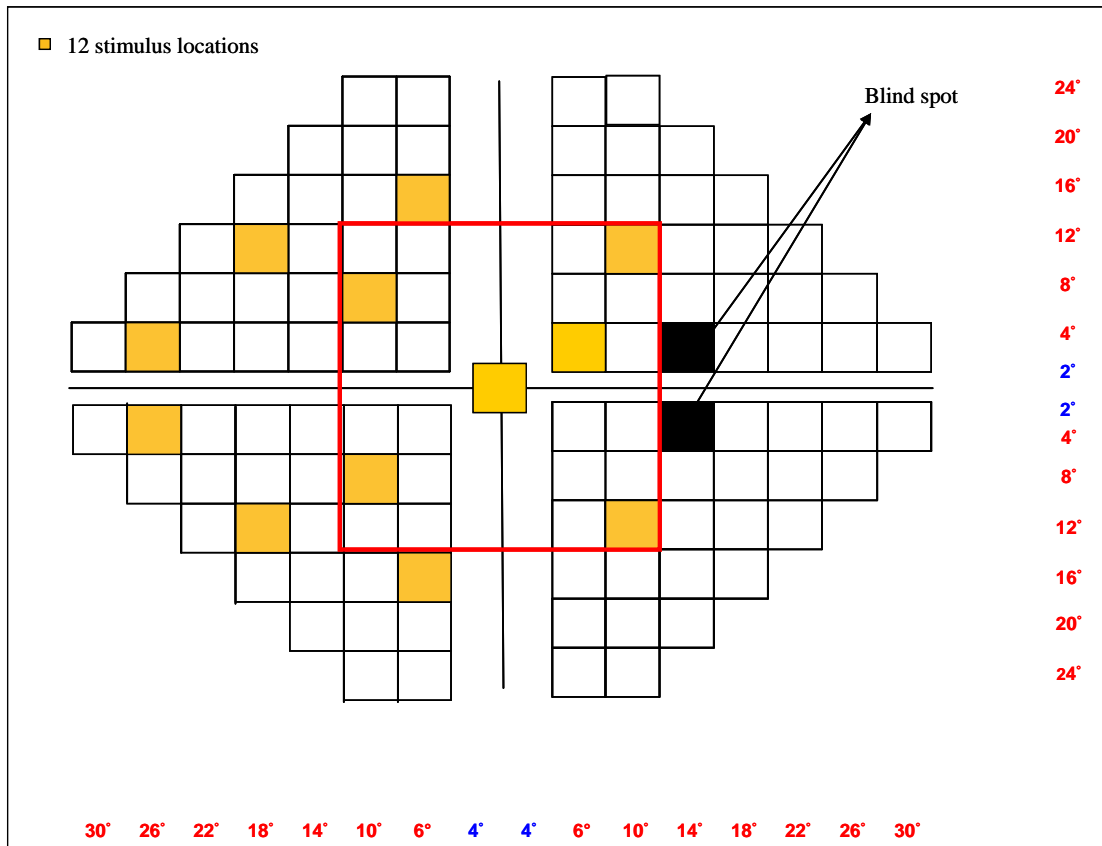


**Figure 10.1** The stimulus grid for DNP in right eye format. The twelve stimulus locations are highlighted in orange. The stimulus locations within the red square, with the exception of the foveal location, are designated, for the purposes of the analysis, as ‘central’ locations and those beyond the red square as ‘peripheral’ locations. The black squares indicate the blind spot.

## **10.4 Results**

### **10.4.1 Mean Sensitivity for the central field**

The summary statistics for each age-group of the Mean Sensitivity (dB) across the 12 stimulus locations in the absence of the noise mask for each of the five visits (mean, SD, median and IQR) are shown in Table 10.1 and in the presence of the noise mask in Table 10.2.

The ANOVA summary table corresponding to the absolute values in Tables 10.1 and 10.2 is shown in Table 10.3.

<b>Without the noise mask</b>					
<b>Young group</b>					
<b>Individual</b>	<b>Visit 1</b>	<b>Visit 2</b>	<b>Visit 3</b>	<b>Visit 4</b>	<b>Visit 5</b>
<b>1</b>	14.52	15.11	16.14	17.00	16.87
<b>2</b>	14.86	15.99	15.38	14.86	16.01
<b>3</b>	12.79	14.79	14.87	15.52	16.50
<b>4</b>	13.47	15.50	15.83	16.07	16.63
<b>5</b>	14.99	16.12	16.58	16.21	16.43
<b>6</b>	13.96	15.48	16.20	16.05	15.85
<b>7</b>	14.25	15.33	15.95	16.34	16.26
<b>8</b>	15.43	16.41	17.19	16.46	16.83
<b>9</b>	15.24	17.19	17.15	17.21	17.45
<b>10</b>	14.96	17.73	17.44	17.38	17.10
<b>Mean</b>	<b>14.45</b>	<b>15.97</b>	<b>16.27</b>	<b>16.31</b>	<b>16.59</b>
<b>SD</b>	<b>0.84</b>	<b>0.93</b>	<b>0.83</b>	<b>0.77</b>	<b>0.49</b>
<b>Median</b>	<b>14.69</b>	<b>15.75</b>	<b>16.17</b>	<b>16.28</b>	<b>16.57</b>
<b>IQR</b>	<b>14.03, 14.98</b>	<b>15.37, 16.34</b>	<b>15.86, 17.01</b>	<b>16.05, 16.86</b>	<b>16.31, 16.86</b>
<b>Elderly group</b>					
<b>Individual</b>	<b>Visit 1</b>	<b>Visit 2</b>	<b>Visit 3</b>	<b>Visit 4</b>	<b>Visit 5</b>
<b>1</b>	13.30	15.27	15.01	15.54	15.23
<b>2</b>	15.70	16.90	16.99	17.27	17.34
<b>3</b>	15.36	17.26	16.99	16.50	16.77
<b>4</b>	13.22	14.68	14.80	15.01	15.42
<b>5</b>	14.05	14.81	15.25	14.65	15.11
<b>6</b>	15.19	16.18	16.03	16.16	16.94
<b>7</b>	13.20	14.22	15.95	16.59	16.52
<b>8</b>	14.83	15.26	16.06	16.06	16.18
<b>Mean</b>	<b>14.36</b>	<b>15.57</b>	<b>15.89</b>	<b>15.97</b>	<b>16.19</b>
<b>SD</b>	<b>1.04</b>	<b>1.09</b>	<b>0.83</b>	<b>0.87</b>	<b>0.85</b>
<b>Median</b>	<b>14.44</b>	<b>15.27</b>	<b>15.99</b>	<b>16.11</b>	<b>16.35</b>
<b>IQR</b>	<b>13.28, 15.23</b>	<b>14.78, 16.36</b>	<b>15.19, 16.29</b>	<b>15.41, 16.52</b>	<b>15.37, 16.81</b>

**Table 10.1** The summary statistics (Mean, SD, Median and IQR) of the mean Michelson contrast in the absence of the noise mask, for the central field, expressed in terms of sensitivity (dB) at each of the five visits for the young group (Top) and for the elderly group (Bottom).

<b>With the noise mask</b>					
<b>Young group</b>					
<b>Individual</b>	<b>Visit 1</b>	<b>Visit 2</b>	<b>Visit 3</b>	<b>Visit 4</b>	<b>Visit 5</b>
<b>1</b>	6.63	8.18	8.18	9.44	9.78
<b>2</b>	6.93	8.69	8.66	8.28	9.10
<b>3</b>	5.85	6.87	9.32	9.42	9.59
<b>4</b>	6.22	7.61	9.26	8.08	8.49
<b>5</b>	8.77	10.28	10.54	11.04	11.02
<b>6</b>	7.13	9.49	8.66	7.70	8.08
<b>7</b>	6.18	7.75	8.19	8.56	8.74
<b>8</b>	7.57	8.78	9.28	9.54	9.21
<b>9</b>	7.29	8.65	8.84	9.24	9.30
<b>10</b>	6.99	9.68	9.16	8.44	8.68
<b>Mean</b>	<b>6.96</b>	<b>8.60</b>	<b>9.01</b>	<b>8.97</b>	<b>9.20</b>
<b>SD</b>	<b>0.84</b>	<b>1.04</b>	<b>0.69</b>	<b>0.97</b>	<b>0.82</b>
<b>Median</b>	<b>6.96</b>	<b>8.67</b>	<b>9.00</b>	<b>8.90</b>	<b>9.15</b>
<b>IQR</b>	<b>6.32, 7.25</b>	<b>7.85, 9.31</b>	<b>8.66, 9.27</b>	<b>8.32, 9.43</b>	<b>8.69, 9.52</b>
<b>Elderly group</b>					
<b>Individual</b>	<b>Visit 1</b>	<b>Visit 2</b>	<b>Visit 3</b>	<b>Visit 4</b>	<b>Visit 5</b>
<b>1</b>	7.47	6.87	7.54	7.61	7.92
<b>2</b>	5.45	5.47	6.35	6.69	7.13
<b>3</b>	6.59	7.58	6.95	7.17	7.27
<b>4</b>	5.85	7.07	7.89	7.70	8.13
<b>5</b>	5.22	6.35	7.14	7.65	8.03
<b>6</b>	7.09	8.29	8.37	8.60	9.14
<b>7</b>	6.83	8.55	8.50	8.85	8.90
<b>8</b>	6.39	7.66	7.88	7.96	8.18
<b>Mean</b>	<b>6.36</b>	<b>7.23</b>	<b>7.58</b>	<b>7.78</b>	<b>8.09</b>
<b>SD</b>	<b>0.80</b>	<b>1.01</b>	<b>0.73</b>	<b>0.70</b>	<b>0.70</b>
<b>Median</b>	<b>6.49</b>	<b>7.33</b>	<b>7.71</b>	<b>7.68</b>	<b>8.08</b>
<b>IQR</b>	<b>5.75, 6.90</b>	<b>6.74, 7.82</b>	<b>7.10, 8.01</b>	<b>7.50, 8.12</b>	<b>7.76, 8.36</b>

**Table 10.2** The summary statistics (Mean, SD, Median and IQR) of the mean Michelson contrast, in the presence of the noise mask, expressed in terms of sensitivity (dB) for the central field at each of the five visits for the young group (Top) and for the elderly group (Bottom).

<b>Factor</b>	<b>Numerator, Degrees of Freedom</b>	<b>Denominator, Degrees of Freedom</b>	<b>F value</b>	<b>P value</b>
<b>Visit</b>	4	148	11.49	<0.0001
<b>Noise mask</b>	1	148	832.44	<0.0001
<b>Age</b>	1	16	8.06	0.0118
<b>Noise*visit</b>	9	148	97.61	<0.0001
<b>Age*visit</b>	4	148	0.67	0.6106
<b>Age*noise</b>	1	148	5.10	0.0255

**Table 10.3** The ANOVA Summary Table for the mean Michelson contrast, expressed in terms of sensitivity (dB), for the central field.

### Visit

Overall, the mean sensitivity for the central field increased over the five visits (<0.0001) by approximately 15%.

The mean MS in the absence of the noise mask increased from Visit 1 to Visit 5 by 2.15dB in the young group and by 1.83dB in the elderly group. The improvement in the MS largely occurred between Visits 1 and 2 (difference between means 1.52dB and 1.22dB in the young and elderly groups, respectively).

The mean MS in the presence of the noise mask increased from Visit 1 to Visit 5 by 2.24dB in the young group and by 1.73dB in the elderly group. The improvement in the MS again largely occurred between Visits 1 and Visit 2 (difference between means 1.64dB and 0.87dB in the young and elderly group, respectively).

The improvement in sensitivity was greater in the presence of the noise mask than in the absence of the noise mask ( $<0.0001$ ) largely due to the extent of improvement in the young group.

#### Noise mask

Overall, the mean sensitivity for the central field was lower in the presence of the noise mask than that in the absence of the noise mask ( $<0.0001$ ). The noise mask attenuated the sensitivity by a greater extent for the elderly group ( $p=0.026$ ).

#### Age

Overall, the mean sensitivity was lower for the elderly group compared to that for the young group ( $p=0.012$ ).

The summary statistics (mean, SD, median and IQR) of the proportionate change from Visit 1 (%) in the Michelson contrast, expressed in terms of sensitivity in dB, for the central field at each of the remaining four visits in the absence and in the presence of the noise mask are shown in Table 10.4.

	Visit 2	Visit 3	Visit 4	Visit 5
<b>Without the noise mask</b>				
<b>Young group</b>				
Mean	11.00	13.26	13.70	15.69
SD	4.80	4.08	6.41	6.57
Median	9.56	12.49	15.29	14.52
IQR	7.82, 14.90	11.79, 16.57	10.07, 17.60	11.21, 16.62
<b>Elderly group</b>				
Mean	9.34	11.75	12.53	14.03
SD	4.21	4.68	7.05	5.77
Median	8.18	10.88	10.20	12.00
IQR	6.91, 12.27	8.80, 13.07	8.00, 15.61	10.41, 16.14
<b>With the noise mask</b>				
<b>Young group</b>				
Mean	27.21	34.69	34.12	37.26
SD	6.64	15.08	17.58	17.09
Median	26.58	29.35	32.15	36.07
IQR	25.16, 30.84	24.17, 38.04	22.90, 40.98	25.70, 43.48
<b>Elderly group</b>				
Mean	17.62	23.07	27.03	32.35
SD	12.50	12.84	13.71	14.75
Median	21.60	23.95	27.85	34.20
IQR	14.20, 25.26	16.69, 30.47	20.26, 35.90	26.06, 37.88

**Table 10.4** The summary statistics (Mean, SD, Median and IQR) of the proportionate change from Visit 1 (%) in the Michelson contrast, expressed in terms of sensitivity (dB), for the central field at each of the remaining four visits in the absence of the noise mask (Top) and in the presence of the noise mask (Bottom) for the young and elderly groups.

#### **10.4.2 Mean Sensitivity at the six central stimulus locations**

The summary statistics for each age-group of the Mean Sensitivity (dB) across the six central stimulus locations in the absence of the noise mask for each of the five visits (mean, SD, median and IQR) are shown in Table 10.5 and in the presence of the noise mask in Table 10.6.

The corresponding ANOVA summary table for the absolute values in Tables 10.5 and 10.6 is shown in Table 10.7.

<b>Without the noise mask</b>					
<b>Young group</b>					
<b>Individual</b>	<b>Visit 1</b>	<b>Visit 2</b>	<b>Visit 3</b>	<b>Visit 4</b>	<b>Visit 5</b>
<b>1</b>	15.62	15.76	16.52	17.46	16.96
<b>2</b>	15.96	16.69	15.94	15.01	15.97
<b>3</b>	13.16	14.56	15.32	15.43	16.63
<b>4</b>	13.83	16.22	16.53	16.41	17.33
<b>5</b>	16.35	16.63	17.19	16.49	17.17
<b>6</b>	14.79	16.80	16.77	16.47	15.92
<b>7</b>	15.06	15.67	16.37	16.63	16.71
<b>8</b>	16.05	17.14	17.36	16.99	17.28
<b>9</b>	15.43	16.63	16.76	16.93	17.17
<b>10</b>	16.28	18.36	18.24	18.16	17.84
<b>Mean</b>	<b>15.25</b>	<b>16.45</b>	<b>16.70</b>	<b>16.60</b>	<b>16.90</b>
<b>SD</b>	<b>1.07</b>	<b>1.00</b>	<b>0.80</b>	<b>0.91</b>	<b>0.61</b>
<b>Median</b>	<b>15.53</b>	<b>16.63</b>	<b>16.65</b>	<b>16.56</b>	<b>17.07</b>
<b>IQR</b>	<b>14.86, 16.03</b>	<b>15.87, 16.78</b>	<b>16.41, 17.08</b>	<b>16.42, 16.97</b>	<b>16.65, 17.25</b>
<b>Elderly group</b>					
<b>Individual</b>	<b>Visit 1</b>	<b>Visit 2</b>	<b>Visit 3</b>	<b>Visit 4</b>	<b>Visit 5</b>
<b>1</b>	13.76	15.62	15.42	15.80	16.04
<b>2</b>	15.45	17.47	17.43	17.63	17.02
<b>3</b>	16.92	17.87	17.75	16.95	17.23
<b>4</b>	14.18	15.62	15.32	15.84	16.32
<b>5</b>	14.75	15.23	15.26	14.50	15.18
<b>6</b>	16.51	17.83	18.06	18.39	18.40
<b>7</b>	14.24	15.42	17.31	17.71	17.53
<b>8</b>	15.79	15.95	17.58	17.55	16.58
<b>Mean</b>	<b>15.20</b>	<b>16.38</b>	<b>16.77</b>	<b>16.80</b>	<b>16.79</b>
<b>SD</b>	<b>1.15</b>	<b>1.14</b>	<b>1.21</b>	<b>1.30</b>	<b>0.99</b>
<b>Median</b>	<b>15.10</b>	<b>15.79</b>	<b>17.37</b>	<b>17.25</b>	<b>16.80</b>
<b>IQR</b>	<b>14.23, 15.97</b>	<b>15.57, 17.56</b>	<b>15.39, 17.62</b>	<b>15.83, 17.65</b>	<b>16.25, 17.31</b>

**Table 10.5** The summary statistics (Mean, SD, Median and IQR) of the Michelson contrast at the six central stimulus locations, in the absence of the noise mask, expressed in terms of sensitivity (dB) at each of the five visits for the young group (Top) and for the elderly group (Bottom).

<b>With the noise mask</b>					
<b>Young group</b>					
<b>Individual</b>	<b>Visit 1</b>	<b>Visit 2</b>	<b>Visit 3</b>	<b>Visit 4</b>	<b>Visit 5</b>
<b>1</b>	6.90	7.94	8.02	9.10	9.41
<b>2</b>	7.08	8.45	8.22	7.85	9.00
<b>3</b>	6.21	6.43	9.12	8.78	9.00
<b>4</b>	6.39	7.34	8.02	7.78	7.67
<b>5</b>	9.02	10.41	10.73	11.25	11.12
<b>6</b>	7.02	9.26	8.31	7.31	7.69
<b>7</b>	6.39	8.01	8.19	8.11	8.23
<b>8</b>	7.64	8.44	9.36	9.74	8.99
<b>9</b>	7.46	8.57	8.75	9.18	9.52
<b>10</b>	6.95	9.31	9.14	7.94	8.52
<b>Mean</b>	<b>7.11</b>	<b>8.42</b>	<b>8.79</b>	<b>8.70</b>	<b>8.91</b>
<b>SD</b>	<b>0.82</b>	<b>1.11</b>	<b>0.85</b>	<b>1.17</b>	<b>1.01</b>
<b>Median</b>	<b>6.99</b>	<b>8.44</b>	<b>8.53</b>	<b>8.45</b>	<b>8.99</b>
<b>IQR</b>	<b>6.51, 7.37</b>	<b>7.96, 9.09</b>	<b>8.19, 9.13</b>	<b>7.87, 9.16</b>	<b>8.30, 9.31</b>
<b>Elderly group</b>					
<b>Individual</b>	<b>Visit 1</b>	<b>Visit 2</b>	<b>Visit 3</b>	<b>Visit 4</b>	<b>Visit 5</b>
<b>1</b>	5.99	6.01	6.36	6.51	7.07
<b>2</b>	5.35	5.54	6.15	6.31	7.26
<b>3</b>	6.50	7.00	6.09	6.52	6.52
<b>4</b>	6.07	6.93	7.55	7.04	7.31
<b>5</b>	4.92	6.54	6.35	6.52	6.86
<b>6</b>	7.04	7.92	8.23	8.48	8.71
<b>7</b>	7.52	8.52	9.13	9.47	9.17
<b>8</b>	6.38	7.41	7.50	7.93	7.94
<b>Mean</b>	<b>6.22</b>	<b>6.98</b>	<b>7.17</b>	<b>7.35</b>	<b>7.60</b>
<b>SD</b>	<b>0.85</b>	<b>0.97</b>	<b>1.12</b>	<b>1.16</b>	<b>0.93</b>
<b>Median</b>	<b>6.22</b>	<b>6.97</b>	<b>6.93</b>	<b>6.78</b>	<b>7.28</b>
<b>IQR</b>	<b>5.83, 6.63</b>	<b>6.41, 7.54</b>	<b>6.30, 7.72</b>	<b>6.52, 8.07</b>	<b>7.02, 8.13</b>

**Table 10.6** The summary statistics (Mean, SD, Median and IQR) of the Michelson contrast at the six central stimulus locations, in the presence of the noise mask, expressed in terms of sensitivity (dB) at each of the five visits for the young group (Top) and for the elderly group (Bottom).

Factor	Numerator, Degrees of Freedom	Denominator, Degrees of Freedom	F value	P value
Visit	4	148	5.87	<0.0001
Noise	1	148	816.54	<0.0001
Age	1	16	2.39	0.1414
Noise*visit	9	148	93.37	<0.0001
Age*visit	4	148	0.23	0.9216
Age*noise	4	148	20.98	<.0001

**Table 10.7** The ANOVA Summary Table for the mean Michelson contrast, expressed in terms of sensitivity (dB), for the six central stimulus locations.

### Visit

Overall, the mean sensitivity for the central six stimulus increased over the five visits (<0.0001).

The mean MS in the absence of the noise mask increased from Visit 1 to Visit 5 by 1.65dB in the young group and by 1.59dB in the elderly group. The improvement in the MS largely occurred between Visits 1 and 2 (mean of the difference 1.20dB and 1.18dB in the young and elderly groups, respectively)

The mean MS in the presence of the noise mask increased from Visit 1 to Visit 5 by 1.80dB in the young group and by 1.38dB in the elderly group. The improvement in the MS again largely occurred between Visits 1 and Visit 2 (mean of the difference 1.31dB and 0.76dB in the young and elderly group, respectively).

The improvement in sensitivity was greater in the presence of the noise mask than in the absence of the noise mask ( $<0.0001$ ) largely due to the extent of the improvement in the young group.

#### Noise mask

Overall, the mean sensitivity for the central field was lower in the presence of the noise mask than that in the absence of the noise mask ( $p<0.0001$ ). The noise mask attenuated the sensitivity to a greater extent for the elderly group ( $p<0.0001$ ).

#### Age

Overall, the mean sensitivity was similar between the two age groups ( $p=0.142$ ).

The summary statistics (mean, SD, median and IQR) of the proportionate change from Visit 1 (%) in the Michelson contrast, expressed in terms of sensitivity in dB, for the six central stimulus locations at each of the remaining four visits in the absence and in the presence of the noise mask are shown in Table 10.8.

	Visit 2	Visit 3	Visit 4	Visit 5
<b>Without the noise mask</b>				
<b>Young group</b>				
Mean	9.14	10.75	9.94	12.05
SD	6.38	6.15	7.72	8.69
Median	8.73	10.48	11.55	9.18
IQR	4.19, 13.53	6.44, 15.77	7.00, 15.24	7.56, 16.10
<b>Elderly group</b>				
Mean	8.34	11.00	11.41	11.52
SD	4.32	5.61	8.27	7.30
Median	8.70	10.98	12.33	11.54
IQR	6.34, 11.02	7.71, 12.22	8.95, 14.76	4.94, 16.40
<b>With the noise mask</b>				
<b>Young group</b>				
Mean	19.09	25.01	23.59	26.54
SD	9.55	9.29	10.71	9.90
Median	16.21	22.50	25.28	26.31
IQR	15.13, 24.70	17.96, 27.82	16.72, 27.85	21.51, 29.13
<b>Elderly group</b>				
Mean	17.03	18.75	22.37	27.51
SD	11.02	11.90	11.13	12.02
Median	16.70	22.61	23.37	27.81
IQR	9.18, 22.48	15.68, 26.75	19.32, 31.94	24.33, 35.51

**Table 10.8** The summary statistics (Mean, SD, Median and IQR) of the proportionate change from Visit 1 (%) in the Michelson contrast, expressed in terms of sensitivity (dB), for the six central stimulus locations at each of the remaining four visits in the absence of the noise mask (Top) and in the presence of the noise mask (Bottom) for the young and elderly groups.

### **10.4.3 Mean Sensitivity at the six peripheral stimulus locations**

The summary statistics for each age-group of the mean sensitivity (dB) across the six peripheral stimulus locations in the absence of the noise mask for each of the five visits (mean, SD, median and IQR) are shown in Table 10.9 and in the presence of the noise mask in Table 10.10.

The corresponding ANOVA summary table for the absolute values in Tables 10.9 and 10.10 is shown in Table 10.11.

<b>Without noise mask</b>					
<b>Young group</b>					
<b>Individual</b>	<b>Visit 1</b>	<b>Visit 2</b>	<b>Visit 3</b>	<b>Visit 4</b>	<b>Visit 5</b>
<b>1</b>	13.41	14.47	15.76	16.54	16.79
<b>2</b>	13.76	15.29	14.83	14.72	16.05
<b>3</b>	12.42	15.01	14.43	15.60	16.38
<b>4</b>	13.12	14.79	15.12	15.73	15.93
<b>5</b>	13.63	15.61	15.98	15.93	15.69
<b>6</b>	13.12	14.15	15.63	15.63	15.78
<b>7</b>	13.43	14.99	15.53	16.06	15.81
<b>8</b>	14.81	15.69	17.02	15.93	16.37
<b>9</b>	15.05	17.76	17.55	17.49	17.72
<b>10</b>	13.63	17.11	16.64	16.60	16.36
<b>Mean</b>	<b>13.64</b>	<b>15.49</b>	<b>15.85</b>	<b>16.02</b>	<b>16.29</b>
<b>SD</b>	<b>0.78</b>	<b>1.14</b>	<b>0.98</b>	<b>0.74</b>	<b>0.61</b>
<b>Median</b>	<b>13.53</b>	<b>15.15</b>	<b>15.70</b>	<b>15.93</b>	<b>16.20</b>
<b>IQR</b>	<b>13.19, 13.73</b>	<b>14.84, 15.67</b>	<b>15.23, 16.48</b>	<b>15.65, 16.42</b>	<b>15.84, 16.38</b>
<b>Elderly group</b>					
<b>Individual</b>	<b>Visit 1</b>	<b>Visit 2</b>	<b>Visit 3</b>	<b>Visit 4</b>	<b>Visit 5</b>
<b>1</b>	12.84	14.92	14.61	15.28	14.41
<b>2</b>	15.96	16.33	16.55	16.91	17.66
<b>3</b>	13.79	16.65	16.23	16.04	16.31
<b>4</b>	12.26	13.74	14.28	14.18	14.52
<b>5</b>	13.34	14.38	15.24	14.80	15.04
<b>6</b>	13.86	14.53	14.01	14.94	15.47
<b>7</b>	12.15	13.02	14.59	15.47	15.51
<b>8</b>	13.88	14.58	14.54	14.57	15.77
<b>Mean</b>	<b>13.51</b>	<b>14.77</b>	<b>15.01</b>	<b>15.27</b>	<b>15.59</b>
<b>SD</b>	<b>1.21</b>	<b>1.22</b>	<b>0.93</b>	<b>0.87</b>	<b>1.05</b>
<b>Median</b>	<b>13.57</b>	<b>14.56</b>	<b>14.60</b>	<b>15.11</b>	<b>15.49</b>
<b>IQR</b>	<b>12.70, 13.87</b>	<b>14.22, 15.27</b>	<b>14.48, 15.49</b>	<b>14.74, 15.61</b>	<b>14.91, 15.90</b>

**Table 10.9** The summary statistics (Mean, SD, Median and IQR) of the Michelson contrast at the six peripheral stimulus locations, in the absence of the noise mask, expressed in terms of sensitivity (dB) at each of the five visits for the young group (Top) and for the elderly group (Bottom).

<b>With the noise mask</b>					
<b>Young group</b>					
<b>Individual</b>	<b>Visit 1</b>	<b>Visit 2</b>	<b>Visit 3</b>	<b>Visit 4</b>	<b>Visit 5</b>
<b>1</b>	6.36	8.41	8.33	9.77	10.15
<b>2</b>	6.78	8.94	9.10	8.71	9.20
<b>3</b>	5.31	7.31	9.53	10.06	10.18
<b>4</b>	5.89	7.87	10.49	8.39	9.31
<b>5</b>	7.05	10.32	11.02	10.83	10.92
<b>6</b>	7.24	9.71	9.00	8.10	8.46
<b>7</b>	5.98	7.48	8.19	9.02	9.26
<b>8</b>	7.50	9.11	9.20	9.33	9.43
<b>9</b>	7.12	8.74	8.93	9.29	9.08
<b>10</b>	7.03	10.05	9.17	8.93	8.83
<b>Mean</b>	<b>6.63</b>	<b>8.80</b>	<b>9.30</b>	<b>9.24</b>	<b>9.48</b>
<b>SD</b>	<b>0.71</b>	<b>1.04</b>	<b>0.87</b>	<b>0.81</b>	<b>0.73</b>
<b>Median</b>	<b>6.90</b>	<b>8.84</b>	<b>9.13</b>	<b>9.16</b>	<b>9.29</b>
<b>IQR</b>	<b>6.07, 7.10</b>	<b>8.01, 9.56</b>	<b>8.95, 9.44</b>	<b>8.77, 9.66</b>	<b>9.11, 9.97</b>
<b>Elderly group</b>					
<b>Individual</b>	<b>Visit 1</b>	<b>Visit 2</b>	<b>Visit 3</b>	<b>Visit 4</b>	<b>Visit 5</b>
<b>1</b>	8.96	7.73	8.72	8.72	8.76
<b>2</b>	5.55	5.41	6.55	6.88	7.01
<b>3</b>	6.69	8.15	7.81	7.82	8.01
<b>4</b>	5.62	7.21	8.74	8.37	8.95
<b>5</b>	5.52	6.16	7.93	8.79	9.20
<b>6</b>	7.14	8.40	8.51	8.81	9.89
<b>7</b>	6.14	8.58	7.88	8.23	8.63
<b>8</b>	6.39	7.91	8.27	8.00	8.42
<b>Mean</b>	<b>6.50</b>	<b>7.44</b>	<b>8.05</b>	<b>8.20</b>	<b>8.61</b>
<b>SD</b>	<b>1.15</b>	<b>1.12</b>	<b>0.71</b>	<b>0.65</b>	<b>0.85</b>
<b>Median</b>	<b>6.27</b>	<b>7.82</b>	<b>8.10</b>	<b>8.30</b>	<b>8.70</b>
<b>IQR</b>	<b>5.61, 6.80</b>	<b>6.95, 8.22</b>	<b>7.86, 8.56</b>	<b>7.95, 8.73</b>	<b>8.32, 9.01</b>

**Table 10.10** The summary statistics (Mean, SD, Median and IQR) of the Michelson contrast at the six peripheral stimulus locations, in the presence of the noise mask, expressed in terms of sensitivity (dB) at each of the five visits for the young group (Top) and for the elderly group (Bottom).

<b>Factor</b>	<b>Numerator, Degrees of Freedom</b>	<b>Denominator, Degrees of Freedom</b>	<b>F value</b>	<b>P value</b>
<b>Visit</b>	4	148	14.10	<0.0001
<b>Noise</b>	1	148	550.78	<0.0001
<b>Age</b>	1	16	20.28	0.0004
<b>Noise*visit</b>	9	148	67.53	<0.0001
<b>Age*visit</b>	4	148	1.39	0.2408
<b>Age*noise</b>	1	148	0.07	0.7916

**Table 10.11** The ANOVA Summary Table for the mean Michelson contrast, expressed in terms of sensitivity (dB), for the six peripheral stimulus locations.

### Visit

Overall, the mean sensitivity for the peripheral six stimulus increased over the five visits ( $p < 0.0001$ ).

The mean MS in the absence of the noise mask increased from Visit 1 to Visit 5 by 2.65dB in the young group and by 2.08dB in the elderly group. The improvement in the MS largely occurred between Visits 1 and 2 (difference between means 1.85dB and 1.26dB in the young and elderly groups, respectively).

The mean MS in the presence of the noise mask increased from Visit 1 to Visit 5 by 2.86dB in the young group and by 2.11dB in the elderly group. The improvement in the MS largely occurred between Visits 1 and 2 (difference between means 2.17dB and 0.94dB in the young and elderly groups, respectively).

The improvement in sensitivity was greater in the absence of the noise mask compared to that in the presence of the noise mask ( $p < 0.0001$ ).

#### Noise mask

Overall, the mean sensitivity for the peripheral field was lower in the presence of the noise mask than that in the absence of the noise mask ( $p < 0.0001$ ).

#### Age

Overall, the mean sensitivity was lower for the elderly group compared to that for the young group ( $p = 0.0004$ ).

The summary statistics (mean, SD, median and IQR) of the proportionate change from Visit 1 (%) in the Michelson contrast, expressed in terms of sensitivity in dB, for the six peripheral stimulus locations at each of the remaining four visits in the absence and in the presence of the noise mask are shown in Table 10.12.

	Visit 2	Visit 3	Visit 4	Visit 5
<b>Without the noise mask</b>				
<b>Young group</b>				
Mean	13.19	16.17	17.88	20.07
SD	6.12	3.79	6.31	5.92
Median	11.43	16.16	19.69	19.56
IQR	9.14, 14.45	15.49, 17.71	14.83, 21.66	17.26, 21.50
<b>Elderly group</b>				
Mean	10.02	12.18	12.52	14.90
SD	7.01	7.52	10.26	8.62
Median	8.13	15.10	14.19	14.33
IQR	5.92, 13.92	5.19, 17.74	4.47, 18.64	13.42, 18.81
<b>With the noise mask</b>				
<b>Young group</b>				
Mean	34.79	43.87	44.08	47.39
SD	8.98	22.62	25.43	25.40
Median	34.83	35.09	38.73	45.79
IQR	28.43, 41.87	27.54, 52.53	28.44, 54.62	27.70, 59.52
<b>Elderly group</b>				
Mean	18.19	27.40	31.68	37.19
SD	18.13	16.63	19.65	22.11
Median	23.58	27.11	27.82	33.87
IQR	8.46, 29.20	20.50, 34.19	24.06, 41.95	29.52, 48.45

**Table 10.12** The summary statistics (Mean, SD, Median and IQR) of the proportionate change from Visit 1 (%) in the Michelson contrast, expressed in terms of sensitivity (dB), for the six peripheral stimulus locations at each of the remaining four visits in the absence of the noise mask (Top) and in the presence of the noise mask (Bottom) for the young and elderly groups.

#### **10.4.4 The ratio of Central to Peripheral Mean Sensitivity**

The summary statistics, for each age-group, of the ratio of Central to Peripheral Mean Sensitivity in the absence of the noise mask for each of the five visits (mean, SD, median and IQR) are shown in Table 10.13 and in the presence of the noise mask in Table 10.14.

The corresponding ANOVA summary table for the absolute values in Tables 10.13 and 10.14 is shown in Table 10.15.

<b>Without the noise mask</b>					
<b>Young group</b>					
<b>Individual</b>	<b>Visit 1</b>	<b>Visit 2</b>	<b>Visit 3</b>	<b>Visit 4</b>	<b>Visit 5</b>
<b>1</b>	1.16	1.09	1.05	1.06	1.01
<b>2</b>	1.16	1.09	1.07	1.02	1.00
<b>3</b>	1.06	0.97	1.06	0.99	1.02
<b>4</b>	1.05	1.10	1.09	1.04	1.09
<b>5</b>	1.20	1.07	1.08	1.03	1.09
<b>6</b>	1.13	1.19	1.07	1.05	1.01
<b>7</b>	1.12	1.05	1.05	1.04	1.06
<b>8</b>	1.08	1.09	1.02	1.07	1.06
<b>9</b>	1.03	0.94	0.96	0.97	0.97
<b>10</b>	1.19	1.07	1.10	1.09	1.09
<b>Mean</b>	<b>1.12</b>	<b>1.06</b>	<b>1.06</b>	<b>1.04</b>	<b>1.04</b>
<b>SD</b>	<b>0.06</b>	<b>0.07</b>	<b>0.04</b>	<b>0.04</b>	<b>0.04</b>
<b>Median</b>	<b>1.12</b>	<b>1.08</b>	<b>1.07</b>	<b>1.04</b>	<b>1.04</b>
<b>IQR</b>	<b>1.07, 1.16</b>	<b>1.05, 1.09</b>	<b>1.05, 1.08</b>	<b>1.02, 1.06</b>	<b>1.01, 1.08</b>
<b>Elderly group</b>					
<b>Individual</b>	<b>Visit 1</b>	<b>Visit 2</b>	<b>Visit 3</b>	<b>Visit 4</b>	<b>Visit 5</b>
<b>1</b>	1.07	1.05	1.06	1.03	1.11
<b>2</b>	0.97	1.07	1.05	1.04	0.96
<b>3</b>	1.23	1.07	1.09	1.06	1.06
<b>4</b>	1.16	1.14	1.07	1.12	1.12
<b>5</b>	1.11	1.06	1.00	0.98	1.01
<b>6</b>	1.19	1.23	1.29	1.23	1.19
<b>7</b>	1.17	1.18	1.19	1.14	1.13
<b>8</b>	1.14	1.09	1.21	1.20	1.05
<b>Mean</b>	<b>1.13</b>	<b>1.11</b>	<b>1.12</b>	<b>1.10</b>	<b>1.08</b>
<b>SD</b>	<b>0.08</b>	<b>0.07</b>	<b>0.10</b>	<b>0.09</b>	<b>0.07</b>
<b>Median</b>	<b>1.15</b>	<b>1.08</b>	<b>1.08</b>	<b>1.09</b>	<b>1.08</b>
<b>IQR</b>	<b>1.10, 1.18</b>	<b>1.07, 1.15</b>	<b>1.05, 1.19</b>	<b>1.04, 1.16</b>	<b>1.04, 1.13</b>

**Table 10.13** The summary statistics (Mean, SD, Median and IQR) of the ratio of the mean Michelson contrast, expressed in terms of sensitivity (dB), at the six central stimulus locations to that at the six peripheral stimulus locations, in the absence of the noise mask, at each of the five visits for the young group (Top) and for the elderly group (Bottom).

<b>With the noise mask</b>					
<b>Young group</b>					
<b>Individual</b>	<b>Visit 1</b>	<b>Visit 2</b>	<b>Visit 3</b>	<b>Visit 4</b>	<b>Visit 5</b>
<b>1</b>	1.08	0.94	0.96	0.93	0.93
<b>2</b>	1.05	0.94	0.90	0.90	0.98
<b>3</b>	1.17	0.88	0.96	0.87	0.88
<b>4</b>	1.08	0.93	0.76	0.93	0.82
<b>5</b>	1.28	1.01	0.97	1.04	1.02
<b>6</b>	0.97	0.95	0.92	0.90	0.91
<b>7</b>	1.07	1.07	1.00	0.90	0.89
<b>8</b>	1.02	0.93	1.02	1.04	0.95
<b>9</b>	1.05	0.98	0.98	0.99	1.05
<b>10</b>	0.99	0.93	1.00	0.89	0.97
<b>Mean</b>	<b>1.08</b>	<b>0.96</b>	<b>0.95</b>	<b>0.94</b>	<b>0.94</b>
<b>SD</b>	<b>0.09</b>	<b>0.05</b>	<b>0.07</b>	<b>0.06</b>	<b>0.07</b>
<b>Median</b>	<b>1.06</b>	<b>0.94</b>	<b>0.97</b>	<b>0.91</b>	<b>0.94</b>
<b>IQR</b>	<b>1.03, 1.08</b>	<b>0.93, 0.97</b>	<b>0.93, 0.99</b>	<b>0.90, 0.97</b>	<b>0.89, 0.97</b>
<b>Elderly group</b>					
<b>Individual</b>	<b>Visit 1</b>	<b>Visit 2</b>	<b>Visit 3</b>	<b>Visit 4</b>	<b>Visit 5</b>
<b>1</b>	0.67	0.78	0.73	0.75	0.81
<b>2</b>	0.96	1.02	0.94	0.92	1.04
<b>3</b>	0.97	0.86	0.78	0.83	0.81
<b>4</b>	1.08	0.96	0.86	0.84	0.82
<b>5</b>	0.89	1.06	0.80	0.74	0.75
<b>6</b>	0.99	0.94	0.97	0.96	0.88
<b>7</b>	1.23	0.99	1.16	1.15	1.06
<b>8</b>	1.00	0.94	0.91	0.99	0.94
<b>Mean</b>	<b>0.97</b>	<b>0.94</b>	<b>0.89</b>	<b>0.90</b>	<b>0.89</b>
<b>SD</b>	<b>0.16</b>	<b>0.09</b>	<b>0.13</b>	<b>0.14</b>	<b>0.11</b>
<b>Median</b>	<b>0.98</b>	<b>0.95</b>	<b>0.89</b>	<b>0.88</b>	<b>0.85</b>
<b>IQR</b>	<b>0.95, 1.02</b>	<b>0.92, 1.00</b>	<b>0.80, 0.95</b>	<b>0.81, 0.97</b>	<b>0.81, 0.97</b>

**Table 10.14** The summary statistics (Mean, SD, Median and IQR) of the ratio of the mean Michelson contrast, expressed in terms of sensitivity (dB), at the six central stimulus locations to that at the six peripheral stimulus locations, in the presence of the noise mask, at each of the five visits for the young group (Top) and for the elderly group (Bottom). A decreasing ratio over the given visits indicates a greater change in the peripheral sensitivity relative to the central sensitivity.

<b>Factor</b>	<b>Numerator, Degrees of Freedom</b>	<b>Denominator, Degrees of Freedom</b>	<b>F value</b>	<b>P value</b>
<b>Visit</b>	4	148	4.26	0.0027
<b>Noise</b>	1	148	2.00	0.1591
<b>Age</b>	1	16	0.22	0.6478
<b>Noise*visit</b>	9	148	2.66	0.007
<b>Age*visit</b>	4	148	0.91	0.4603
<b>Age*noise</b>	1	148	21.83	<0.0001

**Table 10.15** The ANOVA Summary Table for the ratio of the mean Michelson contrast, expressed in terms of sensitivity (dB), at the six central stimulus locations to that at the six peripheral stimulus locations.

### Visit

Overall, the mean ratio declined over the five visits indicating a greater improvement in the peripheral sensitivity compared to that of the central sensitivity ( $p=0.0027$ ).

The ratio in the absence of the noise mask declined from 1.12 at Visit 1 to 1.04 at Visit 5 in the young group and from 1.13 to 1.08 in the elderly group, representing reductions of 0.08 and 0.05, respectively. The ratio in the presence of the noise mask the noise mask declined from 1.08 at Visit 1 to 0.94 at Visit 5 in the young group and from 0.96 to 0.88 in the elderly group, representing reductions of 0.14 and 0.08, respectively. The greater improvements in the peripheral sensitivity compared to the central sensitivity over the five visits were more pronounced in the presence of the noise mask ( $p=0.007$ ).

### Noise mask

Overall, the ratio was not influenced by the noise mask ( $p=0.159$ ) indicating an equivalent effect on both the central and the peripheral sensitivities; however, the mask attenuated the ratio by a greater extent in the elderly group ( $p<0.0001$ ).

#### **10.4.5 Examination Duration**

The summary statistics, for each age-group, of the examination duration in the absence of the noise mask for each of the five visits (mean, SD, median and IQR) are shown in Table 10.16 and in the presence of the noise mask in Table 10.17.

The summary statistics (mean, SD, median and IQR) of the proportionate change from Visit 1 (%) in the examination duration at each of the remaining four visits in the absence, and in the presence of the noise mask are shown in Table 10.18.

<b>Without the noise mask</b>					
<b>Young group</b>					
<b>Individual</b>	<b>Visit 1</b>	<b>Visit 2</b>	<b>Visit 3</b>	<b>Visit 4</b>	<b>Visit 5</b>
<b>1</b>	1015	740	650	504	510
<b>2</b>	859	790	674	768	611
<b>3</b>	1194	771	703	632	553
<b>4</b>	838	747	615	553	583
<b>5</b>	556	493	509	492	496
<b>6</b>	1165	790	819	573	510
<b>7</b>	979	849	722	598	501
<b>8</b>	1045	837	569	580	550
<b>9</b>	1159	768	674	552	492
<b>10</b>	795	680	600	570	490
<b>Mean</b>	<b>960.50</b>	<b>746.50</b>	<b>653.50</b>	<b>582.20</b>	<b>529.60</b>
<b>SD</b>	<b>200.70</b>	<b>101.25</b>	<b>86.76</b>	<b>77.10</b>	<b>42.35</b>
<b>Median</b>	<b>997.00</b>	<b>769.50</b>	<b>662.00</b>	<b>571.50</b>	<b>510.00</b>
<b>IQR</b>	<b>843.25, 1130.50</b>	<b>741.75, 790.00</b>	<b>603.75, 695.75</b>	<b>552.25, 593.50</b>	<b>497.25, 552.25</b>
<b>Elderly group</b>					
<b>Individual</b>	<b>Visit 1</b>	<b>Visit 2</b>	<b>Visit 3</b>	<b>Visit 4</b>	<b>Visit 5</b>
<b>1</b>	673	679	628	658	607
<b>2</b>	754	613	579	722	671
<b>3</b>	859	1350	1350	1257	985
<b>4</b>	1253	1047	874	798	730
<b>5</b>	1362	690	710	720	649
<b>6</b>	1276	756	737	700	695
<b>7</b>	1220	1245	1049	966	686
<b>8</b>	833	573	512	615	438
<b>Mean</b>	<b>1028.75</b>	<b>869.13</b>	<b>804.88</b>	<b>804.50</b>	<b>682.63</b>
<b>SD</b>	<b>274.70</b>	<b>302.01</b>	<b>278.57</b>	<b>211.50</b>	<b>151.50</b>
<b>Median</b>	<b>1039.50</b>	<b>723.00</b>	<b>723.50</b>	<b>721.00</b>	<b>678.50</b>
<b>IQR</b>	<b>813.25, 1258.75</b>	<b>662.50, 1096.50</b>	<b>615.75, 917.75</b>	<b>689.50, 840.00</b>	<b>638.50, 703.75</b>

**Table 10.16** The summary statistics (Mean, SD, Median and IQR) of the examination duration (seconds) in the absence of the noise mask at each of the five visits for the young group (Top) and for the elderly group (Bottom).

<b>With the noise mask</b>					
<b>Young group</b>					
<b>Individual</b>	<b>Visit 1</b>	<b>Visit 2</b>	<b>Visit 3</b>	<b>Visit 4</b>	<b>Visit 5</b>
<b>1</b>	728	804	683	561	530
<b>2</b>	1200	814	780	616	601
<b>3</b>	947	776	678	771	680
<b>4</b>	861	735	759	671	712
<b>5</b>	654	584	610	613	594
<b>6</b>	1184	750	728	589	552
<b>7</b>	1111	722	603	591	550
<b>8</b>	1241	1200	610	613	553
<b>9</b>	1064	720	634	613	594
<b>10</b>	1035	749	712	602	532
<b>Mean</b>	<b>1002.50</b>	<b>785.40</b>	<b>679.70</b>	<b>624.00</b>	<b>589.80</b>
<b>SD</b>	<b>201.48</b>	<b>158.86</b>	<b>64.49</b>	<b>58.70</b>	<b>61.93</b>
<b>Median</b>	<b>1049.50</b>	<b>749.50</b>	<b>680.50</b>	<b>613.00</b>	<b>573.50</b>
<b>IQR</b>	<b>882.50, 1165.75</b>	<b>725.25, 797.00</b>	<b>616.00, 724.00</b>	<b>593.75, 615.25</b>	<b>550.50, 599.25</b>
<b>Elderly group</b>					
<b>Individual</b>	<b>Visit 1</b>	<b>Visit 2</b>	<b>Visit 3</b>	<b>Visit 4</b>	<b>Visit 5</b>
<b>1</b>	727	682	677	683	770
<b>2</b>	659	659	493	780	679
<b>3</b>	994	994	1175	1175	903
<b>4</b>	1045	1202	1257	886	849
<b>5</b>	1053	638	732	767	670
<b>6</b>	1388	791	791	806	906
<b>7</b>	1182	1059	997	916	819
<b>8</b>	673	584	600	611	512
<b>Mean</b>	<b>965.13</b>	<b>826.13</b>	<b>840.25</b>	<b>828.00</b>	<b>763.50</b>
<b>SD</b>	<b>260.92</b>	<b>229.17</b>	<b>275.01</b>	<b>171.61</b>	<b>135.93</b>
<b>Median</b>	<b>1019.50</b>	<b>736.50</b>	<b>761.50</b>	<b>793.00</b>	<b>794.50</b>
<b>IQR</b>	<b>713.50, 1085.25</b>	<b>653.75, 1010.25</b>	<b>657.75, 1041.50</b>	<b>746.00, 893.50</b>	<b>676.75, 862.50</b>

**Table 10.17** The summary statistics (Mean, SD, Median and IQR) of the examination duration (seconds) in the presence of the noise mask at each of the five visits for the young group (Top) and for the elderly group (Bottom).

	Visit 2	Visit 3	Visit 4	Visit 5
<b>Without the noise mask</b>				
<b>Young group</b>				
Mean	-20.63	-30.16	-36.84	-42.19
SD	10.54	11.22	15.63	14.94
Median	-17.18	-28.16	-41.71	-48.10
IQR	-30.92, -11.82	-39.83, -24.96	-49.53, -29.73	-52.70, -32.41
<b>Elderly group</b>				
Mean	-12.04	-18.21	-16.97	-29.62
SD	33.38	33.53	30.62	24.30
Median	-17.57	-26.73	-23.50	-42.76
IQR	-33.60, 1.18	-39.46, -12.18	-38.52, -3.74	-46.00, -10.71
<b>With the noise mask</b>				
<b>Young group</b>				
Mean	-20.01	-29.49	-35.04	-38.39
SD	15.58	16.08	16.02	16.53
Median	-22.84	-33.10	-42.11	-46.39
IQR	-32.29, -11.69	-39.94, -15.99	-48.20, -22.29	-50.35, -27.45
<b>Elderly group</b>				
Mean	-12.15	-11.70	-10.69	-18.09
SD	19.89	22.27	21.08	16.51
Median	-8.30	-13.25	-12.21	-21.34
IQR	-19.77, 0.00	-26.51, -0.61	-23.67, 0.01	-31.71, -6.11

**Table 10.18** The summary statistics (Mean, SD, Median and IQR) of the proportionate change (%) from Visit 1 in the examination duration at each of the remaining four visits in the absence of the noise mask (Top) and in the presence of the noise mask (Bottom) for the young and elderly groups. A negative sign indicates a reduction in the examination duration.

The mean examination duration was longer in the presence of the noise mask. It was also longer for the elderly group compared to the younger group. The mean examination duration decreased over the five visits both in the absence and in the presence of the noise mask.

#### 10.4.6 The derivatives from $MCN_a$ and $MCN_p$

The summary statistics for the proportionate change (%) in the given derivative from Visit 1 is shown in Table 10.19.

	$MCN_a$	$MCN_p$	$N_{eq}$	SE	$LOG_{10}$ Ratio	SDI
<b>Young group</b>						
<b>Mean</b>	-38.1	-39.5	10.2	200.3	9.4	186.8
<b>SD</b>	10.6	10.7	35.6	118.6	6.09	112.5
<b>Median</b>	-38.0	-39.9	6.8	178.4	8.93	160.6
<b>IQR</b>	-41.4; -30.0	-43.6; -33.4	-16.7; 42.0	125.1; 218.3	5.22; 14.69	105.4; 191.1
<b>Elderly group</b>						
<b>Mean</b>	-33.71	-31.77	6.03	133.92	7.7	134.0
<b>SD</b>	9.75	13.08	56.90	81.37	10.2	81.4
<b>Median</b>	-32.33	-35.72	3.06	141.46	10.1	141.6
<b>IQR</b>	-36.78; -27.50	-38.66; -27.68	-33.21; 17.12	96.71; 17.12	0.25; 10.9	96.7; 164.9

**Table 10.19** The summary statistics (Mean, SD, Median and IQR) of the proportionate change (%) between Visit 5 and Visit 1 at the 12 central stimulus locations, for the Michelson contrast in the absence ( $MCN_a$ ) and in the presence ( $MCN_p$ ) of the noise mask and for each of the four derivatives: Equivalent noise ( $N_{eq}$ ); Sampling efficiency (SE);  $LOG_{10}$  of the ratio  $MCN_p: MCN_a$  and Signal Detection Index (SDI) for the young group (Top) and the elderly group (Bottom). A positive sign indicates a deterioration in  $MCN_a$ ,  $MCN_p$ ,  $N_{eq}$  and the  $LOG_{10}$  ratio but an improvement in SE and SDI.

## 10.5 Discussion

In this study, a learning effect for DNP, both in the absence and in the presence of the noise mask, has been illustrated, in absolute and in proportionate terms for both the young and the elderly normal individuals.

The improvement in the group mean Mean Sensitivity in the absence of the noise mask was greatest from Visit 1 to Visit 2 (mean of the differences 1.5 dB [SD 0.66]; 11% and 1.2 dB [SD 0.53]; 9% for the young and elderly groups, respectively). The corresponding differences between Visits 1 and 5 were 2.15dB [SD 0.79]; 16% and 1.83dB [SD 0.70]; 14%, respectively.

The corresponding improvements in the presence of the noise mask were 1.6dB [SD 0.51], 27%, and 0.9dB [SD 0.76]; 18%, from Visit 1 to Visit 2 compared to 2.2dB [SD 0.79], 37%, and 1.7dB [SD 0.80]; 32%, from Visits 1 to 5. The improvement was more pronounced for the peripheral annulus. Commensurate with the improvement in sensitivity was a marked reduction in the examination duration. Clearly, the learning effect was more pronounced in the presence of the noise mask: the improvement was approximately double, and learning effect lasted longer, for both the young and the elderly individuals.

The study of the learning effect was undertaken in one eye, only, of each individual. Clearly, this does not replicate clinical reality. However, the study had been designed as a pilot investigation since it had been anticipated that the measurement of Michelson contrast in the presence of the noise mask would represent a relatively difficult visual task for individuals in experience in visual psychophysics.

The time course, topographical variation and magnitude of the improvement in the Michelson contrast expressed in dB is comparable to the learning effect in SAP expressed as a Weber contrast (Wood et al., 1987; Heijl et al., 1989b; Castro et al., 2008) and to other perimetric stimuli which are expressed in Michelson contrast such as the FDT (Iester et al., 2000; Horani et al., 2002; Contestabile et al., 2007; Castro et al., 2008; Pierre-Filho Pde et al., 2010) and HEP (Lamparter et al., 2011). Unfortunately, the presence of the learning effect in perimetry has never been resolved clinically. Only one study has attempted to address the issue (Olsson, Asman and Heijl, 1997) and that involved the calculation of a Learner's Index. The latter has never been implemented in clinical practice.

## Chapter 11

### General summary, conclusions and proposals for future work

#### 11.1 The influence of the Gaussian filter on Dynamic Noise Perimetry

The study determined the influence of the stimulus edge on the threshold in 15 normal individuals by using different strengths of Gaussian filter (0, 0.25, 0.50 and 1 FWHM). Each of the four levels of Gaussian filter, in the presence or in the absence of the noise mask, exerted little influence on the Michelson contrast, expressed as sensitivity (dB), at each of the three eccentricities and confirmed that the stimulus edge of the DNP did not appear to influence the threshold outcome either in the absence or in the presence of the noise mask ( $p=0.848$ ). Nevertheless, a Gaussian filter of 0.5 FWHM was applied to both vertical edges of the stimulus in the remaining studies to avoid any external negative criticism concerning the influence of the stimulus edge on the threshold.

#### 11.2 The influence of the strength of the noise mask on the outcome of Dynamic Noise Perimetry

The study determined the optimum number of checks per grating cycle to mask the underlying stimulus (a 0.5 cycles per degree grating contained within a  $4^\circ \times 4^\circ$  patch) regardless of eccentricity. Eight checks per grating cycle (1, 2, 3, 4, 5, 8, 12 and 20 checks per grating cycle) were investigated.

Michelson contrast, expressed as sensitivity in dB varied with the number of checks per grating cycle ( $p < 0.0001$ ) and exhibited a minima of approximately 4 checks per grating cycle at the fovea, i.e., the maximum strength of the noise mask. The optimum noise mask at the two more peripheral stimulus locations was less clear; however, 4 checks per grating cycle resulted in the proportionally smallest SD for each of the two peripheral locations. Given that the stimulus size subtended  $4^\circ \times 4^\circ$  and contained 2 grating cycles, it was convenient to utilize the 4 checks per cycle noise mask for each stimulus location. This approach was commensurate with the maximum achievable dynamic range for the chosen stimulus parameters. In terms of Michelson contrast, the 4 checks per grating cycle resulted in the required 3 fold reduction in the Michelson contrast; however, the Michelson contrast in the presence of the noise mask, expressed as sensitivity in dB, increased within increase in eccentricity.

### **11.3 Further development of the ‘Proof of Concept’ DNP Algorithm**

It was essential to develop, further, the ‘Proof of concept’ algorithm in terms of an increase in the number of stimulus locations and a reduction in examination duration without loss of accuracy of the threshold estimates in the absence and in the presence of the noise mask. The algorithm was continually developed through a series of logical deductive iterations. The Final Algorithm comprised 45 locations. The examination duration was approximately 7 minutes in the absence of the noise mask and approximately 9 minutes in the presence of the noise mask. The accuracy of the Final Algorithm was comparable to that of the ‘Proof of Concept’ algorithm and was considered to be suitable for pilot studies of the utility of DNP in the investigation of ocular disease. An example of DNP in the absence and in the



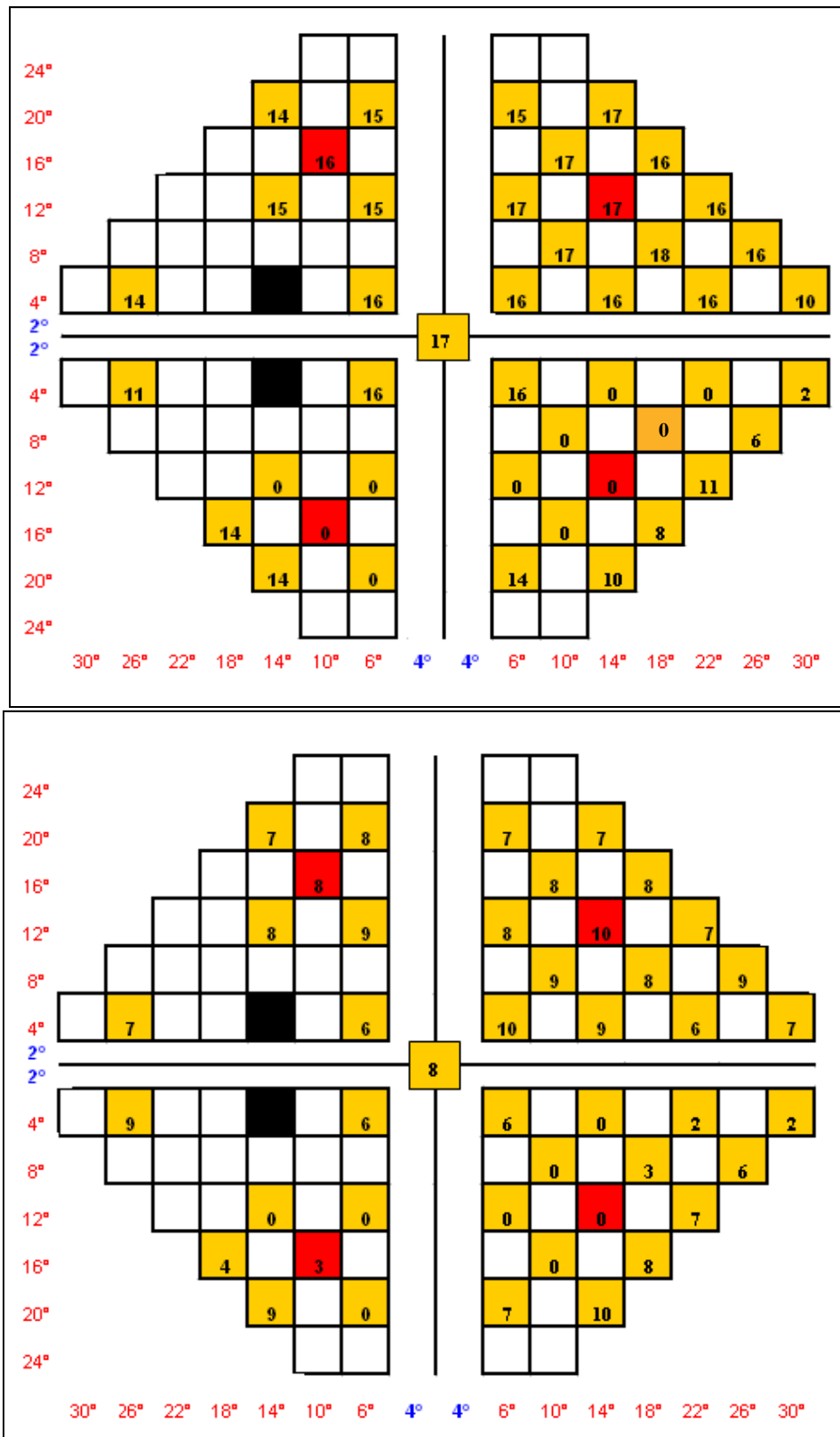


**Figure 11.1.b** The corresponding DNP outcome for the left eye of the 59 year old with open angle glaucoma (Figure 11.1.a) for the final 45 location algorithm in the absence of noise (top) and in the presence of the noise mask (bottom). The red coded stimulus locations indicate the 4 ‘seed’ points and the black coded locations indicate the blind spot. The Michelson contrast, expressed as sensitivity in dB, is given at each stimulus location.

The examination duration of the Final Algorithm for the individual with open angle glaucoma was approximately 20 minutes in the absence of the noise mask and 17 minutes in the presence of the noise mask. However, it was noted that the individual experienced long periods during which the stimulus was ‘not seen’.

#### **11.4 The influence of foveal optical defocus on the Dynamic Noise Perimetry**

The study determined the influence of foveal optical defocus (Plano, +1.00DS, +2.00DS and +4.00DS) on the outcomes of DNP in the absence and in the presence of the noise mask both in the absence and in the presence of the Gaussian filter (0.50FWHM).

The Michelson contrast, in the absence of the noise mask, expressed as sensitivity in dB decreased by approximately 1dB with increase in foveal defocus across the three stimulus locations, and, in the presence of the noise mask, increased by approximately 1dB with increase in defocus across the three locations ( $p < 0.0001$ ). The DNP outcome is, therefore, relatively robust to optical defocus up to +4.00DS. The utilization of the appropriate refractive correction is recommended for the DNP especially in the presence of the noise mask.

#### **11.5 Long-term follow-up of DNP in open angle glaucoma**

The study determined the follow-up visual field by standard automated perimetry and by DNP, at four stimulus locations, using the Proof of Concept algorithm in five of ten

individuals with open angle glaucoma who had undergone an identical protocol at a Baseline examination approximately 3 and a half years earlier (mean 3.6, SD 0.1).

The abnormality at Baseline in a given outcome measure by DNP at a given stimulus location remained abnormal at Follow-up, i.e., the apparent abnormality was repeatable after an interval of approximately three and half years. Additional locations which were normal at Baseline exhibited abnormality in one or more of the outcome measures at follow-up. The opposite was not the case. Abnormality identified by DNP at Baseline was subsequently confirmed as abnormal by standard automated perimetry at Follow-up in two individuals.

### **11.6 The Learning Effect in Dynamic Noise Perimetry**

The study determined the influence of the learning effect on the outcome of DNP in the absence and in the presence of the noise mask, in one designated eye, at each of the five weekly visits, for normal ‘young’ and ‘elderly’ individuals naïve to perimetry. A statistically significant improvement in Michelson contrast, expressed as sensitivity in dB, was present over the five visits ( $p < 0.0001$ ) in both young and elderly groups, in the absence of the noise mask and in the presence of the noise mask (2.1.dB, 1.8.dB and 2.2dB, 1.7dB, respectively); however, the majority of the improvement was between the first and second visits. The improvement in sensitivity was greater in the presence of the noise mask than in the absence of the noise mask ( $p < 0.0001$ ) and was greater for the peripheral annulus compared to the central annulus. The examination durations in the absence of the noise mask and in the presence of the noise mask declined over the five

visits in both the young and elderly groups, in the absence of the noise mask and in the presence of the noise mask, (42%, 38% and, 30%, 18 %, respectively).

### **11.7 Proposals for future work**

Clearly, further development of the algorithm is required, i.e., an extra 10 stimulus locations within 30° eccentricity and a reduction in examination duration to approximately 4 minutes. In addition, with the advent of the importance of the macular ganglion cell thickness/ number in open angle glaucoma, the development of a stimulus grid similar to that of program 10-2 is essential.

The first phase of the development of a new algorithm would be the incorporation of age-corrected start values not only at the seed locations but at all stimulus locations. The required data set would be acquired from a representative range of individuals. Following the response at any given stimulus location with the next iteration of the algorithm, the ‘start’ values at the remaining ‘non-thresholded’ locations would be updated. Such an approach is that used, for example, in the SITA algorithms. In addition, more novel approaches to the investigation of visual field loss could be implemented such as that based upon the concept of the GATE algorithm (Schiefer et al., 2009) and the variability-adjusted algorithm (Gardiner, 2014). The GATE algorithm is novel in that if the initial stimulus, which is presented at 4dB above the expected age-corrected value, is not seen, the subsequent stimulus is at maximum luminance. If the maximum luminance stimulus is not seen the staircase is terminated and if the stimulus is seen the staircase resumes at 4dB above the initial stimulus (Schiefer et al., 2009). The variability-adjusted algorithm is

novel in that the step size increases in direct relation to the variability at locations exhibiting sensitivity of less than 12 (Heijl et al., 1989) to 15dB (Gardiner, 2014).

A further reduction in the examination duration could occur from the introduction of a time window in which the observer either would be required to respond (including guessing) between one of a pair of consecutively presented stimuli. An initial response occurring outside the time window would be discounted and would increase the contrast level of the next presentation by 2dB. Consecutive responses outside the time window would terminate the staircase at the given location. However, the magnitude of the time window is likely to increase with increase in eccentricity, with increase in reaction time, with increase in age and from the absence to the presence of the noise mask and to decrease with increasing familiarity of DNP (i.e., as the learning effect declines).

It will be necessary, once the final algorithm is achieved, to determine the test-retest variability of the threshold estimate.

Eventually, it will also be necessary to acquire a substantial data base of age-corrected normal values for DNP, both in the absence and in the presence of the noise mask, in order to determine, statistically, the status of the outcome by DNP.

It would also be possible to produce a supra threshold algorithm for DNP in the absence and in the presence of the noise mask.

Degradation of the DNP stimulus is likely to occur from forward inter-ocular light scatter arising from age-related cataract. Given the co-existence of age-related cataract with open

angle glaucoma, a knowledge of the effect of cataract on the outcome of DNP is essential. It can be speculated that age-related cataract will have little effect on the 0.5 cycle per degree grating used in DNP given the findings from elsewhere (Elliott, Gilchrist and Whitaker, 1989; Fujikado et al., 2004; Shandiz et al., 2011). However, it can also be speculated that age-related cataract will attenuate the strength of the noise mask. Caution will, therefore, need to be exercised as to whether the noise mask in the presence of cataract will fulfil the criterion of a threefold reduction in Michelson contrast. It will be essential to undertake studies of this nature.

The outcome of DNP in the follow-up of individuals with open angle glaucoma is promising and emphasises the importance of a more extensive study of the impact of DNP in individuals with this condition. Such a study will also necessitate the acquisition of a representative database of age-corrected normal values. Given the length of time for the 45 location Final Algorithm to examine the individual with open angle glaucoma, described above, it will be necessary to modify this algorithm before such studies can be undertaken.

At some point, it would be useful to determine the utility of DNP in the identification of early age-related macular degeneration (AMD). It can be conjectured that if DNP identified wet AMD in advance of current functional and structural investigations, then the technique could be used as sensitive barometer of therapeutic intervention. Similarly, the technique could be applied for example, to multiple sclerosis.

The thesis has concentrated upon the dB outcome measure of DNP and it will be essential to evaluate the utility of each of the derivatives.

## References

Abbey C K, and Eckstein M P (2006) Classification images for detection, contrast discrimination, and identification tasks with a common ideal observer. *J Vis* 6: 335-355.

Acton J H, Gibson J M, and Cubbidge R P (2012) Quantification of visual field loss in age-related macular degeneration. *PLoS One* 7: e39944.

Agarwal R, Gupta S K, Agarwal P, Saxena R, and Agrawal S S (2009) Current concepts in the pathophysiology of glaucoma. *Indian J Ophthalmol* 57: 257-266.

Agudo-Barriuso M, Villegas-Perez M P, de Imperial J M, and Vidal-Sanz M (2013) Anatomical and functional damage in experimental glaucoma. *Curr Opin Pharmacol* 13: 5-11.

Alencar L M, and Medeiros F A (2011) The role of standard automated perimetry and newer functional methods for glaucoma diagnosis and follow-up. *Indian J Ophthalmol* 59 Suppl: S53-58.

Alward W L (2000) Frequency Doubling Technology perimetry for the detection of glaucomatous visual field loss. *Am J Ophthalmol* 129: 376-378.

American Academy of Ophthalmology (2014) Primary open-angle glaucoma. Available at: [http://eyewiki.aaopt.org/Primary\\_Open-Angle\\_Glaucoma](http://eyewiki.aaopt.org/Primary_Open-Angle_Glaucoma) [Accessed: 20-05-2014].

Anderson A J, and Johnson C A (2002) Mechanisms isolated by Frequency Doubling Technology perimetry. *Invest Ophthalmol Vis Sci* 43: 398-401.

Anderson A J, and Johnson C A (2003a) Frequency Doubling Technology perimetry. *Ophthalmol Clin North Am* 16: 213-225.

Anderson A J, and Johnson C A (2003b) Frequency Doubling Technology perimetry and optical defocus. *Invest Ophthalmol Vis Sci* 44: 4147-4152.

Anderson A J, and Johnson C A (2006) Comparison of the ASA, MOBS, and ZEST threshold methods. *Vision Res* 46: 2403-2411.

Anderson A J, Johnson C A, Fingeret M, Keltner J L, Spry P G, Wall M, and Werner J S (2005) Characteristics of the normative database for the Humphrey Matrix perimeter. *Invest Ophthalmol Vis Sci* 46: 1540-1548.

Anderson A J, Johnson C A, and Werner J S (2011) Measuring visual function in age-related macular degeneration with Frequency Doubling (Matrix) perimetry. *Optom Vis Sci* 88: 806-815.

Anderson A J, and McKendrick A M (2007) Quantifying adaptation and fatigue effects in Frequency Doubling perimetry. *Invest Ophthalmol Vis Sci* 48: 943-948.

Anderson A J, and Vingrys A J (2000) Effect of stimulus duration in flicker perimetry. *Clin Experiment Ophthalmol* 28: 223-226.

Anderson D R, and Patella V M (1999) *Automated static perimetry*. Second edition. Mosby, St. Louis, MI.

Anderson R S, McDowell D R, and Ennis F A (2001) Effect of localized defocus on detection thresholds for different sized targets in the fovea and periphery. *Acta Ophthalmol Scand* 79: 60-63.

Anderson R S, and O'Brien C (1997) Psychophysical evidence for a selective loss of M ganglion cells in glaucoma. *Vision Res* 37: 1079-1083.

Aoki Y, Takahashi G, and Kitahara K (2007) Comparison of Swedish Interactive Threshold Algorithm and Full Threshold algorithm for glaucomatous visual field loss. *Eur J Ophthalmol* 17: 196-202.

Artes P H, Hutchison D M, Nicolela M T, LeBlanc R P, and Chauhan B C (2005) Threshold and variability properties of Matrix Frequency Doubling Technology and standard automated perimetry in glaucoma. *Invest Ophthalmol Vis Sci* 46: 2451-2457.

Artes P H, Iwase A, Ohno Y, Kitazawa Y, and Chauhan B C (2002) Properties of perimetric threshold estimates from Full Threshold, SITA Standard, and SITA Fast strategies. *Invest Ophthalmol Vis Sci* 43: 2654-2659.

Artes P H, Nicolela M T, McCormick T A, LeBlanc R P, and Chauhan B C (2003) Effects of blur and repeated testing on sensitivity estimates with Frequency Doubling perimetry. *Invest Ophthalmol Vis Sci* 44: 646-652.

Atchison D A (1987) Effect of defocus on visual field measurement. *Ophthalmic Physiol Opt* 7: 259-265.

Atchison D A, Woods R L, and Bradley A (1998) Predicting the effects of optical defocus on human contrast sensitivity. *J Opt Soc Am A, Opt Image Sci Vis* 15: 2536-2544.

Barlow H B (1958) Temporal and spatial summation in human vision at different background intensities. *J Physiol* 141: 337-350.

Barton J J, Rizzo M, Nawrot M, and Simpson T (1996) Optical blur and the perception of global coherent motion in random dot cinematograms. *Vision Res* 36: 3051-3059.

Bayer A U, and Erb C (2002) Short-wavelength automated perimetry, Frequency Doubling Technology perimetry, and pattern electroretinography for prediction of progressive glaucomatous standard visual field defects. *Ophthalmology* 109: 1009-1017.

Bengtsson B, and Heijl A (1998) Evaluation of a new perimetric threshold strategy, SITA, in patients with manifest and suspect glaucoma. *Acta Ophthalmol Scand* 76: 268-272.

Bengtsson B, and Heijl A (2006) Diagnostic sensitivity of fast blue-yellow and standard automated perimetry in early glaucoma: a comparison between different test programs. *Ophthalmology* 113: 1092-1097.

Bengtsson B, Heijl A, and Olsson J (1998) Evaluation of a new threshold visual field strategy, SITA, in normal subjects. Swedish Interactive Thresholding Algorithm. *Acta Ophthalmol Scand* 76: 165-169.

Bengtsson B, Olsson J, Heijl A, and Rootzen H (1997) A new generation of algorithms for computerized threshold perimetry, SITA. *Acta Ophthalmol Scand* 75: 368-375.

Bergin C, Redmond T, Nathwani N, Verdon-Roe G M, Crabb D P, Anderson R S, and Garway-Heath D F (2011) The effect of induced intraocular straylight on perimetric tests. *Invest Ophthalmol Vis Sci* 52: 3676-3682.

Bernardi L, Costa V P, and Shiroma L O (2007) Flicker perimetry in healthy subjects: influence of age and gender, learning effect and short-term fluctuation. *Arq Bras Oftalmol* 70: 91-99.

Blakemore C, and Vital-Durand F (1986) Organization and post-natal development of the monkey's lateral geniculate nucleus. *J Physiol* 380: 453-491.

Blumenthal E Z, Sample P A, Berry C C, Lee A C, Girkin C A, Zangwill L, Caprioli J et al. (2003) Evaluating several sources of variability for standard and SWAP visual fields in glaucoma patients, suspects, and normals. *Ophthalmology* 110: 1895-1902.

Blumenthal E Z, Sample P A, Zangwill L, Lee A C, Kono Y, and Weinreb R N (2000a) Comparison of long-term variability for standard and short-wavelength automated perimetry in stable glaucoma patients. *Am J Ophthalmol* 129: 309-313.

Blumenthal E Z, Williams J M, Weinreb R N, Girkin C A, Berry C C, and Zangwill L M (2000b) Reproducibility of nerve fiber layer thickness measurements by use of optical coherence tomography. *Ophthalmology* 107: 2278-2282.

Bosworth C F, Sample P A, Gupta N, Bathija R, and Weinreb R N (1998) Motion automated perimetry identifies early glaucomatous field defects. *Arch Ophthalmol* 116: 1153-1158.

Bosworth C F, Sample P A, and Weinreb R N (1997) Perimetric motion thresholds are elevated in glaucoma suspects and glaucoma patients. *Vision Res* 37: 1989-1997.

Bourne R (2010) Image filters. *Fundamentals of digital imaging in medicine*. Springer London, pp. 137-172.

Bourne R R, Jahanbakhsh K, Boden C, Zangwill L M, Hoffmann E M, Medeiros F A, Weinreb R N et al. (2007) Reproducibility of visual field end point criteria for standard automated perimetry, Full Threshold, and Swedish Interactive Thresholding Algorithm strategies: Diagnostic Innovations in Glaucoma Study. *Am J Ophthalmol* 144: 908-913.

Brainard D H (1989) Calibration of a computer controlled color monitor. *Color Research and Application*. 14: 23-34.

Brusini P, and Busatto P (1998) Frequency Doubling perimetry in glaucoma early diagnosis. *Acta Ophthalmol Scand Suppl*: 23-24.

Brusini P, Salvetat M L, Parisi L, and Zeppieri M (2005) Probing glaucoma visual damage by Rarebit perimetry. *Br J Ophthalmol* 89: 180-184.

Brusini P, Salvetat M L, Zeppieri M, and Parisi L (2006) Frequency Doubling Technology perimetry with the Humphrey Matrix 30-2 test. *J Glaucoma* 15: 77-83.

Bullimore M A, Wood J M, and Swenson K (1993) Motion perception in glaucoma. *Invest Ophthalmol Vis Sci* 34: 3526-3533.

Burgansky-Eliash Z, Wollstein G, Patel A, Bilonick R A, Ishikawa H, Kagemann L, Dilworth W D et al. (2007) Glaucoma detection with Matrix and standard achromatic perimetry. *Br J Ophthalmol* 91: 933-938.

Calkins D J, and Horner P J (2012) The cell and molecular biology of glaucoma: axonopathy and the brain. *Invest Ophthalmol Vis Sci* 53: 2482-2484.

Casson E J, Johnson C A, and Nelson-Quigg J M (1993a) Temporal modulation perimetry: the effects of aging and eccentricity on sensitivity in normals. *Invest Ophthalmol Vis Sci* 34: 3096-3102.

Casson E J, Johnson C A, and Shapiro L R (1993b) Longitudinal comparison of temporal-modulation perimetry with white-on-white and blue-on-yellow perimetry in ocular hypertension and early glaucoma. *J Opt Soc Am, A Opt Image Sci Vis* 10: 1792-1806.

Castro D P, Kawase J, and Melo L A, Jr. (2008) Learning effect of standard automated perimetry in healthy individuals. *Arq Bras Oftalmol* 71: 523-528.

Celebisoy N, Ozturk T, and Kose T (2010) Rarebit perimetry in the evaluation of visual field defects in idiopathic intracranial hypertension. *Eur J Ophthalmol* 20: 756-762.

Cello K E, Nelson-Quigg J M, and Johnson C A (2000) Frequency Doubling Technology perimetry for detection of glaucomatous visual field loss. *Am J Ophthalmol* 129: 314-322.

Centofanti M, Fogagnolo P, Oddone F, Orzalesi N, Vetrugno M, Manni G, and Rossetti L (2008) Learning effect of Humphrey Matrix Frequency Doubling Technology perimetry in patients with ocular hypertension. *J Glaucoma* 17: 436-441.

Chauhan B C, House P H, McCormick T A, and LeBlanc R P (1999) Comparison of conventional and High-Pass Resolution perimetry in a prospective study of patients with glaucoma and healthy controls. *Arch Ophthalmol* 117: 24-33.

Chauhan B C, and Johnson C A (1999) Test-retest variability of Frequency Doubling perimetry and conventional perimetry in glaucoma patients and normal subjects. *Invest Ophthalmol Vis Sci* 40: 648-656.

Chauhan B C, LeBlanc R P, McCormick T A, and Rogers J B (1993a) Comparison of High- Pass Resolution perimetry and Pattern Discrimination perimetry to conventional perimetry in glaucoma. *Can J Ophthalmol* 28: 306-311.

Chauhan B C, Tompkins J D, LeBlanc R P, and McCormick T A (1993b) Characteristics of frequency-of-seeing curves in normal subjects, patients with suspected glaucoma, and patients with glaucoma. *Invest Ophthalmol Vis Sci* 34: 3534-3540.

Chin C F, Yip L W, Sim D C, and Yeo A C (2011) Rarebit perimetry: normative values and test-retest variability. *Clin Experiment Ophthalmol* 39: 752-759.

Chiselita D, Crenguta M I, Danielescu C, and Mihaela N M (2006) A comparative analysis of standard automated perimetry and short-wavelength automated perimetry in early diagnosis of glaucoma. *Oftalmologia* 50: 94-102.

Chylack L T, Jr., Wolfe J K, Singer D M, Leske M C, Bullimore M A, Bailey I L, Friend J et al. (1993) The Lens Opacities Classification System III. The Longitudinal Study of Cataract Study Group. *Arch Ophthalmol* 111: 831-836.

Colombo E, and Derrington A (2001) Visual calibration of CRT monitors. *Displays* 22: 87-95.

Contestabile M T, Perdicchi A, Amodeo S, Recupero V, and Recupero S M (2007) The influence of learning effect on Frequency Doubling Technology perimetry (Matrix). *J Glaucoma* 16: 297-301.

Cornsweet T N (1962) The staircase-method in psychophysics. *Am J Psychol* 75: 485-491.

Cubbidge R P, Hosking S L, and Embleton S (2002) Statistical modelling of the central 10-degree visual field in short-wavelength automated perimetry. *Graefes Arch Clin Exp Ophthalmol* 240: 650-657.

Dacey D M (1993) Morphology of a small-field bistratified ganglion cell type in the macaque and human retina. *Vis Neurosci* 10: 1081-1098.

Dacey D M, and Petersen M R (1992) Dendritic field size and morphology of midget and parasol ganglion cells of the human retina. *Proc Natl Acad Sci USA* 89: 9666-9670.

De Tarso Pierre-Filho P, Gomes P R, Pierre E T, and Pierre L M (2010) Learning effect of Humphrey Matrix Frequency Doubling Technology perimetry in patients with open-angle glaucoma. *Eur J Ophthalmol* 20: 538-541.

Delgado M F, Nguyen N A, Cox T A, Singh K, Lee D A, Dueker D k, Fechtner R D et al. (2002) Automated perimetry: a report by the American Academy of Ophthalmology. *Ophthalmology* 109: 2362-2374.

Drasdo N, Mortlock K E, and North R V (2008) Ganglion cell loss and dysfunction: relationship to perimetric sensitivity. *Optom Vis Sci* 85: 1036-1042.

Dul M W (2013) Optimizing contrast sensitivity perimetry for clinical use. *J Ophthalmic Vis Res* 8: 74-76.

Elliott D B, Gilchrist J, and Whitaker D (1989) Contrast sensitivity and glare sensitivity changes with three types of cataract morphology: are these techniques necessary in a clinical evaluation of cataract? *Ophthalmic Physiol Opt* 9: 25-30.

Falkenberg H K, and Bex P J (2007) Sources of motion sensitivity loss in glaucoma. *Invest Ophthalmol Vis Sci* 48: 2913-2921.

Falkenberg H K, Simpson W A, and Dutton G N (2014) Development of sampling efficiency and internal noise in motion detection and discrimination in school-aged children. *Vision Res* 100: 8-17.

Fankhauser F, and Bebie H (1978) Threshold fluctuations, interpolations and spatial resolution in perimetry. *Docum Ophthalmol Proc Ser* 19: 295-309.

Farkas R H, and Grosskreutz C L (2001) Apoptosis, neuroprotection, and retinal ganglion cell death: an overview. *Int Ophthalmol Clin* 41: 111-130.

Ferreras A, Polo V, Larrosa J M, Pablo L E, Pajarin A B, Pueyo V, and Honrubia F M (2007) Can Frequency Doubling Technology and short-wavelength automated perimetries detect visual field defects before standard automated perimetry in patients with preperimetric glaucoma? *J Glaucoma* 16: 372-383.

Flammer J (1994) The vascular concept of glaucoma. *Surv Ophthalmol* 38 Suppl: S3-6.

Flanagan J G, Moss I D, Wild J M, Hudson C, Prokopich L, Whitaker D, and O'Neill E C (1993) Evaluation of FASTPAC: a new strategy for threshold estimation with the Humphrey Field Analyser. *Graefes Arch Clin Exp Ophthalmol* 231: 465-469.

Fogagnolo P, Rossetti L, Ranno S, Ferreras A, and Orzalesi N (2008) Short-wavelength automated perimetry and Frequency Doubling Technology perimetry in glaucoma. *Prog Brain Res* 173: 101-124.

Fogagnolo P, Tanga L, Rossetti L, Oddone F, Manni G, Orzalesi N, and Centofanti M (2010) Mild learning effect of short-wavelength automated aerimetry using SITA Program. *J Glaucoma* 19: 319-323.

Frisen L (1987) High-Pass resolution targets in peripheral vision. *Ophthalmology* 94: 1104-1108.

Frisen L (1993) High-Pass Resolution perimetry. A clinical review. *Doc Ophthalmol* 83: 1-25.

Frisen L (2002) New, sensitive window on abnormal spatial vision: Rarebit probing. *Vision Res* 42: 1931-1939.

Frisen L, and Jensen C (2008) How robust is the optic chiasm? Perimetric and neuro-imaging correlations. *Acta Neurol Scand* 117: 198-204.

Fujikado T, Kuroda T, Maeda N, Ninomiya S, Goto H, Tano Y, Oshika T et al. (2004) Light scattering and optical aberrations as objective parameters to predict visual deterioration in eyes with cataracts. *J Cataract Refract Surg* 30: 1198-1208.

Fujimoto N, Minowa K, Miyauchi O, Hanawa T, and Adachi-Usami E (2002) Learning effect for Frequency Doubling perimetry in patients with glaucoma. *Am J Ophthalmol* 133: 269-270.

Gardiner S K (2014) Effect of a variability-adjusted algorithm on the efficiency of perimetric testing. *Invest Ophthalmol Vis Sci* 55: 2983-2992.

Gardiner S K, Demirel S, and Johnson C A (2008a) Is there evidence for continued learning over multiple years in perimetry? *Optom Vis Sci* 85: 1043 -1048.

Gardiner S K, Demirel S, Johnson C A, and Swanson W H (2011) Assessment of linear-scale indices for perimetry in terms of progression in early glaucoma. *Vision Res* 51: 1801-1810.

Gardiner S K, Swanson W H, Demirel S, McKendrick A M, Turpin A, and Johnson C A (2008b) A two-stage neural spiking model of visual contrast detection in perimetry. *Vision Res* 48: 1859-1869.

Garway-Heath D F, Caprioli J, Fitzke F W, and Hitchings R A (2000a) Scaling the hill of vision: the physiological relationship between light sensitivity and ganglion cell numbers. *Invest Ophthalmol Vis Sci* 41: 1774-1782.

Garway-Heath D F, Holder G E, Fitzke F W, and Hitchings R A (2002) Relationship between electrophysiological, psychophysical, and anatomical measurements in glaucoma. *Invest Ophthalmol Vis Sci* 43: 2213-2220.

Garway-Heath D F, Poinoosawmy D, Fitzke F W, and Hitchings R A (2000b) Mapping the visual field to the optic disc in normal tension glaucoma eyes. *Ophthalmology* 107: 1809-1815.

Gedik S, Akman A, and Akova Y A (2007) Efficiency of Rarebit perimetry in the evaluation of homonymous hemianopia in stroke patients. *Br J Ophthalmol* 91: 1065-1069.

Georgeson M A, May K A, Freeman T C, and Hesse G S (2007) From filters to features: scale-space analysis of edge and blur coding in human vision. *J Vis* 7: 1-21.

Glass E, Schaumberger M, and Lachenmayr B J (1995) Simulations for FASTPAC and the standard 4-2 dB Full Threshold strategy of the Humphrey Field Analyzer. *Invest Ophthalmol Vis Sci* 36: 1847-1854.

Glovinsky Y, Quigley H A, and Dunkelberger G R (1991) Retinal ganglion cell loss is size dependent in experimental glaucoma. *Invest Ophthalmol Vis Sci* 32: 484-491.

Glovinsky Y, Quigley H A, and Pease M E (1993) Foveal ganglion cell loss is size dependent in experimental glaucoma. *Invest Ophthalmol Vis Sci* 34: 395-400.

Goldstick B J, and Weinreb R N (1987) The effect of refractive error on automated global analysis Program G-1. *Am J Ophthalmol* 104: 229-232.

Gonzalez-Hernandez M, Garcia-Feijoo J, Mendez M S, and de la Rosa M G (2004) Combined spatial, contrast, and temporal functions perimetry in mild glaucoma and ocular hypertension. *Eur J Ophthalmol* 14: 514-522.

Gonzalez de la Rosa M, and Gonzalez-Hernandez M (2013) Pulsar perimetry. A review and new results. *Ophthalmologe* 110: 107-115.

Goren D, and Flanagan J G (2008) Is flicker-defined form (FDF) dependent on the contour? *J Vis* 8: 15 11-11.

Green D G, and Campbell F W (1965) Effect of focus on the visual response to a sinusoidally modulated spatial stimulus. *J Opt Soc Am* 55: 1154-1157.

Greve E L (1973) Single and multiple stimulus static perimetry in glaucoma; the two phases of perimetry. Thesis. *Doc Ophthalmol* 36: 1-355.

Gupta N, Ly T, Zhang Q, Kaufman P L, Weinreb R N, and Yucel Y H (2007) Chronic ocular hypertension induces dendrite pathology in the lateral geniculate nucleus of the brain. *Exp Eye Res* 84: 176-184.

Hackett D A, and Anderson A J (2011) Determining mechanisms of visual loss in glaucoma using Rarebit perimetry. *Optom Vis Sci* 88: 48-55.

Hankins M W, Peirson S N, and Foster R G (2008) Melanopsin: an exciting photopigment. *Trends Neurosci* 31: 27-36.

Hart W M J R, Silverman S E, Trick G L, Nesher R, and Gordon M O (1990) Glaucomatous visual field damage. Luminance and color-contrast sensitivities. *Invest Ophthalmol Vis Sci* 31: 359-367.

Harwerth R S, and Quigley H A (2006) Visual field defects and retinal ganglion cell losses in patients with glaucoma. *Arch Ophthalmol* 124: 853-859.

Harwerth R S, Vilupuru A S, Rangaswamy N V, and Smith E L (2007) The relationship between nerve fiber layer and perimetry measurements. *Invest Ophthalmol Vis Sci* 48: 763-773.

Harwerth R S, Wheat J L, Fredette M J, and Anderson D R (2010) Linking structure and function in glaucoma. *Prog Retin Eye Res* 29: 249-271.

Hayes R D, and Merigan W H (2007) Mechanisms of sensitivity loss due to visual cortex lesions in humans and macaques. *Cereb Cortex* 17: 1117-1128.

Heeg G P, Ponsioen T L, and Jansonius N M (2003) Learning effect, normal range, and test-retest variability of Frequency Doubling perimetry as a function of age, perimetric experience, and the presence or absence of glaucoma. *Ophthalmic Physiol Opt* 23: 535-540.

Heijl A (1989) Visual field changes in early glaucoma and how to recognize them. *Surv Ophthalmol* 33: 403-404.

Heijl A, Lindgren G and Olsson J (1989) Test-retest variability in glaucomatous visual fields. *Invest Ophthalmol Vis Sci* 108:130-135.

Heijl A, and Bengtsson B (1996) The effect of perimetric experience in patients with glaucoma. *Arch Ophthalmol* 114: 19-22.

Heijl A, and Greve E L (1985) The Humphrey Field Analyzer, Construction and Concepts. In Heijl A, and Greve E L (Eds) Proceedings of the Sixth International Visual Field Symposium. *Docum Ophthalmol Proc Ser* 42: 77-84.

Heijl A, Lindgren A, and Lindgren G (1989a) Test-retest variability in glaucomatous visual fields. *Am J Ophthalmol* 108: 130-135.

Heijl A, Lindgren G, and Olsson J (1989b) The effect of perimetric experience in normal subjects. *Arch Ophthalmol* 107: 81-86.

Heijl A, Lindgren G, Olsson J, and Asman P (1989c) Visual field interpretation with empiric probability maps. *Arch Ophthalmol* 107: 204-208.

Herse P R (1992) Factors influencing normal perimetric thresholds obtained using the Humphrey Field Analyzer. *Invest Ophthalmol Vis Sci* 33: 611-617.

Hesse G S, and Georgeson M A (2005) Edges and bars: where do people see features in 1-D images? *Vision Res* 45: 507-525.

Heuer D K, Anderson D R, Feuer W J, and Gressel M G (1987) The influence of refraction accuracy on automated perimetric threshold measurements. *Ophthalmology* 94: 1550-1553.

Hogg R E, and Anderson A J (2009) Appearance of the Frequency Doubling stimulus at threshold. *Invest Ophthalmol Vis Sci* 50: 1477-1482.

Hood D C, and Kardon R H (2007) A framework for comparing structural and functional measures of glaucomatous damage. *Prog Retin Eye Res* 26: 688-710.

Horani A, Frenkel S, Yahalom C, Farber M D, Ticho U, and Blumenthal E Z (2002) The learning effect in visual field testing of healthy subjects using Frequency Doubling Technology. *J Glaucoma* 11: 511-516.

Horn F K, Link B, Mardin C Y, Junemann A G, and Martus P (2007) Long-term reproducibility of screening for glaucoma with FDT perimetry. *J Glaucoma* 16: 448-455.

Horner D G, Dul M W, Swanson W H, Liu T, and Tran I (2013) Blur-resistant perimetric stimuli. *Optom Vis Sci* 90: 466-474.

Hot A, Dul M W, and Swanson W H (2008) Development and evaluation of a contrast sensitivity perimetry test for patients with glaucoma. *Invest Ophthalmol Vis Sci* 49: 3049-3057.

Hutchings N, Hosking S L, Wild J M, and Flanagan J G (2001) Long-term fluctuation in short-wavelength automated perimetry in glaucoma suspects and glaucoma patients. *Invest Ophthalmol Vis Sci* 42: 2332-2337.

Hylkema B S (1942) Examination of the visual field by determining the fusion frequency *Acta Ophthalmol* 20: 181-193.

Iester M, Capris P, Pandolfo A, Zingirian M, and Traverso C E (2000) Learning effect, short-term fluctuation, and long-term fluctuation in Frequency Doubling Technique. *Am J Ophthalmol* 130: 160-164.

Jampel H D, Singh K, Lin S C, Chen T C, Francis B A, Hodapp E, Samples J R et al. (2011) Assessment of visual function in glaucoma: a report by the American Academy of Ophthalmology. *Ophthalmology* 118: 986-1002.

Johnson C A (1994) Selective versus non-selective losses in glaucoma. *J Glaucoma* 3: 532-544.

Johnson C A (1995) Early losses of visual function in glaucoma. *Optom Vis Sci* 72: 359-370.

Johnson C A (2008) FDT perimetry for the detection of glaucomatous visual field loss. The effectiveness of the FDT and Humphrey Matrix Perimeters. *Glaucoma Today* 6: 26-28.

Johnson C A, Adams A J, Casson E J, and Brandt J D (1993a) Blue-on-yellow perimetry can predict the development of glaucomatous visual field loss. *Arch Ophthalmol* 111: 645-650.

Johnson C A, Adams A J, Casson E J, and Brandt J D (1993b) Progression of early glaucomatous visual field loss as detected by blue-on-yellow and standard white-on-white automated perimetry. *Arch Ophthalmol* 111: 651-656.

Johnson C A, Cioffi G A, and Van Buskirk E M (1999) Frequency Doubling Technology perimetry using a 24-2 stimulus presentation pattern. *Optom Vis Sci* 76: 571-581.

Johnson C A, and Marshall D, Jr. (1995) Aging effects for opponent mechanisms in the central visual field. *Optom Vis Sci* 72: 75-82.

Johnson C A, and Samuels S J (1997) Screening for glaucomatous visual field loss with Frequency Doubling perimetry. *Invest Ophthalmol Vis Sci* 38: 413-425.

Joson P J, Kamantigue M E, and Chen P P (2002) Learning effects among perimetric novices in Frequency Doubling Technology perimetry. *Ophthalmology* 109: 757-760.

Kelly D H (1966) Frequency Doubling in visual responses. *J Opt Soc Am* 56: 1628-1633.

Kelly D H (1981) Nonlinear visual responses to flickering sinusoidal gratings. *J Opt Soc Am* 71: 1051-1055.

Kerrigan-Baumrind L A, Quigley H A, Pease M E, Kerrigan D F, and Mitchell R S (2000) Number of ganglion cells in glaucoma eyes compared with threshold visual field tests in the same persons. *Invest Ophthalmol Vis Sci* 41: 741-748.

Kersten D, Hess R, and Plant G (1988) Assessing contrast sensitivity behind cloudy media. *Clinical Vision Sciences* 2: 143-158.

Kim Y Y, Kim J S, Shin D H, Kim C, and Jung H R (2001) Effect of cataract extraction on blue-on-yellow visual field. *Am J Ophthalmol* 132: 217-220.

Kuehn M H, Fingert J H, and Kwon Y H (2005) Retinal ganglion cell death in glaucoma: mechanisms and neuroprotective strategies. *Ophthalmol Clin North Am* 18: 383-395.

Kukkonen H, Rovamo J, Donner K, Tammikallio M, and Raninen A (2002) Noise frame duration, masking potency and whiteness of temporal noise. *Invest Ophthalmol Vis Sci* 43: 3131-3135.

Kukkonen H, Rovamo J, and Nasanen R (1995) Masking potency and whiteness of noise at various noise check sizes. *Invest Ophthalmol Vis Sci* 36: 513-518.

Kukkonen H, Rovamo J, Tiippana K, and Nasanen R (1993) Michelson contrast, RMS contrast and energy of various spatial stimuli at threshold. *Vision Res* 33: 1431-1436.

Kukkonen H T (1994) Effects of pixel noise and stimulus structure on visual detection performance. PhD, Aston University.

Kulze J C, Stewart W C, and Sutherland S E (1990) Factors associated with a learning effect in glaucoma patients using automated perimetry. *Acta Ophthalmol (Copenh)* 68: 681-686.

Kwon Y H, Park H J, Jap A, Ugurlu S, and Caprioli J (1998) Test-retest variability of blue-on-yellow perimetry is greater than white-on-white perimetry in normal subjects. *Am J Ophthalmol* 126: 29-36.

Lachenmayr B, Gleissner M, and Rothbacher H (1989) Automated flicker perimetry. *Fortschr Ophthalmol* 86: 695-701.

Lachenmayr B J, and Gleissner M (1992) Flicker perimetry resists retinal image degradation. *Invest Ophthalmol Vis Sci* 33: 3539-3542.

Lachenmayr B J, Kojetinsky S, Ostermaier N, Angstwurm K, Vivell P M, and Schaumberger M (1994) The different effects of aging on normal sensitivity in flicker and light-sense perimetry. *Invest Ophthalmol Vis Sci* 35: 2741-2748.

Lamarter J, Aliyeva S, Schulze A, Berres M, Pfeiffer N, and Hoffmann E M (2013) Standard automated perimetry versus Matrix Frequency Doubling Technology perimetry in subjects with ocular hypertension and healthy control subjects. *PLoS One* 8: e57663.

Lamarter J, Russell R A, Schulze A, Schuff A C, Pfeiffer N, and Hoffmann E M (2012) Structure-function relationship between FDF, FDT, SAP, and scanning laser ophthalmoscopy in glaucoma patients. *Invest Ophthalmol Vis Sci* 53: 7553-7559.

Lamarter J, Schulze A, Schuff A C, Berres M, Pfeiffer N, and Hoffmann E M (2011) Learning curve and fatigue effect of Flicker Defined Form perimetry. *Am J Ophthalmol* 151: 1057-1064 e1051.

Leeprechanon N, Giacconi J A, Manassakorn A, Hoffman D, and Caprioli J (2007a) Frequency Doubling perimetry and short-wavelength automated perimetry to detect early glaucoma. *Ophthalmology* 114: 931-937.

Leeprechanon N, Giangiacomo A, Fontana H, Hoffman D, and Caprioli J (2007b) Frequency-Doubling perimetry: comparison with standard automated perimetry to detect glaucoma. *Am J Ophthalmol* 143: 263-271.

Legge G E, Kersten D, and Burgess A E (1987) Contrast discrimination in noise. *J Opt Soc Am A* 4: 391-404.

Liu M, Duggan J, Salt T E, and Cordeiro M F (2011a) Dendritic changes in visual pathways in glaucoma and other neurodegenerative conditions. *Exp Eye Res* 92: 244-250.

Liu S, Lam S, Weinreb R N, Ye C, Cheung C Y, Lai G, Lam D S et al. (2011b) Comparison of standard automated perimetry, Frequency-Doubling Technology perimetry,

and short-wavelength automated perimetry for detection of glaucoma. *Invest Ophthalmol Vis Sci* 52: 7325-7331.

Maddess T, Goldberg I, Dobinson J, Wine S, Welsh A H, and James A C (1999) Testing for glaucoma with the spatial frequency doubling illusion. *Vision Res* 39: 4258-4273.

Maddess T, and Henry G H (1992) Performance of nonlinear visual units in ocular hypertension and glaucoma. *Clin Vis Sci* 7: 371-383.

Malik R, Swanson W H, and Garway-Heath D F (2012) Structure-function relationship in glaucoma: past thinking and current concepts. *Clin Experiment Ophthalmol* 40: 369-380.

Martin L, and Wanger P (2004) New perimetric techniques: a comparison between Rarebit and Frequency Doubling Technology perimetry in normal subjects and glaucoma patients. *J Glaucoma* 13: 268-272.

Martin P R, White A J, Goodchild A K, Wilder H D, and Sefton A E (1997) Evidence that blue-on cells are part of the third geniculocortical pathway in primates. *Eur J Neurosci* 9: 1536-1541.

Martinez G A, Sample P A, and Weinreb R N (1995) Comparison of High-Pass resolution perimetry and standard automated perimetry in glaucoma. *Am J Ophthalmol* 119: 195-201.

Matsumoto C, Okuyama S, Iwagaki A, Otsuki T, Uyama K, and Otori T (1997) The influence of target blur on perimetric threshold values in automated light-sensitive perimetry and flicker perimetry. In: Wall M, and Heijl A [eds.] *Perimetry Update 1996/1997*. Amsterdam, The Netherlands: Kugler Publications, pp. 191-200.

Matsumoto C, Takada S, Okuyama S, Arimura E, Hashimoto S, and Shimomura Y (2006) Automated flicker perimetry in glaucoma using Octopus 311: a comparative study with the Humphrey Matrix. *Acta Ophthalmol Scand* 84: 210-215.

Matsuo H, Tomita G, Suzuki Y, and Araie M (2002) Learning effect and measurement variability in Frequency-Doubling Technology perimetry in chronic open-angle glaucoma. *J Glaucoma* 11: 467-473.

McAnany J J, and Alexander K R (2009) Contrast thresholds in additive luminance noise: Effect of noise temporal characteristics. *Vision Res* 49: 1389-1396.

McKendrick A M (2005) Recent developments in perimetry: test stimuli and procedures. *Clin Exp Optom* 88: 73-80.

Medeiros F A, Zangwill L M, Bowd C, Mansouri K, and Weinreb R N (2012) The structure and function relationship in glaucoma: implications for detection of progression and measurement of rates of change. *Invest Ophthalmol Vis Sci* 53: 6939-6946.

Miles P W (1950) Flicker fusion fields; III. Findings in early glaucoma. *Arch Ophthalmol* 43: 661-677.

Morgan J E (2002) Retinal ganglion cell shrinkage in glaucoma. *J Glaucoma* 11: 365-370.

Morgan J E, Uchida H, and Caprioli J (2000) Retinal ganglion cell death in experimental glaucoma. *Br J Ophthalmol* 84: 303-310.

Moss I D, Wild J M, and Whitaker D J (1995) The influence of age-related cataract on blue-on-yellow perimetry. *Invest Ophthalmol Vis Sci* 36: 764-773.

Mozaffarieh M, and Flammer J (2013) New insights in the pathogenesis and treatment of normal tension glaucoma. *Curr Opin Pharmacol* 13: 43-49.

Nevalainen J, Paetzold J, Krapp E, Vonthein R, Johnson C A, and Schiefer U (2008) The use of semi-automated kinetic perimetry (SKP) to monitor advanced glaucomatous visual field loss. *Graefes Arch Clin Exp Ophthalmol* 246: 1331-1339.

Ng M, Racette L, Pascual J P, Liebmann J M, Girkin C A, Lovell S L, Zangwill L M et al. (2009) Comparing the Full-Threshold and Swedish Interactive Thresholding Algorithms for short-wavelength automated perimetry. *Invest Ophthalmol Vis Sci* 50: 1726-1733.

Nilsson M, Abdiu O, Laurell C G, and Martin L (2010) Rarebit perimetry and fovea test before and after cataract surgery. *Acta Ophthalmol* 88: 479-482.

Nordmann J P, Brion F, Hamard P, and Mouton-Chopin D (1998) Evaluation of the Humphrey perimetry programs SITA Standard and SITA Fast in normal probands and patients with glaucoma. *J Fr Ophtalmol* 21: 549-554.

Nowomiejska K, Paetzold J, Zagorski Z, and Schiefer U (2004) Recent developments in kinetic perimetry. *Klin Oczna* 106: 798-801.

Nowomiejska K, Vonthein R, Paetzold J, Zagorski Z, Kardon R, and Schiefer U (2005) Comparison between semi-automated kinetic perimetry and conventional Goldmann manual kinetic perimetry in advanced visual field loss. *Ophthalmology* 112: 1343-1354.

- Nucci C, Martucci A, Cesareo M, Mancino R, Russo R, Bagetta G, Cerulli L et al. (2013) Brain involvement in glaucoma: advanced neuroimaging for understanding and monitoring a new target for therapy. *Curr Opin Pharmacol* 13: 128-133.
- Nurminen L, Kilpelainen M, and Vanni S (2013) Fovea-periphery axis symmetry of surround modulation in the human visual system. *PLoS One* 8: e57906.
- O'Brien C, Poinoosawmy D, Wu J, and Hitchings R (1994) Evaluation of the Humphrey FASTPAC threshold program in glaucoma. *Br J Ophthalmol* 78: 516-519.
- Olds E S, Cowan W B, and Jolicoeur P (1999) Effective color CRT calibration techniques for perception research. *J Opt Soc Am A Opt Image Sci Vis* 16: 1501-1505.
- Oleszczuk J D, Bergin C, and Sharkawi E (2012) Comparative resilience of clinical perimetric tests to induced levels of intraocular straylight. *Invest Ophthalmol Vis Sci* 53: 1219-1224.
- Olsson J, Asman P, and Heijl A (1997) A perimetric learner's index. *Acta Ophthalmol Scand* 75: 665-668.
- Olsson J, Heijl A, Bengtsson B, and Rootzen H (1993) Frequency-of-seeing in computerized perimetry. In: Mills R P [ed.] *Perimetry Update 1992/1993*. Proceedings of the Xth International Perimetric Society meeting, Kyoto, Japan. Kugler Publications, Amsterdam/ New York 1993: 551-556.
- Osborne N N (2010) Mitochondria: their role in ganglion cell death and survival in primary open angle glaucoma. *Exp Eye Res* 90: 750-757.
- Pardhan S (2004) Contrast sensitivity loss with aging: sampling efficiency and equivalent noise at different spatial frequencies. *J Opt Soc Am, A Opt Image Sci Vis* 21: 169-175.
- Pardhan S, Gilchrist J, Elliott D B, and Beh G K (1996) A comparison of sampling efficiency and internal noise level in young and old subjects. *Vision Res* 36: 1641-1648.
- Pelli D G (1990) The Quantum Efficiency of Vision. In: Blakemore, C [ed.]. *Vision: Coding and Efficiency*. Cambridge: Cambridge University Press.
- Pelli D G, and Farell B (1999) Why use noise? *J Opt Soc Am, A Opt Image Sci Vis* 16: 647-653.

Phipps J A, Zele A J, Dang T, and Vingrys A J (2001) Fast psychophysical procedures for clinical testing. *Clin Exp Optom* 84: 264-269.

Pierre-Filho Pde T, Gomes P R, Pierre E T, and Pierre L M (2010) Learning effect in visual field testing of healthy subjects using Humphrey Matrix Frequency Doubling Technology perimetry. *Eye (Lond)* 24: 851-856.

Quaid P T, and Flanagan J G (2005a) Defining the limits of Flicker Defined Form: effect of stimulus size, eccentricity and number of random dots. *Vision Res* 45: 1075-1084.

Quaid P T, and Flanagan J G (2005b) The effect of dioptric blur on Flicker Defined Form phase contrast thresholds. *Invest Ophthalmol Vis Sci* 46: ARVO meeting Abstract 5660

Quaid P T, Simpson T, and Flanagan J G (2004) Monocular and dichoptic masking effects on the Frequency Doubling illusion. *Vision Res* 44: 661-667.

Quigley H A (1998) Identification of glaucoma-related visual field abnormality with the screening protocol of Frequency Doubling Technology. *Am J Ophthalmol* 125: 819-829.

Quigley H A (2011) Glaucoma. *Lancet* 377: 1367-1377.

Quigley H A, and Broman A T (2006) The number of people with glaucoma worldwide in 2010 and 2020. *Br J Ophthalmol* 90: 262-267.

Quigley H A, Dunkelberger G R, and Green W R (1988) Chronic human glaucoma causing selectively greater loss of large optic nerve fibers. *Ophthalmology* 95: 357-363.

Quigley H A, Sanchez R M, Dunkelberger G R, L'Hernault N L, and Baginski T A (1987) Chronic glaucoma selectively damages large optic nerve fibers. *Invest Ophthalmol Vis Sci* 28: 913-920.

Racette L, and Sample P A (2003) Short-wavelength automated perimetry. *Ophthalmol Clin North Am* 16: 227-236.

Raninen A, and Rovamo J (1986) Perimetry of Critical Flicker Frequency in human rod and cone vision. *Vision Res* 26: 1249-1255.

Rao H L, Jonnadula G B, Addepalli U K, Senthil S, and Garudadri C S (2013) Effect of cataract extraction on Visual Field Index in glaucoma. *J Glaucoma* 22: 164-168.

Rattan R (2010) The development of Dynamic Noise Perimetry. PhD Thesis, Cardiff University.

Reed H, and Drance S M (1972) *The Essentials of Perimetry, Static and Kinetic*. Second ed. Oxford, United Kingdom: Oxford University Press: Ulster Med J.

Robinson D A (1963) A method of measuring eye movement using a scleral search coil in a magnetic field. *IEEE Trans Biomed Eng* 10: 137-145.

Rodieck R W, Binmoeller K F, and Dineen J (1985) Parasol and midget ganglion cells of the human retina. *J Comp Neurol* 233: 115-132.

Rogers-Ramachandran D C, and Ramachandran V S (1998) Psychophysical evidence for boundary and surface systems in human vision. *Vision Res* 38: 71-77.

Roggen X, Herman K, Van Malderen L, Devos M, and Spileers W (2001) Different strategies for Humphrey automated perimetry: FASTPAC, SITA Standard and SITA Fast in normal subjects and glaucoma patients. *Bull Soc Belge Ophthalmol*: 23-33.

Rossetti L, Fogagnolo P, Miglior S, Centofanti M, Vetrugno M, and Orzalesi N (2006) Learning effect of short-wavelength automated perimetry in patients with ocular hypertension. *J Glaucoma* 15: 399-404.

Rovamo J, and Kukkonen H (1996) The effect of noise check size and shape on grating detectability. *Vision Res* 36: 271-279.

Rovamo J, Kukkonen H, Tiippa K, and Nasanen R (1993a) Effects of luminance and exposure time on contrast sensitivity in spatial noise. *Vision Res* 33: 1123-1129.

Rovamo J, Luntinen O, and Nasanen R (1993b) Modelling the dependence of contrast sensitivity on grating area and spatial frequency. *Vision Res* 33: 2773-2788.

Russell R A, Crabb D P, Malik R, and Garway-Heath D F (2012) The relationship between variability and sensitivity in large-scale longitudinal visual field data. *Invest Ophthalmol Vis Sci* 53: 5985-5990.

Salvetat M L, Zeppieri M, Parisi L, and Brusini P (2007) Rarebit perimetry in normal subjects: test-retest variability, learning effect, normative range, influence of optical defocus, and cataract extraction. *Invest Ophthalmol Vis Sci* 48: 5320-5331.

Salvetat M L, Zeppieri M, Parisi L, Johnson C A, Sampaolesi R, and Brusini P (2013) Learning effect and test-retest variability of Pulsar perimetry. *J Glaucoma* 22: 230-237.

Sample P A, Bosworth C F, Blumenthal E Z, Girkin C, and Weinreb R N (2000) Visual function-specific perimetry for indirect comparison of different ganglion cell populations in glaucoma. *Invest Ophthalmol Vis Sci* 41: 1783-1790.

Sample P A, Medeiros F A, Racette L, Pascual J P, Boden C, Zangwill L M, Bowd C et al. (2006) Identifying glaucomatous vision loss with visual-function-specific perimetry in the Diagnostic Innovations in Glaucoma Study. *Invest Ophthalmol Vis Sci* 47: 3381-3389.

Sample P A, Taylor J D, Martinez G A, Lusky M, and Weinreb R N (1993) Short-wavelength color visual fields in glaucoma suspects at risk. *Am J Ophthalmol* 115: 225-233.

Sample P A, and Weinreb R N (1990) Color perimetry for assessment of primary open-angle glaucoma. *Invest Ophthalmol Vis Sci* 31: 1869-1875.

San Laureano J (2007) When is glaucoma really glaucoma? *Clin Exp Optom* 90: 376-385.

Saunders R M (1975) The critical duration of temporal summation in the human central fovea. *Vision Res* 15: 699-703.

Schiefer U, Pascual J P, Edmunds B, Feudner E, Hoffmann E M, Johnson C A, Lagreze W A et al. (2009) Comparison of the new perimetric GATE strategy with conventional Full-Threshold and SITA Standard strategies. *Invest Ophthalmol Vis Sci* 50: 488-494.

Schiefer U, Patzold J, and Dannheim F (2005) Conventional perimetry I: Introduction-basics. *Ophthalmologe* 102: 627-644; quiz 645-626.

Schmidt T (1955) Visual field examination with Goldmann perimeter. *Klin Monbl Augenheilkd Augenarztl Fortbild* 126: 209-217.

Searle A E, Wild J M, Shaw D E, and O'Neill E C (1991) Time-related variation in normal automated static perimetry. *Ophthalmology* 98: 701-707.

Sekhar G C, Naduvilath T J, Lakkai M, Jayakumar A J, Pandi G T, Mandal A K, and Honavar S G (2000) Sensitivity of Swedish Interactive Threshold Algorithm compared with standard Full Threshold algorithm in Humphrey visual field testing. *Ophthalmology* 107: 1303-1308.

Shafi A, Swanson W H, and Dul M W (2011) Structure and function in patients with glaucomatous defects near fixation. *Optom Vis Sci* 88: 130-139.

Shandiz J H, Derakhshan A, Daneshyar A, Azimi A, Moghaddam H O, Yekta A A, Yazdi S H et al. (2011) Effect of cataract type and severity on visual acuity and contrast sensitivity. *J Ophthalmic Vis Res* 6: 26-31.

Siddiqui M A, Azuara-Blanco A, and Neville S (2005) Effect of cataract extraction on Frequency Doubling Technology perimetry in patients with glaucoma. *Br J Ophthalmol* 89: 1569-1571.

Silverman S E, Trick G L, and Hart W M, Jr. (1990) Motion perception is abnormal in primary open-angle glaucoma and ocular hypertension. *Invest Ophthalmol Vis Sci* 31: 722-729.

Soliman M A, de Jong L A, Ismaeil A A, van den Berg T J, and de Smet M D (2002) Standard achromatic perimetry, short-wavelength automated perimetry, and Frequency Doubling Technology for detection of glaucoma damage. *Ophthalmology* 109: 444-454.

Spry P G, Johnson C A, Mansberger S L, and Cioffi G A (2005) Psychophysical investigation of ganglion cell loss in early glaucoma. *J Glaucoma* 14: 11-19.

Strang N C, Atchison D A, and Woods R L (1999) Effects of defocus and pupil size on human contrast sensitivity. *Ophthalmic Physiol Opt* 19: 415-426.

Sun H, Swanson W H, Arvidson B, and Dul M W (2008) Assessment of contrast gain signature in inferred magnocellular and parvocellular pathways in patients with glaucoma. *Vision Res* 48: 2633-2641.

Swanson W H, Pan F, and Lee B B (2008) Chromatic temporal integration and retinal eccentricity: psychophysics, neurometric analysis and cortical pooling. *Vision Res* 48: 2657-2662.

Swanson W H, Sun H, Lee B B, and Cao D (2011) Responses of primate retinal ganglion cells to perimetric stimuli. *Invest Ophthalmol Vis Sci* 52: 764-771.

Taberner J, Ohlendorf A, Fischer M D, Bruckmann A R, Schiefer U, and Schaeffel F (2011) Peripheral refraction profiles in subjects with low foveal refractive errors. *Optom Vis Sci* 88: 388-394.

Tafreshi A, Sample P A, Liebmann J M, Girkin C A, Zangwill L M, Weinreb R N, Lalezary M et al. (2009) Visual function-specific perimetry to identify glaucomatous visual

loss using three different definitions of visual field abnormality. *Invest Ophthalmol Vis Sci* 50: 1234-1240.

Taylor M M, and Douglas Creelman C (1967) PEST: Efficient estimates on probability functions. *J Acoust Soc Am* 41: 782-787.

Tezel G (2013) Immune regulation toward immunomodulation for neuroprotection in glaucoma. *Curr Opin Pharmacol* 13: 23-31.

Tonagel F, Voykov B, and Schiefer U (2012) Conventional perimetry. Antiquated or indispensable for functional glaucoma diagnostics? *Ophthalmologe* 109: 325-336.

Treutwein B (1995) Adaptive psychophysical procedures. *Vision Res* 35: 2503-2522.

Trick G L, Steinman S B, and Amyot M (1995) Motion perception deficits in glaucomatous optic neuropathy. *Vision Res* 35: 2225-2233.

Turpin A, McKendrick A M, Johnson C A, and Vingrys A J (2003) Properties of perimetric threshold estimates from Full Threshold, ZEST, and SITA-like strategies, as determined by computer simulation. *Invest Ophthalmol Vis Sci* 44: 4787-4795.

Tyler C W (1981) Specific deficits of flicker sensitivity in glaucoma and ocular hypertension. *Invest Ophthalmol Vis Sci* 20: 204-212.

Tyrrell R A, and Owens D A (1988) A rapid technique to assess the resting states of eyes and other threshold phenomena: The modified binary search (MOBS). *Behav Res Meth Instrum Comput* 20: 137-141.

van der Schoot J, Reus N J, Colen T P, and Lemij H G (2010) The ability of short-wavelength automated perimetry to predict conversion to glaucoma. *Ophthalmology* 117: 30-34.

Verdon-Roe G M, Westcott M C, Viswanathan A C, Fitzke F W, and Garway-Heath D F (2006) Exploration of the psychophysics of a motion displacement hyperacuity stimulus. *Invest Ophthalmol Vis Sci* 47: 4847-4855.

Vidal-Fernandez A, Garcia Feijoo J, Gonzalez-Hernandez M, Gonzalez De La Rosa M, and Garcia Sanchez J (2002) Initial findings with Pulsar perimetry in patients with ocular hypertension. *Arch Soc Esp Oftalmol* 77: 321-326.

Vislisel J M, Doyle C K, Johnson C A, and Wall M (2011) Variability of Rarebit and standard perimetry sizes I and III in normals. *Optom Vis Sci* 88: 635-639.

Vohra R, Tsai J C, and Kolko M (2013) The role of inflammation in the pathogenesis of glaucoma. *Surv Ophthalmol* 58: 311-320.

Vonthein R, Rauscher S, Paetzold J, Nowomiejska K, Krapp E, Hermann A, Sadowski B et al. (2007) The normal age-corrected and reaction time-corrected isopter derived by semi-automated kinetic perimetry. *Ophthalmology* 114: 1065-1072.

Wall M (1991) High-Pass resolution perimetry in optic neuritis. *Invest Ophthalmol Vis Sci* 32: 2525-2529.

Wall M (2012) Motion detection perimetry [Online]. Available at:

<http://www.perimetry.org/PerimetryHistory/Motion/index.htm> [Accessed: 10-03-2014].

Wall M, Brito C F, Woodward K R, Doyle C K, Kardon R H, and Johnson C A (2008) Total Deviation probability plots for stimulus size V perimetry: a comparison with size III stimuli. *Arch Ophthalmol* 126: 473-479.

Wall M, Doyle C K, Eden T, Zamba K D, and Johnson C A (2013) Size threshold perimetry performs as well as conventional automated perimetry with stimulus sizes III, V, and VI for glaucomatous loss. *Invest Ophthalmol Vis Sci* 54: 3975-3983.

Wall M, and Ketoff K M (1995) Random dot motion perimetry in patients with glaucoma and in normal subjects. *Am J Ophthalmol* 120: 587-596.

Wall M, Lefante J, and Conway M (1991) Variability of High-Pass Resolution Perimetry in normals and patients with idiopathic intracranial hypertension. *Invest Ophthalmol Vis Sci* 32: 3091-3095.

Wall M, Woodward K R, Doyle C K, and Artes P H (2009) Repeatability of automated perimetry: a comparison between standard automated perimetry with stimulus size III and V, Matrix, and Motion Perimetry. *Invest Ophthalmol Vis Sci* 50: 974-979.

Wall M, Woodward K R, Doyle C K, and Zamba G (2010) The effective dynamic ranges of standard automated perimetry sizes III and V and Motion and Matrix perimetry. *Arch Ophthalmol* 128: 570-576.

Watanabe M, and Rodieck R W (1989) Parasol and midget ganglion cells of the primate retina. *J Comp Neurol* 289: 434-454.

Watson A B, and Pelli D G (1983) QUEST: a Bayesian adaptive psychometric method. *Percept Psychophys* 33: 113-120.

Weber A J, Kaufman P L, and Hubbard W C (1998) Morphology of single ganglion cells in the glaucomatous primate retina. *Invest Ophthalmol Vis Sci* 39: 2304-2320.

Weber J, and Rau S (1992) The properties of perimetric thresholds in normal and glaucomatous eyes. *Ger J Ophthalmol* 1: 79-85.

Weijland A, Flammer J, Bebie H, and Fankhauser F (2004) Automated Perimetry Visual Field Digest. Haag-Streit AG, Fifth Edition.

Weinreb R N, and Perlman J P (1986) The effect of refractive correction on automated perimetric thresholds. *Am J Ophthalmol* 101: 706-709.

Werkmeister R M, Cherecheanu A P, Garhofer G, Schmidl D, and Schmetterer L (2013) Imaging of retinal ganglion cells in glaucoma: pitfalls and challenges. *Cell Tissue Res* 353: 261-268.

Werner E B, Adelson A, and Krupin T (1988) Effect of patient experience on the results of automated perimetry in clinically stable glaucoma patients. *Ophthalmology* 95: 764-767.

Werner E B, Krupin T, Adelson A, and Feitl M E (1990) Effect of patient experience on the results of automated perimetry in glaucoma suspect patients. *Ophthalmology* 97: 44-48.

Wetherill G B, and Levitt H (1965) Sequential estimation of points on a psychometric function. *Br J Math Stat Psychol* 18: 1-10.

White A J, Sun H, Swanson W H, and Lee B B (2002) An examination of physiological mechanisms underlying the Frequency-Doubling illusion. *Invest Ophthalmol Vis Sci* 43: 3590-3599.

Wild J M (2001) Short-wavelength automated perimetry. *Acta Ophthalmol Scand* 79: 546-559.

Wild J M, Cubbidge R P, Pacey I E, and Robinson R (1998) Statistical aspects of the normal visual field in short-wavelength automated perimetry. *Invest Ophthalmol Vis Sci* 39: 54-63.

Wild J M, Dengler-Harles M, Searle A E, O'Neill E C, and Crews S J (1989) The influence of the learning effect on automated perimetry in patients with suspected glaucoma. *Acta Ophthalmol (Copenh)* 67: 537-545.

Wild J M, Hussey M K, Flanagan J G, and Trope G E (1993) Pointwise topographical and longitudinal modeling of the visual field in glaucoma. *Invest Ophthalmol Vis Sci* 34: 1907-1916.

Wild J M, Kim L S, Pacey I E, and Cunliffe I A (2006) Evidence for a learning effect in short-wavelength automated perimetry. *Ophthalmology* 113: 206-215.

Wild J M, and Moss I D (1996) Baseline alterations in blue-on-yellow normal perimetric sensitivity. *Graefes Arch Clin Exp Ophthalmol* 234: 141-149.

Wild J M, Pacey I E, Hancock S A, and Cunliffe I A (1999a) Between-algorithm, between-individual differences in normal perimetric sensitivity: Full Threshold, FASTPAC, and SITA. Swedish Interactive Threshold algorithm. *Invest Ophthalmol Vis Sci* 40: 1152-1161.

Wild J M, Pacey I E, O'Neill E C, and Cunliffe I A (1999b) The SITA perimetric threshold algorithms in glaucoma. *Invest Ophthalmol Vis Sci* 40: 1998-2009.

Wild J M, Searle A E, Dengler-Harles M, and O'Neill E C (1991) Long-term follow-up of baseline learning and fatigue effects in the automated perimetry of glaucoma and ocular hypertensive patients. *Acta Ophthalmol (Copenh)* 69: 210-216.

Williams P A, Howell G R, Barbay J M, Braine C E, Sousa G L, John S W, and Morgan J E (2013) Retinal ganglion cell dendritic atrophy in DBA/2J glaucoma. *PLoS One* 8: e72282.

Wilson M E (1970) Invariant features of spatial summation with changing locus in the visual field. *J Physiol* 207: 611-622.

Winther C, and Frisen L (2010) A compact Rarebit test for macular diseases. *Br J Ophthalmol* 94: 324-327.

Wood J M, Wild J M, Hussey M K, and Crews S J (1987) Serial examination of the normal visual field using Octopus automated projection perimetry. Evidence for a learning effect. *Acta Ophthalmol (Copenh)* 65: 326-333.

Yoon M K, Hwang T N, Day S, Hong J, Porco T, and McCulley T J (2012) Comparison of Humphrey Matrix Frequency Doubling Technology to standard automated perimetry in neuro-ophthalmic disease. *Middle East Afr J Ophthalmol* 19: 211-215.

Yoshiyama K K, and Johnson C A (1997) Which method of flicker perimetry is most effective for detection of glaucomatous visual field loss? *Invest Ophthalmol Vis Sci* 38: 2270-2277.

Yucel Y, and Gupta N (2008) Glaucoma of the brain: a disease model for the study of transsynaptic neural degeneration. *Prog Brain Res* 173: 465-478.

Zeppieri M, Brusini P, Parisi L, Johnson C A, Sampaolesi R, and Salvetat M L (2010) Pulsar perimetry in the diagnosis of early glaucoma. *Am J Ophthalmol* 149: 102-112.

Zeppieri M, Demirel S, Kent K, and Johnson C A (2008) Perceived spatial frequency of sinusoidal gratings. *Optom Vis Sci* 85: 318-329.